Anti-obesity Study of Indonesian Medicinal Plants: An *in vitro* Study in Adipocytes

脂肪細胞を対象としたインドネシア薬用植物の抗肥満研究

Hokkaido University Graduate School of Agriculture
Division of Applied Bioscience Doctor Course

LUCY LAHRITA

HOKKAIDO UNIVERSITY

Anti-obesity Study of Indonesian Medicinal Plants: An *in vitro* Study in Adipocytes

Lucy Lahrita

A thesis submitted to
Graduate School of Agriculture, Hokkaido University
in partial fulfillment of the requirements for the
Degree of PhD

September 2018

DECLARATION

I here declare that this thesis is my own work and that, to the best of my knowledge and belief, it reproduces no material previously published or written, nor material that has been acceded for the award of any other degree or diploma, except where due acknowledgement has been in the text.

_____

Lucy Lahrita

Abstract

Obesity has become a global health problem due to its association with major life-threatening diseases including cardiovascular diseases, type 2 diabetes and numerous cancers. Over the past decades, only few anti-obesity drugs have been developed and approved. In fact, some drugs have been withdrawn from the market due to their serious side-effects. With the alarming rise of obese individuals globally and in view of the dissatisfactions with synthetic drugs, there is a growing shift towards natural product-based medications.

In this study, investigation of potential anti-obesogenic agents was conducted from Indonesian medicinal plants. Indonesia, a Southeast Asian country, is rich in flora diversity which have been used as herbal medicines. Two plants, *Eurycoma longifolia* and *Brucea javanica* (both from family Simaroubaceae) were investigated for their lipolytic activity, a bioactivity to break down triglyceride into glycerol in adipocytes. Several lipolytic compounds were isolated from these plants and were further studied for their cellular mechanisms of actions. In addition, an anti-obesogenic screening was conducted to explore different mode of action from Indonesian medicinal plants.

1. Study of lipolytic activity from *E. longifolia*

The roots extract of *E. longifolia* have been widely used as aphrodisiac in Southeast Asian traditional medicine. Our previous study demonstrated its activity to reduce lipid accumulation in 3T3-L1 white adipocytes without cytotoxicity, indicating an anti-obesogenic activity. In current study, further investigation on lipolytic activity from this plant was conducted, including isolation of its active compounds, and lipolytic mechanisms for its extract and active compounds. Additionally, explorative study on the bioactivities of the active compounds in brown adipocytes, different type of adipocytes known for its thermogenesis, was studied.

Based on glycerol release assay, the extract of *E. longifolia* (EL) exerted lipolytic activity in 3T3-L1 adipocytes in a concentration-dependent manner. Subsequent molecular mechanistic study using several specific inhibitors to lipolytic signaling pathways showed that PKA and ERK inhibitors attenuate the lipolytic activity of EL. Further immunoblotting analysis confirmed that EL activates PKA and ERK phosphorylation by 200% and 250%, respectively.

Based on bioassay-guided fractionation, two lipolytic compounds, eurycomanone (**1**) and 13β,21-epoxyeurycomanone (**2**), were isolated from *E. longifolia*. Compound **1** enhanced lipolysis in adipocytes with an EC_{50} of 14.6 μM, while its epoxy derivate, compound **2**, had a stronger activity with an EC_{50} of 8.6 μM. Molecular mechanistic study found that PKA inhibitor totally diminishes the lipolytic activity of **1** and **2**. Furthermore, immunoblotting analysis confirmed the activation of phosphorylated PKA by both **1** and **2**. When tested in WT-1 brown adipocytes, compounds **1** and **2** also reduced lipid accumulation and exerted lipolytic activity, suggesting a potential of thermogenesis stimulation.

2. Lipolytic activity of *B. javanica*

The fruit of *B. javanica* has been used by local Indonesian people in traditional medicine for the treatment of dysentery, malaria, and cancers. So far, there was not much research that studies its activity in glucose and lipid metabolisms. This is the first study to explore potential anti-obesity activity from *B. javanica*.

In this study, *B. javanica* demonstrated strong lipolytic activity in white adipocytes, thus further study was conducted to identify its lipolytic compounds. Bioassay-guided fractionation from *B. javanica* has isolated several lipolytic compounds, including brucein A (**5**), brusatol (**6**), brucenatinol (**7**), brucein B (**8**), 3'-hydroybrucein A (**9**), and bruceine C (**10**). Some isolated compounds from this plant have demonstrated much stronger lipolytic activity compared to two isolated compounds from *E. longifolia*.

3. Anti-obesogenic screening of Indonesian medicinal plants

The 76 selected Indonesian plant extracts were subjected to two bioassays, namely lipid accumulation and glycerol release assays. The results of this screening revealed plant species that exert different lipid metabolism regulatory effects in adipocytes.

There are plants that reduce lipid accumulation and enhance lipolysis, *B. javanica*, *Melaleuca leucadendra*, *Zingiber purpureum*, and *Clerodendrum serratum*. There are some plants that enhance lipolysis but not reduce lipid accumulation, *Leucas lavandulifolia*, *Mentha arvensis*, *Pimpinella anisum*, *E. longifolia*, *Piper crocatum*, *Guazuma ulmifolia*, and *Sapindus rarak*. There is also a plant that reduces lipid accumulation but not enhance lipoysis, *Momordica charantia*.

Taken together, the findings of this study provide significant contributions to the body of knowledge in anti-obesity research from Indonesian medicinal plants. Not only has this study provided scientific basis and rationale for the use of those potential plants for medicinal purposes, but it has also provided information on different mode of anti-obesity effects to address this global health problem.

List of Publications during Graduate Study

Peer-reviewed journal

Lahrita, L., Hirosawa, R., Kato, E., Kawabata, J. (2017). Isolation and lipolytic activity of eurycomanone and its epoxy derivative from *Eurycoma longifolia*. Bioorg. Med. Chem. *25*, 4829-4834.

Lahrita, L., Kato, E. and Kawabata, J. (2015).Uncovering potential of Indonesian medicinal plants on glucose uptake enhancement and lipid suppression in 3T3-L1 adipocytes. J. Ethnopharmacol. *168*, 229–236.

Oral presentation

JSBBA National Meeting 2018. Presented in Nagoya (Japan) in March 2018.
Received JSBBA Hokkaido Branch Travel Award.
Lahrita, L., Kato, E., Tseng, YH., Kawabata, J. Activity of Eurycomanone and Epoxy-eurycomanone on Lipid Metabolism in WT-1 Brown Adipocytes.

65th International Congress and Annual Meeting of the Society for Medicinal Plant and Natural Product Research. Presented in Basel (Switzerland) in September 2017.
Received overseas travel grant from Hokkaido University's Agriculture alumni association.
Lahrita, L., Kato, E., Kawabata, J. *Eurycoma longifolia* Jack and Its Quassinoids Stimulate Lipolysis in 3T3-L1 Adipocytes.

The 3rd Myanmar-Japan Symposium. Presented in Pathein (Myanmar) in December 2016.
Lahrita, L., Hirosawa, R., Kato, E., Kawabata, J. Anti-diabetes and anti-obesity studies of Indonesian medicinal plants.

JSBBA Hokkaido Branch 2016. Presented in Sapporo (Japan) in November 2016.
Received 2016 JSBBA Hokkaido Branch Outstanding Student Award.
Lahrita, L. Study on anti-obesity and anti-diabetes properties of Indonesian medicinal plants.

International Symposium on Natural Products for the Future 2016. Presented in Tokushima (Japan) in September 2016.
Lahrita, L., Kato, E., Hendra, P., Fenty, Julianus, J., Kawabata, J. Lipid-suppressing activity of *Eurycoma longifolia* Jack in animal and cell models and its mechanism of action.

The International Chemical Congress of Pacific Basin Societies 2015. Presented in Honolulu (USA) in December 2015.
Received overseas travel grant from Hokkaido University.
Lahrita, L., Kato, E., Kawabata, J. Uncovering potential of Indonesian medicinal plants for dual actions as anti-diabetes and anti-obesity.

JSBBA National Meeting 2015. Presented in Okayama (Japan) on Mar 28, 2015.
Lahrita, L., Kato, E. and Kawabata, J. (2015). *In vitro* screening on 3T3-L1 adipocytes reveals *Eurycoma longifolia* Jack and *Piper nigrum* L. as dual active Indonesian medicinal plants for anti-diabetes and anti-obesity.

Poster presentation

50th Miami Winter Symposium on 'Diabetes: Today's Research-Tomorrow's Therapies'. Presented in Miami (USA) in January 2017.
Received Symposium Travel Awards from IUBMB.
Lahrita, L., Kato, E., Kawabata, J. Plant-based insulin mimetic and insulin sensitizer augmented with lipid reduction property. Miami Winter Symposium 2017. Miami: USA.

JSBBA National Meeting 2016. Presented in Sapporo (Japan) in March 2016.
Lahrita, L., Kato, E., Kawabata, J. Mechanism of lipid-suppressing activity of *Eurycoma longifolia* Jack in 3T3-L1 adipocytes.

19th International Conference of FFC - 7th International Symposium of ASFFBC. Presented in Kobe (Japan) in November 2015.
Lahrita, L., Kato, E., Kawabata, J. Piper nigrum L. and Eurycoma longifolia Jack as dual actions (anti-diabetes and anti-obesity) in 3T3-L1 adipocytes.

JSBBA Hokkaido Regional Meeting 2014. Presented in Sapporo (Japan) in December 2014.
Lahrita, L., Kato, E. and Kawabata, J. Bioassay-guided screening of Indonesian medicinal plants for anti-diabetes and anti-obesity against 3T3-L1 adipocytes.

List of Academic Awards and Grants

March 2018	Japan Society for Bioscience, Biotechnology and Agrochemistry (JSBBA) Hokkaido Branch Travel Award
November 2017	Nitobe School Advanced Program for Graduate Students (Scholarship and Research Grant) from Hokkaido University Frontier Foundation
September 2017	Overseas Travel Grant from Hokkaido University's Agriculture alumni association
April 2017	Leave A Nest Grant International Student Award 2017
January 2017	Symposium Travel Awards from International Union of Biochemistry and Molecular Biology (IUBMB)
November 2016	JSBBA Hokkaido Branch Outstanding Student Award 2016
December 2015	Overseas Travel Grant from Hokkaido University

Acknowledgement

It is a great honor and special privilege for the author to complete her graduate study at the Laboratory of Food Biochemistry, Graduate School of Agriculture at Hokkaido University (Japan), under the supervision of Dr. Eisuke Kato (lecturer). During her study, Dr. Kato has supported the author's research ideas to explore and develop her research projects, and to allow considerable freedom to challenge and introduce new research perspectives. The author is very grateful to complete her Master and Doctoral courses under his supervision. His research guidance has helped the author to publish her works in peer reviewed journals and to disseminate them in national/international conferences prior to this PhD dissertation.

The author's deepest gratitude is directed toward the Japanese Ministry of Education, Culture, Sports, Science, and Technology (MEXT) that awarded her with the highly prestigious MEXT scholarship; thus, enabling her to pursue and accomplish her graduate study at Hokkaido University. The author would like to express gratitude to Prof. Jun Kawabata for his academic guidance and direction during the author's study. From his service at Hokkaido University, the author learns about dedication, perseverance and passion for science. The author would also like to extend her profound gratitude to academic referees; Prof. Hiroshi Hara, Prof. Hideyuki Matsuura, and Associate Prof. Kei Sonoyama for their feedback and useful suggestions in improving the quality of her PhD dissertation.

The author would like to express gratitude to Prof. Yu-hua Tseng at Joslin Diabetes Center (Boston, USA) to welcome her in Tseng Lab to conduct a research project in her final year. As a research institution affiliated to Harvard University, this visiting research has exposed the author to seminars and discussions with world renowned scientists from Harvard University and other global universities. The author would like to extend her gratitude to the lab. manager and other postdoctoral fellows for assisting her to adjust to new research environment and sharing their research experiences and best practices. The author has gained invaluable research experience, resulting in a fruitful research outcome in such a short period of time. This visiting research would not have been conducted without the funding through Nitobe School Advanced Program, thus the author would also like to express her gratitude to Hokkaido University Frontier Foundation for the financial support.

Above all, the author would like to thank JESUS CHRIST, the Lord God Almighty and the Creator of Life, for continuously blessing her with sufficient strength, health, wisdom, and knowledge day after day to accomplish her graduate study. What are best in the author, she returns to His grace alone. Furthermore, the author personally dedicates this small piece of work to her loving parents, who have continuously blessed her with unceasing love, care, support, and constant encouragement. Dearest gratitude is fully directed to her 'other-half' for persistently teaching her the importance and benefits of hard work, self-discipline, self-dependence, prayer, and perseverance to achieve the goals of life. The author profoundly appreciates all the invaluable sacrifices, continuous prayer, and great efforts he vigorously made for her throughout her study. Next chapter of life awaits us, as we welcome and nurture our 'beloved' with the power of our Lord.

Last, but not least, the author would like to express her gratitude to the members of the Laboratory of Food Biochemistry for their hand-on assistance and words of encouragement. Particularly, the author would like to thank and remember the late Ryota Hirosawa, for his outstanding research works that give remarkable contribution to the author's research projects.

Table of Contents

List of Figures

List of Tables

List of Abbreviations

2-DG	2-deoxyglucose
8-Br-cAMP	8-bromoadenosine 3′,5′-cyclic monophosphate
β-NADP+	β-nicotineamide adenine dinucleotide phosphate
aq.	aqueous
ANOVA	analysis of variance
APS	ammonium persulfate
ATP	adenosine 5-triphosphate disodium salt
BSA	bovine serum albumin
CCK-8	cell counting kit-8
CMC	sodium carboxymethylcellulose
DEX	dexamethasone
DMSO	dimethyl sulfoxide
DMEM	Dulbecco's modified Eagle's Medium
EC_{50}	half maximal effective concentration
EDTA	ethylenediaminetetraacetic acid
ERK	extracellular signal-regulated kinase
ESI	electrospray ionization
FBS	fetal bovine serum
G6PDH	glucose 6-phosphate dehydrogenase
HDL	high-density lipoprotein
HMBC	heteronuclear multiple bond correlation
HPLC	high performance liquid chromatography
HSL	hormone-sensitive lipase
IBMX	3-isobutyl-1-methylxanthine
IDF	International Diabetes Federation
JNK	c-Jun N-terminal Kinases
KRPH	Krebs–Ringer–phosphate–Hepes
LDL	low-density lipoprotein
NMR	nuclear magnetic resonance
NOESY	nuclear Overhauser effect spectroscopy
OD	optical density

ORO	oil red O
p38 MAPK	p38 mitogen-activated protein kinase
PBS	phosphate buffered saline
PKA	c-AMP dependent protein kinase
PMSF	phenylmethylsulfonyl fluoride
PPARγ	peroxisome proliferator activated receptor gamma
SEM	standard error of the mean
SD	standard deviation
SDS	sodium dodecyl sulfate
SDS-PAGE	sodium dodecyl sulfate-polyacrylamide gel electrophoresis
T2DM	type-2 diabetes mellitus
TEA	triethanolamine hydrochloride
TEMED	N,N,N′,N′-tetramethylethylenediamine
TG	triglycerides
TLC	thin layer chromatography
Tris Base	2-amino-2-hydroxymethyl-1,3-propanediol
Tris-HCl	tris(hydroxymethyl)aminomethane hydrochloride
TZDs	thiazolidinediones
WHO	World Health Organization

List of Units

°C	degree Celcius
g	gram
h	hour
L	liter
µg/mL	microgram per milliliter
µL	microliter
µm	micrometer
µM	micromolar
mg	milligram
mg/mL	milligram per milliliter
mL	milliliter
mM	millimolar
min	minute
M	molar
nm	nanometer
U/mL	unit per milliliter
v/v	volume per volume
w/w	weight per weight

Chapter I
Introduction

This chapter provides background for conducting the anti-obesity study of Indonesian traditional medicinal plants. This chapter is divided into three sections. The first section identifies the global problems of obesity and its significance in public health issues. The following section describes the rationale of the study, reviews its current medications/non-medications treatment options and introduces natural product-based potential agents. The third section presents the general objective of this anti-obesity study from Indonesian medicinal plants and elaborates several specific objectives that would be achieved through this *in vitro* study.

In general, this chapter aims to establish and justify the need for this study to fill the existing research gap in drug development from natural sources, particularly from Indonesian medicinal plants. This represents a scientific effort to address current obesity issues in the world and to give contribution to the body of knowledge.

1.1 Problem Identification

1.1.1 Obesity: A Global Epidemic Disease

Obesity is a severe chronic metabolic disorder, characterized by the accumulation of excess fat in adipose tissue, as a result of imbalance between energy intake and energy expenditure. The World Health Organization (WHO) recognizes Body Mass Index (BMI), weight in kilograms divided by the square of the height in metres (kg/m^2), as a simple index of obesity to classify overweight (BMI $\geq$ 25) and obese (BMI $\geq$ 30).

On a global scale, obesity is an epidemiological problem and a major contributor to the global burden of non-communicable chronic diseases. According to the recent data from WHO (2018), more than 1.9 billion adults worldwide are overweight and at least 650 million of them are clinically obese (Figure 1.1).

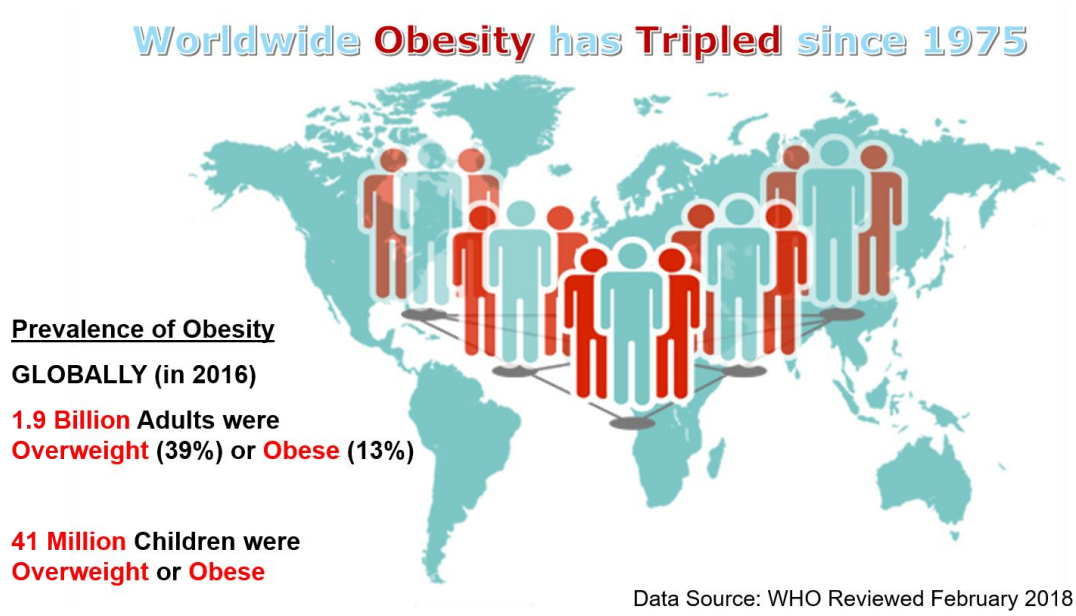

Figure 1.1 Worldwide prevalence of obesity

Source: http://welcomehealthy.com/obesity-risk-related-conditions-know/

The prevalence of obesity and overweight individuals is highest in the USA (26% obese and 62% overweight in both sexes) when lowest rate of obesity (3%) and overweight (14%) has been observed in Southeast Asia (Nahal et al., 2012). It is more prevalent in the developed countries, but in recent years, it dramatically increased in the developing countries. Over 50% people are either overweight or obese in India, Indonesia, Pakistan, Russia, Mexico, Brazil, Egypt, South Africa, Europe, the Eastern Mediterranean, and Americas (WHO, 2018).

In recent times lifestyle changes, less physical activity, excessive food intake, sedentary lifestyles, junk food and alcohol consumption, and wide access to high calorie foods are crucial factors for the development of obesity in adult and children. Obesity has been observed in the people those who consume more daily calories compared to their requirement. The excess calories taken in are converted into lipid components, primarily triglycerides, and is stored in liver, adipose and other tissues.

Obesity and obesity-related healthcare will become major global medical expenditures over the next 25–50 years. It is estimated that presently more than GBP 4 billions are incurred per year on obesity treatment and are likely to double by 2040 (Withrow and Alter 2011). Furthermore, obese individuals were found to have

medical costs that were approximately 30% higher than their peers with normal weight. Although medical community is aware of the various health risks concerning obesity, the number of obese people keeps increasing and worldwide obesity has tripled in the last three decades (WHO, 2018). These alarming facts underline the urgency to prevent and treat obesity in order to minimize treatment costs.

1.1.2 Obesity-related Diseases

Obesity is a complex health problem worldwide and a potential risk factor for a number of lifestyle-related chronic diseases (Figure 1.2). Obese individuals are more likely to develop diabetes, cardiovascular diseases, hypertension, metabolic syndrome, osteoarthritis, infertility, urinary incontinence, pulmonary disease, and certain types of cancer (Canning et al., 2014). In addition to medical complications, obese individuals are also prone to psychological issues, such as prejudice and discrimination, negative self-image, and are more likely to suffer an early death due to depression (Balaji et al., 2016).

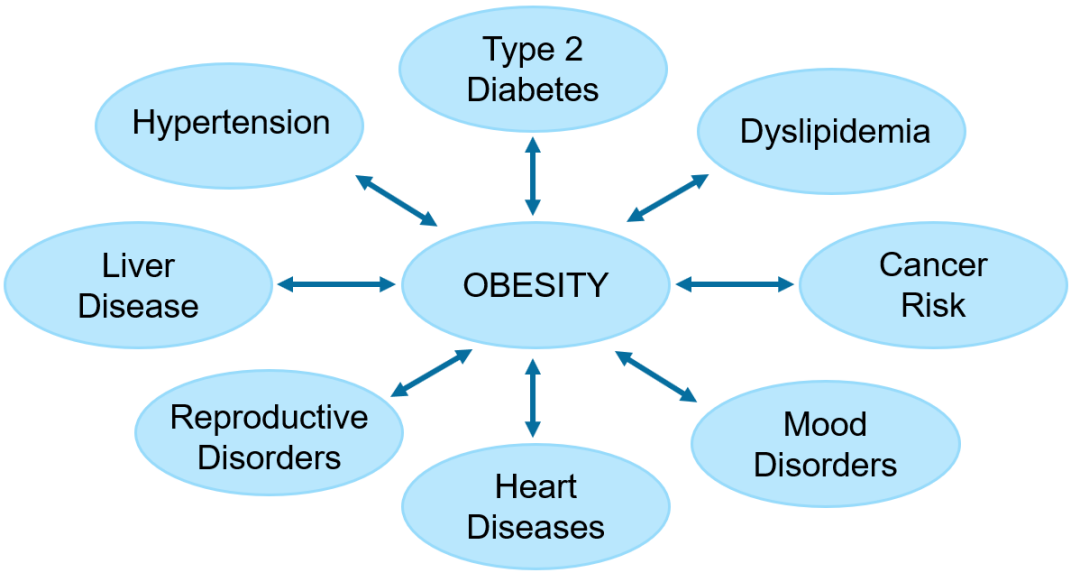

Figure 1.2 Obesity-related diseases

1.2 Rationale for Study

1.2.1 Treatment of Obesity

Obesity is a growing health problem in our global society and its treatment has been challenging. Currently, multiple therapeutic options are available to treat obesity such as caloric restriction, exercise, surgery, and medications.

Caloric restriction-induced weight loss is known to decrease serum free fatty acids (FFA) levels, and this may be also responsible for favorable improvements in insulin sensitivity (Mattison et al., 2017). Although non-medication weight control is one effective option, people tend to be reluctant to comply with recommended caloric restrictions and adequate levels of exercise. There were only 20% of people who attempt weight loss, actually utilize exercise training (Weiss et al., 2006). On the other hand, bariatric surgery is associated with health risks and high cost. As a result, obese patients seek treatment on medications and other supplements to manage their weight.

1.2.2 Anti-obesity Medications

Synthetic medication is one of therapeutic options to treat obesity. In spite of the importance of controlling obesity, available anti-obesity medications are limited. Over the past three decades, only few obesity-treatment drugs have been developed or approved by the US Food and Drug Administration (FDA). On the other hand, several anti-obesity drugs have been withdrawn from the market because of reported and documented adverse effects.

For instance, in 2010, the FDA has directed the withdrawal of Sibutramine from the US and Canadian markets due to cardiovascular concerns (James et al., 2010). Sibutramine is the first new drug for treating obesity via appetite suppression to be approved by the FDA within the past 30 years. Its main mechanism causes an increase in the feeling of satiety by controlling noradrenalin, serotonin or 5-hydroxytryptamine (5-HT), and dopamine (Fink and Gothert, 2007).

Rimonabant, an anorectic anti-obesity drug worked in cannabinoid system, was approved by the European authorities in 2006 but later withdrawn in 2008 due to serious psychiatric side effects (Balaji et al., 2016). Other drug, fenfluramine, reduces food intake and increase satiety by acting on 5-HT receptor. However, because of their side effects, they were withdrawn from the market.

After years of interruption, the FDA has recently approved additional new anti-obesity drugs, expanding treatment options for overweight/obese patients. The majority of these medications are taken orally, and only one is administered subcutaneously (Figure 1.3). The efficacy, mechanism of action, as well as the adverse effects of all five FDA-approved drugs are briefly summarized below:

1. Orlistat (Xenical®)

Orlistat is the only anti-obesity medication approved for long-term use worldwide. It was initially approved in 1990 under prescription, but since 2007 it has been available as a nonprescription drug in the US. Orlistat inhibits lipase, an enzyme produced in the pancreas and stomach, that breaks triglycerides down into fatty acids. This results in a lower rate of fat absorption by 30% and reduced total cholesterol and low-density lipoprotein (LDL) cholesterol (Hvizdos and Markham, 1999). Compared with other anti-obesity drugs, its side effects are mild, such as flatulence and steatorrhea (oily stool), but cases of severe liver injury have been reported (Weir et al., 2011).

2. Lorcaserin (Belviq®)

Lorcaserin, approved in 2012, is a serotonin or 5-HT agonist, that selectively activates the 5-HT2C receptors, which control caloric intake (Thomsen et al., 2008). Serotonin is involved in the regulation of appetite and food intake behavior. Lorcaserin does not reduce LDL cholesterol and has no effect on HDL cholesterol, but it reduces total cholesterol and triglyceride levels (Smith et al., 2010, Fidler et al., 2011). This medication appears to be more beneficial in the first few months and slowly loses its ability to maintain long-term weight loss, thus it is an option for patients who require short-term anti-obesity treatment and for women who have no known risk factors for breast cancer due to cancer risks in animal studies.

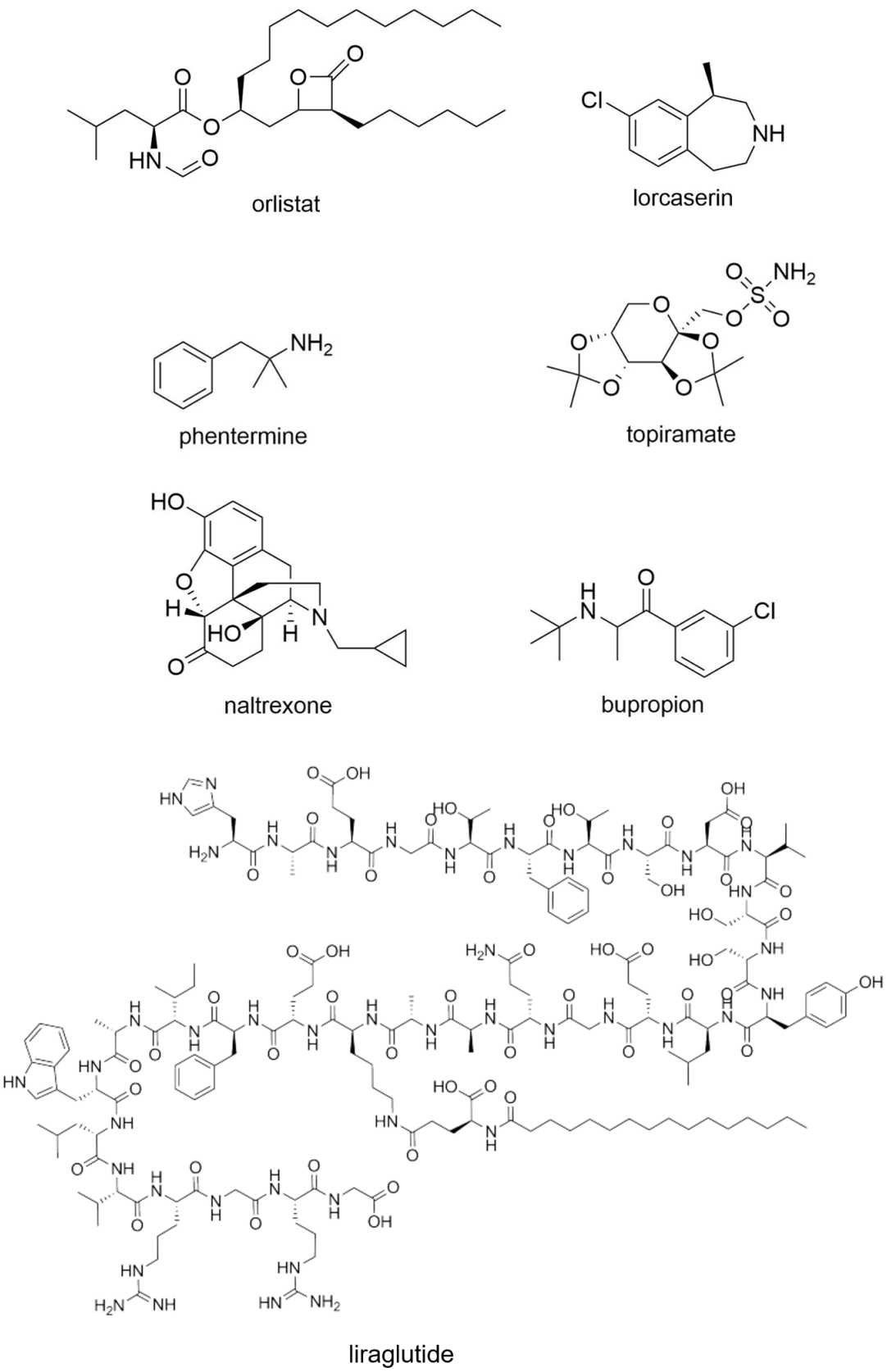

Figure 1.3 FDA-approved anti-obesity drugs

3. Phentermine/topiramate (Qysmia®)

Phentermine/topiramate is a combination drug, approved by the FDA in 2012. Phentermine is a nonselective stimulator of synaptic noradrenaline, dopamine, and serotonin release. Topiramate is an anticonvulsant drug that blocks voltage-dependent sodium channels, glutamate receptors, and carbonic anhydrase, and augments the activity of γ-aminobutyric acid (Antel and Hebebrand, 2012). Its effect on total cholesterol, LDL cholesterol, and HDL cholesterol levels gives positive profile. This drug combination would be beneficial in patients who need greater weight loss compared to other available strategies. One of the major concerns with this treatment is the higher rate of new-onset anxiety and depression, thus it is not a good option for patients with risk factors for anxiety and depression.

4. Naltrexone/bupropion (Contrave®)

Naltrexone/bupropion was approved by the FDA in 2014. Naltrexone is an opioid receptor antagonist used for alcohol and narcotic addiction. Bupropion is a selective reuptake inhibitor of dopamine and noradrenaline (antidepressant) that is also beneficial to promoting weight loss (Croft et al., 2002, White and Grilo, 2013). The effect of this combination is to reduce hunger, although it has no effect on energy metabolism. This combination provides a larger degree of weight loss than orlistat, and its side-effect including nausea is considered tolerable.

5. Liraglutide (Saxenda®, Victoza®)

Liraglutide (Saxenda®) is the only currently available FDA-approved injectable weight loss medication, and is a glucagon-like peptide-1 (GLP-1) receptor agonist. This medication is primarily used to treat type 2 diabetes, marketed under different name as Victoza®. Liraglutide is indicated as an adjunct to a low-calorie diet and increased physical activity for chronic weight management, thus it is suitable for patients needed to lower blood cholesterol and triglyceride but higher HDL cholesterol levels (Daneschvar et al., 2016). For weight loss medication, one of the major side effects of this medication is hypoglycemia, thus this medication would be beneficial for obese patients with hyperglycemia or for diabetic patients.

In the continuous effort to treat obesity, there are a number of new anti-obesity drugs currently under clinical trials, including centrally-acting drugs (radafaxine and oleoylestrone), drugs targeting peripheral episodic satiety signals (APD356) and drugs blocking fat absorption (cetilistat and AOD9604) (Halford, 2006).

1.2.3 Plant-based Anti-obesogenic Products

With the alarming rise of overweight and obese individuals globally, there is a growing need for cost-effective treatment of obesity. Recent approvals of additional drugs by the FDA have apparently expanded the treatment options for clinicians who care for overweight and obese patients. However, they are not affordable for all obese people, particularly in the developing countries. In view of these drawbacks and dissatisfaction with synthetic medications, there is a growing shift towards natural product-based medications.

A huge number medicinal plant parts and their extracts, fractions and isolated pure compounds have been investigated to examine their potential anti-obesity activity and possible mechanisms of actions. The easy accessibility without the need for laborious pharmaceutical synthesis has drawn considerable attention toward herbal medicines. Research on potential anti-obesity agents can be conducted in *in vitro, in vivo*, and clinical studies. Most of the *in vitro* studies were conducted via enzyme inhibition assay and using cell culture techniques which poses more advantage not only due to less chemical usage but also due to the early determination of the efficacy of drugs or plant compounds. In fact, many medicinal plants were exposed to scientific world by identifying their anti-obesogenic activity by *in vitro* methods (Mopuri and Islam, 2017).

In *in vitro* study, anti-obesogenic agents derived from natural products can be classified into categories based on their distinct mechanisms of actions: (1) pancreatic lipase inhibitory effect, (2) appetite suppressive effect, (3) energy expenditure stimulatory effect, (4) adipocyte differentiation inhibitory effect, and (5) lipid metabolism regulatory effect.

1.2.3.1 Pancreatic Lipase Inhibitory Effect

One of the prominent strategies to combat obesity is through inhibition of pancreatic lipase in gastrointestinal system. Pancreatic lipase is a key enzyme in dietary fat absorption, hydrolyzing triglycerides to monoglycerides and fatty acids. Dietary fat is not directly absorbed by the intestine unless the fat has been subjected to the action of lipase. The decreased digestion and absorption of ingested fats lead to overall decreased caloric absorption ultimately leading to decreased obesity.

Pancreatic lipase inhibition is one of the most widely studied mechanisms for determining natural products' potential efficacy as anti-obesity agents. Orlistat (tetrahydrolipstatin), the only FDA-approved anti-obesity drug for long term use, in fact, is a derivative of the naturally-occurring lipase inhibitor produced from *Streptomyces toxytricini* (Ballinger and Peikin, 2002). However, researchers continue to screen novel inhibitors, derived from plants or other natural sources, that lack some of the unpleasant side-effects orlistat has.

The active ingredients of *Panax japonicus* (family Araliaceae), *Clusia nemorosa* (family Clusiaceae), *Gardenia jasminoides* (family Rubiaceae), *Acanthopanax senticosus* (family Araliaceae), *Aesculus turbinate* (family Sapindaceae) and *Glycyrrhiza uralensis* (family Fabaceae) have been reported to possess pancreatic lipase inhibitory effects (Table 1.1). Among the vast natural sources of pancreatic lipase inhibitors, different types of tea (green, oolong, and black tea) received considerable interest on pancreatic lipase inhibition. (-)-Epicatechin (EC), (-)-epicatechin gallate (ECG), (-)-epigallocatechin (EGC), and (-)-epigallocatechin gallate (EGCG) are among the polyphenols that were isolated from tea leaves. These polyphenols require galloyl moieties within their chemical structures and/or polymerization of their flavan-3-ols for enhancement of pancreatic lipase inhibition (Nakai et al., 2005).

As the IC_{50} value of orlistat is 0.75 μg/mL, the inhibitory potencies of natural sources are significantly weaker than that of orlistat (Kim and Kang, 2005). For instance, Yoshikawa et al. (2002) reported that EGC and (-)-epicatechin-(4b→8)-(-)-4′-O-methylepigallocatechin inhibited the pancreatic lipase activity with an IC_{50} of 88 and 68 μg/ml, respectively.

A wide array of plants, including crude extracts from *Nelumbo nucifera* (Ono et al., 2006), *Salacia reticulata* (Kishino et al., 2006), and saponins from *Platycodi radix* (Han et al., 2000) have been also studied for their pancreatic lipase inhibitory effects. Because crude extracts include not only active substances, but also non-active components, the reported IC_{50} values are significantly weaker than that of orlistat (Kim and Kang, 2005).

Table 1.1 Isolated compounds inhibiting pancreatic lipase

No.	Isolated compounds	Natural source	Inhibition
1.	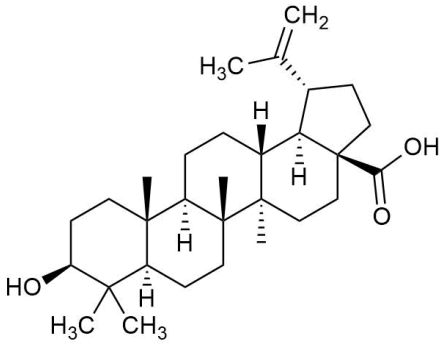 Betulinic acid ($C_{30}H_{48}O_3$), Molecular weight (MW): 456.711 g/mol	*Clusia nemorosa*	IC_{50} 21.1 µM, and induces adipocyte lipolysis (Kim et al., 2012)
2.	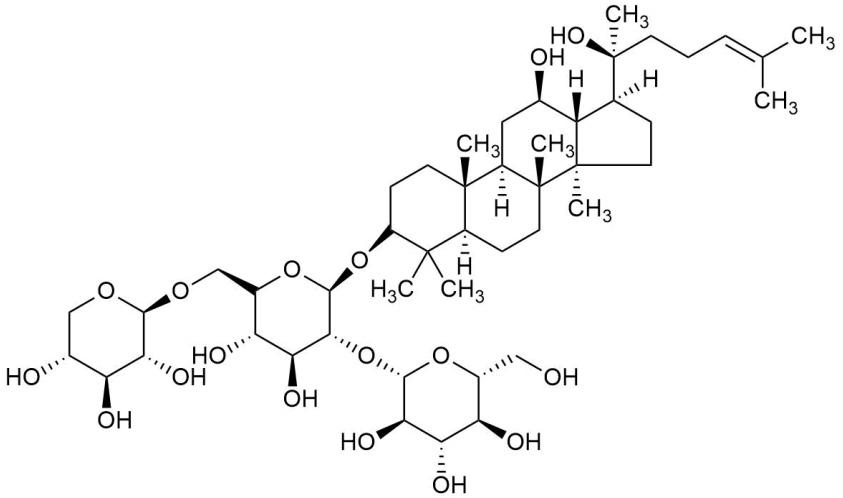 Chikusetsusaponins III ($C_{47}H_{80}O_{17}$), MW: 917.14 g/mol	*Panax japonicus*	IC_{50} 0.25 mg/mL, 22% decrease in body weight gain (Han et al., 2005)

Continued on the following page

No.	Isolated compounds	Natural source	Inhibition
3.	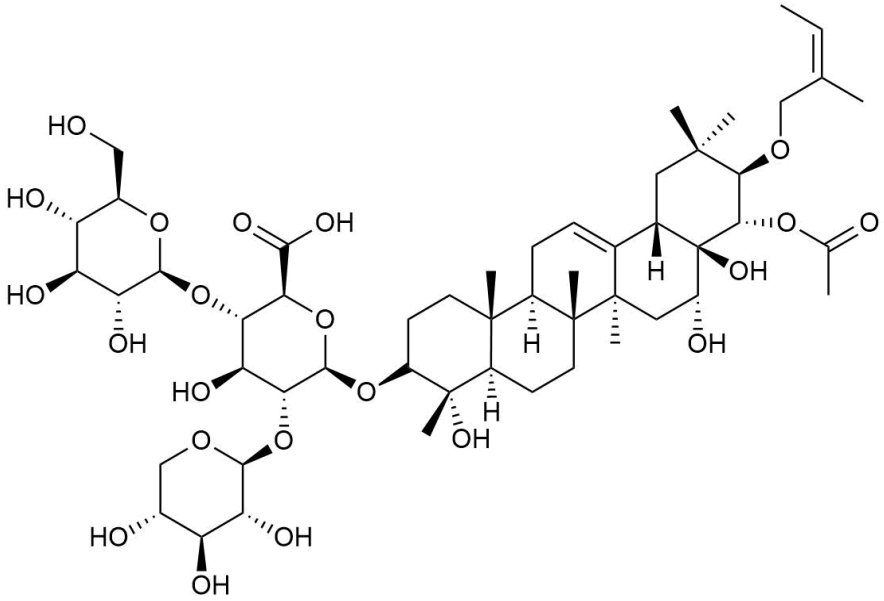 Escin IIb ($C_{54}H_{84}O_{23}$), MW: 1101.243 g/mol	*Aesculus turbinata*	IC_{50} 14 µg/mL (Kimura et al., 2006)
4.	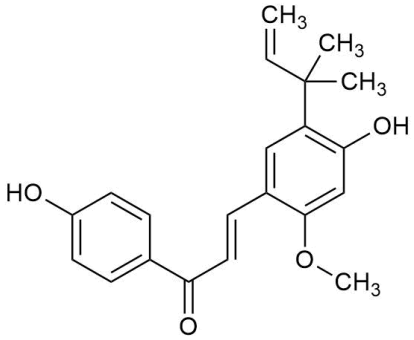 Licochalcone A ($C_{21}H_{22}O_4$), MW: 338.403 g/mol	*Glycyrrhiza uralensis*	IC_{50} 35 µg/mL (Won et al., 2007)

Continued on the following page

No.	Isolated compounds	Natural source	Inhibition
5.	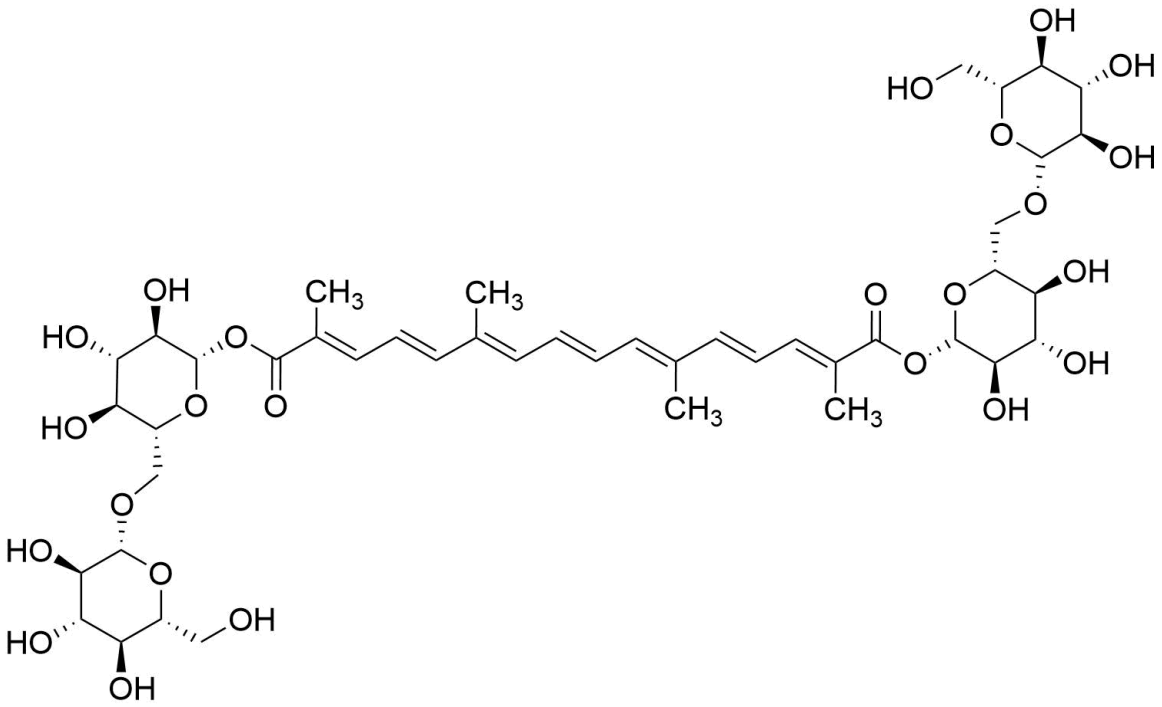 Crocin ($C_{44}H_{64}O_{24}$), MW: 976.972 g/mol 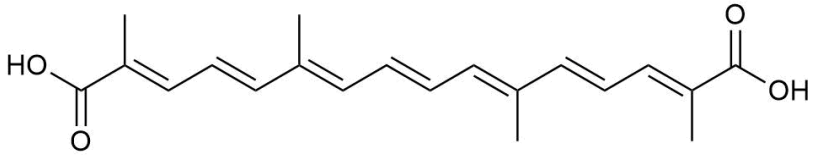 Crocetin ($C_{20}H_{24}O_4$), MW: 328.408 g/mol	*Gardenia jasminoides*	IC_{50} (2.1 and 2.6 mg/mL, respectively), reduced 25% body weight and suppressed serum TG, TC, and LDL-C in hyperlipidemic mice (Lee et al., 2005, Sheng et al., 2006)

Continued on the following page

No.	Isolated compounds	Natural source	Inhibition
6.	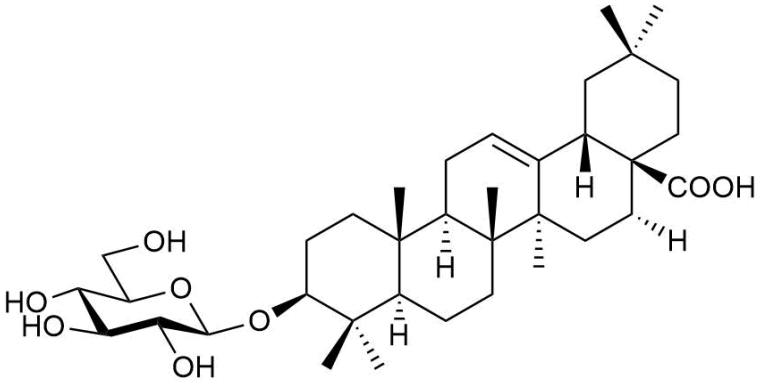 Silphioside F ($C_{48}H_{78}O_{18}$), MW: 943.134 g/mol 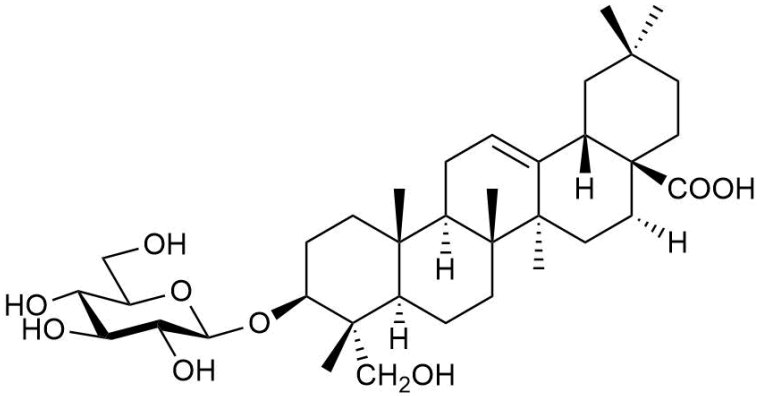 Copteroside B ($C_{36}H_{56}O_{10}$), MW: 648.834 g/mol	*Acanthopanax senticosus*	IC_{50} = 0.22 and 0.25 mM, respectively (Li et al., 2007)

Continued on the following page

No.	Isolated compounds	Natural source	Inhibition
7.	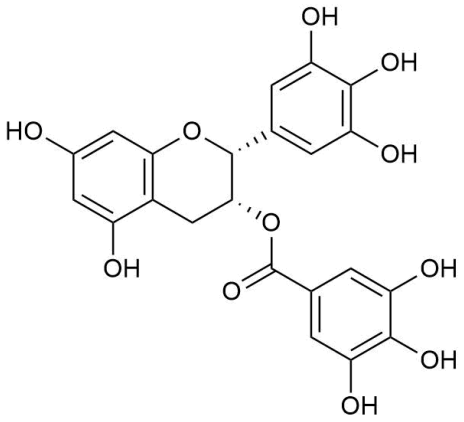 Epigallocatechin gallate (EGCG) 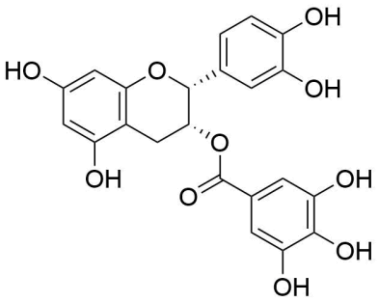 Epicatechin gallate (ECG) 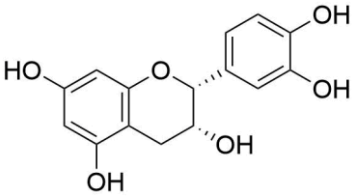 Epicatechin (EC) 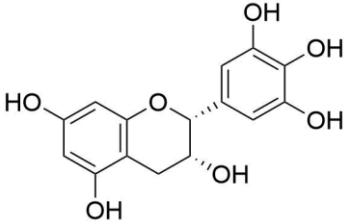 Epigallocatechin (EGC) 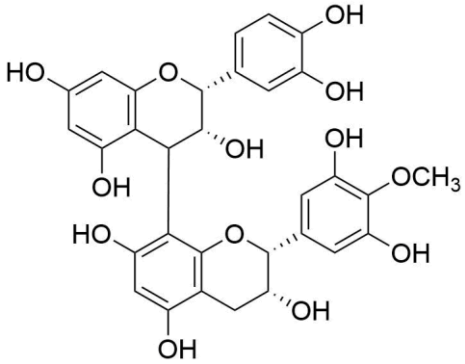 Epicatechin-4'-O-methylepigallocatechin	Tea polyphenols	IC_{50} EGC and Epicatechin-4'-O-methylepigallocatechin (88 and 68 µg/mL, respectively) (Yoshikawa et al., 2002)

1.2.3.2 Appetite suppressive effect

Body weight regulation through appetite control is a multifactorial event resulting from neurological and hormonal interrelationships. Numerous studies indicate that neurotransmitters, such as serotonin, histamine, dopamine, and their associated receptor activities play key role in appetite and satiety regulation. These receptors may enable researchers to better target their searches for suitable candidates anti-obesity agents that suppress appetite.

Appetite suppressant mechanisms of action typically affect hunger control centers in the brain, resulting in a sense of fullness. Many natural appetite suppressants found to mediate the reduced expression of hypothalamic neuropeptide Y (NPY) or serum leptin levels (Kim et al., 2005, Weigle, 2003). Besides leptin, ghrelin is also a peripheral signal with central effects, secreted from the stomach. They are key players in appetite regulation, which consequently influences body weight/fat and may be a potential means for obesity treatment. To provide safer drugs, therefore, researchers continue to study natural products for appetite regulation (Table 1.2).

For natural appetite suppressant, *Hoodia gordonii*, a leafless, spiny, succulent plant growing in some South African countries, is a phenomenal example. *H. gordonii* regulates appetite and significantly reduces calorie intake and boosts weight loss (MacLean and Luo, 2004, van Heerden et al., 2007). There are currently more than 20 international patents on compounds originating in *H. gordonii*, and many hoodia-containing commercial preparations are available on the market, including P57AS3 (van Heerden et al., 2007).

Other potential active compounds were isolated from *Garcinia cambogia* (family Clusiaceae), *Evodia rutaecarpa* (family Rutaceae), *Gymnema sylvestre* (family Apocynaceae), and including chilli *Capsicum annuum* (family Solanaceae), that worked in different targets to suppress appetite and reduce calorie intake, resulting in weight loss (Table 1.2).

Table 1.2 Isolated compounds suppressing appetite

No.	Isolated compounds	Natural source	Mechanism
1.	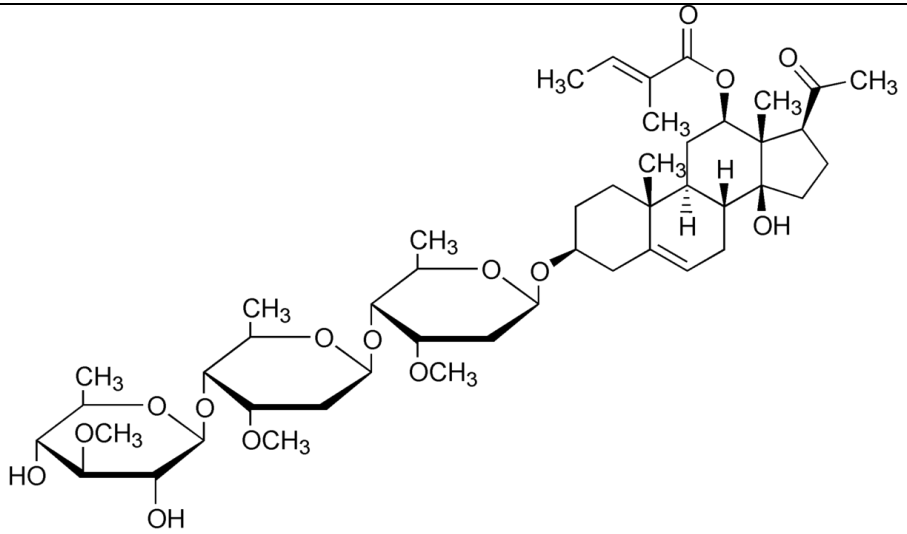 Steroidal glycoside (P57AS3) ($C_{47}H_{74}O_{15}$), MW: 879.08 g/mol	*Hoodia gordonii*	Increased ATP content/production in the hypothalamus, 40–60% reduction in food intake (MacLean and Luo, 2004, van Heerden et al., 2007)
2.	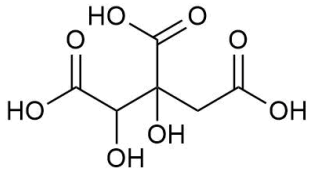 (-)-hydroxycitric acid (HCA) ($C_6H_8O_8$), MW: 208.122 g/mol	*Garcinia cambogia*	Increases satiety, decreases [^{3}H]-5-HT uptake by 20%, enhances the release of neurotransmitter (Ohia et al., 2002)
3.	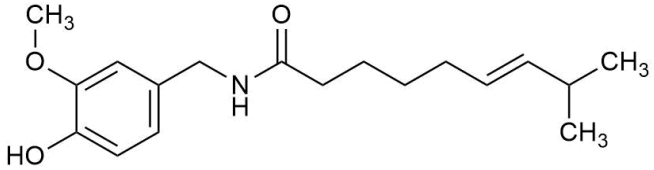 Capsaicin ($C_{18}H_{27}NO_3$), MW: 305.418 g/mol	*Capsicum annuum*	Increases the level of GLP-1, tended to decrease ghrelin content (Smeets and Westerterp-Plantenga, 2009)

Continued on the following page

No.	Isolated compounds	Natural source	Mechanism
4.	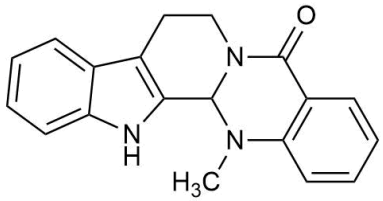 Evodiamine ($C_{19}H_{17}N_3O$), MW: 303.365 g/mol 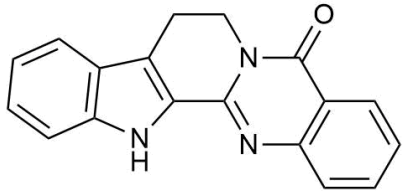 Rutecarpine ($C_{18}H_{13}N_3O$), MW: 287.322 g/mol	*Evodia rutaecarpa*	Decrease the mRNA expression of NPY and AgRP, decrease the protein expression of NPY peptide, enhance leptin level, decrease blood cholesterol, nonfasting glucose level (Shi et al., 2009, Kim et al., 2009)
5.	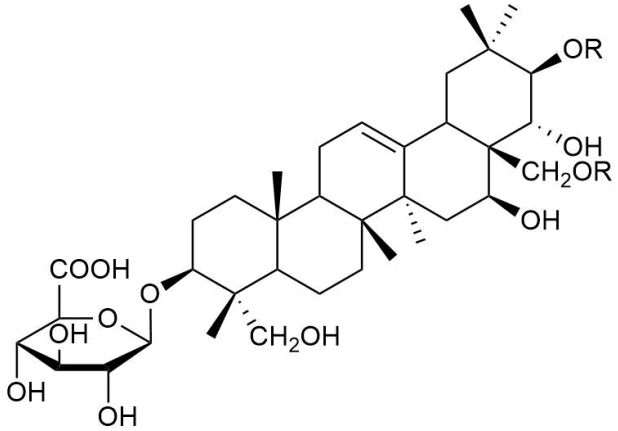 Gymnemic acids ($C_{43}H_{66}O_{14}$), MW: 806.987 g/mol	*Gymnema sylvestre*	Prevents sugar molecular absorption, reduces food intake (Kim et al., 2016)

1.2.3.3 Energy Expenditure Stimulatory Effect

Adipose tissue is a complex organ with a profound influence on physiology and pathophysiology. Adipose tissues can be classified as white (WAT) or brown (BAT) (Figure 1.3).

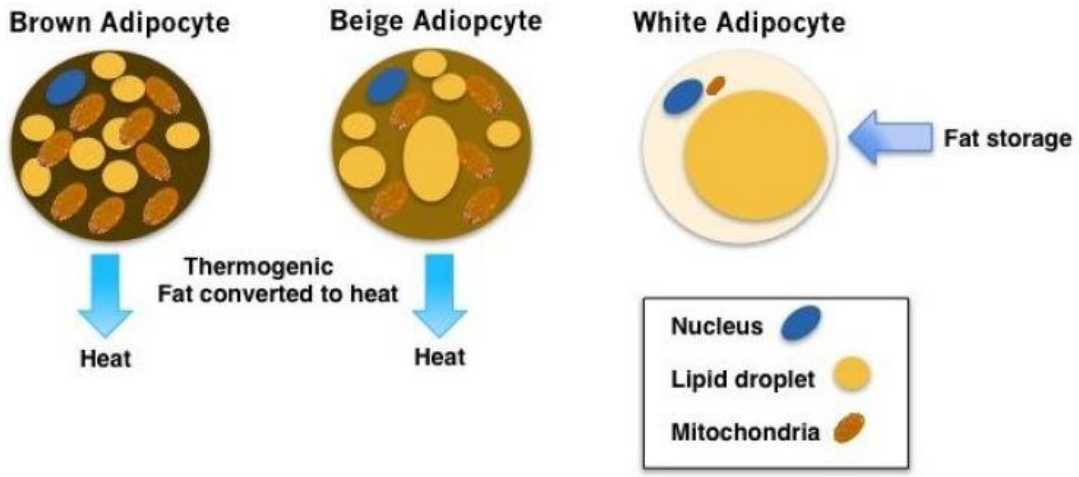

Figure 1.4 Classification of adipocytes
Source: https://www.eurekalert.org/multimedia/pub/109143.php

Credit: Cassie Tan, University of Pennsylvania

In adult humans, brown fat can be found in the supraclavicular region, deep neck and in the perirenal region (Jesperson et al., 2013, Lidell et al., 2013, Cypess et al., 2013, Betz et al., 2013). The uncovering of substantial amounts of active brown fat that exists in adult humans (Figure 1.5) has paved the ways for the development of new anti-obesity treatments by targeting this particular tissue.

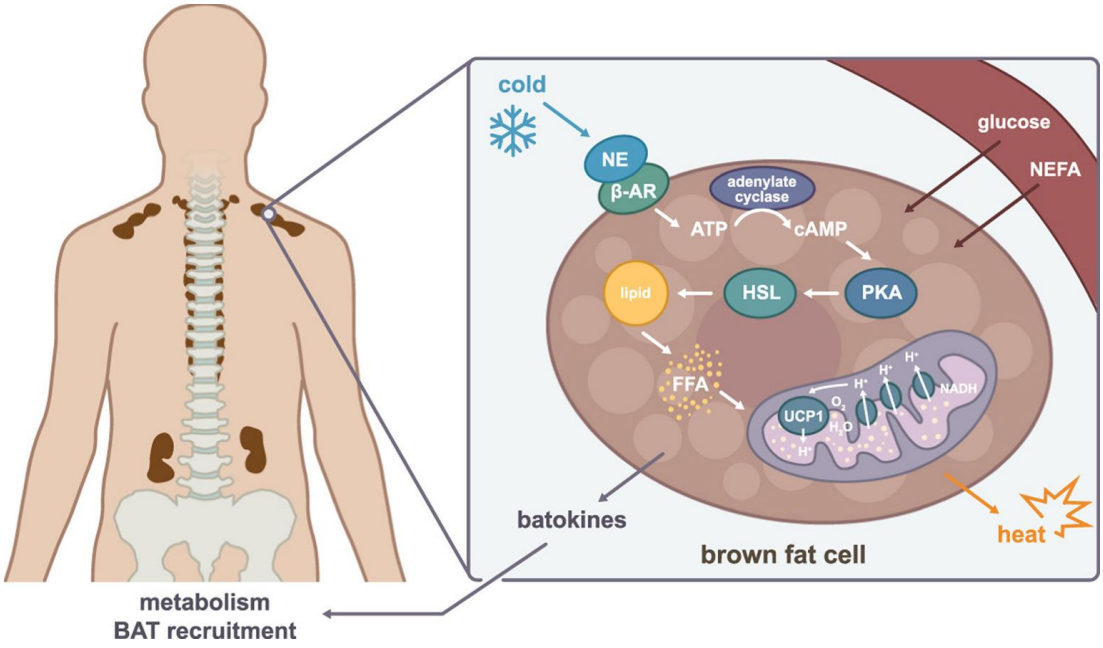

Figure 1.5 Human brown fat
(Scheele and Nielsen, 2017)

Brown adipocytes are highly specialized cells that dissipate stored energy as heat through β-adrenergic receptors. To regulate body weight and energy expenditure, mammalian BAT establishes non-shivering thermogenesis through dissipation of excess energy as heat in response to cold/β adrenogen-1 (Cannon and Nedergaard, 2004). Mechanism of thermogenesis involved in the response to chronic cold exposure, in which brown fat is activated through sympathetic signalling. The key player in this process is uncoupling protein-1 (UCP-1), in which substances that upregulate UCP1 gene expression may be a worthy strategy for achieving obesity control.

Norepinephrine activates β3-adrenergic receptors on the brown adipocytes, initiating lipolysis of the intracellular triglyceride storage. Free fatty acids are released as substrate, triggering mitochondrial respiration, which generates a mitochondrial membrane potential. This stimulates UCP-1, a mitochondrial BAT-specific protein, resulting in dissipation of the energy as heat (called thermogenesis). One analogue of UCP1, UCP3, is also a potential anti-obesity target, because it mediates the thermogenesis regulated by the thyroid hormone, β3-adrenergic agonists, and/or leptin in some organs (Gong et al., 1997). Therefore, researching for substances that can

upregulate UCPs gene expression may be an effective strategy to combat obesity through increased energy expenditure.

Moreover, UCP1-expressing thermogenic adipocytes have also been identified in WAT in the form of WAT-browning (beige adipocytes) (Peirce et al., 2014). BAT can be recruited from WAT under certain conditions, by remodeling mature WAT into mitochondria-rich cells with a high capacity for fatty acid oxidation (Cinti, 2002; Mercader et al., 2006). Therefore, the expansion of BAT or WAT-browning to enhance mitochondrial UCP1 expression-mediated thermogenic effects is thought to be a potential therapeutic target for treating obesity.

Numerous plant compounds have been proposed as treatments for weight loss via enhanced energy expenditure, including EGCG from tea leaves, celastrol from *Tripterygium wilfordii* (family Celastraceae), and capsaicin and piperine as spice components from chilli and pepper (Table 1.3). Besides plant-based products, there are numerous naturally occurring agents from marine sources, such as fucoxanthin, DHA and EPA, that also stimulate the process of thermogenesis in BAT.

Table 1.3 Isolated compounds promoting energy expenditure

No.	Isolated compounds	Natural source	Mechanism
1.	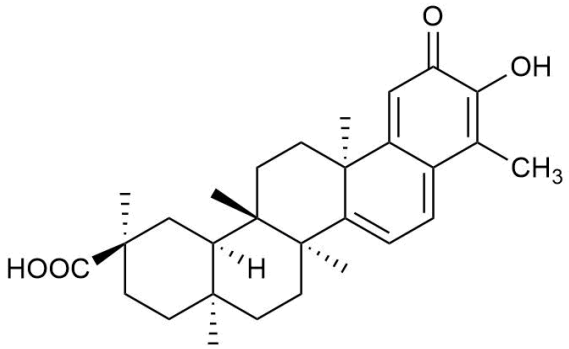 Celastrol ($C_{29}H_{38}O_4$), MW: 450.62 g/mol	*Tripterygium wilfordii*	Improves thermogenesis (BAT level), white fat remodeling, and mitochondrial function, increases plasma leptin, activates the HSF1-PGC1α transcriptional axis (Liu et al., 2015, Ma et al., 2015)
2.	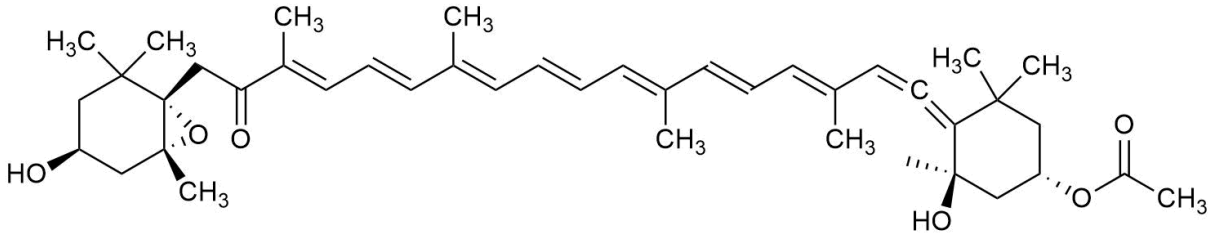 Fucoxanthin ($C_{42}H_{58}O_6$), MW: 658.92 g/mol	*Undaria pinnatifida* (brown algae)	UCP1 expression in WAT (Maeda et al., 2005)
3.	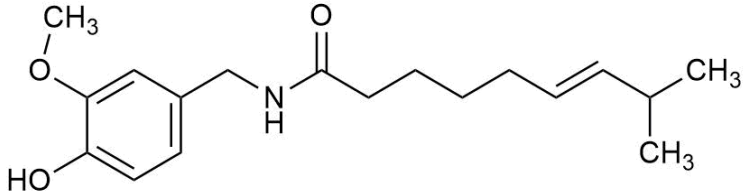 Capsaicin ($C_{18}H_{27}NO_3$), MW: 305.418 g/mol	*Capsicum annuum*	Increases diet-induced Thermogenesis, upregulation of UCP2 and UCP3 (Clegg et al., 2013)

Continued on the following page

No.	Isolated compounds	Natural source	Mechanism
4.	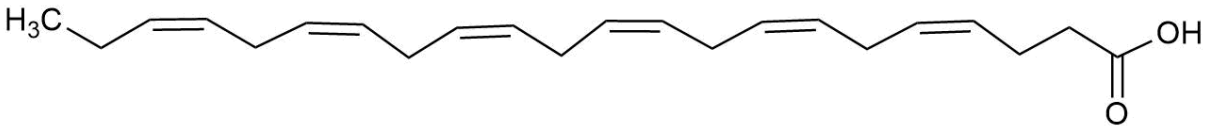 Docosahexaenoic acid (DHA) ($C_{22}H_{32}O_2$), MW: 328.488 g/mol 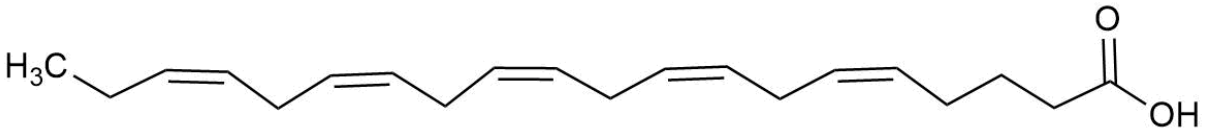 Eicosapentaenoic acid (EPA) ($C_{20}H_{30}O_2$), MW: 302.451 g/mol	Fish oil	Upregulation of UCP2 in liver (Tsuboyama-Kasaoka et al., 1999)
5.	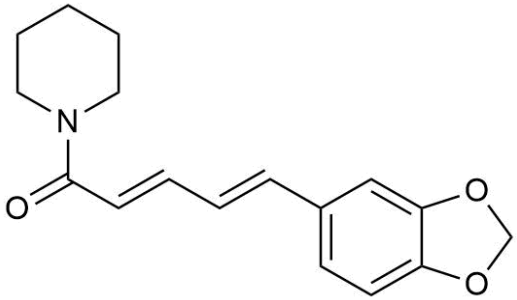 Piperine ($C_{17}H_{19}NO_3$), MW: 285.34 g/mol	*Piper nigrum*	Upregulation of UCP1 (Brahma et al. 2014).

Continued on the following page

No.	Isolated compounds	Natural source	Mechanism
6.	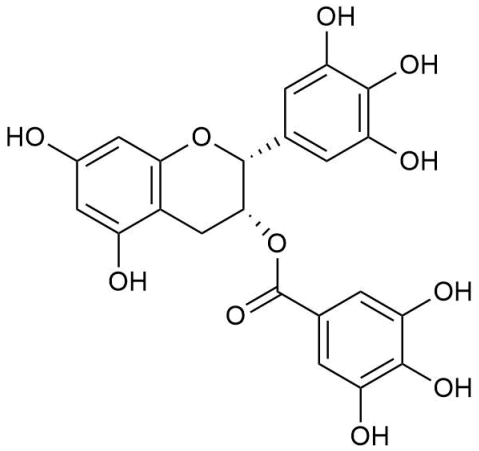 EGCG ($C_{22}H_{18}O_{11}$), MW: 458.372 g/mol	*Camellia sinensis*	Stimulates thermogenesis through inhibition of the catechol-O-methyltransferase involved in the degradation of norepinephrine (Boschmann and Thielecke, 2007)

1.2.3.4 Adipocyte Differentiation Inhibitory Effect

Adipocytes is crucial metabolic organ that controls energy homeostasis, through the regulation of both food intake and energy expenditure. Adipose tissue stores triglycerides, and releases glycerol and FFA in response to changes in energy demands. Obesity involves an abnormal growth of adipose tissue, characterized by an increasing adipocyte number (hyperplasia) and size (hypertrophy). The obese condition is generally aggravated by excess accumulation of lipid in adipose tissue, particularly in white adipose tissue (WAT).

The amount of adipose tissue mass can be regulated by the suppression of adipogenesis, which is the development of mature fat cells from fibroblastic preadipocytes (Figure 1.6).

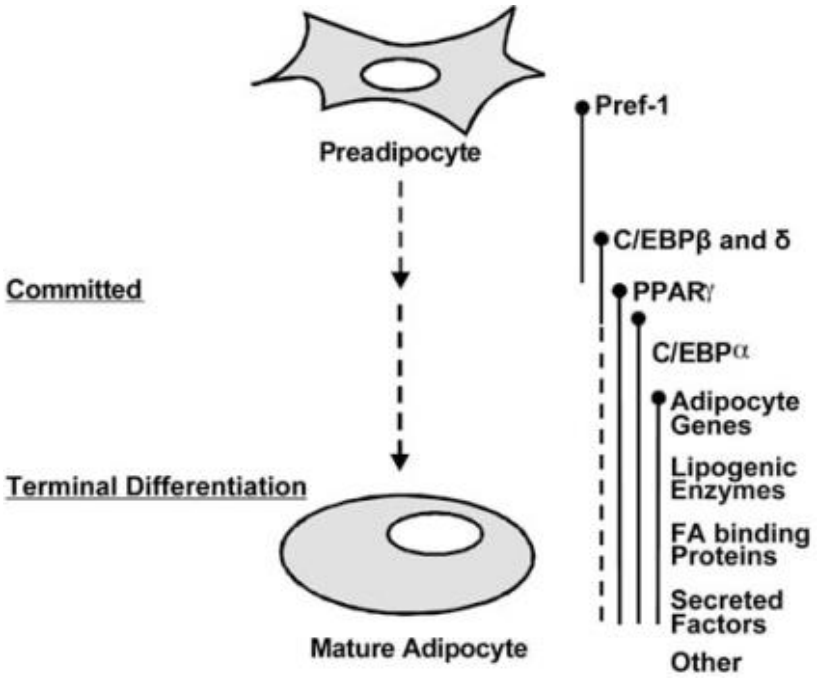

Figure 1.6 Development of mature adipocytes from preadipocytes
(Prokesch et al., 2009)

Adipogenesis is a differentiation process by which undifferentiated preadipocytes are converted to fully differentiated adipocytes. Adipocyte differentiation is characterized by a coordinate increase in adipocyte-gene expression.

The first wave of adipogenesis starts with the transient dramatic induction of CCAAT/enhancer binding protein-β (C/EBPβ) and -δ (C/EBPδ), stimulated by 3-isobutyl-1-methylxanthine (IBMX) and dexamethasone (DEX) respectively (Ramji and Foka, 2002). Subsequently, both C/EBPβ and C/EBPδ directly induce expression of peroxisome proliferator activated receptor-γ (PPARγ) and C/EBPα, the key transcriptional regulators of adipocyte differentiation and adipogenesis. PPARγ and C/EBPα subsequently activate a large number of downstream target genes whose expression determine the adipogenesis. PPARγ activation in mature adipocytes regulates several genes involved in the insulin signaling cascade as well as glucose and lipid metabolism (Lehrke and Lazar, 2005). Furthermore, the expression of the transcription factor sterol regulatory element binding protein (SREBP-1) also increases PPAR-γ activity during adipocyte differentiation.

The course of adipocyte differentiation has been well studied using 3T3-F422A and 3T3-L1 cells, two cell lines from murine white adipocytes that are committed to the adipocyte lineage (Green and Kehinde, 1974; 1975). In the presence of hormonal cocktail consisting of insulin, DEX, and IBMX; 3T3-L1 preadipocytes differentiate into mature adipocyte cells, thus expressing specific adipocyte genes such as PPARγ and C/EBPβ and accumulating TG lipid droplets (Cornelius et al., 1994; Lefterova and Lazar, 2009). The 3T3-L1 adipocytes have been served as well-established cell culture system that can be used to study adipogenesis and lipid metabolism.

As the generation of new fat cells plays key roles in the development of obesity, understanding the modulation of adipocyte differentiation is essential to regulate the number and function of these cells. Therefore, several studies screening for anti-obesity agents have focused on the processes of adipocyte proliferation and differentiation (Ikarashi et al., 2012; Richard et al., 2014).

In literature, various phytoconstituents like polyphenols, phytosterols, guggulsterone, tannins and dietary flavonoids found in green tea, vegetables, fruits, and herbs are reported to downregulate the adipogenesis through transcriptional regulation of PPAR-γ, C/EBPα, and SREBP-1, leading to inhibition of adipocyte differentiation during the early stage (Yang et al., 2008). For instance, curcumin, the phenolic yellowish pigment from *Curcuma longa* rhizomes, suppresses 3T3-L1

adipocyte differentiation. In addition, curcumin significantly decreased the expression of PPARγ and C/EBPα which are two key transcription factors in adipogenesis (Lee et al., 2009b). Other isolated compounds such as genistein from soy-bean, fucoxanthin from marine algae, isorhamnetin from Seabuckthorn, shikonin from *Lithospermum erythrorhizon*, vitisin A from *Vitis vinifera* and berberine from *Cortidis rhizoma* were also found as potential anti-obesity agents by inhibiting adipocyte differentiation (Table 1.4).

Table 1.4 Isolated compounds inhibiting adipocyte differentiation

No.	Isolated compounds	Natural source	Inhibition
1.	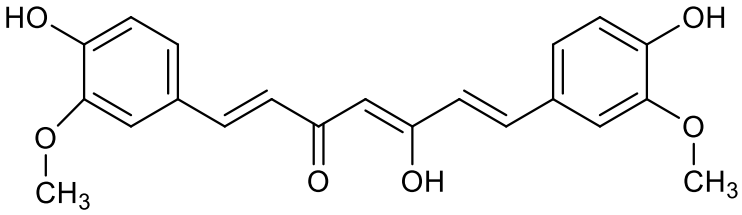 Curcumin ($C_{21}H_{20}O_6$), MW: 368.39 g/mol	*Curcuma longa*	Concentration of 50 μM, 2.4-fold decrease in TG accumulation (Lee et al., 2009b)
2.	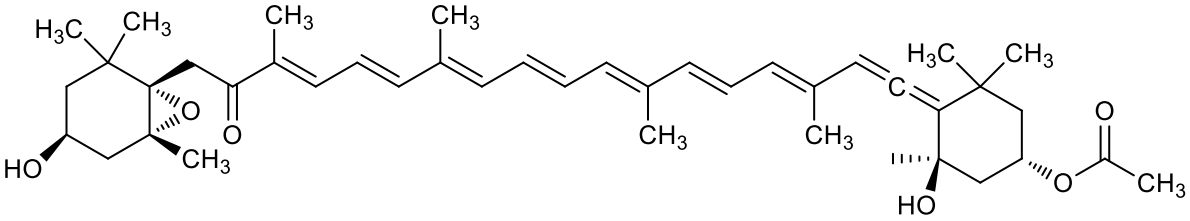 Fucoxanthin ($C_{42}H_{58}O_6$), MW: 658.92 g/mol	*Undaria pinnatifida* (brown algae)	Concentration of 15 μM, 70% inhibition of adipocyte differentiation (Maeda et al., 2006)
3.	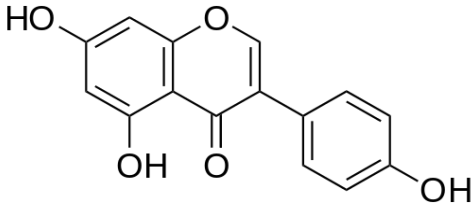 Genistein ($C_{15}H_{10}O_5$), MW: 270.24 g/mol	*Glycine max* (soy isoflavone)	Concentration of 200 μM, 90% inhibition of adipocyte differentiation with 43% decrease in viability (Hwang et al., 2005)

Continued on the following page

No.	Isolated compounds	Natural source	Inhibition
4.	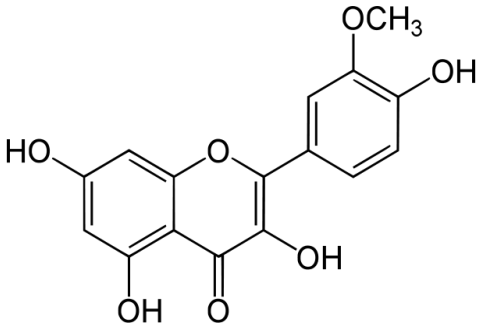 Isorhamnetin ($C_{16}H_{12}O_7$), MW: 316.26 g/mol	Seabuckthorn	Concentration of 50 μM, 2.75-fold decrease in TG accumulation (Lee et al., 2009a)
5.	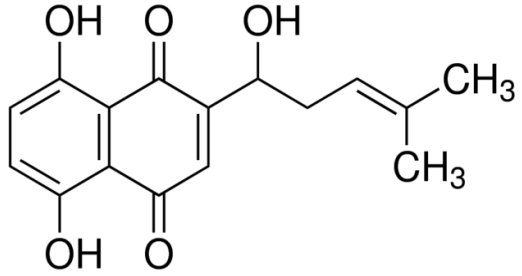 Shikonin ($C_{16}H_{16}O_5$), MW: 288.299 g/mol	*Lithospermum erythrorhizon*	IC_{50} = 1.1 μM (Lee et al., 2010)

Continued on the following page

No.	Isolated compounds	Natural source	Inhibition
6.	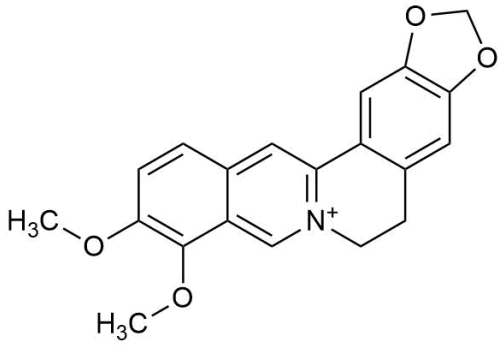 Berberine ($C_{20}H_{18}NO_4^+$), MW: 336.37 g/mol	*Cortidis rhizoma*	Inhibits 3T3-L1 adipocyte differentiation through the PPARγ pathway (Huang et al., 2006a)
7.	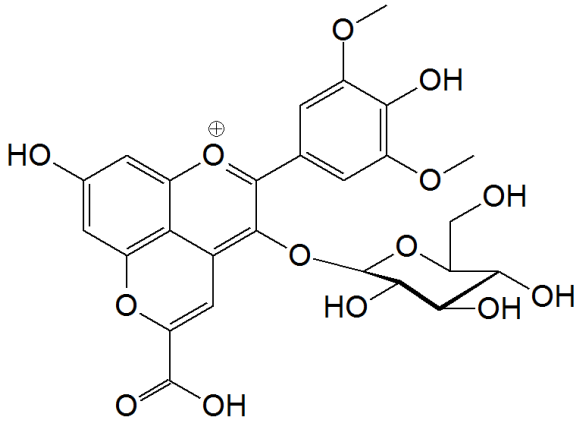 Vitisin A $C_{26}H_{25}O_{14}^+$), MW: 561.46 g/mol	*Vitis vinifera*	Inhibits adipocyte differentiation through cell cycle arrest (Kim et al., 2008)

1.2.3.5 Lipid Metabolism Regulatory Effect

Fat cells have the ability to synthesize triglycerides from fatty acids that are provided by circulating lipoproteins or via endogenous fatty acid biosynthesis. AMP-activated protein kinase (AMPK) signalling plays a key role in regulating lipid metabolism. AMPKs regulate lipogenesis genes including, sterol regulatory element-binding protein-1 (SREBP1). SREBP1c regulates the expression of genes involved in lipogenesis, metabolism of lipids and cholesterol, and fatty acid desaturation (Chen et al., 2011; Oppi-Williams et al., 2013). AMPK also regulates capacity for fatty acid oxidation by phosphorylation of transcription factors, such as cAMP response element binding protein (CREB) or co-activators such as peroxisome proliferator-activated receptor gamma coactivator 1-alpha (PGC-1α). Hence, AMPK is now recognised as a potential target to develop drugs/formulations for effective treatment of obesity.

The activation of SREBP1c promotes the expression of fatty acid synthase (FAS), lipoprotein lipase (LPL) and steroylcoenzyme A desaturase 1 (SCD-1) (Lee et al., 2013). FAS is a large enzyme that can synthesize fatty acids *de novo* from C2 acetyl coenzyme A subunits, to be biosynthesized further into triglycerides (Kim et al., 2014). Meanwhile, SCD-1 is involved in the synthesis and regulation of unsaturated fatty acids. Pharmacological approach revolves around targeting key enzymes in lipogenesis can be a target of obesity treatment.

As shown in Figure 1.7, reduced lipogenesis and enhanced lipolysis is vital in the regulation of lipid metabolism in adipocytes.

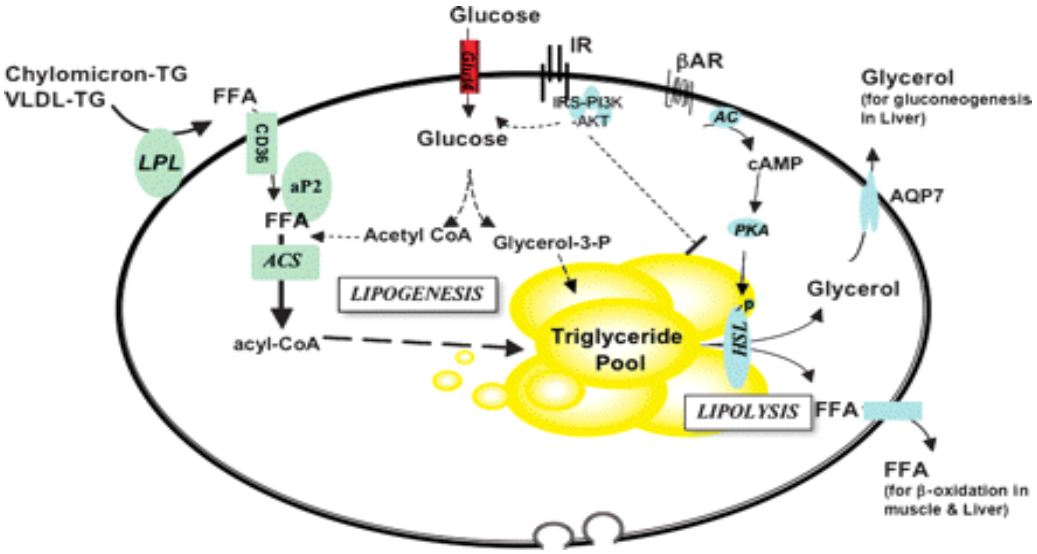

Figure 1.7 Lipid metabolism in adipocytes
(Sethi and Vidal-Puig, 2010)

Lipolysis is one of the most important mechanisms to reduce adipose mass, leading to the breakdown of triacylglycerols stored in adipocytes and release of free fatty acids (FFA) and glycerol (Figure 1.8). The lipolytic process occurs through consecutive steps that require the action of at least three different lipases: adipose triglyceride lipase (ATGL), hormone-sensitive lipase (HSL), and monoacylglycerol lipase (MGL) (Zechner et al., 2012). However, ATGL and HSL are responsible for more than 95% of TG hydrolysis in adipocytes.

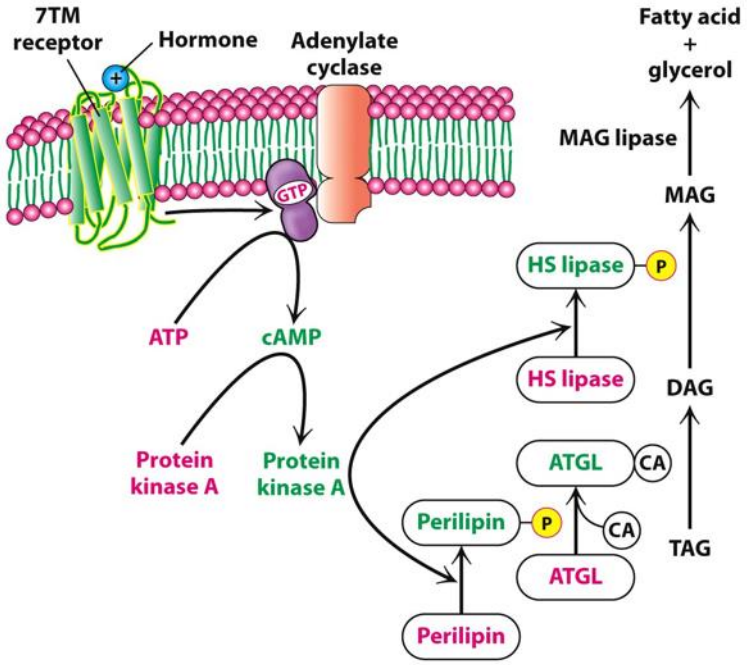

Figure 1.8 Adenylyl cyclase/c-AMP/PKA pathways in lipolysis
(Ahern, 2012)

cAMP/PKA pathway is the main pathway leading to the stimulation of lipolysis through the activation of (PKA) (Greenberg et al., 2001). Cyclic AMP (cAMP) is an important second messenger in the signaling pathways that mobilize fat stores. Catecholamines stimulate adipocyte lipolysis by binding to β-adrenoceptors, which activate adenylyl cyclase via the stimulatory guanine nucleotide binding protein (Gs), leading to an increase in intracellular cAMP and activation of cAMP-dependent protein kinase (PKA). Activated PKA phosphorylates HSL, a prominent lipase in the lipolysis, that leads to catalysis of triglycerides and diglycerides breakdown, producing the subsequent release of FFA and glycerol.

In addition to PKA pathway, it has been shown that components regulating adipocyte lipolysis are cytoplasmic targets of mitogen-activated protein kinase (MAPK) and that a portion of β-adrenergic-stimulated lipolysis in 3T3-L1 adipocytes is mediated via extracellular signal-regulated kinase (ERK) (Greenberg et al., 2001). MAPK/ERK pathway responds to growth factors and activates Ras, leading to the activation of Raf, which subsequently activates MEK, which in turn phosphorylates the MAPK, ERK1 and ERK2 (Chang and Karin, 2001). HSL was reported as one of the ERK's substrates (Greenberg et al., 2001), and the activation of ERK 1/2 leads to

adipocyte lipolysis by phosphorylation, thus increasing the activity of HSL. Targeting lipolysis can be of therapeutic interest, since stimulation of triglyceride hydrolysis that leads to reduced fat stores will ultimately combate obesity.

In regulating lipid metabolism, natural occurring compounds act in different target mechanisms (Table 1.5). Cerulenin from *Cephalosporium caerulens* inhibits biosynthesis of sterols and fatty acids via FAS inhibition. In addition to inhibiting adipocyte differentiation, curcumin also activates Wnt/β-catenin signalling in lipid metabolism (Ahn et al., 2010). Raspberry ketone (RK), sinensetin from citrus fruits and isolates from *Coprinus atramentarius* (illudin C2 and C3) were found to increase lipolysis (Morimoto et al., 2005, Kim et al., 2014, Kan et a., 2015). While berberine works through AMPK activation to regulate lipid metabolism (Lee et al., 2006).

Table 1.5 Isolated compounds regulating lipid metabolism

No.	Isolated compounds	Natural source	Mechanism
1.	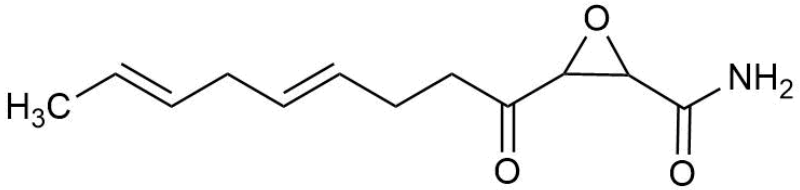 Cerulenin ($C_{12}H_{17}NO_3$), MW: 223.2695 g/mol	*Cephalosporium caerulens*	FAS inhibitor (Tomoda et al., 2002)
2.	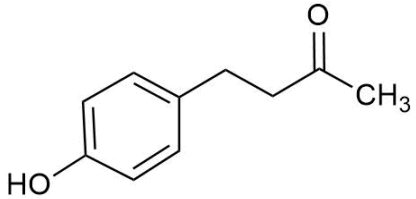 4-(4-Hydroxyphenyl)butan-2-one (RK) ($C_{10}H_{12}O_2$), MW: 164.20 g/mol	*Rubus idaeus* (raspberry)	Increases lipolysis (Morimoto et al., 2005)
3.	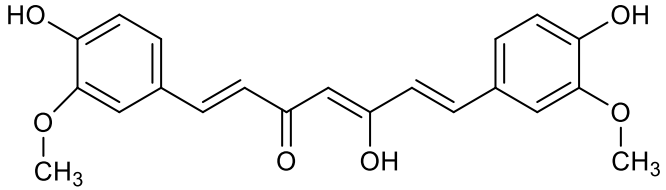 Curcumin ($C_{21}H_{20}O_6$), MW: 368.39 g/mol	*Curcuma longa*	Activation of Wnt/β-catenin signalling (Ahn et al., 2010)

No.	Isolated compounds	Natural source	Mechanism
4.	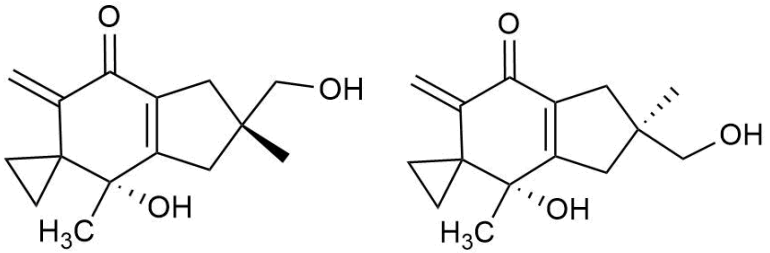 Illudins C2 and C3 ($C_{15}H_{20}O_2$), MW: 232.323 g/mol	*Coprinus atramentarius*	Stimulate lipolysis (Kim et al., 2014)
5.	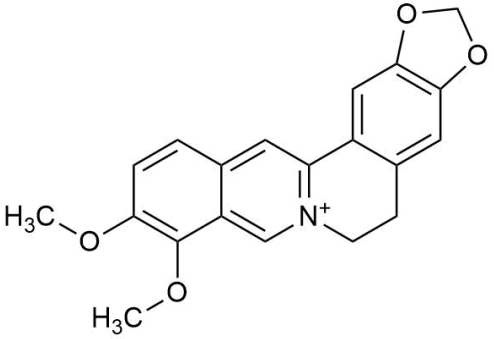 Berberine ($C_{20}H_{18}NO_4^+$), MW: 336.37 g/mol	*Cortidis rhizoma*	AMPK activation (Lee et al., 2006)
5.	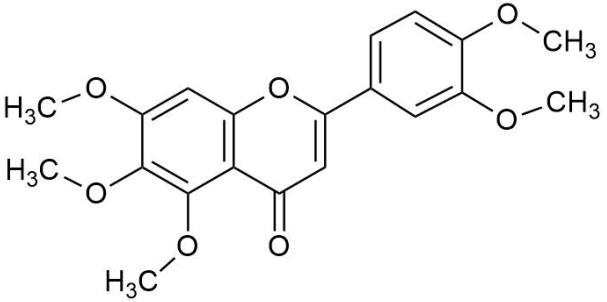 Sinensetin ($C_{20}H_{20}O_7$), MW: 372.36 g/mol	Citrus fruits	Enhances adipogenesis and lipolysis by increasing cAMP (Kang et al., 2015)

1.2.3.6 Combined Effects for Obesity Treatment

Some natural biomaterials possessing multi-functional anti-obesity activities have been discovered. Catechins from green tea, curcumin, and capsaicin are examples of multi-target compounds with anti-obesity effects.

Researchers originally studied green tea for its anti-oxidant activity than anti-obesity activity, owing to its high concentration of catechins, including epicatechin, ECG, and EGCG. However, subsequent research proved the strong anti-obesity effects of catechins resulted from the combined actions of appetite reduction, greater lipolytic activity and energy expenditure, and less lipogenic activity and adipocyte differentiation (Boschmann and Thielecke, 2007).

Curcumin, the phenolic yellowish pigment from *Curcuma longa* rhizomes, lower lipid levels and prevent obesity-associated complications in multiple mechanisms. It suppresses 3T3-L1 adipocyte differentiation through PPARγ and C/EBPα, which are two key transcription factors in adipogenesis (Lee et al., 2009b). It also modifies lipid metabolism in adipocytes through phosphorylation of AMPK and activation of Wnt/β-catenin signalling (Ahn et al., 2010).

Capsaicin, the major ingredient in *Capsicum annuum*, also acts in multiple target in adipocytes. This compound not only possesses anti-adipogenic effect but also increases thermogenesis (Hwang et al., 2005). It up-regulates UCP2 and UCP3 expression (analogs of UCP1) in mature adipocytes, thus promoting fat oxidation and energy expenditure (Smeets and Westerterp-Plantenga, 2009).

G. cambogia extract with its main active compound (-)-hydroxycitric acid (HCA), has also displayed multifunctional anti-obesity effects. Research has shown that it inhibits lipogenesis, burns excess fats, and suppresses appetite (Kim et al., 2004a). Its commercially-available extract, derived from the dried fruit of the *G. cambogia* tree, which grows in the forests of South India and Southeast Asia, has been on the market over 10 years with no adverse side-effects (Ohia et al., 2002).

There are many other natural products that possess anti-obesity activity with varying mechanisms. Perhaps, achieving synergistic effects of natural products can be a strategy to develop effective anti-obesity drugs. Thus, multiple products or products having multiple activities can be the recommended approach for obesity treatments from natural products.

1.2.4 Development of Anti-obesogenic Products from Indonesian Medicinal Plants

Traditionally, Indonesians believe that all diseases are curable, assuming that their medicines are available in nature. *Jamu*, an Indonesian word adopted from Javanese tribe language, is commonly used to refer to traditional medicines. To cure illnesses or diseases, they made decoctions from certain part of plants, such as leaf, bark, fruit, flower, and roots. Those plant materials, which are collected from their home gardens or surrounding forest, are used as *jamu* ingredients. The prescriptions of *jamu* were obtained from local practitioners, who had been trained to cure sick people using herbal medicines. They have evolved for centuries on experiences and practices, and now served as a major source of lead compounds for producing modern medicine.

The modern *jamu* is manufactured in various big and modem industries that are registered in the Indonesian Ministry of Health. According to Pramono (2002), there were more than 840 *jamu* industries in Indonesia and this number has grown to 872 companies in 2005. In terms of business, *jamu* industries have a promising growth of 25%-30% annually. Apart from domestic consumption, *jamu* are exported to other countries. Considering its potential commercial value, Indonesian government takes strategic approaches to preserve *jamu* quality by developing its standardization through strict and proper quality control and quality assurance.

Due to long history of consumption, there are various ways to classify *jamu*. It can be used for internal consumption as drinking decoction and external application such as ointment on wounded skin or gargle solution. It is available not only in traditional forms of decoctions, but also in the form of tablets, pills, powder, pastilles, capsules, extracts, creams, and ointments. In its development, *jamu* is used not only for medicinal purposes, but also for healthcare, beauty care, and healthy drinks (Tilaar et al., 1992).

The utilization of plants as traditional medicines is extensive nationwide because *jamu* has been a part of living culture in Indonesia. Species belonging to the families of Zingiberaceae, Asteraceae, Fabaceae, Euphorbiaceae and Lamiaceae are commonly used in *jamu*. Among them, Zingiberaceae (ginger family) is the most frequently found in its formulation (Sangat-Roemanty and Riswan, 1990). With 25,000-30,000 species of flowering plants in the country, there were 1,260 tree species in tropical rain forests, which had been used as traditional medicine (Zuhud et al. 1994). This indicates the small percentage of medicinal plants that has been phytochemically investigated and evaluated for

pharmacological potential. Even from the plants known for traditional medicinal use, many still have not been studied for their effectiveness and safety. Moreover, the potential of plants, herbs and their derivatives of Indonesian medicinal plants for the treatment of obesity is still largely unexplored and can be an excellent alternative to develop new safe and effective natural product-based anti-obesity drugs. Therefore, a necessity has arisen for alternative treatment for obesity, with minimal or no side effects in place of the present medications.

In this current study, *Eurycoma longifolia* Jack and *Brucea javanica* (L.) Merr., were investigated for their potential lipolytic activity. From the same family (Simaroubaceae), both plants are commonly used Indonesian medicinal plants but less studied for their potential anti-obesogenic activity. The following sub-sections provide descriptions of the plants, chemical constituents and their reported bioactivities.

1.2.4.1 *Eurycoma longifolia* Jack

Eurycoma longifolia Jack (family Simaroubaceae), locally known as *tongkat ali* in Indonesia, is a shrubby tree indigenous to Southeast Asian countries. This flowering plant can be found not only in Indonesia, but also in Malaysia, Vietnam, and some parts of Cambodia, Myanmar, Laos, and Thailand. The root of this tree is a popular material used in health foods and in traditional herbal medicine in this region. *E. longifolia* is prepared as a water decoction, as a commercial capsule of the root powder mixed with other herbs, and is used as an additive in several health food products.

E. longifolia is a rich source of various classes of bioactive compounds, which includes quassinoids, β-carboline alkaloids, canthin-6-one alkaloids, triterpene-type tirucallane, squalene derivatives, and eurycolactone, eurycomalactone, laurycolactone, biphenyl neolignan and bioactive steroids (Ang et al., 2000, Tran et al., 2000, Kuo et al., 2004, Mahfudh and Pihie, 2008, Miyake et al., 2009). Among these, bitter tasting quassinoid phytoconstituents account for a major portion in the *E. longifolia* root contents. Quassinoids are a group of nortriterpenoids with dynamic pharmacological properties. The quassinoids that have been isolated from the roots of *E. longifolia*, including eurycomanone (pasakbumin-A), eurycomanols, pasakbumin-B, hydroxyklaineanones, eurycomalactones, eurycomadilactones, eurylactones, laurycolactones, longilactones, and hydroxyglaucarubol

(Darise et al., 1982, Chan et al., 1989; 1991; 1992; Tada et al., 1991, Meng et al., 2014, Park et al., 2014).

Over the years, numerous studies have reported diverse biological activities of *E. longifolia*, including anti-malarial, anti-angiogenesis and anti-tumor (Al-Salahi et al., 2013; Chan et al., 2004; Jiwajinda et al., 2002). However, water decoction of the roots of *E. longifolia* remains a popular folk medicine for male aphrodisiac since it is believed to increase vitality and virility (Ang et al., 2003). In addition to the reported pharmacological effects, we recently reported that extracts from the roots of *E. Longifolia* suppressed intracellular lipid accumulation in 3T3-L1 adipocytes without cytotoxic side-effects, suggesting anti-obesogenic effects (Lahrita et al., 2015b). This newly identified anti-obesogenic effect of *E. longifolia* means that there is potential to develop an efficient method to prevent obesity in humans, and/or to treat obese patients, by means of herbal medication or functional food supplement. Also, identification of the bioactive compounds in this plant may be useful for the development of an anti-obesity drug. Thus, to further investigate the anti-obesogenic effect of *E. longifolia*, elucidation of the bioactive compounds and mechanistic studies were conducted in this current study.

1.2.4.2 *Brucea javanica* (L.) Merr.

Brucea javanica (L.) Merr (family Simaroubaceae), known as *buah Makassar* in Indonesia, is a shrub of about three-meter height. It grows in tropical areas distributing from Southeast Asia to Northern Australia (Kamperdick et al., 1995; Kim et al., 2003). The fruit of *B. javanica* has been used by local Indonesian and Thai people in traditional medicine for the treatment of dysentery, malaria, and cancer (Elkhateeb et al., 2008). In Malaysia, the seeds of this plant are used by the traditional practitioners for the treatment of diabetes, in which diabetic patients are recommended to take 5–10 seeds a day. (Shamsul et al., 2003).

Various chemical compounds have been reported to be isolated from *B. javanica* including alkaloids (Karin et al. 1990), lignans and terpenoids (Luyengi et al., 1996), alkaloid glycosides (Kitagawa et al., 1994), quassinoid glycosides (Sasaki et al., 1986a), and quassinoids (Kim et al., 2003). Quassinoids are known to be the major compounds isolated from Simaroubaceae family; and *B. javanica* is one of the most intensely investigated plants of this family, thus nearly 50 quassinoids have been isolated from this plant. Quassinoids

including bruceine C, bruceantinol, javanicolides A-D, and javanicosides A-F (Polonsky et al., 1980; Kim et al., 2003; 2004) and quassinoid glycosides including bruceosides A-C, and Yadanzioside P (Lee et al., 1979, Sakaki et al., 1986b, Fukamiya et al., 1992) have been isolated from *B. javanica*.

In addition to the traditional medicinal uses, compounds from *B. javanica* exhibited various biological activities such as antimalarial, amoebicidal, cytotoxic and antileukemic, anti-protozoan, anti-HIV, anti-inflammatory, and anti-babesial effects (Hall et al., 1983, Sakaki et al., 1986b, O'Neill et al., 1987, Wright et al., 1988, Okano et al., 1996, Sawangjaroen and Sawangjaroen, 2005, Subeki et al., 2007). To the best of author's knowledge, so far, there was no report on the anti-obesity potential from *B. javanica*. Therefore, a bioassay-guided fractionation performed in order to 'find and follow' the anti-obesogenic activity will reveal the active compounds and provide new alternative treatment for obese patients.

1.3 Objectives of the Study

The general objective of this laboratory study is to investigate potential anti-obesogenic activities of Indonesian medicinal plants, conducted *in vitro* in adipose model cells. The series of investigational works are divided into three sections; namely study of lipolytic activity from *Eurycoma longifolia* Jack, lipolytic activity of *Brucea javanica* (L.) Merr., and anti-obesogenic screening of Indonesian medicinal plants.

The specific objectives of each section are presented as follows:

A. Study of lipolytic activity from *Eurycoma longifolia* Jack

1. To elucidate mechanism of lipolytic activity of *E. longifolia* root extract
2. To isolate lipolytic compounds from *E. longifolia*
3. To elucidate mechanism of the lipolytic compounds
4. To investigate anti-obesogenic effects of the lipolytic compounds in brown adipocytes

B. Lipolytic activity of *Brucea javanica* (L.) Merr.

1. To investigate lipid metabolic-regulation of *B. javanica* fruit extract
2. To isolate lipolytic compounds from *B. javanica*

C. Anti-obesogenic screening of Indonesian medicinal plants

1. To identify Indonesian plant species with potential to enhance glycerol release

(enhancement of lipolysis)

2. To identify Indonesian plant species with potential to reduce lipid accumulation and enhance glycerol release
3. To identify Indonesian plant species with potential to reduce lipid accumulation but not enhance glycerol release (anti-lipogenesis)

Chapter II
Materials and Methods

This chapter describes detailed methodologies of anti-obesogenic activity the author carried out on a variety of Indonesian medicinal plants. The routine bioactivity assays consist of lipid accumulation (Oil Red O Staining and Nile Red Staining), lipolysis (glycerol release), and cell viability assays. Mechanistic studies include inhibitory challenges on the glycerol release and immunoblot analysis on protein kinases. Each section in this chapter elaborates the principles, chemical reagents, instruments and procedures of all the experiments conducted to investigate potential anti-obesogenic activities of *Eurycoma longifolia* Jack and its isolated active compounds, lipolytic activity and isolation of the lipolytic activity of *Brucea javanica* (L.) Merr., and anti-obesogenic screening of selected Indonesian medicinal plants.

2.1 Chemicals and Instruments for Extraction and Isolation of Bioactive Compounds

Unless otherwise stated, commercially available chemicals were purchased from Wako Pure Chemical Industries, Ltd. (Osaka, Japan). Water is of 'ultrapure' water Type 1, produced by Milli-Q purification system (Milli-Q water). A Bruker AMX 500 instrument (Bruker BioSpin K.K., Bruker Instruments, Billerica, MA, USA) was used to obtain NMR spectra, and residual solvents were used as an internal standard (pyridine-d_5: ^{1}H 7.22 ppm, ^{13}C 135.91 ppm). Mass spectra were obtained using LCT-Premier mass spectrometer (Waters Corp., Milford, MA, USA). For the LC-MS analysis, Waters Acquity UPLC system (Waters Corp., Milford, MA, USA) was combined with LCT-Premier mass spectrometer.

Dried plant materials were extracted in a mixture of solvent and each supernatant was then filtered through an Advantec filter paper no.101 and evaporated by a rotary evaporator (EYELA, Tokyo, Japan) under vacuum at 30°C (Figure 2.1). The temperature of the water bath was kept below 30°C to avoid decomposition of natural compounds. Each dried extract was re-dissolved in 10% (v/v) aq. DMSO before tested in adipocytes.

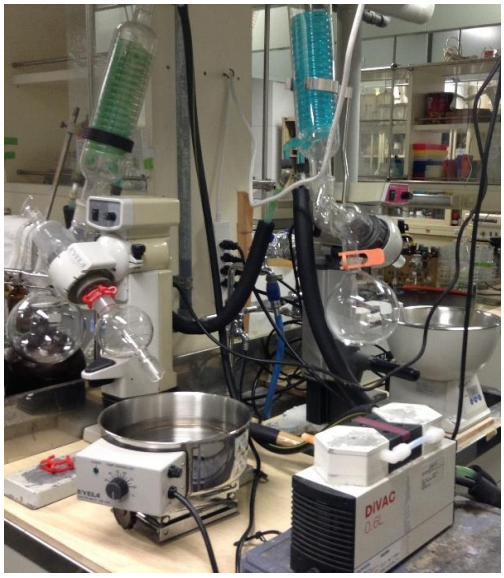

Figure 2.1 EYELA rotary evaporator

2.2 Extraction of *Eurycoma longifolia* Jack and Isolation of the Bioactive Compounds

2.2.1 Plant Materials

Dried roots of *E. longifolia* (Figure 2.2) were purchased from Merapi Farma Herbal Co. (Yogyakarta, Indonesia), a local herbs supplier, in February 2015. The plants, collected from the Kalimantan Island, were certified by the company's herbalist. The voucher specimens (SL. 1A.2015.PB) were deposited at the same company.

Figure 2.2 Dried roots of *E. longifolia*

2.2.2 Procedure

2.2.2.1 Extraction of *Eurycoma longifolia* Jack

The dried roots were reduced to coarse powder (Figure 2.3) and macerated at ambient temperature with 5%, 50% or 95% (v/v) aq. methanol for 24 hours. Different ratio of methanol and water was used to examine the optimal solvent with the highest reduction of lipid accumulation in 3T3-L1 adipocytes. Extracts of 95% (v/v) aq. methanol was used in mechanistic studies, while extract in 50% (v/v) aq. methanol was used in lipolysis-guided isolation.

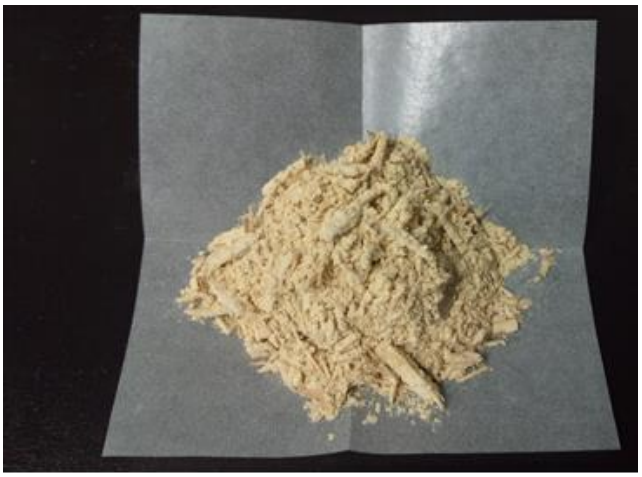

Figure 2.3 Coarse powder of *E. longifolia*

2.2.2.2 Isolation of Compounds 1-3

Powdered root of *E. longifolia* (200 g) was extracted with 50% aq. methanol for 24 h to obtain 6.84 g extract. The extract was suspended in water and partitioned with ethyl acetate and then with 1-butanol to obtain a water-soluble fraction (4.10 g), a 1-butanol-soluble fraction (1.17 g), and an ethyl acetate-soluble fraction (1.17 g). The 1-butanol-soluble fraction was adsorbed onto DIAION HP-20 (φ40 mm × 240 mm, Mitsubishi Chemical Co., Tokyo, Japan), washed with water, and eluted with 50% aq. methanol. The 50% aq. methanol-eluted fraction (580 mg) was then separated using Cosmosil® 75C18-OPN (Nakalai Tesque Inc., Kyoto, Japan) column chromatography (φ20 mm × 120 mm) by stepwise elution with water, 10% aq. methanol, 20% aq. methanol, 30% aq. methanol, 50% aq. methanol, 70% aq. methanol, and methanol. The active fraction eluted with 10% aq. methanol (130 mg) was further purified by Toyopearl HW-40F (Tosoh Co., Tokyo, Japan) column chromatography

(φ15 mm × 160 mm) with water as the eluent. The active fraction was finally purified by HPLC using an InertSustain C18 column (φ20×250 mm; GL Science Co., Tokyo, Japan) with 20% aq. methanol as an eluent to obtain compound **1** (16.3 mg), compound **2** (4.8 mg), and compound **3** (3.6 mg). The water-soluble fraction (4.10 g) was similarly separated to obtain additional compounds **1** (68.2 mg), **2** (14.0 mg), and **3** (8.6 mg).

2.2.2.3 Acetylation of Compound 2

Because there were two reported compound **2** with two different stereochemistry (Tada et al., 1991, Morita et al., 1993), compounds **2** were acetylated to confirm the correct stereochemistry assignments. Compound **2** (3.6 mg) was dissolved in pyridine (0.3 mL) and then acetic anhydride (0.15 mL) was added. The mixture was stirred for 1 h at room temperature under nitrogen, and then diluted with water and extracted with ethyl acetate. The organic layer was dried over sodium sulfate, evaporated, and then the residue was separated by preparative TLC (hexane/acetone = 1/1) to obtain the di-acetylated derivative compound **4** (4.4 mg, quant.). The positions of acetyl groups were confirmed from chemical shift changes and the HMBC spectrum.

2.3 Extraction of *Brucea javanica* (L.) Merr. and Isolation of the Bioactive Compounds

2.3.1 Plant Materials

Dried roots of *B. javanica* (Figure 2.4) were purchased from Merapi Farma Herbal Co. (Yogyakarta, Indonesia), a local herbs supplier, in February 2015. The plants were certified by the company's herbalist. The voucher specimens (SL. 1A. 2015. BMKS) were deposited at the same company.

Figure 2.4 Dried fruits of *B. javanica*

2.3.2 Procedure

2.3.2.1 Extraction of *Brucea javanica (L.) Merr.*

The dried fruits were reduced to powder and macerated at ambient temperature with 50% (v/v) aq. methanol for 24 hours. The supernatant was then filtered through an Advantec filter paper no.101 and evaporated by a rotary evaporator.

2.3.2.2 Isolation of Compounds 5-10

Powdered fruits of *B. javanica* (200 g) was extracted with 50% (v/v) aq. methanol to obtain 22.7 g extract. The extract was suspended in water and partitioned with ethyl acetate and then with 1-butanol to obtain a water-soluble fraction (17.80 g), a 1-butanol-soluble fraction (1.40 g), and an ethyl acetate-soluble fraction (1.84 g). The ethyl acetate layer was separated by silica gel column to obtain six fractions in which four fractions showed higher lipolytic activities. Through subsequent silica gel column and purification by TLC and HPLC, the four active fractions yielded in six lipolytic compounds; compound **5** (5.5 mg), compound **6** (1.6 mg), compound **7** (4.5 mg), compound **8** (4.6 mg), compound **9** (2.2 mg), and compound **10** (5.4 mg).

2.4 Cell Maintenance

2.4.1 Principle

Two types of adipose cells were used in this study, namely 3T3-L1 white adipocytes and WT-1 brown adipocytes. *In vitro* study with 3T3-L1 adipocytes was conducted at the Laboratory of Food Biochemistry (Graduate School of Agriculture, Hokkaido University) while *in vitro* study with WT-1 adipocytes was conducted at Tseng Lab, Section on Integrative Physiology and Metabolism (Joslin Diabetes Center, Boston, MA, USA), a research institute affiliated to Harvard Medical School.

Maintenance of 3T3-L1 and WT-1 adipose cells involves changes of different supplemented culture media during proliferation, differentiation, and development of adipocytes. The culture media include culturing medium, differentiation medium, and insulin medium that were replaced periodically. There are some differences on supplemented media between 3T3-L1 white adipocytes and WT-1 brown adipocytes. All supplements are described separately in different sections below. In addition to the mediums, the culture environment was controlled under aseptic conditions to avoid any contaminations. To maintain their optimum growth, the cells were incubated under controlled temperature and humidity.

2.4.2 Mouse 3T3-L1 White Adipocytes

2.4.2.1 Materials

The murine 3T3-L1 pre-adipocytes (cell no. JCRB9014) were supplied by the Japanese Collection of Research Bioresources Cell Bank in Osaka, Japan (Figure 2.5).

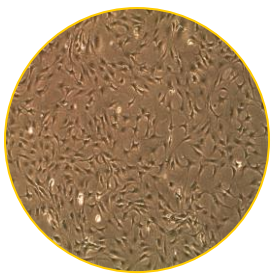

Figure 2.5 3T3-L1 pre-adipocytes
(Magnification 40x)

Various materials applied for growing 3T3-L1 cells and their suppliers, are listed in Table 2.1.

Table 2.1 Materials for 3T3-L1 cell culture

Material	**Supplier**	**Product Code**
D-MEM (high glucose) with L-Glutamine and Phenol Red	Wako Chem.	044-29765
Fetal Bovine Serum (FBS)	Gibco	10270-106
10× D-PBS(-)	Wako Chem.	048-29805
Penicillin G potassium salt	Sigma-Aldrich	P7794-10MU
Streptomycin sulfate	Wako Chem.	196-08511
Gentamicin sulfate Source: *Micromonospora purpurea*	Wako Chem.	073-04914
Trypsin Source: Porcine pancreas	Wako Chem.	207-09891
Insulin, human, recombinant Source: *Pichia pastoris*	Wako Chem.	093-06471
3-isobutyl-1-methylxanthine (IBMX)	Sigma-Aldrich	I5879
Dexamethasone (DEX)	Sigma-Aldrich	D4902
Dimethyl sulfoxide (DMSO)	Wako Chem.	043-07216

2.4.2.2 Preparation of Reagent Solutions and Medium

The solutions of reagents for cell culture were prepared as described in Table 2.2.

Table 2.2 Reagents and preparation for 3T3-L1 cell culture

Antibiotic stock solution	Gentamicin sulfate (100 mg), Streptomycin sulfate (200 mg), and 200,000 unit of Penicillin G potassium salt (125.8 mg) were dissolved in 2 mL of Milli-Q water. The solution was then filter-sterilized through a 0.2 μm syringe filter* and stored in a freezer (-20ºC).
Culture medium (10% FBS/D-MEM)	FBS (55 mL) and antibiotic stock solution (0.5 mL) were added into 500 mL of D-MEM (high glucose). The culture medium was mixed well and stored in a refrigerator.
Phosphate-buffered saline (PBS) buffer	10× D-PBS(-) (50 mL) was diluted in 450 mL of sterilized Milli-Q water and kept in a refrigerator.
Trypsin solution	Trypsin (40 mg) and EDTA 2Na (4 mg) were dissolved in 40 mL of PBS buffer. The solution was kept in a refrigerator for 1 day and then filter-sterilized through a 0.2 μm syringe filter*.
Insulin stock solution (10 mg/mL)	Insulin (10 mg) was dissolved in 1 mL of PBS buffer by adding 1 M HCl dropwise. The solution was then filter-sterilized through a 0.2 μm syringe filter* and stored in a freezer (-20ºC).
IBMX stock solution	IBMX (112 mg) was dissolved in 0.5 mL of DMSO, filter-sterilized through a 0.2 μm syringe filter** and then stored in a freezer (-20ºC).
DEX stock solution	DEX (5 mg) was dissolved in 2.55 mL of DMSO and then diluted 10 times to reach 0.5 mM of concentration. The solution was then filter-sterilized through a 0.2 μm syringe filter** and stored in a freezer (-20ºC).
Differentiation medium (differentiation inducer)	IBMX stock solution (25 μL), DEX stock solution (25 μL), and insulin stock solution (50 μL) was added into 50 mL of culture medium (10% FBS/D-MEM). The differentiation medium was mixed well and stored in a refrigerator.

	The differentiation medium was D-MEM supplemented with 10% (v/v) FBS, antibiotics, 0.5 mM IBMX, 0.25 μM DEX, and 5 μg/mL insulin.
Insulin medium (differentiation enhancer)	Insulin stock solution (277.5 μL) was added into 555 mL of culture medium (10% FBS/D-MEM). The insulin medium was mixed well and stored in a refrigerator.

Remarks*:*
[*]Advantec 25CS020AS (Toyo Roshi Ltd., Tokyo, Japan)
[**]Minisart RC 15 No. 17761--ACK (Sartorius Stedim, Goettingen, Germany)

2.4.2.3 Procedure

Figure 2.6 describes the 3T3-L1 cell maintenance that consists of timely medium changes and the application of the sample treatment. The 3T3-L1 pre-adipocytes were seeded into different types of well plates (Greiner Bio-one, Tokyo, Japan), depending on the experiments. The pre-adipocytes were seeded into 96-well plate, 48-well plate, and 12-well plate for cell viability, lipid accumulation, and protein extraction, respectively. The pre-adipocytes were then incubated in culture medium at 37°C in a humidified atmosphere of 10% CO_2.

To induce adipocyte differentiation, a day after reaching confluence, the cells were cultured in differentiation medium (day 0). To enhance the differentiation, two days after the induction (day 2), the culture medium was replaced with insulin medium. These cells (day 4) were used in lipid accumulation reduction assay. For other assays, the cells were further cultured in insulin medium for two more days (day 6) and then replaced with culture medium for another two days. These cells (day 8) were used in the glycerol release enhancement assay.

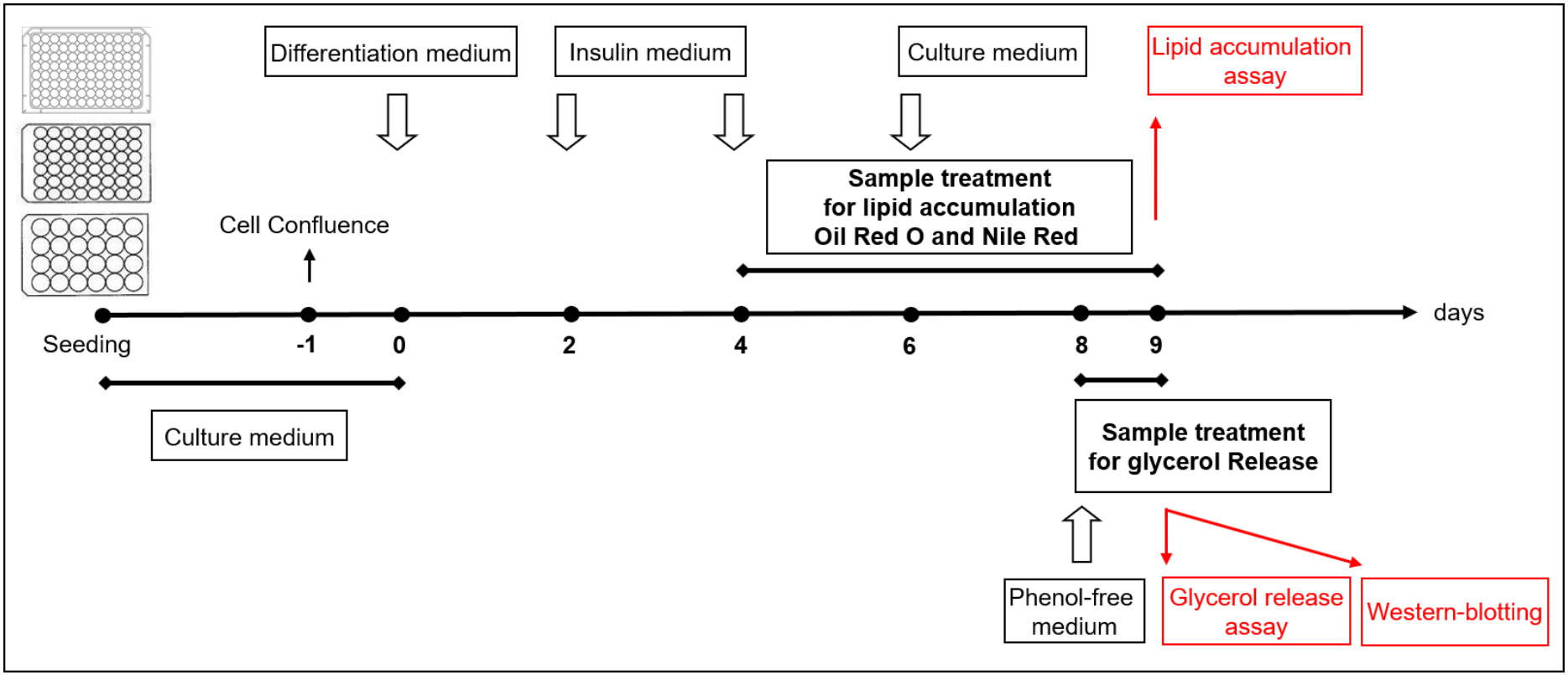

Figure 2.6 Scheme of 3T3-L1 cell culture and sample treatment

2.4.3 Mouse WT-1 Brown Adipocytes

2.4.3.1 Materials

The murine WT-1 pre-adipocytes used in this study were provided from the Tseng Lab. (Joslin Diabetes Center) (Figure 2.7).

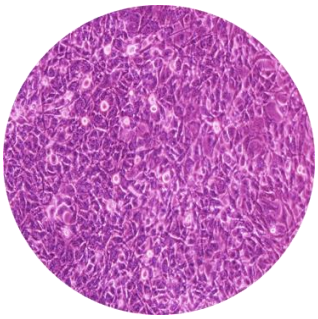

Figure 2.7 WT-1 pre-adipocytes (Magnification 20x)
Credit: Mari Sato, School of Dentistry (Hokkaido University)

Solutions for growing WT-1 cells and their suppliers (Tseng Lab), are listed in Table 2.3.

Table 2.3 Materials for WT-1 cell culture

Material	**Supplier**	**Product Code**
D-MEM (high glucose) with L-Glutamine and Phenol Red	Joslin MediaCore	
Fetal Bovine Serum (FBS)	Gemini	FetalPlex 100-702
PBS pH 7.4	Gibco	10010023
Penicillin-Streptomycin (Pen/Strep) ▪ Stock solution 100x (10,000 units Penicillin, 10 mg Streptomycin) ▪ 1x (100 units Penicillin, 100 μg Streptomycin)	Invitrogen	15140-155
0.25% Trypsin-EDTA	Gibco	25200-056
Insulin, human, recombinant ▪ Stock solution (10 mg/mL) in milliQ water		

3-isobutyl-1-methylxanthine (IBMX) ▪ Stock solution 100x (50 mM) in 0.1 mM KOH	Sigma-Aldrich	I5879
Dexamethasone (DEX) ▪ Stock solution 1000x (2 mg/mL or 5mM) in 2 mL of EtOH	Sigma-Aldrich	D1756
Triiodothyronine (T3) ▪ Stock solution 10000x (10 μM) in milliQ water	Sigma-Aldrich	T-2877
Indomethacin ▪ Stock solution 1000x (0.125 mM) in MeOH	Sigma-Alrich	I7378

2.4.3.2 Reagents and Preparation

The solutions of reagents for cell culture were prepared as described in Table 2.4.

Table 2.4 Reagents and preparation for WT-1 cell culture

Growth medium for pre-adipocytes (10% FBS/D-MEM)	FBS (50 mL) was added into 450 mL of D-MEM (high glucose) supplemented with Pen/Strep (Joslin MediaCore). The culture medium was filter-sterilized through a 500 mL bottle top filter with PES 0.22 μm filter** and then stored in a refrigerator.
Culture medium (2% FBS/D-MEM)	Growth medium 10% FBS/D-MEM (100 mL) was added into 400 mL of D-MEM (high glucose) supplemented with Pen/Strep (Joslin MediaCore). The culture medium was then stored in a refrigerator.
Induction medium (differentiation inducer)	IBMX stock solution (500 μL), DEX stock solution (50 μL), T3 stock solution (5 μL), Indomethacin (50 μL), and insulin stock solution (0.6 μL) was added into 49.5 mL of culture medium (2% FBS/D-MEM). The induction medium was mixed well and stored in a refrigerator. The induction medium was D-MEM supplemented with 2% (v/v) FBS, antibiotics, 0.5 mM IBMX, 5 μM DEX, 1 nM T3, 0.125 mM Indomethacin, and 20 nM insulin.

Differentiation medium (differentiation enhancer)	T3 stock solution (5 μL), and insulin stock solution (0.6 μL) was added into 50 mL of culture medium (2% FBS/D-MEM). The differentiation medium was mixed well and stored in a refrigerator. The differentiation medium was D-MEM supplemented with 2% (v/v) FBS, antibiotics, 1 nM T3, and 20 nM insulin.

Remarks*:*
*CELLTREAT Scientific Products 229717 (Pepperell, MA, USA)

2.4.3.3 Procedure

Figure 2.8 describes the WT-1 cell maintenance that consists of timely medium changes and the application of the sample treatment. Initially, the WT-1 pre-adipocytes were seeded into a 96-well plate and cultured in growth medium at 37°C in a humidified atmosphere of 5% CO_2. To induce adipocyte differentiation, a day after reaching confluence, the cells were cultured in induction medium (day 0). To enhance the differentiation, two days after the induction (day 2), the induction medium was replaced with differentiation medium. The differentiation medium was refreshed every two days (i.e day 4, day 6, day 8). Cells on day 4 were used in lipid accumulation reduction assay. For glycerol release enhancement assay, the cells were further cultured in the differentiation medium for two or more days. The fully differentiated cells (day 7 or day 8) were then ready to be used in the glycerol release enhancement assay.

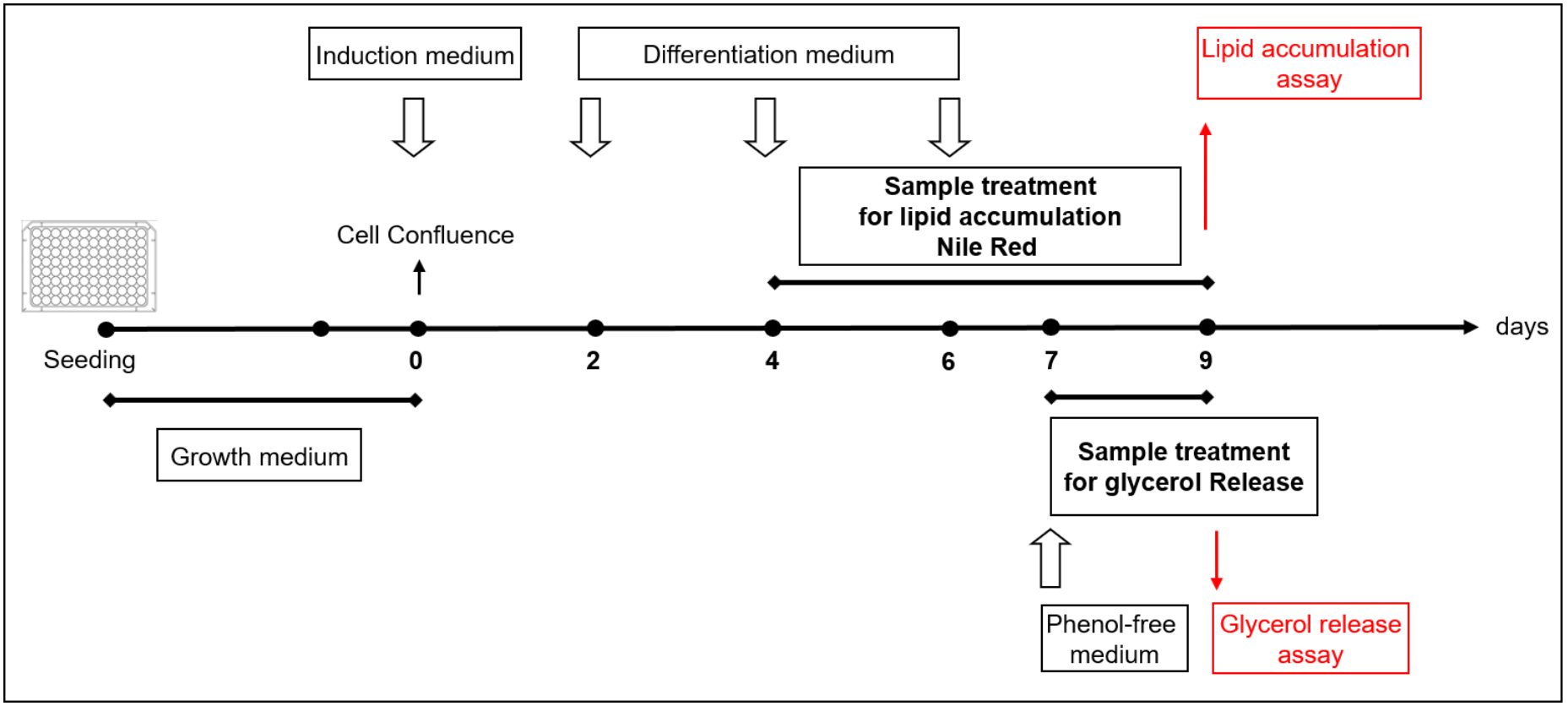

Figure 2.8 Scheme of WT-1 cell culture and sample treatment

2.5 Lipid Accumulation Assay

There were two staining methods to determine intracellular lipid accumulation in adipocytes in this study, namely Oil Red O (ORO) staining and Nile Red staining (AdipoRed). The principle, materials, reagent preparation, procedure and measurement are elaborated in the following sub-sections.

2.5.1 Oil Red O Staining

2.5.1.1 Principle

After the differentiation induction, adipose cells start producing lipid components. The lipid droplets were stained with Oil Red O (ORO), a fat-soluble dye (lysochrome), that is based on the solubility of the dye in the lipoid substances (Figure 2.9).

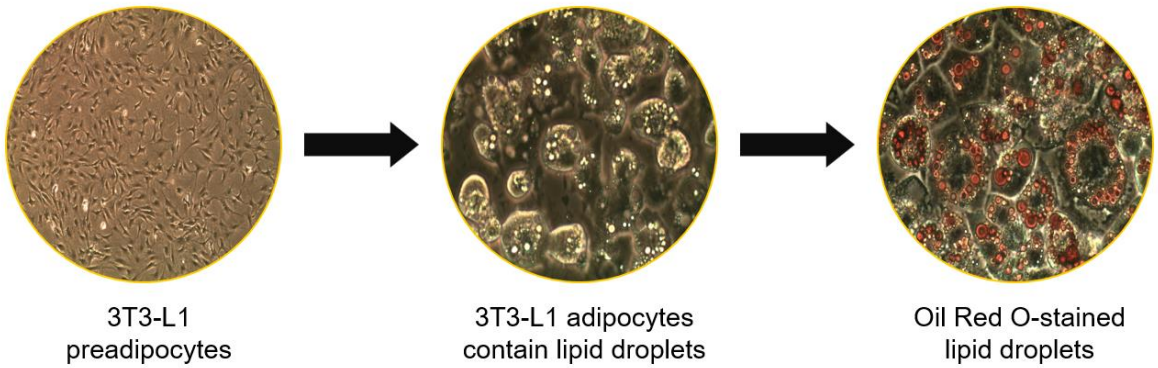

Figure 2.9 Oil Red O staining of lipid droplets of 3T3-L1 as seen under microscope (Magnification 200x)

2.5.1.2 Materials

Oil Red O (Solvent Red 27), 1-(2,5-dimethyl-4-(2-5-dimethylphenyl) phenyldiazenyl) azonapthalen-2-ol, is a lysochrome that is commonly used for dyeing lipid. Reagents used in Oil Red O assay and their suppliers are listed in Table 2.5.

Table 2.5 Materials for ORO staining

Material	Supplier	Product Code
ORO	Sigma-Aldrich	O0625-25G
2-propanol (isopropyl alcohol)	Wako Chem.	166-04836
Formalin in formaldehyde solution 37%	Wako Chem.	064-00406

2.5.1.3 Reagents and Preparation

An ORO stock was prepared as previously described by Kuri-Harcuch and Green (1978) with minor modifications. The ORO stock solution and the working solution were prepared as described in Table 2.6.

Table 2.6 Preparation of ORO solution

ORO solution	To prepare a stock solution, ORO (150 mg) was dissolved in 50 mL of isopropyl alcohol. Ten minutes prior to the staining process, a working solution was prepared by mixing the ORO stock solution with Milli-Q water with a volume ratio of 3:2. The working solution was filtered through an Advantec filter paper no. 101.
10% formalin	The formaldehyde solution was diluted 10 times in PBS buffer.

2.5.1.4 Procedure

Figure 2.10 describes the lipid accumulation assay (Oil Red O) of 3T3-L1 white adipocytes in the absence or presence of tested compounds or plant extracts.

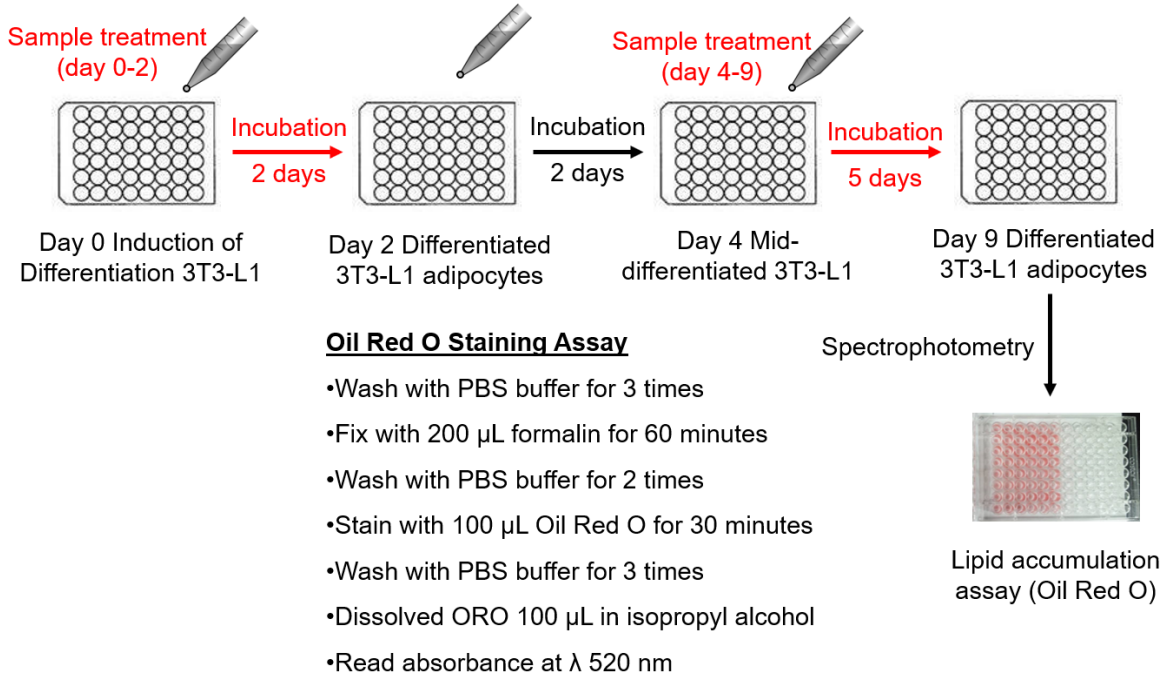

Figure 2.10 Scheme of Oil Red O staining assay

To detect inhibition at the earlier stage of differentiating pre-adipocytes, the tested compounds or plant extracts were added on day 0 for 2 days (day 0-2). Meanwhile, the tested compounds or plant extracts were added on day 4 for 5 days (day 4-9) to observe inhibition of lipid droplet accumulation at the latter stage.

The Oil Red O staining was performed on day 9 to detect the accumulated lipid droplets. First, the cells were washed twice with PBS buffer and fixed with 200 µL of 10% (v/v) formalin for 1 hour at room temperature. The cells were then washed twice with PBS buffer and subsequently stained with 100 µL of ORO solution (0.36% ORO in 60% (v/v) isopropyl alcohol) for another 30 minutes. To remove the excess of the ORO solution, the cells were washed three times with PBS buffer. For visualization, the stained lipid droplets were photographed using an Olympus CKX41 microscope (Tokyo, Japan) (Figure 2.11).

Figure 2.11 Olympus CKX41 microscope
(Tokyo, Japan)

For quantitative analysis, the ORO stained-lipid droplets were dissolved with 100 µL of isopropyl alcohol and remained for 30 minutes prior to transferring into a 96-clear well plate (Figure 2.12).

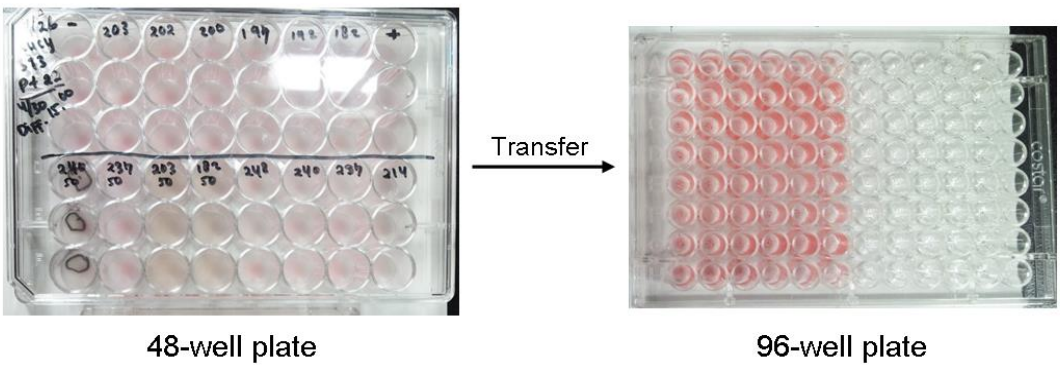

Figure 2.12 ORO staining assay in well plates

The optical density (OD) was measured at a wavelength of 520 nm using a Synergy™ MX spectrophotometer (Bio-tech Instruments Inc., Winooski, USA) (Figure 2.13). The accumulated lipids of control cells were set as 100% and the lipid contents from the treated

cells were calculated relative to the non-treatment value. Each compound or plant extract was tested in triplicate and the sample was tested in six wells. Three independent experiments were performed to confirm reproducibility and the representative result is selected for the figures.

Figure 2.13 Synergy™ MX microplate reader
(Bio-tech Instruments Inc., Winooski, USA)

2.5.2 Nile Red Staining

2.5.2.1 Principle

Nile Red (9-diethylamino-5H-benzo[alpha]phenoxazine-5-one) is a dye for the detection of intracellular lipid droplets by fluorescence microscopy and flow cytofluorometry. It is strongly fluorescent when partitioned in a hydrophobic environment (Figure 2.14).

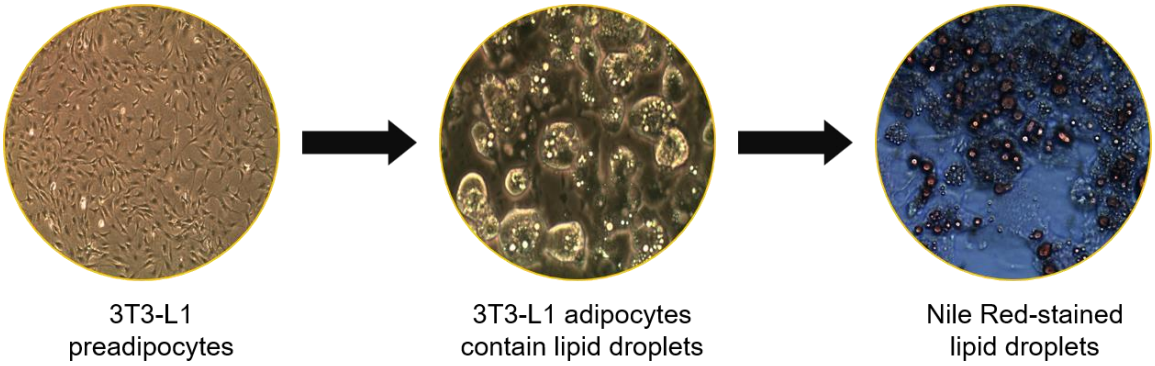

Figure 2.14 Nile Red staining of lipid droplets of 3T3-L1 as seen under microscope (Magnification 200x)

2.5.2.2 Materials

AdipoRed™ Assay Reagent PT-7009 (Lonza Walkersville, MD, USA) is used for Nile Red staining.

2.5.2.3 Reagents and Preparation

Following the manual instructions, volume of the Reagent and PBS buffer is optimized as stated in Table 2.7.

Table 2.7 Volume of AdipoRed™ Assay Reagent

Well-plate used	Wash volume/well	Final volume of PBS/well	Volume of AdipoRed/well
6-well plate	2 mL	5 mL	140 µL
12-well plate	1 mL	2 mL	60 µL
24-well plate	1 mL	1 mL	30 µL
48-well plate	0.4 mL	0.4 mL	12 µL
96-well plate	0.2 mL	0.2 mL	5 µL

2.5.2.4 Procedure

Figure 2.15 describes the lipid accumulation assay (Nile Red AdipoRed) of WT-1 brown adipocytes in the absence or presence of tested compounds or plant extracts.

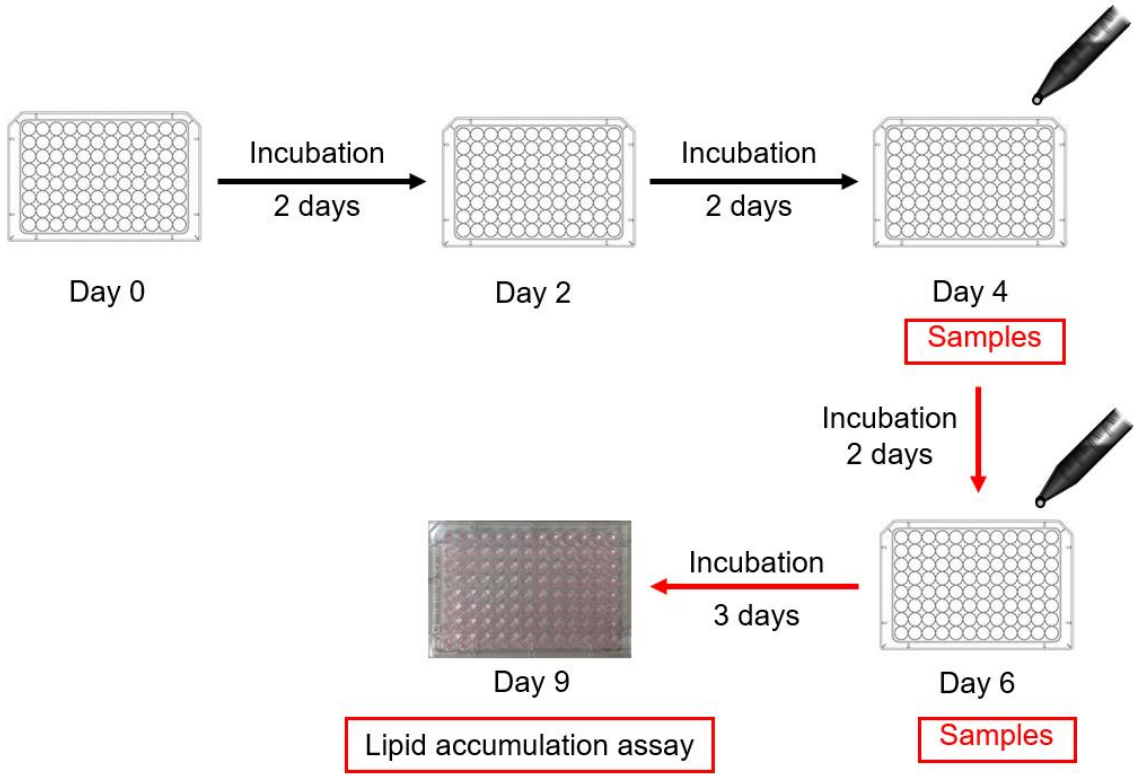

AdipoRed™ Assay Reagent

- Wash cells with 200 µL PBS buffer
- Add 200 µL PBS buffer
- Add 5 µL reagent, shake immediately
- Sit for 10 min
- Read fluorescence at E_x 485 nm E_m 572 nm

Figure 2.15 Scheme of Nile Red staining assay

Tested compounds were added to WT-1 cells on day 4 after differentiation induction, and were refreshed on day 6. Nile Red staining was performed on the fully differentiated brown adipocytes (day 9) to quantify the accumulated lipid droplets. For 96-well plate, the cells were once washed with 200 µL PBS buffer and the same amount of PBS buffer was added to each well. Setting the 96-well plate on a rapid shaker, an exact 5 µL AdipoRed™

Reagent was added to each well using a multichannel pipette (Figure 2.16). The shaker was switch-on immediately upon addition of the Reagent to each row of wells. After sitting for 10 minutes in room temperature, the 96-well plate was placed in the fluorometer.

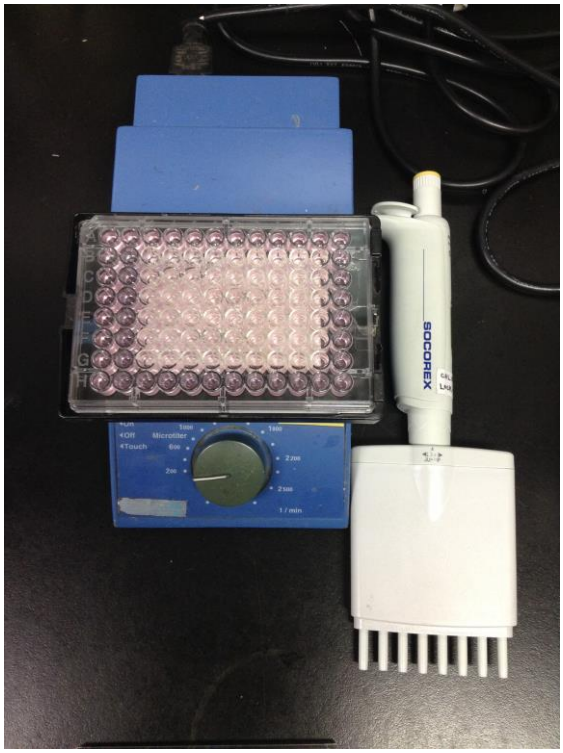

Figure 2.16 Shaker and multichannel pipette for Nile Red staining

Fluorescence excitation and emission wavelengths were measured at wavelengths of, 485 nm and 572 nm, respectively, using a Synergy™ MX microplate reader (Bio-tech Instruments Inc., Winooski, USA) (Figure 2.12). While conducting research at the Tseng Lab (Joslin Diabetes Center, Boston, MA, USA), fluorescence excitation and emission wavelengths were measured at 475 nm and 580-640 nm, respectively. The fluorescence value relative to that of the control was then calculated (Figure 2.17).

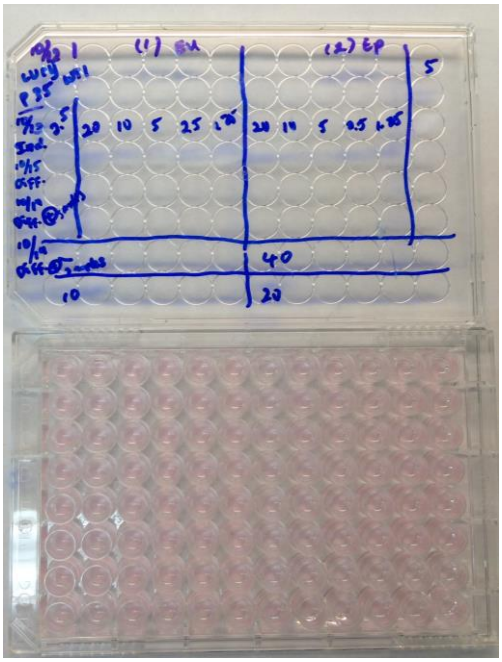

Figure 2.17 Nile Red staining assay in a 96-well plate

2.6 Cell Viability Assay

2.6.1 Principle

Cell Counting Kit (CCK)-8 kit solution contains water-soluble tetrazolium salt WST-8(2-(2-methoxy-4-nitrophenyl)-3-(4-nitrophenyl)-5-(2,4-disulfophenyl)-2H-tetrazolium, monosodium salt) to measure the NADH produced by the dehydrogenase activity of viable cells (Ishiyama et al., 1997). The orange-colored formazan product, which results from the reduction of the WST-8, directly corresponds to the number of living cells (Figure 2.18).

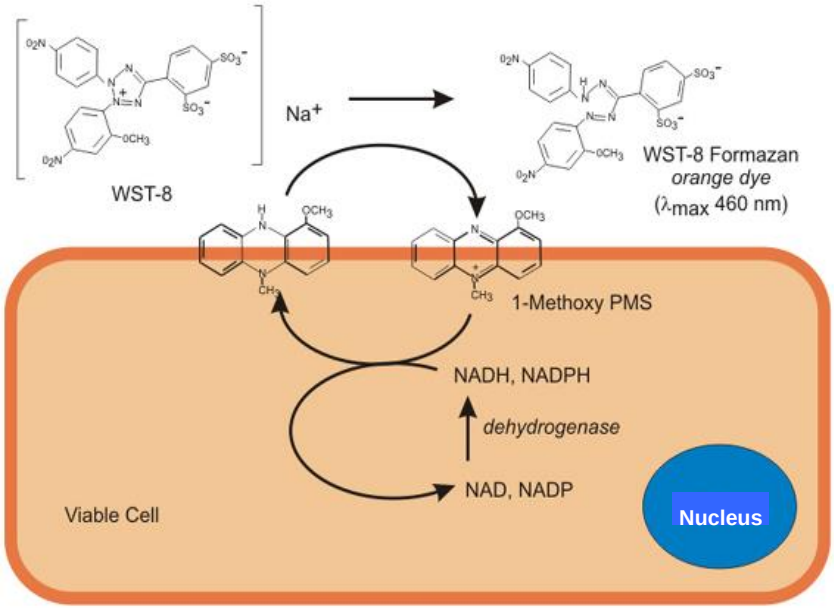

Figure 2.18 Reaction of WST-8 in cytotoxicity assay
(Dojindo, 2014)

2.6.2 Materials

The cell viability was tested using the CCK-8 supplied by Dojindo Molecular Laboratories Inc., no. 343-07623 (Kumamoto, Japan).

2.6.3 Procedure

The 3T3-L1 pre-adipocytes were seeded in 96-well plates and incubated for 24 hours. From the author's previous study, optimal incubation time with the tested compounds or plant extracts was set to 24 hours, because no cell death was seen after 6 and 12 hour incubation, meanwhile no significant change in cell death occurred from 24 hours to 48 hours.

Cell viability assay was conducted in two phases of adipocyte growth; pre-adipocytes and differentiated adipocytes. For pre-adipocytes, undifferentiated 3T3-L1 cells were seeded in 96-well plates at a density of 5×10^3 cells per well and incubated for 24 hours. The cells were incubated with the tested compounds or plant extracts for another 24 hours. For differentiated adipocytes, cells were maintained and differentiation was induced as described in Figure 2.5; and the tested compounds or plant extracts were added on day 4 for 24 hours. Both 0.1% DMSO and 1% Triton X-100 served as the negative control and cytotoxic

reference, respectively. After treatment of the samples for 24 hours, 10 µL of CCK-8 solution was added to each well, and the 96-well plate was incubated at 37°C for an additional 3 hours (Figure 2.19).

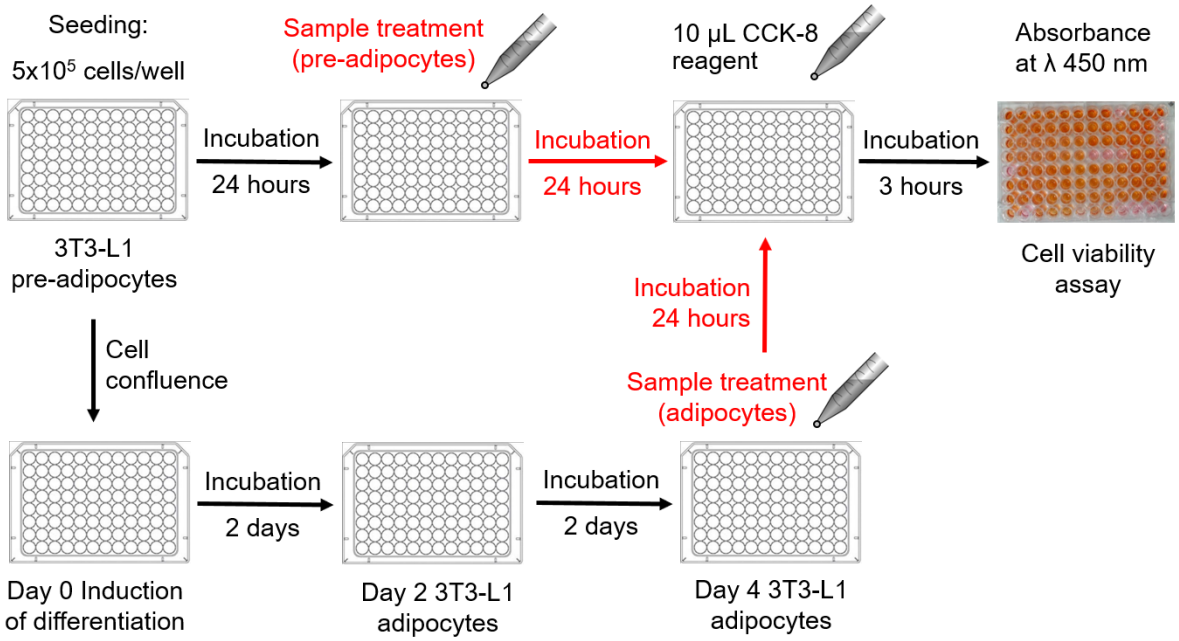

Figure 2.19 Scheme of CCK-8 cell viability assay

The optical density (OD) was measured at 450 nm of wavelength using a Synergy™ MX microplate reader. Each experiment was done in triplicate. The cell viability (% of control) was calculated using the following formula:

$$\% \text{ cell viability} = [OD]_{test}/[OD]_{control} \times 100 \quad (2.1)$$

where $[OD]_{test}$ is the absorbance of the tested extracts, while $[OD]_{control}$ represents the absorbance of the negative control.

2.7 Lipolysis Assay

2.7.1 Principle

Lipolysis in adipocytes is a breakdown of lipids, and it involves hydrolysis of triglyceride (TG) to release fatty acids (FAs) and glycerol. Free Glycerol Reagent F6428 (Sigma-Aldrich, Saint Louis, MO, USA) was used to quantify glycerol released to the culture

medium. The Free Glycerol Reagent measures the glycerol by coupled enzymatic reactions (Figure 2.20).

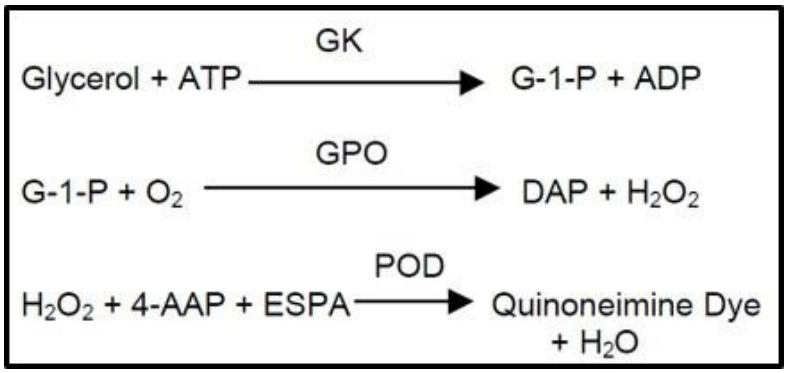

Figure 2.20 Glycerol assay enzymatic reactions
(Sigma-Aldrich, 2015)

Glycerol is phosphorylated by adenosine-5'-triphosphate (ATP) forming glycerol-1-phosphate (G-1-P) and adenosine-5'-diphosphate (ADP) in the reaction catalyzed by glycerol kinase (GK). G-1-P is then oxidized by glycerol phosphate oxidase (GPO) to dihydroxyacetone phosphate (DAP) and hydrogen peroxide (H_2O_2). Peroxidase (POD) catalyzes the coupling of H_2O_2 with 4-aminoantipyrine (4-AAP) and sodium *N*-ethyl-*N*-(3-sulfopropyl) *m*-anisidine (ESPA) to produce a quinoneimine dye that shows an absorbance maximum at 540 nm. The increase in absorbance at 540 nm is directly proportional to the free glycerol concentration of the sample.

2.7.2 Materials

Reagent, inhibitors, activators and medium used in lipolysis assay and their suppliers are listed in Table 2.8.

Table 2.8 Materials for lipolysis assay

Material	**Supplier**	**Product Code**
Free Glycerol Reagent	Sigma-Aldrich	F6428
D-MEM (high glucose) Phenol Red Free	Wako Chem.	040-30095
Isoproterenol	Sigma-Aldrich	I6504

Propranolol	Wako Chem.	167-11593
8-Br-cAMP	Nacalai Tesque, Inc.	05450-02
H-89	Apollo Scientific	BIH127
Ceramide C6	Cayman Chemical Co.	62525
PD 98059	Tokyo Chemical Industry Co.	A2529
Anisomycin	Tokyo Chemical Industry Co.	A2613
SP 600125	Tokyo Chemical Industry Co.	A2548
SB 203580	Apollo Scientific	BIS0733

2.7.3 Reagents and Preparation

Prior to usage, the Free Glycerol Reagent needs to be reconstituted with 40 ml of ultrapure deionized water. After addition of the water, the reagent was immediately mix several times by inversion. The reconstituted Free Glycerol Reagent was stored in an amber bottle to protect from light, and it was stable for 60 days when stored at 2–8 °C.

A series of glycerol solutions was used as the standard to determine a calibration curve (Table 2.9).

Table 2.9 Preparation of glycerol solution for calibration curve

Glycerol solution	Glycerol (1 mg) was dissolved in 1 mL of Milli-Q water to reach 1 mg/mL glycerol of stock solution. A series of 0, 3.125, 6.25, 12.5, 25, 50, 100, 200 μg/mL glycerol standard solutions.

Prior to the measurement of glycerol release, the glycerol standard solutions were reacted with the Free Glycerol Reagent and their absorbance data were recorded to determine a calibration curve. A representative calibration curve is presented in **Appendix 1** and **2**.

2.7.4 Procedure

2.7.4.1 Glycerol Release Enhancement Assay

Following the scheme of cell culture, medium was changed to sample-containing medium (D-MEM Phenol Red Free) on day 7 (for WT-1 brown adipocytes) or day 8 (for 3T3-L1 white adipocytes) when the adipocytes reached maturity (Figure 2.21). Isoproterenol (1 μM), a β-adrenoreceptor agonist that enhances lipolysis, was used as positive control.

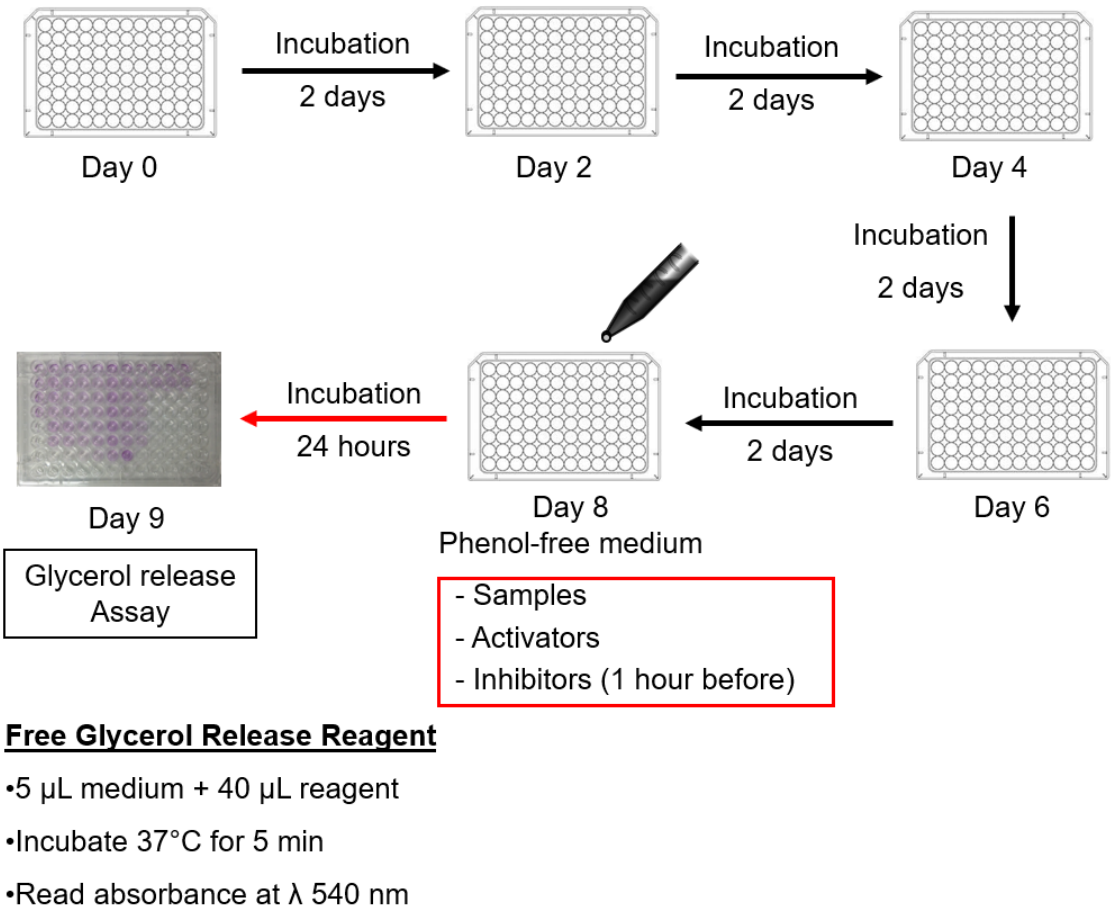

Figure 2.21 Scheme of glycerol release enhancement assay

On day 9, after sample incubation for 24 hours (for 3T3-L1 white adipocytes) or 48 hours (for WT-1 brown adipocytes), 5 μL medium supernatants were collected and mixed with 80 μL Free Glycerol Reagent. The mixture was incubated for 5 min at 37 °C and absorbance at 540 nm was measured to calculate the released glycerol. While conducting research at the Tseng Lab (Joslin Diabetes Center, Boston, MA, USA), the absorbance was

measured at 560 nm. The glycerol release (% of control) was calculated using the following formula:

$$\%\ \text{glycerol release} = ([OD]_{sample}-[OD]_{blank})/([OD]_{control}-[OD]_{blank}) \times 100 \quad (2.2)$$

where $[OD]_{sample}$ is the absorbance of the tested sample, $[OD]_{blank}$ is the absorbance of water, while $[OD]_{control}$ represents the absorbance of the control.

2.7.4.2 Inhibitory Challenges on Glycerol Release

For inhibitory challenges, 3T3-L1 mature adipocytes on day 8 were pre-incubated with inhibitors for 1 hour prior to sample treatments (Figure 2.21). Activators for each respective pathway were used as the positive control. After incubation for 24 hours, medium supernatants were collected and the amount of glycerol released into the medium was measured using a Free Glycerol Reagent, as described in the previous §2.7.4.1.

There were four specific inhibitors (for plant extracts) and five specific inhibitors (for tested compounds) used in these inhibitory challenges (Figure 2.22).

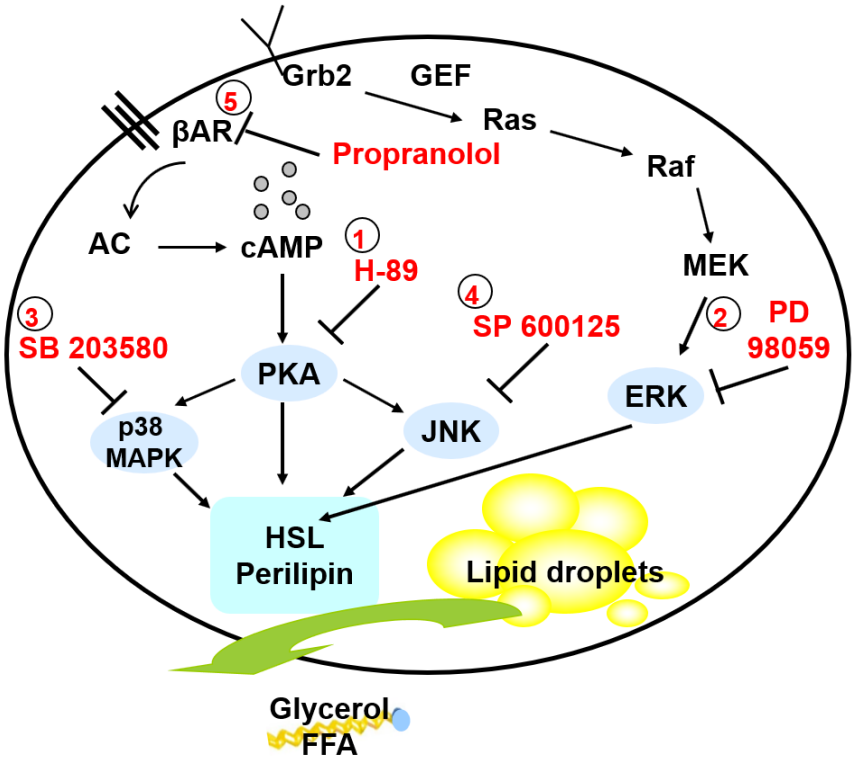

Figure 2.22 Inhibitory challenges on glycerol release in 3T3-L1 adipocytes

Inhibitors and activators for each respective pathway are listed in Table 2.10.

Table 2.10 Inhibitors and activators used for inhibitory challenges on glycerol release

Target protein	Inhibitor	Activator
1. PKA	H-89 (20 µM)	8-Br-cAMP (100 µM)
2. ERK	PD 98059 (50 µM)	Ceramide C6 (20 µg/mL)
3. p38 MAPK	SB 203580 (20 µM)	Anisomycin (25 µg/mL)
4. JNK	SP 600125 (50 µM)	
5. β-adrenoreceptor	Propranolol (1 µM)	Isoproterenol (1 µM)

2.8 Protein Immunoanalysis

2.8.1 Principle

Protein immunoanalysis was performed using Western-blot, a widely used analytical technique to detect specific proteins in a sample of tissue homogenate or cell lysate. In this study; PKA, ERK 1/2 and their phosphorylated forms were analyzed, while β-actin was used as loading control.

As the procedure consisted of several steps, including protein extraction followed by determination of protein concentration, protein denaturation and protein separation (gel electrophoresis), electroblotting, protein detection and visualization, the following sub-sections described materials, preparation, and procedure for the protein immunoanalysis.

2.8.2 Materials

Various chemicals and antibodies used in the protein immunoanalysis and their suppliers are listed in Table 2.11 and Table 2.12.

Table 2.11 Materials for protein extraction

Material	Supplier	Product Code
Protein Extraction (lysis buffer)		
Triethanolamine hydrochloride (Tris-HCl	Kanto Chem.	146-07271
NaCl	Wako Chem.	191-01665
EDTA.2Na	Dojindo	345-01865
NaF		
Sodium orthovanadate (Na_3VO_4)	Wako Chem.	168-09752
PMSF	Wako Chem.	164-12181
Sodium pyrophosphate	Alfa Aesar	A17546
2-propanol	Wako Chem.	166-04836
Protease inhibitor cocktail (cOmplete, Mini)	Roche	118361530001
Triton X-100	Wako Chem.	169-21105
Quick Start Bradford 1X Dye Reagent	Bio-Rad Lab. Inc.	500-0205

Table 2.12 Materials for Western-blotting

Material	Supplier	Product Code
Protein separation (SDS-PAGE)		
Mini-Protean®	Bio-Rad Lab. Inc.	
PowerPac™ Basic Power Supply	Bio-Rad Lab. Inc.	
Acrylamide	Wako Chem.	016-00765

N, N'-methylene-bis (Acrylamide)	Wako Chem.	138-06032
Sodium dodecyl sulfate (SDS)	Wako Chem.	192-14042
Ammonium persulfate (APS)	Sigma-Aldrich	A3678
Precision Plus Protein™ Dual Color Standards	Bio-Rad Lab. Inc.	1610374
Electroblotting and Protein Detection		
Transblot® SD Semi-dry Transfer Cell	Bio-Rad Lab. Inc.	
LumiVision PRO 400EX	Aisin Seiki Co.	
Amersham Protran 0.2 µM Nitrocellulose membrane	GE Healthcare	10600104
Glycine	Kanto Chem.	01194-00
Tris (2-amino-2-hydroxymethyl-1,3-propanediol)	Kanto Chem.	40326-00
Tween-20 (Polyoxyethylene (20) sorbitan monolaurate)	Wako Chem.	166-21213
Albumin, from Bovine Serum, Cohn Fraction V, pH 7.0	Wako Chem.	019-23293
Rabbit PKA C-α antibody	Cell Signaling Technology Inc	#4782
phospho-PKA C (Thr197) antibody		#4781
ERK 1/2 antibody		#4695
phospho-ERK 1/2 (Thr202/Tyr204) antibody		#4370
β-actin antibody		#4967
anti-rabbit IgG HRP-linked antibody		#7074
ImmunoStar® LD	Wako Chem.	292-6990

2.8.3 Reagents and Preparation

Formula of lysis buffer and Laemmli sample buffer is described in Table 2.13.

Table 2.13 Preparation of lysis buffer and Laemmli sample buffer

Lysis buffer stock solution	
Tris-HCl pH 7.5 stock solution (2 M)	To prepare 2 M stock solution, 2.42 g Tris-HCl was initially dissolved in 7 mL of Milli-Q water. The pH of the buffer solution was adjusted to 7.5 by adding 6 M HCl. The total volume of Tris-HCl buffer was then adjusted to 10 mL with Milli-Q water.
NaCl stock solution (5 M)	To prepare a stock solution of 5 M NaCl, 2.922 g NaCl was dissolved in 10 mL of Milli-Q water.
EDTA stock solution (0.2 M)	To prepare a stock solution of 0.2 M EDTA, 0.744 g EDTA.2Na was initially dissolved in 7 mL of Milli-Q water. The pH of the solution was adjusted to 8.0 by adding 0.5 M NaOH. The total volume of EDTA solution was then adjusted to 10 mL with Milli-Q water.
NaF stock solution (100 mM)	To prepare a stock solution of 100 mM NaF, 6.29 mg NaF was dissolved in 1.5 mL of Milli-Q water. The NaF stock solution was then stored in a freezer (-20ºC).
Na_3VO_4 stock solution (100 mM)	To prepare a stock solution of 100 mM Na_3VO_4, 27.5 g Na_3VO_4 was initially dissolved in 1 mL of Milli-Q water. The pH of the solution was adjusted to 9.0 by adding 1 M HCl. The total volume of Na_3VO_4 solution was then adjusted to 1.5 mL with Milli-Q water. The Na_3VO_4 stock solution was then stored in a freezer (-20ºC).
PMSF stock solution (100 mM)	To prepare a stock solution of 100 mM PMSF, 26.1 g PMSF was dissolved in 1.5 mL of 2-propanol. The PMSF stock solution was then stored in a freezer (-20ºC).
Sodium pyrophosphate stock solution (100 mM)	To prepare a stock solution of 100 mM Sodium pyrophosphate, 39.8 mg Sodium pyrophosphate was dissolved in 1.5 mL of Milli-Q water. The Sodium pyrophosphate stock solution was then stored in a freezer (-20ºC).

Lysis buffer	To prepare 10 mL of lysis buffer, 2 M Tris-HCl (250 µL), 5 M NaCl (300 µL), 0.2 M EDTA (50 µL), 100 mM NaF (400 µL), 100 mM Na_3VO_4 (100 µL), 100 mM PMSF (100 µL), 100 mM Sodium pyrophosphate (250 µL), and 150 µL Triton X-100 were added to Milli-Q water up to 10 mL. A tablet of protease inhibitor cocktail (cOmplete, Mini) was added to the solution and mixed well by inversion. The lysis buffer was then stored in a refrigerator and used within 10 days. The lysis buffer contained 50 mM Tris-HCl, 150 mM NaCl, 2 mM EDTA, 4 mM NaF, 1 mM Na_3VO_4, 1 mM PMSF, 2.5 mM Sodium pyrophosphate, and 1.5% Triton X-100 in water solution.
X2 Laemmli sample buffer (10 mL)	
4% SDS	0.4 g
20% glycerol	2 mL
0.004% bromophenol blue	0.4 mg
0.125 M Tris-HCI	2.5 mL of 0.5 M Tris-HCl
10% 2-mercaptoethanol	Change to 0.5 M Dithiothreitol (DTT)
Milli-Q water	Up to 10 mL

Gel matrix for SDS-PAGE (12.5 % polyacrylamide gel) was prepared as described in Table 2.14.

Table 2.14 Preparation of polyacrylamide gel

		Running gel 'R'	**Stacking gel 'S'**
30% Acrylamide	To prepare 30% Acrylamide, 29.2 g Acrylamide and 0.8 g Bis-acrylamide were dissolved in 100 mL Milli-Q water.	5 mL	1.6 mL

1.5 M Tris-HCl, pH 8.8	To prepare 1.5 M Tris-HCl, 36.4 g Tris was initially dissolved in 150 mL Milli-Q water. The pH of the solution was adjusted to 8.8 by adding 6 M HCl. The total volume of the solution was then adjusted to 200 mL with Milli-Q water.	3 mL	-
0.5 M Tris-HCl, pH 6.8	To prepare 0.5 M Tris-HCl, 6.05 g Tris was initially dissolved in 70 mL Milli-Q water. The pH of the solution was adjusted to 6.8 by adding 6 M HCl. The total volume of the solution was then adjusted to 100 mL with Milli-Q water.	-	3 mL
10% SDS	To prepare 10% SDS, 1 g SDS was dissolved in 10 mL Milli-Q water.	120 µL	120 µL
10% APS	To prepare 10% APS, 0.1 g APS was dissolved in 1 mL Milli-Q water.	60 µL	60 µL
Milli-Q water		3.82 mL	7.22 mL
Tetramethylethylenediamine (TEMED) Added before use		8.5 µL	8.5 µL

To prepare the polyacrylamide gel, running gel mixture (R) and stacking gel mixture (S) were degas using a vacuum pump for 15 min. Tetramethylethylenediamine (TEMED) 8.5 µL was added into R mixture and quickly mixed without creating any bubbles. The R mixture was then loaded into gel cassette (up to 7-8 mm below the comb-end). Water may be added to avoid dryness during the the formation of R gel. After the R gel was formed (30-40 min), the water was then removed.

For preparing S gel, 8.5 µL TEMED was added into S mixture and quickly mixed without creating any bubbles. The S mixture was then loaded into gel cassette (up to the top-end), and the comb was inserted to the gel cassette. Laying the gel cassette in a horizontal position, the 12.5 % polyacrylamide gel was ready to be used in another 30-40 min.

Running buffer for the gel electrophoresis was prepared as described in Table 2.15.

Table 2.15 Running buffer for gel electrophoresis

X10 Running buffer (Tris glycine SDS buffer)	
Glycine (1,920 mM)	144.0 g
Tris (250 mM)	30.3 g
SDS (1%)	10.0 g
Milli-Q water	Up to 1 L

The CBB solution and CBB de-staining solution were prepared as described in Table 2.16.

Table 2.16 CBB staining solutions

CBB solution	
CBB R-250 (0.25%)	0.5 g
Ethanol (EtOH) 5%	10.0 g
Acetic acid (AcOH) 7.5%	15.0 g
Milli-Q water	200 mL
CBB de-staining solution	
EtOH	100 mL
AcOH	30 mL
Milli-Q water	400 mL

There are several buffers used in electro-transfer and antibody solutions in Western-blotting, the preparation for the buffers are described in Table 2.17.

Table 2.17 Preparation for Western-blotting buffer

Transfer buffer	
Glycine (192 mM)	14.4 g
Tris (25 mM)	3.0 g
Milli-Q water	800 mL
Methanol (20%)	200 mL
X10 TBS buffer	
Tris (200 mM)	24.23 g
NaCl (1,370 mM)	80.06 g
Milli-Q water	800 mL, and add up to 1 L after 1 M HCl
1 M HCl	Adjust to pH 7.6
TBS-T	
X10 TBS	50 mL
Tween-20 (0.1%)	500 μL
Milli-Q water	450 mL

2.8.4 Procedure

Figure 2.23 describes the 3T3-L1 cell culture and sample treatment prior to western blot assay that consists of protein extraction, determination of protein concentration, protein denaturation and protein separation (gel electrophoresis), electroblotting, protein detection and visualization.

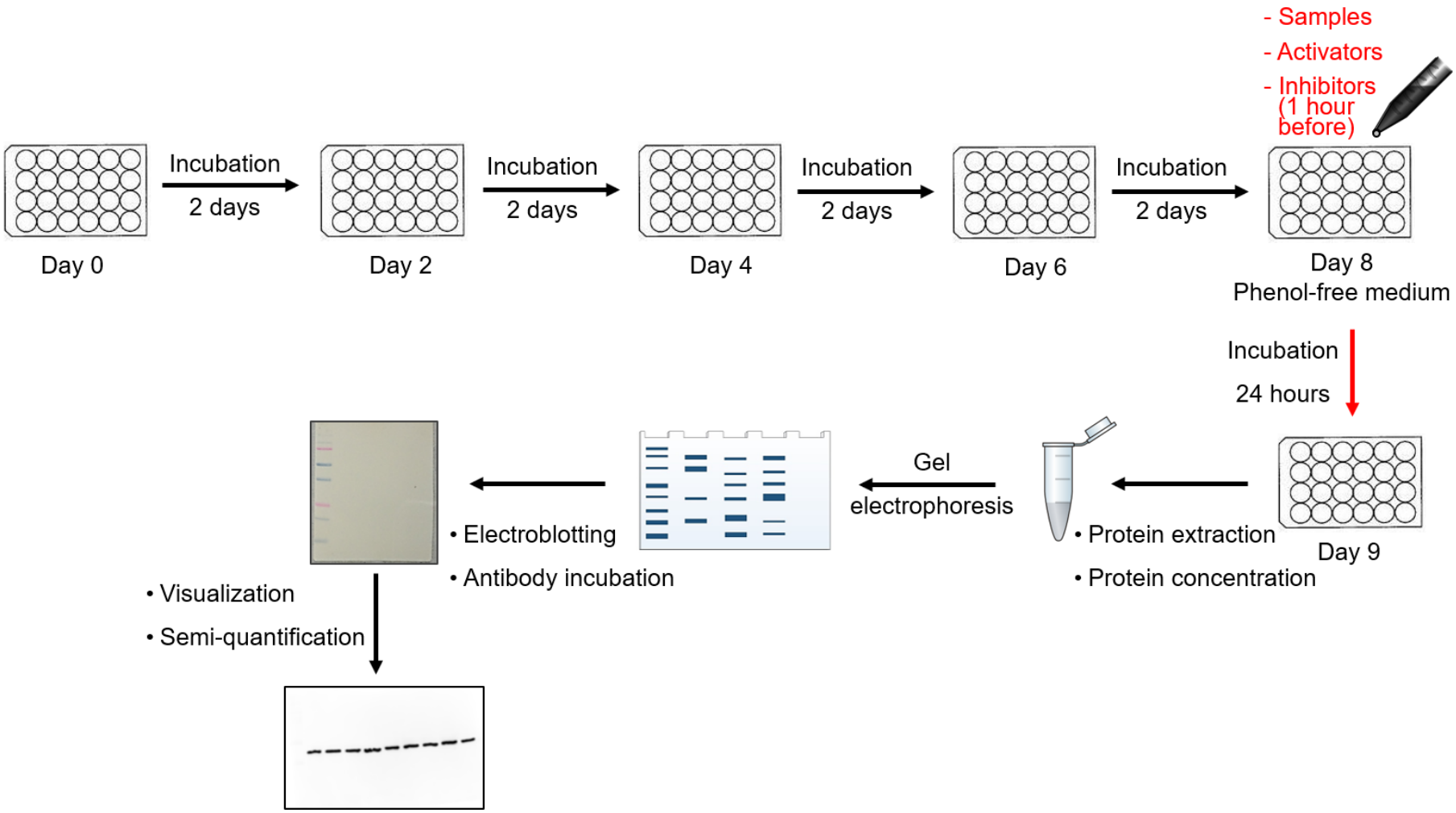

Figure 2.23 Scheme of cell culture and sample treatment prior to western blot assay

2.8.4.1 Protein Extraction

3T3-L1 adipocytes were cultured in 24-well plates and treated accordingly as shown in Figure 2.23. Mature adipocytes were washed twice with ice-cold PBS buffer and lysed in ice-cold lysis buffer (Table 2.13) on ice. The cell homogenate was centrifuged at 14,000 × g for 10 min at 4°C. The supernatant was collected, and the protein concentration was determined by Bradford assay as described in the following sub-section.

2.8.4.2 Determination of Protein Concentration

Protein concentration was determined by Bradford assay using a Quick Start Dye Reagent (Bio-Rad Laboratories, Inc., Hercules, CA, USA). The absorbance was detected at a wavelength of 595 nm. Bovine serum albumin (BSA) was used as the protein standard. The BSA standard solutions were reacted with the Quick Start Dye Reagent, and their absorbance data were recorded to determine a calibration curve. A representative calibration curve is presented in **Appendix 3.** Once the concentration of each protein sample has been determined, the protein samples can be freezed and stored at -20°C or -80°C for later use, or it can be prepared for loading onto a gel.

2.8.4.3 Protein Denaturation and Protein Separation (Gel Electrophoresis)

Extracted proteins were then denatured by heating at 95°C for 5 min in a Laemmli sample buffer supplemented with 0.05 M DTT (Table 2.13). Different amounts of proteins 5, 10, and 15 μg were separated using a 12.5% polyacrylamide gel. Gel electrophoresis was run using Mini-Protean® and PowerPac™ Basic Power Supply at 15 Volts (Figure 2.24) with appropriate amount of running buffer (Table 2.15).

Figure 2.24 Mini-Protean® and PowerPac™ Basic Power Supply

2.8.4.4 CBB Staining

Upon SDS-PAGE, the gel was stained in CBB solution (Table 2.16) for 30-40 min on a shaker, and then de-stained with CBB de-staining solution for 10-20 min and the CBB de-staining solution was refreshed for several times. The results of the CBB staining and de-staining are shown in Figure 2.25.

A. 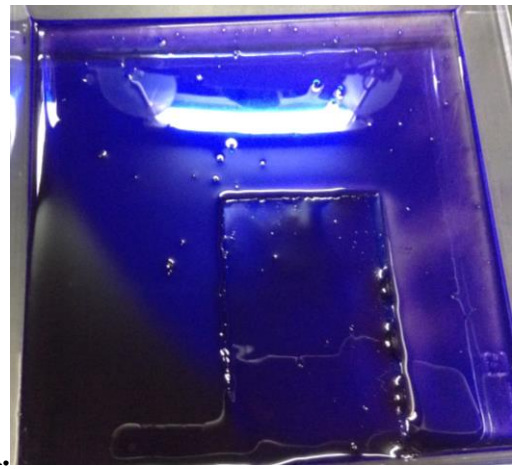 **B.** 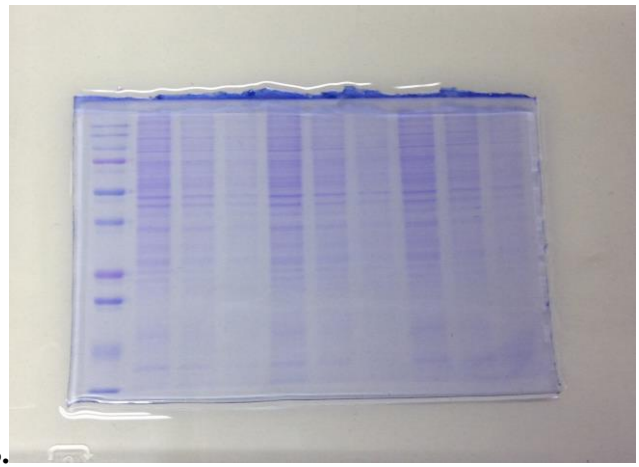

Figure 2.25 CBB staining A) and CBB de-staining B)

The SDS-PAGE successfully separated the proteins in the samples, and as little as 5 μg protein samples was sufficient to be separated by the gel electrophoresis (Figure 2.25). Therefore, 5 μg for total protein and 10 μg for phosphorylated protein would be loaded into acrylamide gel.

2.8.4.5 Electroblotting, Protein Detection and Visualization

The proteins within the acrylamide gel were transferred onto a PVDF or nitrocellulose membrane using a Transblot® SD Semi-dry Transfer Cell at 15 Volts for 15 minutes. The membrane was placed below the gel, and a stack of blotting papers were placed on top of the gel (3 blotting papers) and below the membrane (3 blotting papers). The gel, membrane and blotting papers was soaked in an appropriate amount of transfer buffer (Table 2.17) for 30 min before running the semi-dry electroblotting (Figure 2.26).

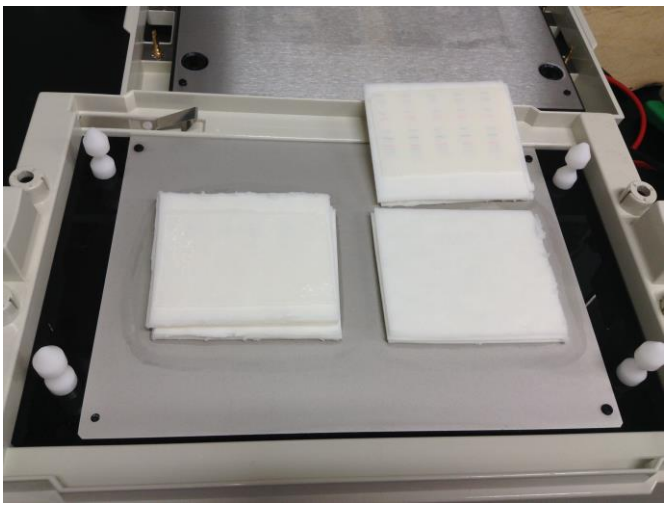

Figure 2.26 Electroblotting using a Transblot® SD Semi-dry Transfer Cell

Nitrocellulose membrane was chosen based on the results of electroblotting shown in Figure 2.27, in which nitrocellulose membrane gave more clear protein bands than PVDF membrane did.

A. 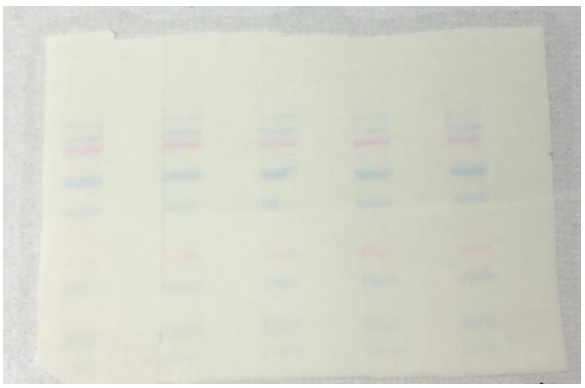 **B.** 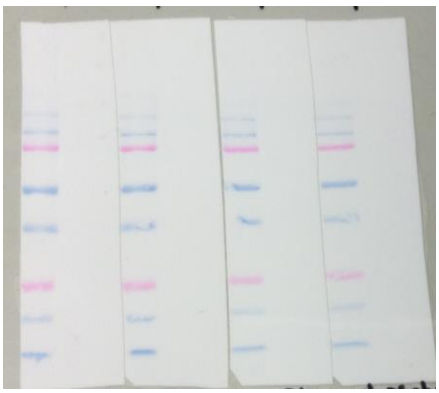

Figure 2.27 Electroblotting to PVDF membrane A) and nitrocellulose membrane B)

Blocking of non-specific binding is achieved by placing the membrane in a 5% BSA in TBS-T solution (Table 2.17) (blocking solution) for 1 hour at room temperature. After blocking, to detect the protein, the membrane is probed for the target protein. The list of primary antibodies and secondary antibody is presented in Table 2.12. β-actin was used as the internal loading control to validate equal loading in each lane.

Incubation with primary antibody was performed after washing the membrane 3 times with TBS-T for 5 min each time. The membrane was then incubated overnight at 4°C with primary antibody in BSA/TBS-T (1:1000) under gentle agitation. Primary antibody incubation was followed with washing the membranes 3 times with TBS-T for 5 min each time, to minimize background and remove unbound antibody.

After washing the membrane to remove unbound primary antibody, the membrane was exposed to secondary antibody. For secondary antibody, the membrane was incubated for 1 hour at room temperature with horseradish peroxidase-conjugated antibody (1:2000) under gentle agitation (Figure 2.28).

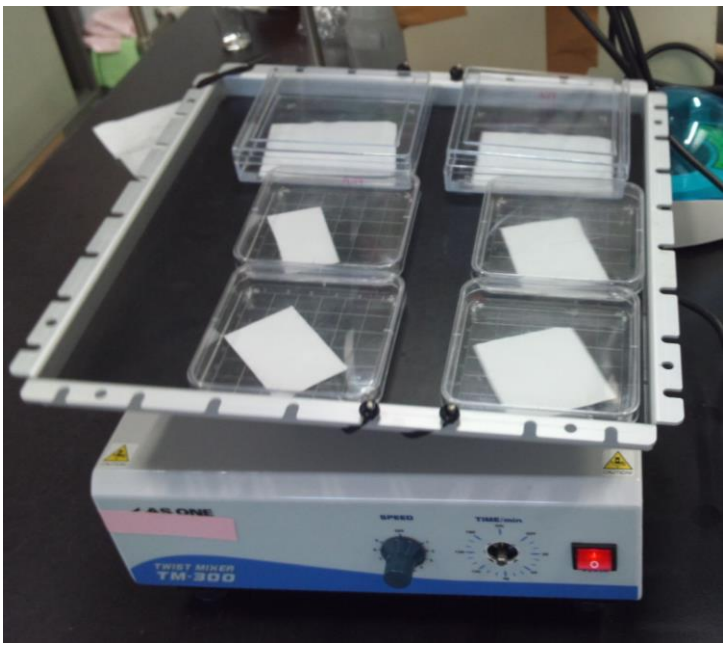

Figure 2.28 Antibody incubation with gentle agitation

After washing the membrane 3 times with TBS-T for 5 min each time, the membrane was incubated with a ImmunoStar® LD reagent for 1 minute. The light is then detected using LumiVision PRO 400EX (Aisin Seiki Co., Aichi, Japan), a CCD camera, which captures a digital image of the western blot. The luminescence intensity was then quantified and analyzed using ImageJ software.

2.9 Statistical Analysis

For the *in vitro* study, experiments were undertaken at least in triplicate under identical conditions. The mean values ± standard error of the mean (SEM) of the representative data are presented. Statistical differences were determined using the one-way analysis of variance (ANOVA) followed by Dunnett’s or Student's t-test, with *p*-values being indicated for each figure.

Chapter III
Results and Discussion

This chapter analyzes and discusses findings of the present study in anti-obesogenic research from Indonesian medicinal plants. The focus of the mechanism of action is lipid metabolism regulatory effect as described in the §1.2.3.5. The first section presents extensive study of *Eurycoma longifolia* Jack, exploring its bioactivities on lipid metabolisms in 3T3-L1 white adipocytes, isolation of lipolytic compounds, cellular mechanisms of actions, and exploration on its bioactivities in WT-1 brown adipocytes. The second section presents study of *Brucea javanica* (L.) Merr. and its isolation of lipolytic compounds in 3T3-L1 white adipocytes. Furthermore, the last section offers an original screening method with different mode of anti-obesogenic effects to identify potential anti-lipogenic products, that can be universally applicable for screening of other natural resources. In this last section, the author also discusses future anti-obesity research of Indonesian medicinal plants.

3.1 Study of Lipolytic Activity from *Eurycoma longifolia* Jack

3.1.1 Effects of EL on Lipid Accumulation and Cell Viability of White Adipocytes

In the previous screening study of 76 Indonesian medicinal plant samples (Lahrita, 2015a), *Eurycoma longifolia* Jack root extracts (EL) exerted reduction of lipid accumulation in 3T3-L1 white adipocytes without cytotoxicity. Samples EL were incubated after the induction of differentiation (from day 4 to day 9), and cytotoxicity test was performed in pre-adipocytes. In current study, subsequent experiments were needed to examine if EL also disrupts differentiation process in which pre-adipocytes turn into adipocytes, or if EL only reduces lipid droplets produced by mature adipocytes. Thus, the inhibition of lipid accumulation in 3T3-L1 adipocytes was observed at two phases; namely differentiating pre-adipocytes (sample incubation from day 0 to day 2) and differentiated adipocytes (sample incubation from day 4 to day 9) using ORO staining assay (Figure 3.1). Cell viability assay to examine cytotoxicity of EL was also conducted in two phases, differentiating pre-adipocytes and differentiated adipocytes.

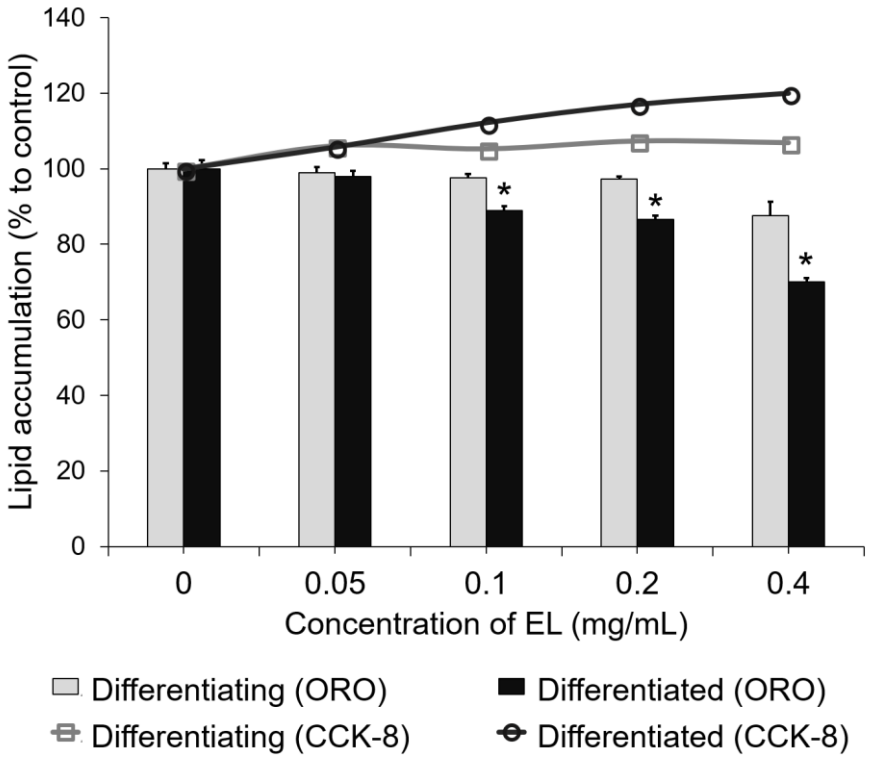

Figure 3.1 Lipid reducing-activity and cytotoxicity of EL in differentiating and differentiated 3T3-L1 adipocytes. Bars represent the percentages of lipid accumulation, while lines represent the percentages of viable cells. Data are expressed as mean ± SEM (n=6) and are representative of 3–4 independent experiments. * p<0.05 *vs.* control.

The results of ORO showed that lipid content in differentiated 3T3-L1 adipocytes (incubation from day 4 to day 9) was significantly reduced by 20%, 25%, and 30% when treated with 0.1, 0.2, and 0.4 mg/mL of EL respectively, indicating a reduction in triglycerides (TG) lipid droplets (p<0.05, Student's t-test). On the contrary, treatment with EL during the induction of the differentiation period (day 0 to day 2), indicated no inhibition of lipid accumulation. Treatment with EL also did not exhibit cytotoxic effects, either in differentiating pre-adipocytes or in differentiated adipocytes. These results eliminated the possibility of cytotoxicity of EL, thus avoiding bias in reduction of lipid accumulation in the lipid accumulation assay. These results not only reconfirm the results of previous screening study, but also fill the research gap on the effects of EL in different phases of differentiation of adipocytes.

Adipocytes play key roles in maintaining lipid homeostasis, both by storing TG and by releasing free fatty acids. Although several studies on anti-obesogenic activities have focused on adipocyte proliferation and differentiation processes, this study showed no significant lipid reduction by EL observed in early phase of differentiation. This suggests that

the inhibition of lipid accumulation was not mediated by transcriptional genes involved in the adipocyte proliferation and induction of differentiation, which transformed pre-adipocytes into differentiated (mature) adipocytes. Instead, 30% of lipid reduction (0.4 mg/mL of EL) occurred in the differentiated adipocytes, that led the author to the study of lipolysis, a process of breaking down of fat storage in differentiated adipocytes.

3.1.2 Effects of EL on Lipolysis in White Adipocytes

As summarized in the §3.1.1, 30% of lipid reduction that occurred in the differentiated adipocytes leads to the hypothesis that EL stimulates lipolysis process in adipocytes. Lipolysis, a catabolism process to break down TG lipid droplets in adipocytes, is one well-known mechanism to reduce fat mass. Increasing the breakdown of TG lipid droplets in the lipolysis process has been considered a promising therapeutic target in the treatment of obesity (Ahmadian et al., 2010; Lass et al., 2011). Hydrolysis of the TG lipid droplets results in the release of free-fatty acid and glycerol, thus the concentration of glycerol released into the culture medium was assayed as an indicator of lipolysis.

The results of glycerol release assay of EL in 3T3-L1 white adipocytes are presented in Figure 3.2.

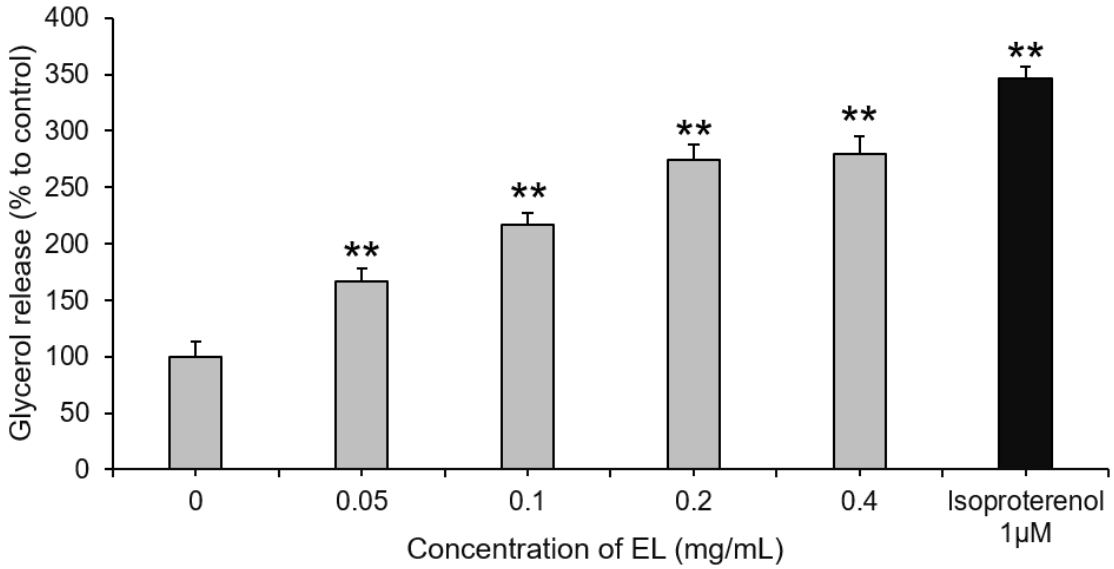

Figure 3.2 Effects of EL on lipolysis in 3T3-L1 adipocytes. Isoproterenol 1 μM was used as the positive control. Lipolysis was stimulated by EL at various concentrations. Data are expressed as mean ± SEM (n = 6) and are representative of three independent experiments. ** $p < 0.001$ versus untreated cells.

Isoproterenol, an activator of β-adrenoceptor, was used as a reference compound for lipolysis stimulation. Treatment of isoproterenol strongly elevated glycerol release by 3.46-fold compared with basal conditions (p<0.001). Treatment with various concentrations of EL (0.05, 0.1, 0.2, and 0.4 mg/mL) significantly enhanced glycerol release in a concentration-dependent manner. These results confirm the indication of lipolytic stimulation, leading to the reduction of TG lipid droplets in adipocytes.

As EL showed stimulation of lipolysis in white adipocytes, further study leads to the mechanism of the lipolytic stimulation. Mechanistic studies in this study were conducted in two steps, inhibitory challenge on the lipolytic pathway and confirmation by protein immunoanalysis. The inhibitory challenge and protein immunoanalysis are presented in the following §3.1.3.

3.1.3 Mechanistic Studies of EL-stimulated Lipolysis

3.1.3.1 Effects of Lipolysis Inhibitors on EL-stimulated Lipolysis

Since EL stimulated lipolysis, the signaling molecules related to the activation of hormone-sensitive lipase (HSL) were predicted to involve. As described in the introduction section, cAMP/PKA and MAPK/ERK pathways are two widely known lipolytic pathways that activate phosphorylation of HSL, the prominent lipase in the lipolytic process. To assess the involvement of PKA, ERK, and other MAPK cascades (JNK and p38 MAPK) pathways in the EL-stimulated lipolysis, respective inhibitors and activators to the pathways were added in the glycerol release assay (Figure 3.3).

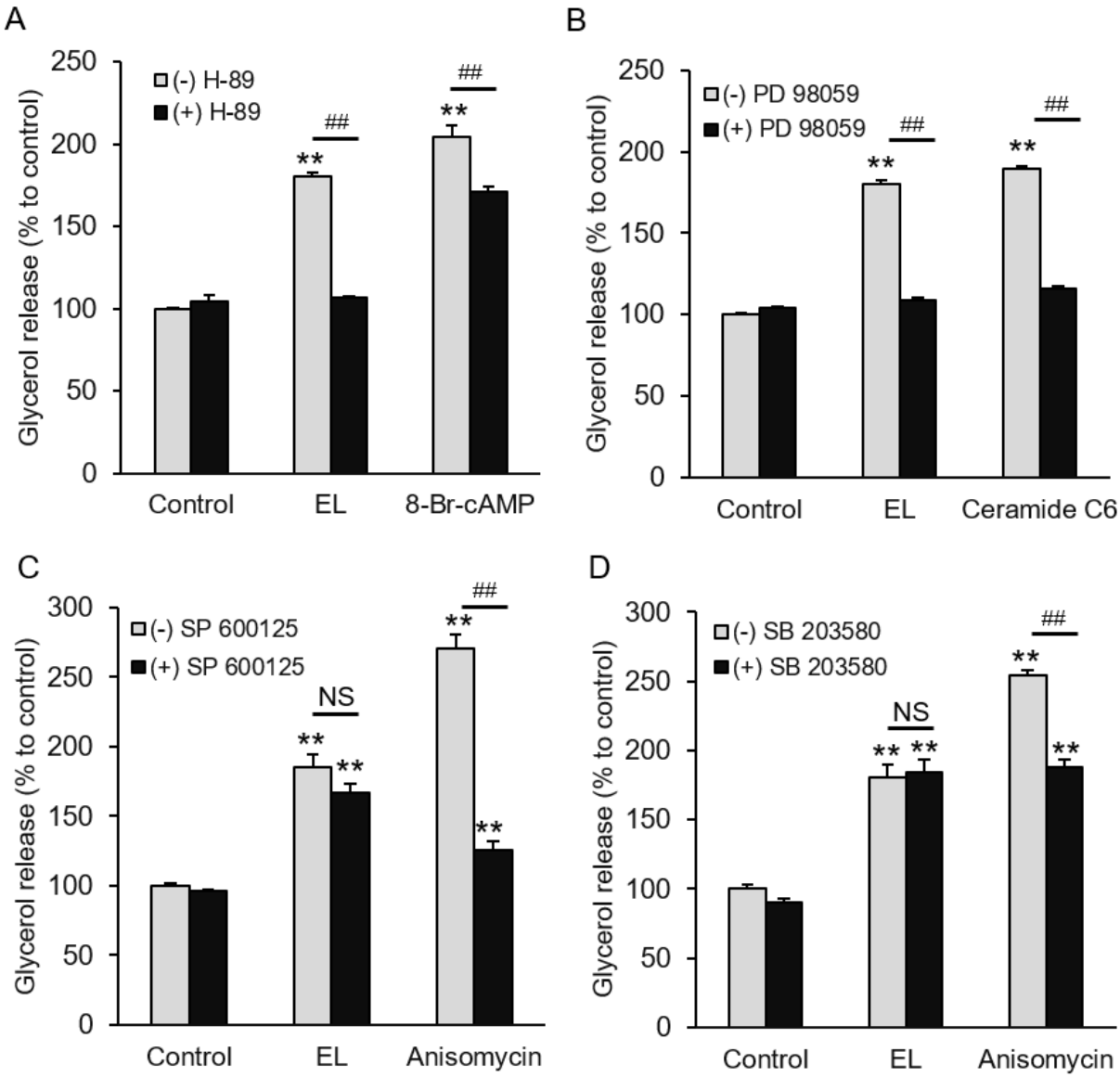

Figure 3.3 Effects of PKA, ERK, JNK, and p38 MAPK inhibitors on the EL-stimulated lipolysis. 3T3-L1 adipocytes were pre-treated with inhibitor of **(A)** PKA (20 µM H-89), **(B)** ERK (50 µM PD 98059), **(C)** JNK (50 µM SP 600125), or **(D)** p38 MAPK (20 µM SB 203580) for 1 hour. Concentration of EL was 0.1 mg/mL. 8-Br-cAMP (100 µM) and ceramide C6 (20 µg/mL) were used as positive controls for PKA and ERK pathways, respectively, while anisomycin (25 µg/mL) was used as the positive control for both JNK and p38 MAPK pathways. Glycerol release values are percentages to control without inhibitor. Data are expressed as mean ± SEM (n = 6) and are representative of three independent experiments. $^{**}p < 0.01$ versus control without inhibitor (Dunnett's test); $^{\#\#}p < 0.01$ versus no inhibitor (t-test); NS: No Significance.

Among the four tested inhibitors, PKA and ERK inhibitors completely abolished EL-stimulated lipolysis (93.1% and 91.2%, respectively) (Figure 3.3A and 3.3B). Meanwhile, there were no changes on EL-stimulated lipolysis with the presence of p38 MAPK and JNK inhibitors, although the inhibitors attenuated lipolysis stimulated by the activator (Figure

3.3C and 3.3D). These results suggest that both kinases, PKA and ERK, were involved in mediating the lipolytic activity of EL. In order to confirm the involvement of PKA and ERK kinases on EL-stimulated lipolysis, a protein immunoassay using western-blotting method was performed subsequently. The protein immunoanalysis is presented in the following §3.1.3.2.

3.1.3.2 Protein Immunoanalysis of EL-stimulated Lipolysis

To confirm the results of inhibitory challenges, protein immunoanalysis was conducted to determine the activation of PKA and ERK kinases by EL treatment (0.1 mg/mL), in the presence or absence of their respective inhibitors. Western blot analysis was performed to examine the activation of both target proteins: phosphorylated PKA (p-PKA) and total PKA (PKA), and phosphorylated ERK (p-ERK) and total ERK 1/2 (ERK). The amount of the phosphorylated protein and the total protein was quantified, and the ratios the two-forms as well as the representative immunoblots are presented (Figure 3.4).

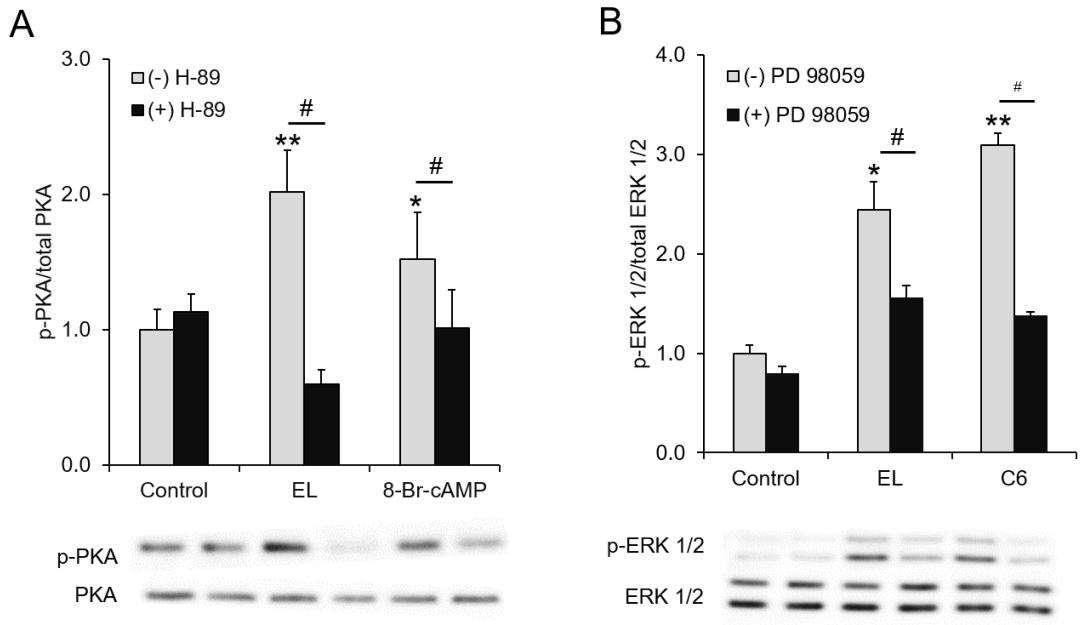

Figure 3.4 Immunoblotting analysis of PKA and ERK 1/2 after EL treatment. 3T3-L1 adipocytes were pre-treated with inhibitor of **(A)** PKA (20 µM H-89) or **(B)** ERK 1/2 (50 µM PD 98059) for 1 hour. Concentration of EL was 0.1 mg/mL. 8-Br-cAMP (100 µM) and ceramide C6 (20 µg/mL) were used as positive controls for PKA and ERK, respectively. Cells were harvested, lysed, and subjected to SDS-PAGE and western blotting. Phosphorylation indicates luminescence intensity of ratio of phosphorylated fraction to their respective total fractions. Data are expressed as mean ± SEM (n = 4). A representative immunoblot is shown. *$p < 0.05$, **$p < 0.01$ versus control without inhibitor (Dunnett's test); $^{\#}p < 0.05$ versus no inhibitor (t-test).

As shown in Figure 3.4A, EL treatment increased phosphorylation of PKA by 2-fold higher than that of untreated cells, and the activation was abolished by the addition of PKA inhibitor (H-89). Similarly, EL-treated cells increased phosphorylation of ERK 1/2 by 2.5-fold higher than that of untreated cells, which was substantially reduced by the presence of ERK 1/2 inhibitor (PD 98059) (Figure 3.4B). These results confirmed that EL stimulated lipolysis in 3T3-L1 adipocytes by enhancing phosphorylation of PKA and ERK kinases (Figure 3.5).

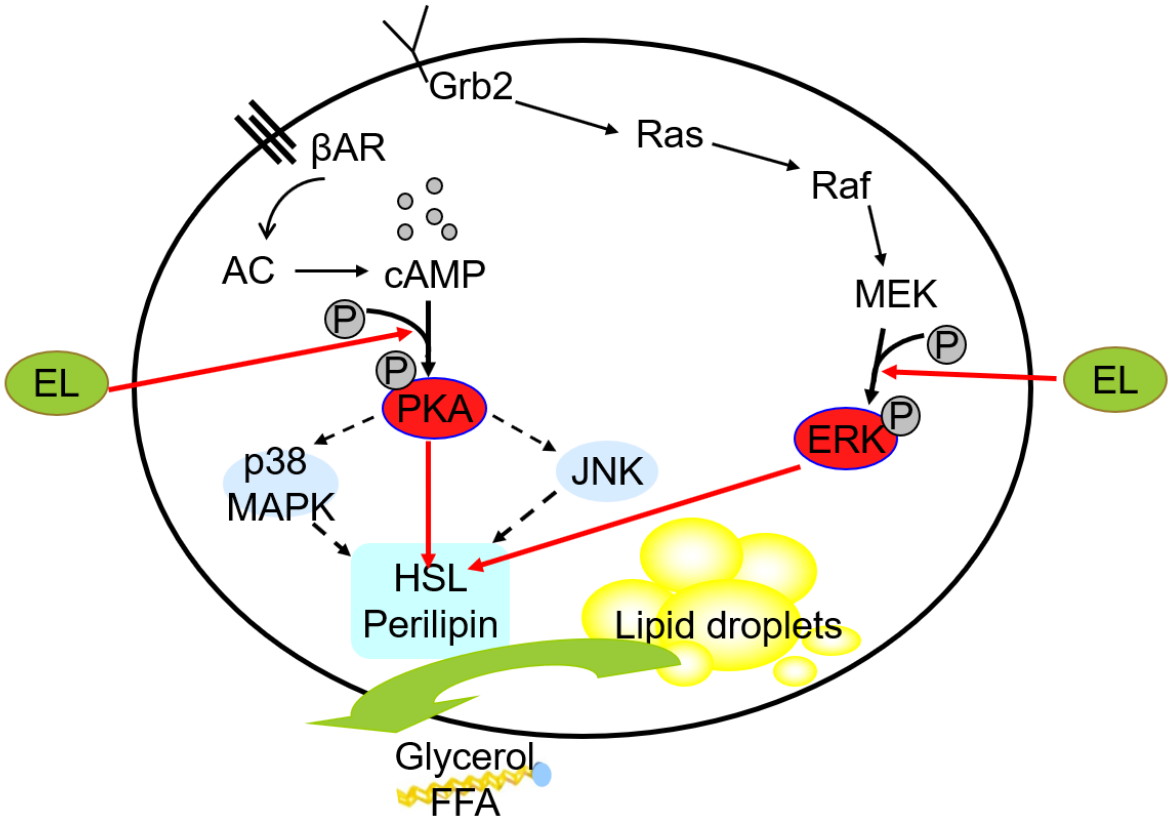

Figure 3.5 *E. longifolia* stimulates lipolysis in 3T3-L1 adipocytes through the activation of PKA and ERK

Lipolytic promoting activity has been increasingly studied with the goal of developing efficient treatments for obese patients. Various plant extracts were found to promote lipolysis via either PKA or ERK pathways. For example, extract of *Hemerocallis fulva* (Mori et al., 2009) was reported to stimulate lipolysis through increases in cAMP levels and activation of PKA in adipocytes. Extract of an African plant, *Mesembryanthemum crystallinum*, was shown to augment lipolysis of adipocytes by enhancing ERK 1/2 phosphorylation (Drira et al., 2016).

Although similar to the above reports, the ability of EL to enhance lipolysis is different in that it increases phosphorylation of both PKA and ERK kinases. This dual activation was previously reported for *Brassica campestris* spp. *Rapa*, in which this species demonstrated lipolysis enhancement via β_3-adrenergic receptor, leading to the phosphorylation of PKA and ERK (An et al., 2010).

3.1.4 Discussion on Bioactivities of *Eurycoma longifolia* Jack

Eurycoma longifolia Jack (Simaroubaceace), locally known as *pasak bumi* in Indonesia, is a medicinal plant in Southeast Asian region. The plant has been widely known for its male aphrodisiac effects. Water decoctions and extract-in-capsules from the roots are commercialized not only in Malaysia and Indonesia, but also in global market. For the first time, the author has reported the potential anti-obesogenic effects of *E. longifolia* and elucidated the mechanism of action *in vitro* (Lahrita et al., 2015b; 2017). This anti-obesogenic effect of this medicinal plant is scarcely studied. So far, there was a randomized clinical trial (RCT) on sexual improvement using water-extract of *E. longifolia* roots, that unintentionally found a significant fat mass loss in male subjects with BMI $\geq$ 25 kg/m^2 (p = 0.008) (Ismail et al., 2012).

Obesity has been identified among other causal factors contributing to male infertility. Although *E. longifolia* extract has been reported to improve spermatogenesis and male fertility index in animal study (Low et al., 2013), there was no report that links between male infertility improvement and anti-obesity effect from this medicinal plant. The finding on the activation of ERK by *E. longifolia* in this study, has become a key molecular signaling in the nexus of obesity and male infertility. The author suggests that ERK is not only involved in lipolysis process, but also in spermatogenesis (Figure 3.6).

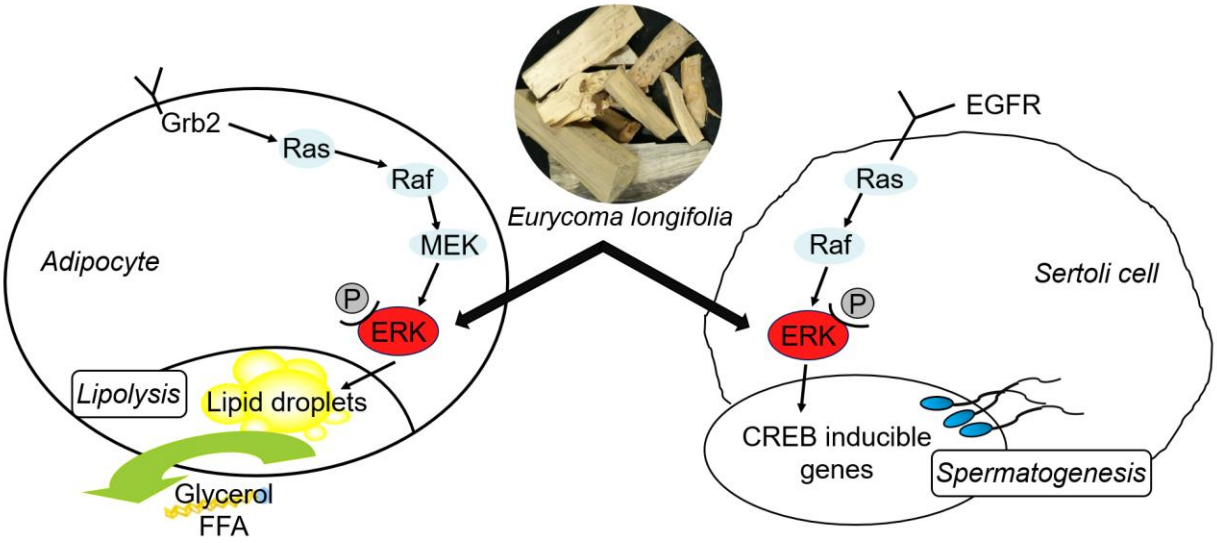

Figure 3.6 *E. longifolia* activates ERK, the signaling molecule in adipocytes' lipolysis and testosterone action. Figure is adapted from (Lahrita et. al., 2017) and (Burton and McKnight, 2007).

Spermatogenesis is a complex biological process of the male reproductive system, culminating in the generation of mature motile spermatozoa (Almog and Naor, 2008). Despite its complexity process, there is increasing data on the role of MAPK cascades (ERK, JNK and p38 MAPK) in spermatogenesis (Almog and Naor, 2010). Particularly, a number of studies have shown the involvement of ERK activation in various functions of the spermatozoa life cycle, emphasizing the important role of ERK in male reproductive system. The activation of ERK 1, 2 was reported to induce the production of testosterone (Martinat et al., 2005, Walker, 2009) and regulate spermatogenesis and spermatozoa function (Hasegawa et al., 2013, Sette et al., 1999). The fact that lipolysis and spermatogenesis share common signaling pathways, any herbal medicines that have such activities to modulate MAPK cascades can be considered as potential agents to combat male obesity-related infertility. The current study provides scientific background for further research on the efficacy of *E. longifolia* to address these two phenomena in our male society.

3.1.5 Study of the Lipolytic Compounds from *Eurycoma longifolia* Jack

As EL showed stimulation of lipolysis in white adipocytes, the study leads to isolation of responsible compounds that possess lipolytic-activity, and further examination of bioactivities the isolated compounds *in vitro*. First parts, the bioassay-guided fractionation

and structure determination of the lipolytic compounds are presented in the following sub-section 3.1.5.1.

3.1.5.1 Bioassay-guided Fractionation of Compounds 1-3

In order to isolate the responsible compounds that possess lipolytic-activity, a bioassay-guided fractionation was performed using glycerol release enhancement assay in 3T3-L1 adipocytes as described in §2.6. Multiple fractionation steps of separation by column chromatography and HPLC were performed to give three purified compounds: compounds **1**, **2**, and **3**. The fractionation scheme is presented in Figure 3.7

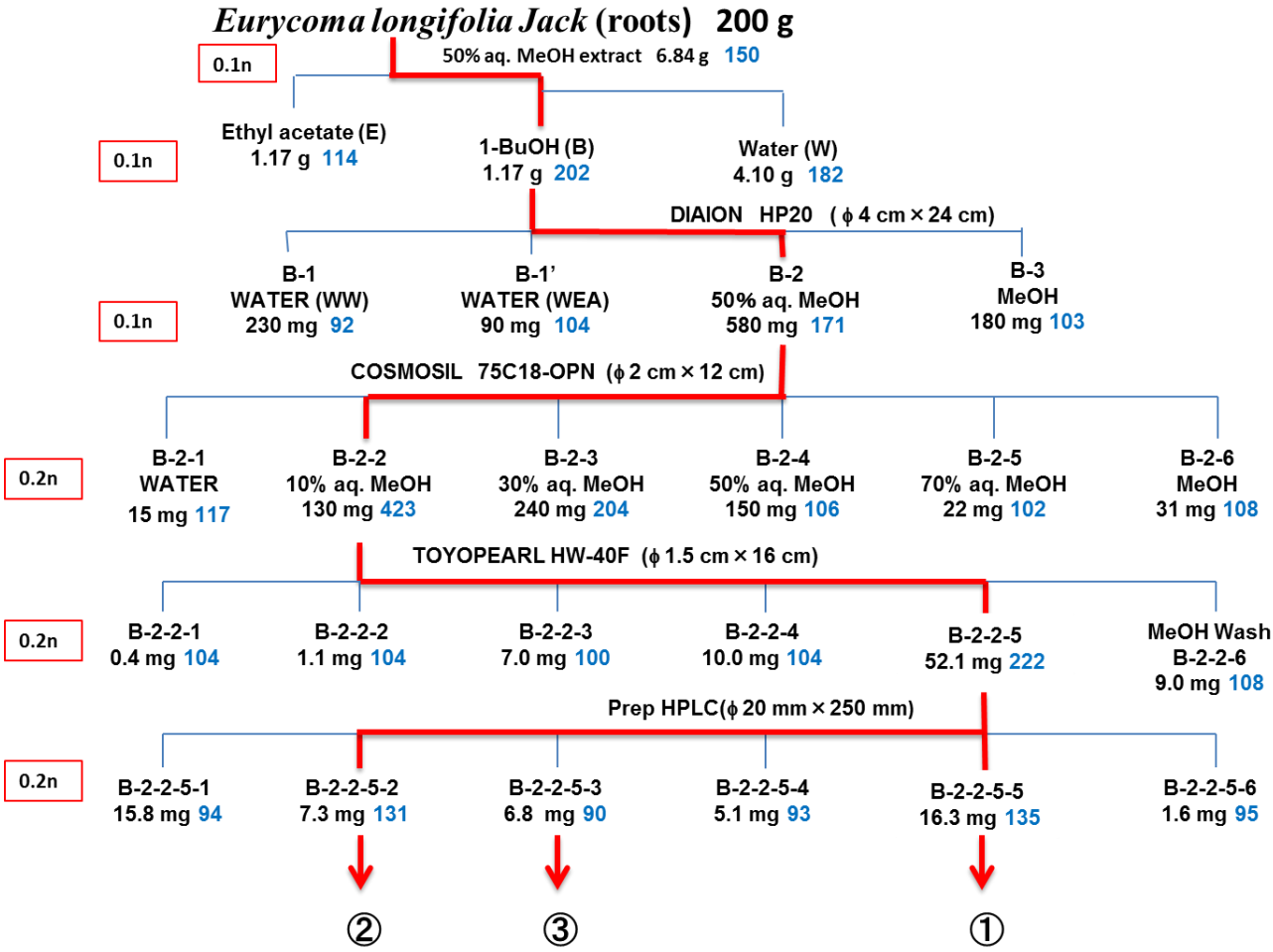

Figure 3.7 Fractionation scheme of *E. longifolia* from its *n*-butanol layer.
Remarks:
200 = percentage of glycerol release (% to control)

$$1\ n = \frac{\text{extracted material (1 g)}}{\text{solution volume (10 mL)}}$$

Powdered root of *E. longifolia* was extracted with 50% (v/v) aq. methanol. The extract was dried and partitioned with water, 1-butanol, and ethyl acetate. The 1-butanol layer was adsorbed to DIAION HP-20 and eluted with 50% (v/v) aq. methanol. The obtained 50% aq. methanol eluate was separated by Cosmosil 75C_{18}-OPN and then Toyopearl HW-40F column chromatography to obtain its active fraction. This fraction was finally purified by preparative HPLC with an InertSustain C18 column to isolate compounds **1**, **2**, and **3**.

There are 3 quassinoids that were isolated from *E. longifolia* roots: eurycomanone (**1**), 13β,21-epoxyeurycomanone (**2**), and 13β,21-dihydroxyeurycomanone (**3**). Each compound was identified by comparing its ^{1}H,^{13}C-NMR and optical rotation with the reported values.

Eurycomanone (1)

^{1}H-NMR and ^{13}C-NMR spectra of compound (**1**) are shown in Figure 3.8 and 3.9, respectively.

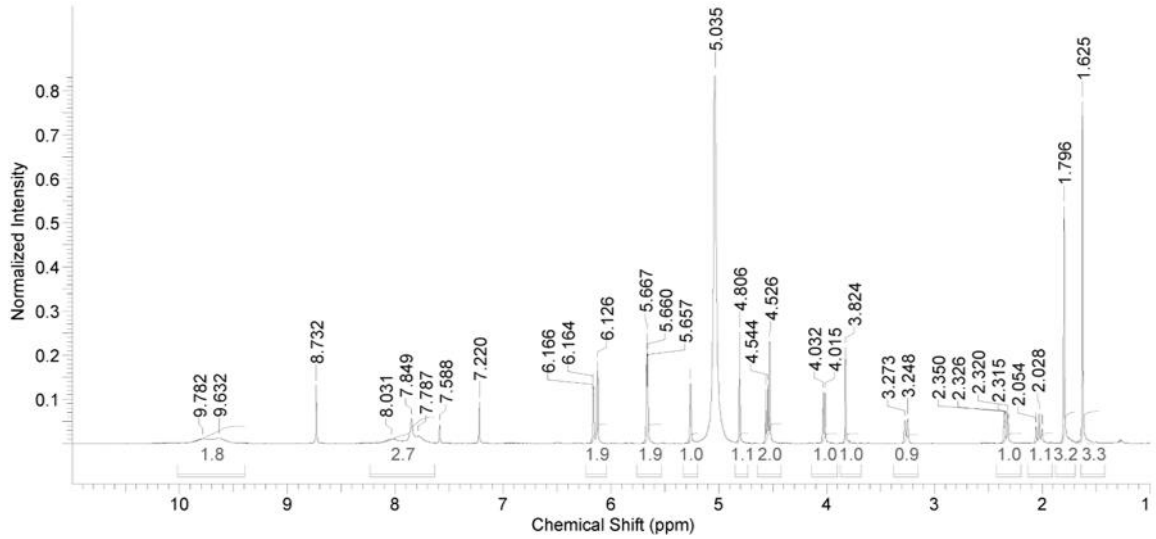

Figure 3.8 ^{1}H-NMR spectrum of compound **1**

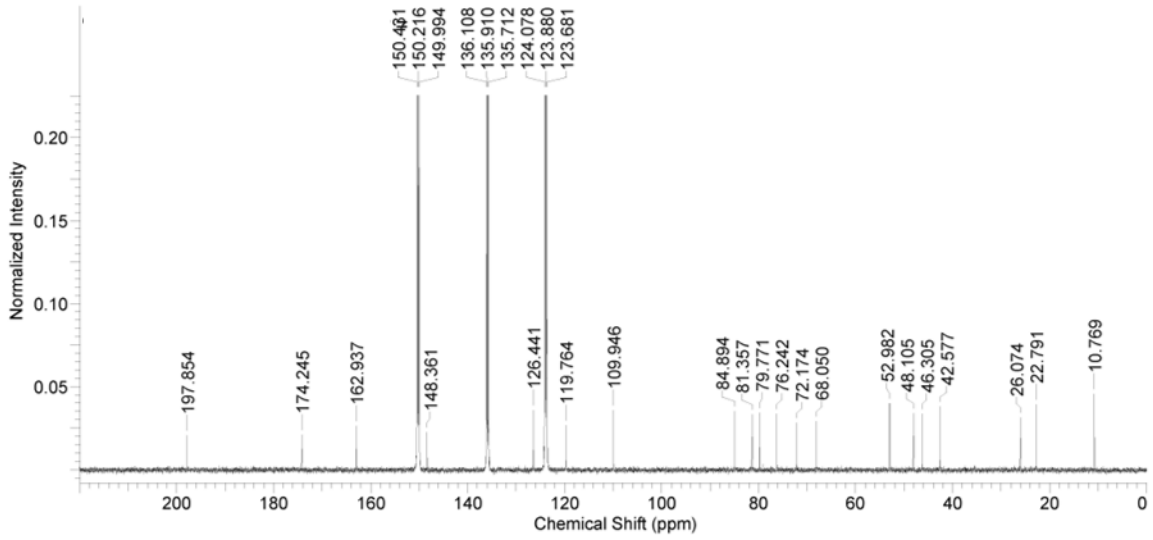

Figure 3.9 ^{13}C-NMR spectrum of compound **1**

The NMR data of compound **1** are consistent with those reported for eurycomanone (Tada et al., 1991, Morita et al., 1990), thus compound **1** was confirmed as eurycomanone (Figure 3.10).

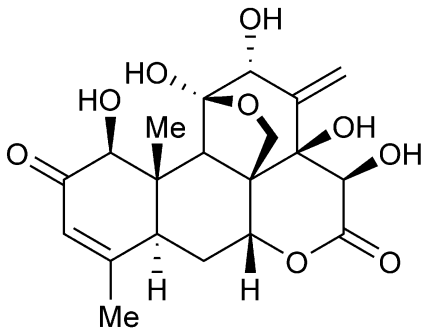

Figure 3.10 Structure of eurycomanone (**1**)
^{1}H-NMR (500 MHz, pyridine-d_5, rt): 1.63 (3H, s), 1.80 (3H, br s), 2.03 (1H, ddd, *J* = 2.4, 13.3, 14.4 Hz), 2.33 (1H, td, *J* = 2.4, 14.4 Hz), 3.26 (1H, br d, *J* = 12.6 Hz), 3.82 (1H, s), 4.02 (1H, d, *J* = 8.8 Hz), 4.53 (1H, s), 4.55 (1H, d, *J* = 8.8 Hz), 4.81 (1H, s), 5.26 (1H, t, *J* = 2.4 Hz), 5.66 (1H, d, *J* = 1.5 Hz), 5.67 (1H, s), 6.12 (1H, d, *J* = 1.5 Hz), 6.16 (1H, q, *J* = 1.3 Hz), 7.79 (1H, br s, OH), 7.85 (1H, s, OH), 8.03 (1H, br s, OH), 9.63 (1H, br s, OH), 9.78 (1H, br s, OH) ppm.
^{13}C-NMR (125 MHz, pyridine-d_5, rt): 10.77, 22.79, 26.07, 42.58, 46.30, 48.10, 52.98, 68.05, 72.17, 76.24, 79.77, 81.36, 84.89, 109.95, 119.76, 126.44, 148.36, 162.94, 174.25, 197.85 ppm.
HR-ESI-MS (positive): $[M+Na]^+$, found *m/z* = 431.1322, $C_{20}H_{24}O_9Na$, requires *m/z* 431.1318; $[\alpha]_D^{24}$ +32.1° (*c* = 1.0, pyridine)

Eurycomanone, commonly used as marker compound in commercial *E. longifolia* extract, is a major quassionoid in *E. longifolia* roots. In the tested *E. longifolia* extract (EL), eurycomanone appeared at 18.6 min as indicated by the HPLC chromatograms (Figure 3.11)

The content of eurycomanone in MeOH extract was 5.1% as quantified by LC-MS (**Appendix 8**).

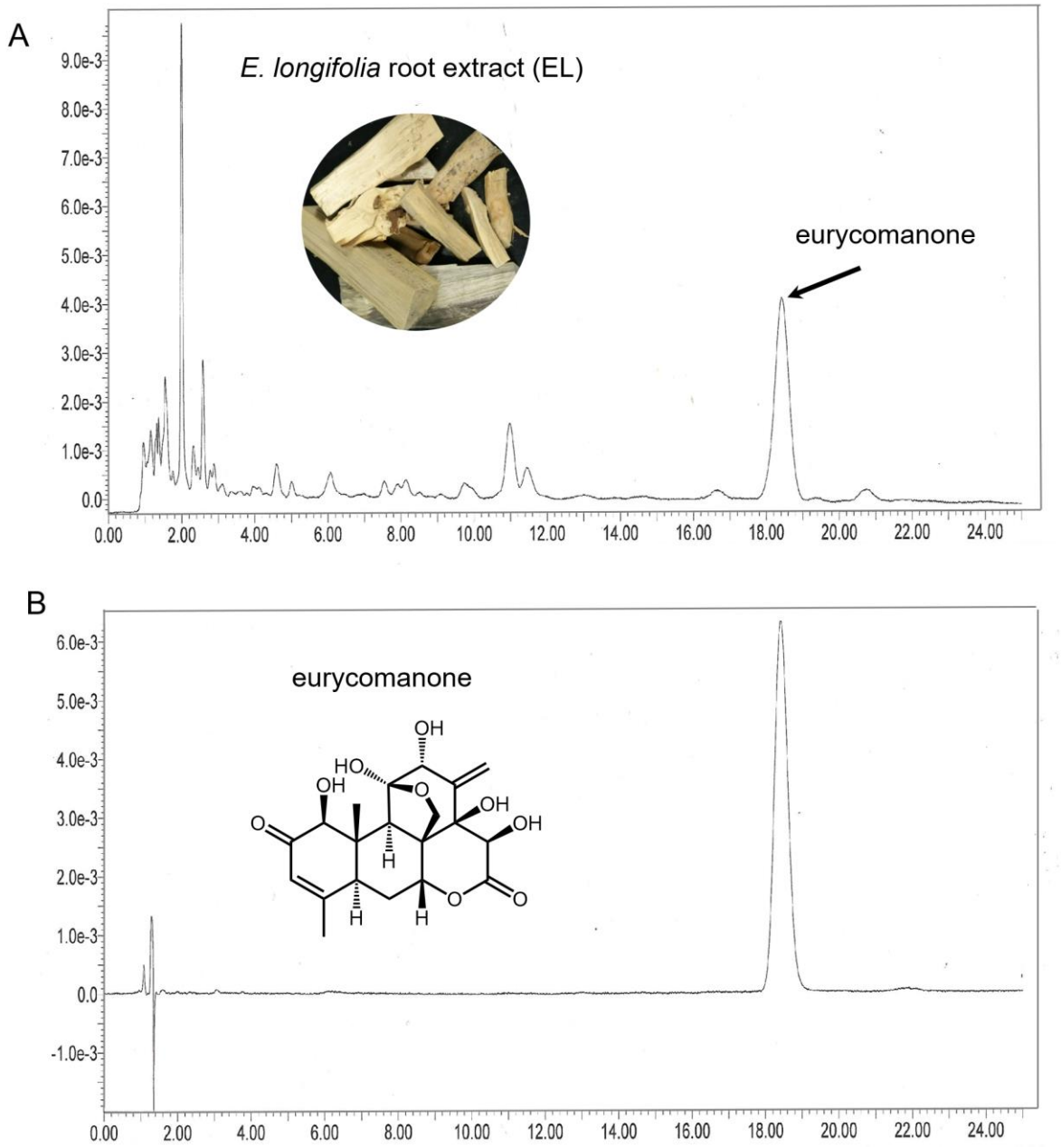

Figure 3.11 HPLC chromatograms of EL (A) and eurycomanone (B)
Remarks:
The analytical column was an Inertsustain C18 column (2.1 mm X 100 mm; GL Science Co., Tokyo, Japan).The mobile phase consisted of 10% methanol aq. containing 10 mM ammonium acetate. The flow rate was set at 0.2 mL/min and UV detection wavelength was set at 254 nm. In the HPLC chromatogram, eurycomanone was found at 18.6 min.

13β,21-epoxyeurycomanone (2)

^{1}H-NMR and ^{13}C-NMR spectra of compound **2** are shown in Figure 3.12 and 3.13, respectively.

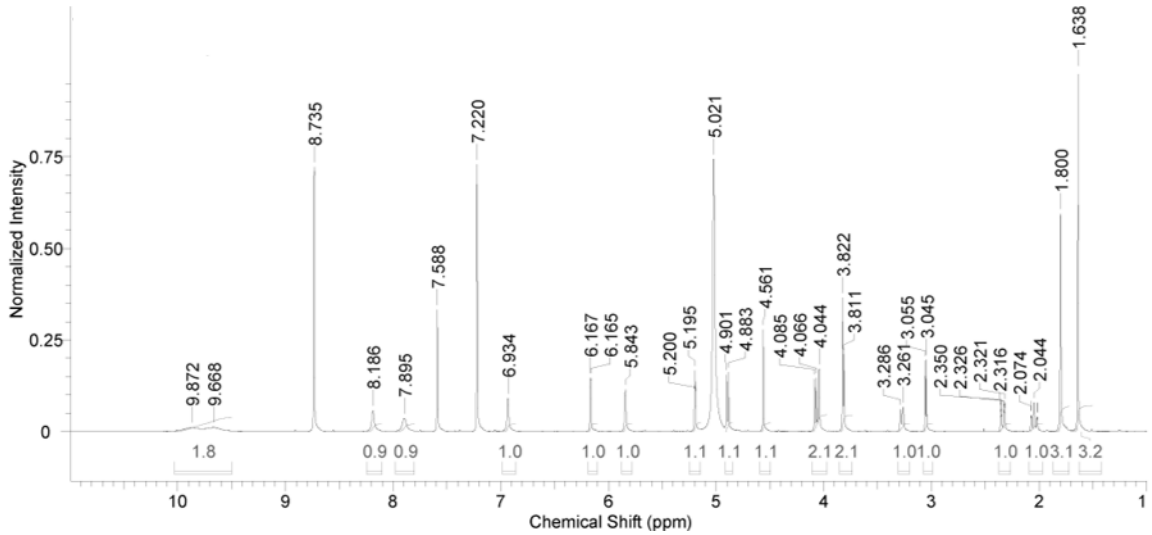

Figure 3.12 ^{1}H-NMR spectrum of compound **2**

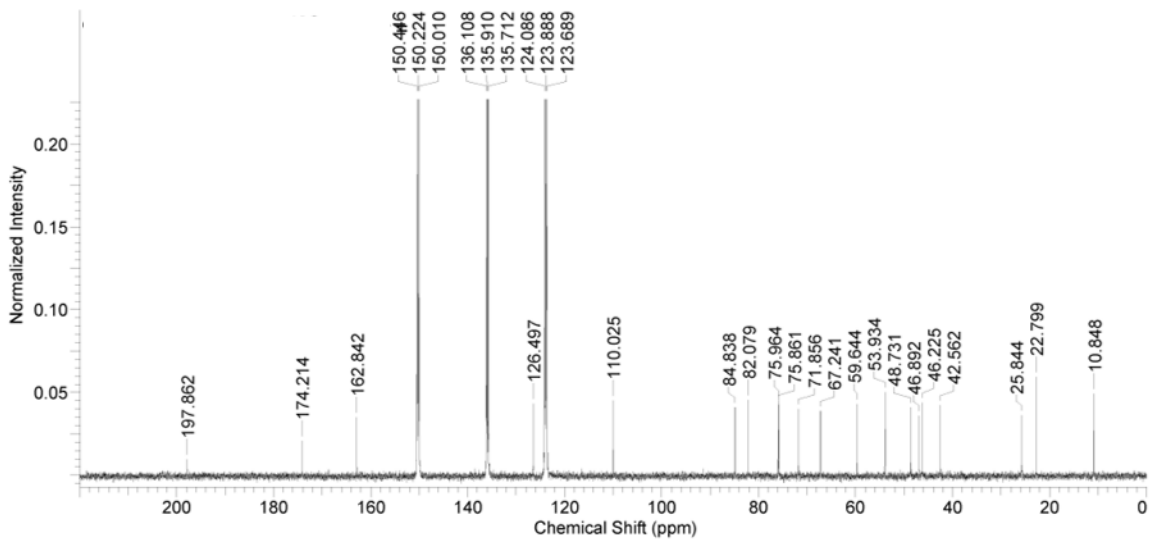

Figure 3.13 ^{13}C-NMR spectrum of compound **2**

The NMR data of compound **2** are consistent with those reported for 13β,21-epoxyeurycomanone (Tada et al. 1991), thus compound **2** was confirmed as 13β,21-epoxyeurycomanone (Figure 3.14).

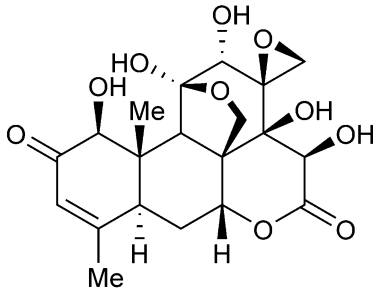

Figure 3.14 Structure of 13β,21-epoxyeurycomanone (**2**)
^{1}H-NMR (500 MHz, pyridine-d_5, rt): 1.64 (3H, s), 1.80 (3H, br s), 2.04 (1H, ddd, *J* = 2.7, 13.2, 14.4 Hz), 2.33 (1H, td, *J* = 2.7, 2.7, 14.8 Hz), 3.05 (1H, d, *J* = 5.3 Hz), 3.27 (1H, br d, *J* = 13.2 Hz), 3.817 (1H, d, *J* = 5.3 Hz), 3.822 (1H, s), 4.04 (1H, s), 4.07 (1H, d, *J* = 9.0 Hz), 4.56 (1H, s), 4.89 (1H, d, *J* = 9.0 Hz), 5.20 (1H, t, *J* = 2.7 Hz), 5.84 (1H, s), 6.17 (1H, q, *J* = 1.3 Hz), 6.93 (1H, br s, OH), 7.90 (1H, s, OH), 8.19 (1H, br s, OH), 9.67 (1H, br s, OH), 9.87 (1H, br s, OH) ppm.
^{13}C-NMR (125 MHz, pyridine-d_5, rt): 10.85, 22.80, 25.84, 42.56, 46.23, 46.89, 48.73, 53.93, 59.64, 67.24, 71.86, 75.86, 75.96, 82.08, 84.84, 110.03, 126.50, 162.84, 174.21, 197.86 ppm.
HR-ESI-MS (positive): $[M+Na]^+$, found *m*/*z* = 447.1287, $C_{20}H_{24}O_{10}Na$, requires *m*/*z* 447.1267; $[\alpha]_D^{24}$ +34.2° (*c* = 1.0, pyridine)

Although compound **2** was determined to be a quassinoid, 13,21-epoxyeurycomanone, the stereochemistry of the epoxide in Tada et al. (1991) was reported as beta, while in another reference it was identified as alpha (Morita et al., 1993). Since both of the reported NMR spectra and optical rotations were the same as those obtained for compound **2** here, it indicated that one of the previous stereochemistry assignments is incorrect (See **Appendix 4**). To examine and verify its stereochemistry, compound **2** was then acetylated to obtain di-*O*-acetyl product **4** and the NOESY experiment was performed using compound **4**. ^{1}H-NMR, ^{13}C-NMR and NOESY spectra of compound **4** are shown in Figure 3.15, 3.16 and 3.17, respectively.

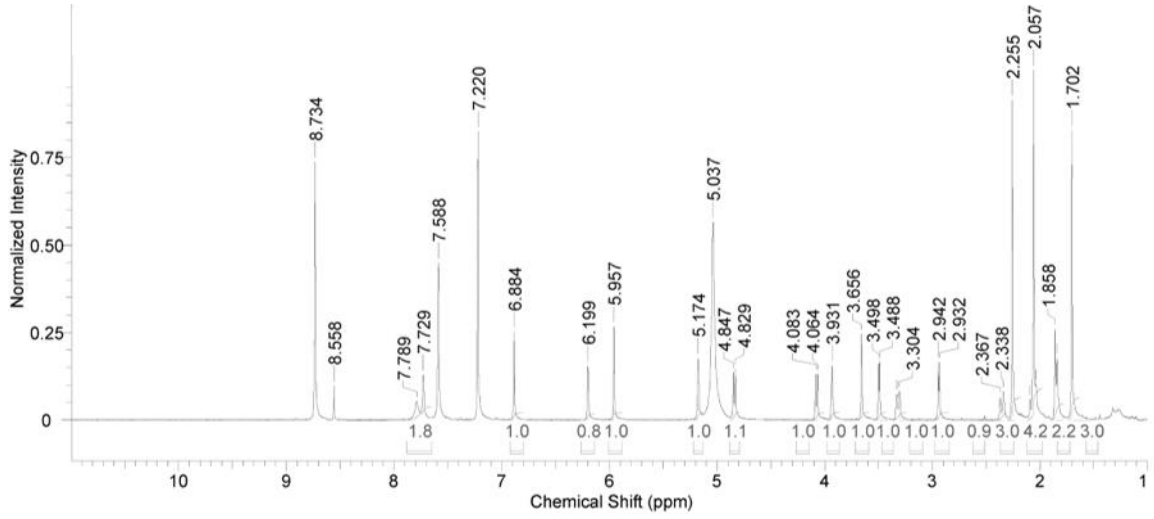

Figure 3.15 ^{1}H-NMR spectrum of compound **4**

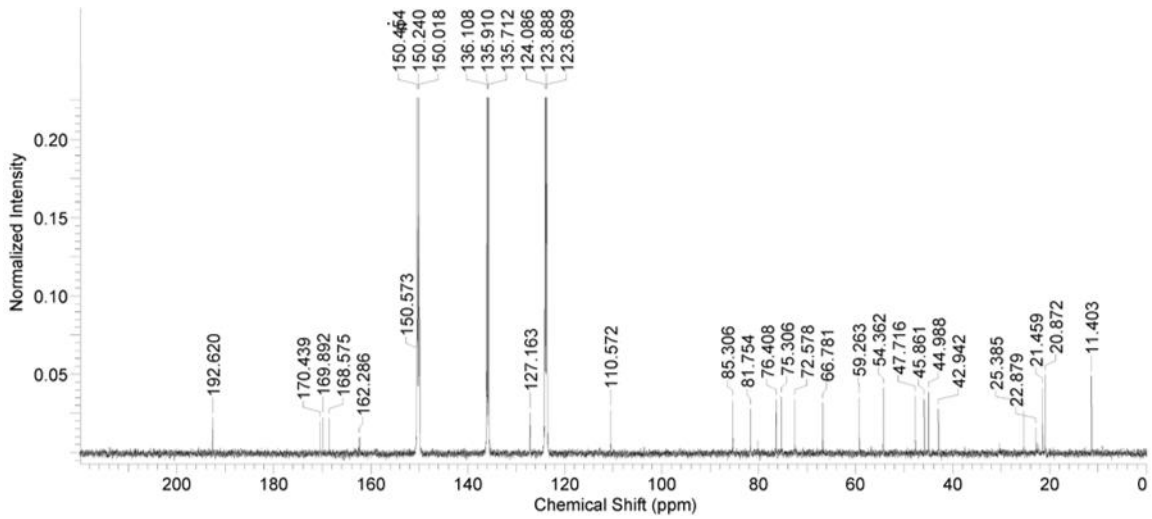

Figure 3.16 ^{13}C-NMR spectrum of compound **4**

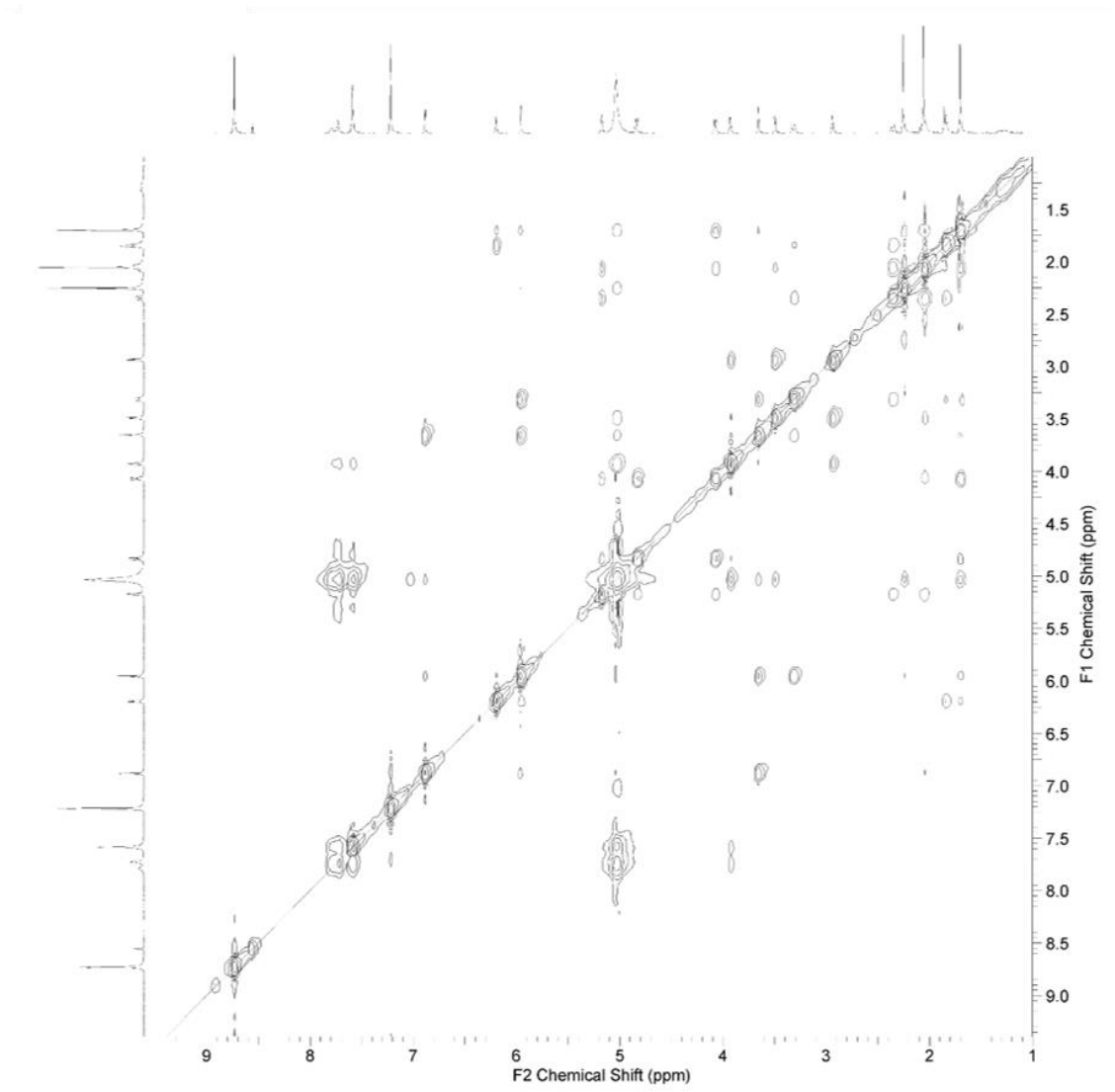

Figure 3.17 NOESY spectrum of 1,15-di-*O*-acetyl-13β,21-epoxyeurycomanone (**4**)

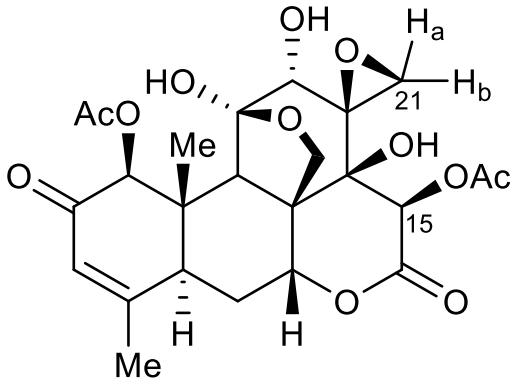

Figure 3.18 Structure of 1, 15- di-*O*-acetyl-13β,21-epoxyeurycomanone (**4**)

^{1}H-NMR (500 MHz, pyridine-d_5, rt): 1.70 (3H, s), 1.86 (3H, s), 2.06 (3H, s), 2.03-2.09 (1H, m), 2.26 (3H, s), 2.35 (1H, br d, *J* = 14.8 Hz), 2.94 (1H, d, *J* = 5.0 Hz), 3.32 (1H, br d, *J* = 12.9 Hz), 3.49 (1H, d, *J* = 5.0 Hz), 3.66 (1H, s), 3.93 (1H, s), 4.07 (1H, d, *J* = 9.1 Hz), 4.84 (1H, d, *J* = 9.1 Hz), 5.17 (1H, br s), 5.96 (1H, s), 6.20 (1H, br s), 6.88 (1H, s), 7.73 (1H, br s, OH), 7.79 (1H, br s, OH) ppm.

^{13}C-NMR (125 MHz, pyridine-d_5, rt): ^{13}C-NMR (125 MHz, pyridine-d_5, rt): 11.39, 20.86, 21.44, 22.86, 25.37, 42.92, 44.97, 45.84, 47.70, 54.34, 59.25, 66.76, 72.56, 75.29, 76.39, 81.74, 85.29, 110.55, 127.15, 162.27, 168.56, 169.87, 170.42, 192.60 ppm.

HR-ESI-MS (positive): $[M+Na]^+$, found *m*/*z* = 531.1495, $C_{24}H_{28}O_{12}Na$, requires *m*/*z* 531.1478; $[\alpha]_D^{25}$ +14.3° (*c* = 0.314, pyridine).

Measurement of the NOESY spectra of this compound showed a correlation between H-12 and H_a-21, which was considered as an evidence of the α-epoxide in the previous study of Morita et al. (1993). However, the distance between those two hydrogen atoms was similar between the α- and β-epoxide structure models. Therefore, the observed NOESY correlation was considered insufficient evidence to determine its stereochemistry. In compound **4**, a NOESY correlation was observed between H_b-21 and AcO-15 (See **Appendix 5**). Thus, the stereochemistry of the epoxide was confirmed to be beta, which is a biosynthetically reasonable configuration if the epoxide (**2**) is hydrolyzed to produce its dihydroxy derivative (**3**) *in planta*. In light of this finding, we need to consider that previous studies on the use, detection, and isolation of 13α,21-epoxyeurycomanone from *E. longifolia* probably refer to the β-epoxide (Ikram et al., 2015, Han et al., 2015).

13β,21-dihydroxyeurycomanone (3)

^{1}H-NMR and ^{13}C-NMR spectra of compound **3** are shown in Figure 3.19 and 3.20, respectively.

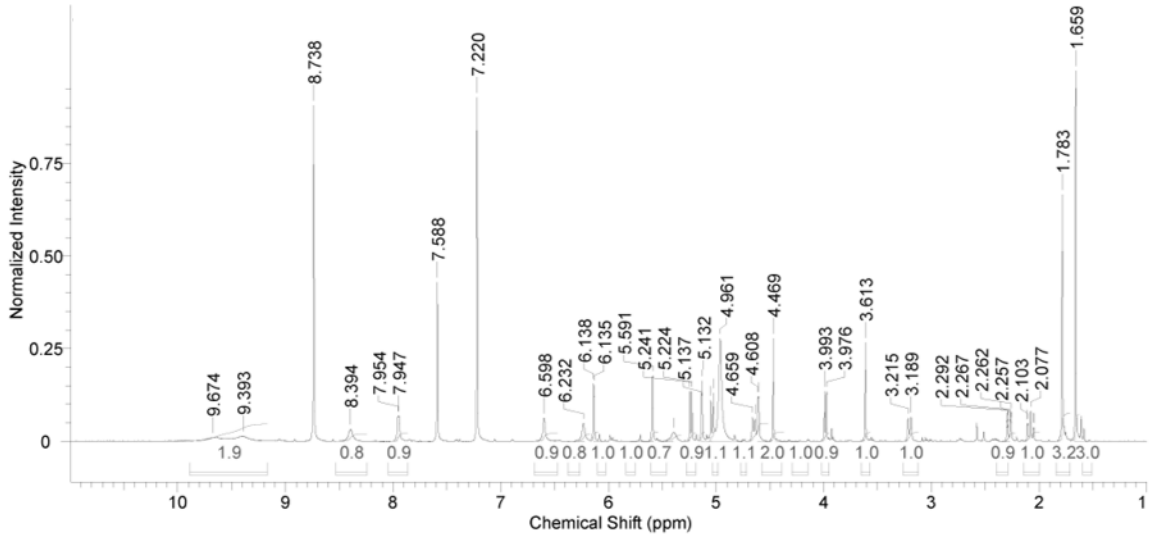

Figure 3.19 ^{1}H-NMR spectrum of compound **3**

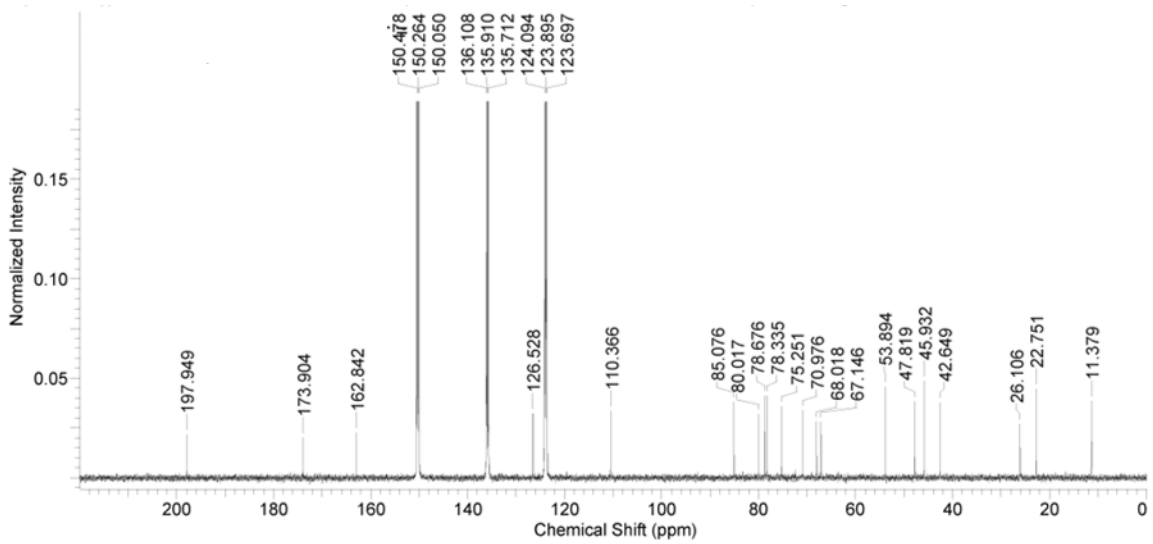

Figure 3.20 ^{13}C-NMR spectrum of compound **3**

The NMR data of compound **3** are consistent with those reported for 13β,21-dihydroxyeurycomanone (Kuo et al., 2004, Morita et al., 1990), thus compound **3** was confirmed as 13β,21-dihydroxyeurycomanone (Figure 3.21).

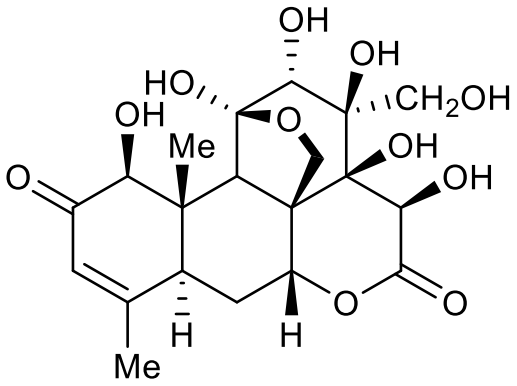

Figure 3.21 Structure of 13β,21-dihydroxyeurycomanone (**3**)
^{1}H-NMR (500 MHz, pyridine-d_5, rt): 1.66 (3H, s), 1.78 (3H, s), 2.08 (1H, ddd, *J* = 2.4, 13.2, 14.0 Hz), 2.28 (1H, td, *J* = 2.4, 14.0 Hz), 3.20 (1H, br d, *J* = 13.2 Hz), 3.61 (1H, s), 3.98 (1H, d, *J* = 8.7 Hz), 4.47 (1H, s), 4.60 (1H, d, *J* = 3.3 Hz), 4.65 (1H, d, *J* = 11.7 Hz), 5.04 (1H, d, *J* = 11.7 Hz), 5.13 (1H, t, *J* = 2.4 Hz), 5.23 (1H, d, *J* = 8.7 Hz), 5.39 (1H, br s, OH), 5.59 (1H, s), 6.14 (1H, q, *J* = 1.3 Hz), 6.23 (1H, br s, OH), 6.60 (1H, br s, OH), 7.59 (1H, s, OH), 7.95 (1H, d, *J* = 3.3 Hz), 8.39 (1H, br s, OH), 9.39 (1H, br s, OH), 9.67 (1H, br s, OH) ppm.
^{13}C-NMR (125 MHz, pyridine-d_5, rt): 11.38, 22.75, 26.11, 42.65, 45.93, 47.82, 53.89, 67.15, 68.02, 70.98, 75.25, 78.34, 78.68, 80.12, 85.08, 110.37, 126.53, 162.84, 173.90, 197.95 ppm
HR-ESI-MS (positive): $[M+Na]^+$, found *m*/*z* = 465.1390, $C_{20}H_{26}O_{11}Na$, requires *m*/*z* 465.1373; $[\alpha]_D^{24}$ +17.5° (*c* = 1.0, pyridine)

The three isolated quassinoid compounds **1**, **2** and **3** were further examined for their anti-obesogenic activities. The results are presented in the following sub-sections.

3.1.5.2 Effects of Compounds 1-3 on Lipid Accumulation, Lipolysis and Cell Viability of White Adipocytes

Compounds **1**, **2**, and **3** were evaluated for anti-obesogenic activities, including reduction of lipid accumulation and enhancement of lipolysis. The three isolated compounds were subjected to lipid accumulation, glycerol release, and cell viability assays. The results are presented in Figure 3. 22.

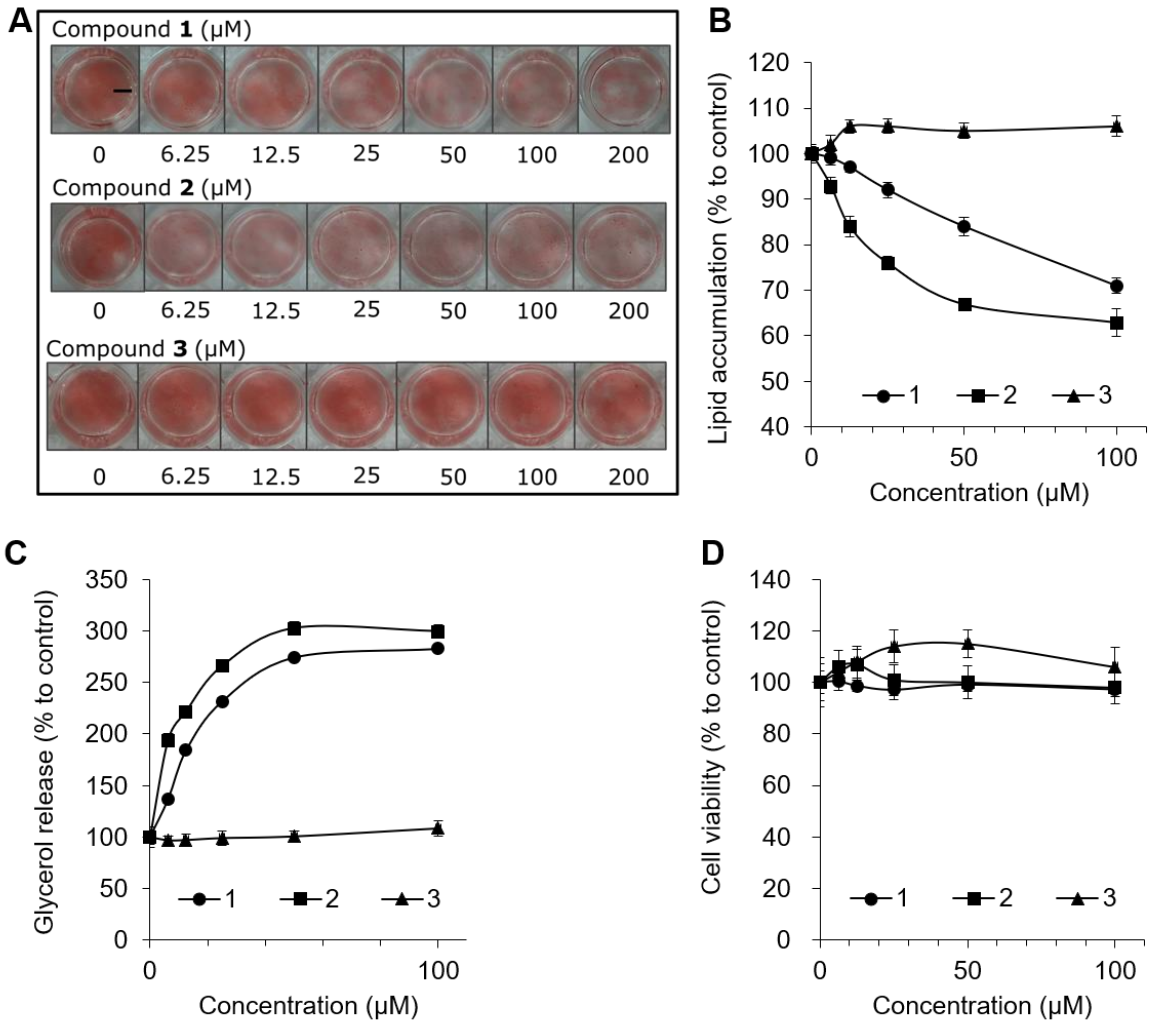

Figure 3.22 Photograph of Oil Red O-stained lipid droplets (A), lipid accumulation reduction effect (B), glycerol release enhancement activity (C), and cell viability (D) of compounds **1**–**3**. (A) Scale bar corresponds to 3 mm. (B) Compound **1** showed significant difference above 25 μM (p<0.01). Compound **2** showed significant difference above 6.25 μM (p<0.05) and above 12.5 μM (p<0.01). (C) Compounds **1** and **2** showed significant difference above 6.25 μM. Isoproterenol (1 μM) was used as positive control (322±1%). Data are expressed as mean ± SEM (n=6). Dunnett's test was used.

Compounds **1** and **2** showed concentration-dependent activity in the enhancement of glycerol release, and the reduction of lipid accumulation without cytotoxic effects (Figure 3.21). The EC_{50} value for the glycerol release enhancement was 14.6 μM for **1**, while **2** had a lower EC_{50} (8.6 μM). The stronger bioactive effects of **2** indicates the importance of the epoxide group in exerting its bioactivity. In contrast, the hydrolyzed derivative **3** did not show any biological activity in either of the two assays (Figure 3.21B and 3.21C), even at the highest tested concentration.

There are two possible reasons for the total absence of bioactivity in **3**. First, the presence of two hydroxyl groups might have strongly interfered with the interaction between the compound and the target. However, this explanation is unlikely to happen for the following reason. Although various derivatives of eurycomanones have been isolated from plants using various methods (Rehman et al., 2016, Kuo et al., 2004, Morita et al., 1990; 1993, Han et al., 2015, Chan et al., 1991, Meng et al., 2014, Park et al., 2014), in this study, compounds **1**–**3** were isolated through an activity-guided fractionation. If steric hindrance or ionic repulsion were the reason for the lack of bioactivity of **3**, then other related compounds, for example 13β-methyl,21-dihydroeurycomanone, would have been obtained as bioactive compounds during the isolation process.

The second possibility is that the epoxide group is the essential moiety for the bioactivity. This would suggest that eurycomanone (**1**) is oxidized in the cells to form its bioactive epoxide (**2**). However, there has been no evidence for supporting this hypothesis yet. Therefore, subsequent research on structure-activity relationship (SAR) of these quassinoids is being conducted to determine whether the epoxide group is the essential part of the bioactivity.

After evaluating their biological activities in reducing lipid accumulation and enhancing lipolysis, molecular mechanism of the lipolytic activity of **1** and **2** was further investigated.

3.1.5.3 Mechanistic Studies of 1- and 2-stimulated Lipolysis

As demonstrated in the mechanistic studies of EL extract (§3.1.3), in which EL stimulated lipolysis by activating PKA and ERK kinases, the isolated compounds **1** and **2** might also activate both PKA and ERK or only activate either of the kinases.

3.1.5.3.1 Effects of Lipolysis Inhibitors on 1- and 2-stimulated Lipolysis

First mechanistic study was conducted with co-incubation with two specific inhibitors to the lipolytic pathways (PKA and ERK), as well as additional β3-adrenergic receptor to investigate the upstream signaling (Figure 3.23).

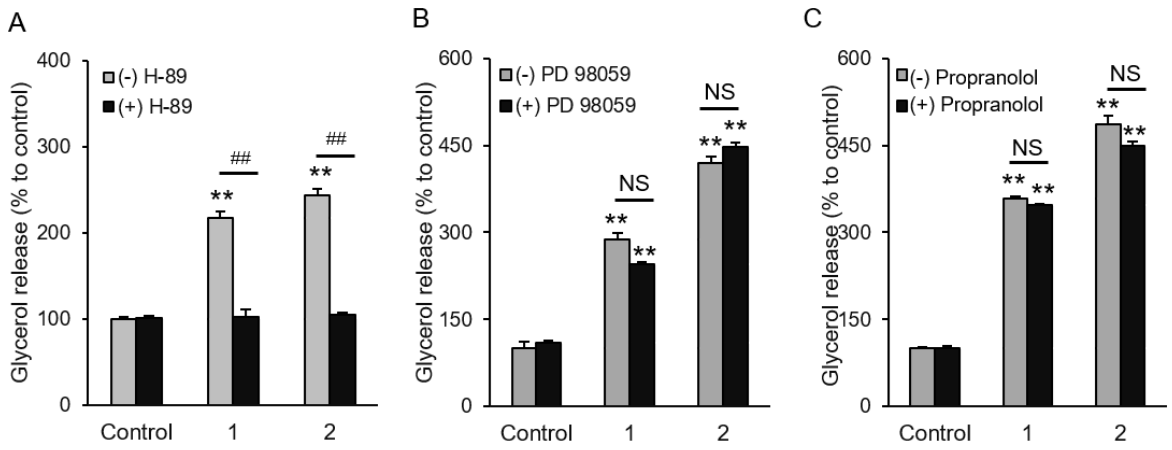

Figure 3.22 Effect of specific inhibitors on glycerol release enhancement activity of compounds **1** and **2**. 3T3-L1 adipocytes were pre-treated with (A) inhibitor of PKA (H-89, 20 μM), (B) inhibitor of ERK (PD 98059, 50 μM), or (C) inhibitor of β3-adrenergic receptor (propranolol 1 μM) and then treated with **1** and **2** (25 μM). Glycerol release values are percentages to control without inhibitor. Data are expressed as mean ± SEM (n=6). **p<0.01 *vs.* control without inhibitor (Dunnett's test); $^{\#\#}p$<0.01 (t-test); NS: No significance.

Initially, the two well-known lipolytic signaling molecules; protein-kinase A (PKA) and extracellular signal-regulated kinase (ERK), were tested by co-incubating compounds **1** and **2** with the respective specific inhibitors (Fig. 3.22A and 3.22B). Inhibitor of PKA (H-89) totally diminished the activity of both compounds, but inhibitor of ERK (PD 98059) had no significant effect on the lipolytic activity. To further investigate the target of compounds **1** and **2**, β3-adrenergic receptor, the major upstream target of PKA, was examined (Mori et al., 2009). Compounds **1** and **2** were co-incubated with propranolol, an antagonist of β3-adrenergic receptor, but the antagonist had no effect on the lipolytic activity of the both compounds (Fig. 3.22C). Lipolytic activity of compounds **1** and **2** might also work through the other upstream related signaling proteins, but not through the β3-adrenergic receptor located at the cell membrane.

3.1.5.3.2 Protein Immunoanalysis of 1- and 2-stimulated Lipolysis

To confirm the results of inhibitory challenges, protein immunoanalysis was conducted to determine the activation of PKA by compounds **1** and **2**. Western blot analysis was performed to examine the activation of the target protein, phosphorylated PKA (p-PKA) and total PKA (PKA). The amount of the phosphorylated protein and the total protein was quantified, and the ratios the two-forms as well as the representative immunoblots are presented in Figure 3.24.

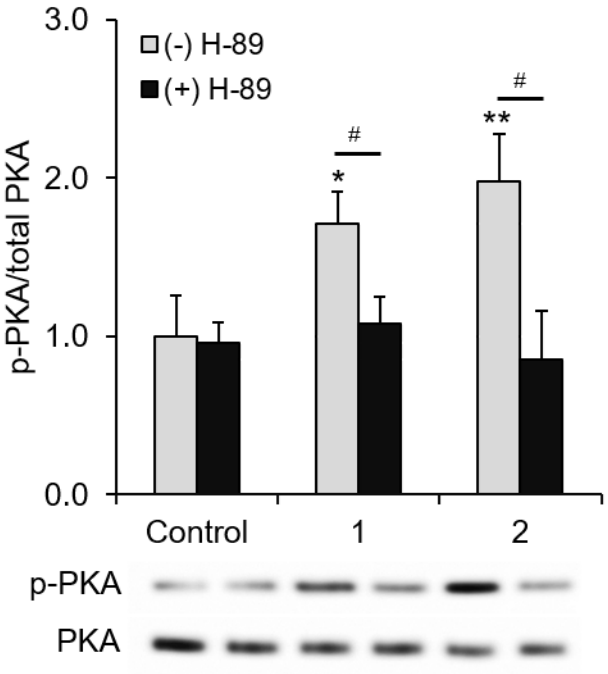

Figure 3.23 Analysis of PKA activation after treatment of **1** and **2**. 3T3-L1 adipocytes were pre-treated with or without inhibitor of PKA (H-89, 20 µM) and then treated with **1** or **2** (12.5 µM). Cells were lysed and subjected to SDS-PAGE followed by western blotting. Data are expressed as mean ± SEM (n=4). A representative immunoblot is shown. *p<0.05, **p<0.01 *vs.* blank (Dunnett's test); $^{\#}p$<0.05 (t-test).

Protein immunoblotting analysis also confirmed the activation of PKA by both compounds **1** and **2** (Figure 3.23). Based on these findings, it is conclusively evident that compounds **1** and **2** induce their lipolytic effects in white adipocytes through the activation of PKA (Figure 3.25).

The results of lipolytic mechanisms between EL extract and the isolated compounds (compounds **1** and **2**) shows that EL activated both PKA and ERK, while compounds **1** and **2** activated PKA but not ERK. The absence of ERK activation by the isolated compounds suggests that there might be other lipolytic compounds that activated ERK but they were not successfully isolated. Although these compounds might be present in trace concentrations, they might have synergistically activated ERK in mixture form in the plant extract. Other possibility is that the compounds in EL extract that activate ERK may be the compounds that also involve in spermatogenesis, as postulated in §3.1.4.

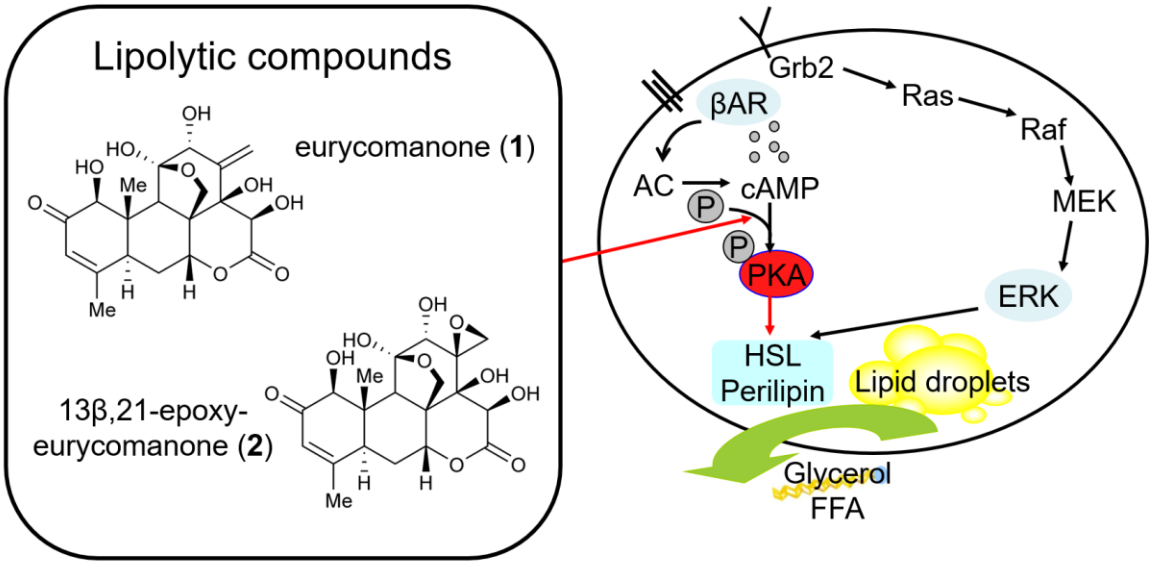

Figure 3.25 Isolated compounds **1** and **2** exert lipolytic activity through PKA activation

Further study on the anti-obesogenic activity of the isolated compounds **1** and **2** was conducted in brown adipocytes, a different type of adipocytes with distinguished physiological properties from white adipocytes. This collaborative research with the Tseng Lab (Joslin Diabetes Center, USA) is an explorative research to investigate other potential mode of anti-obesogenic activity in different cell line. The results of the anti-obesogenic activity of compounds **1** and **2** in brown adipocytes are presented in the following sub-section.

3.1.5.4 Effects of Compounds 1 and 2 on Lipid Accumulation and Lipolysis in Brown Adipocytes

Due to its distinguished properties in utilizing lipid and thermogenesis, brown adipocytes have been recently studied for new approach in anti-obesity research. Compounds **1** and **2** were examined for their anti-obesogenic activities; reduction of lipid accumulation and enhancement of lipolysis, in WT-1 brown adipocytes. The results of the two assays are presented in Figure 3.26.

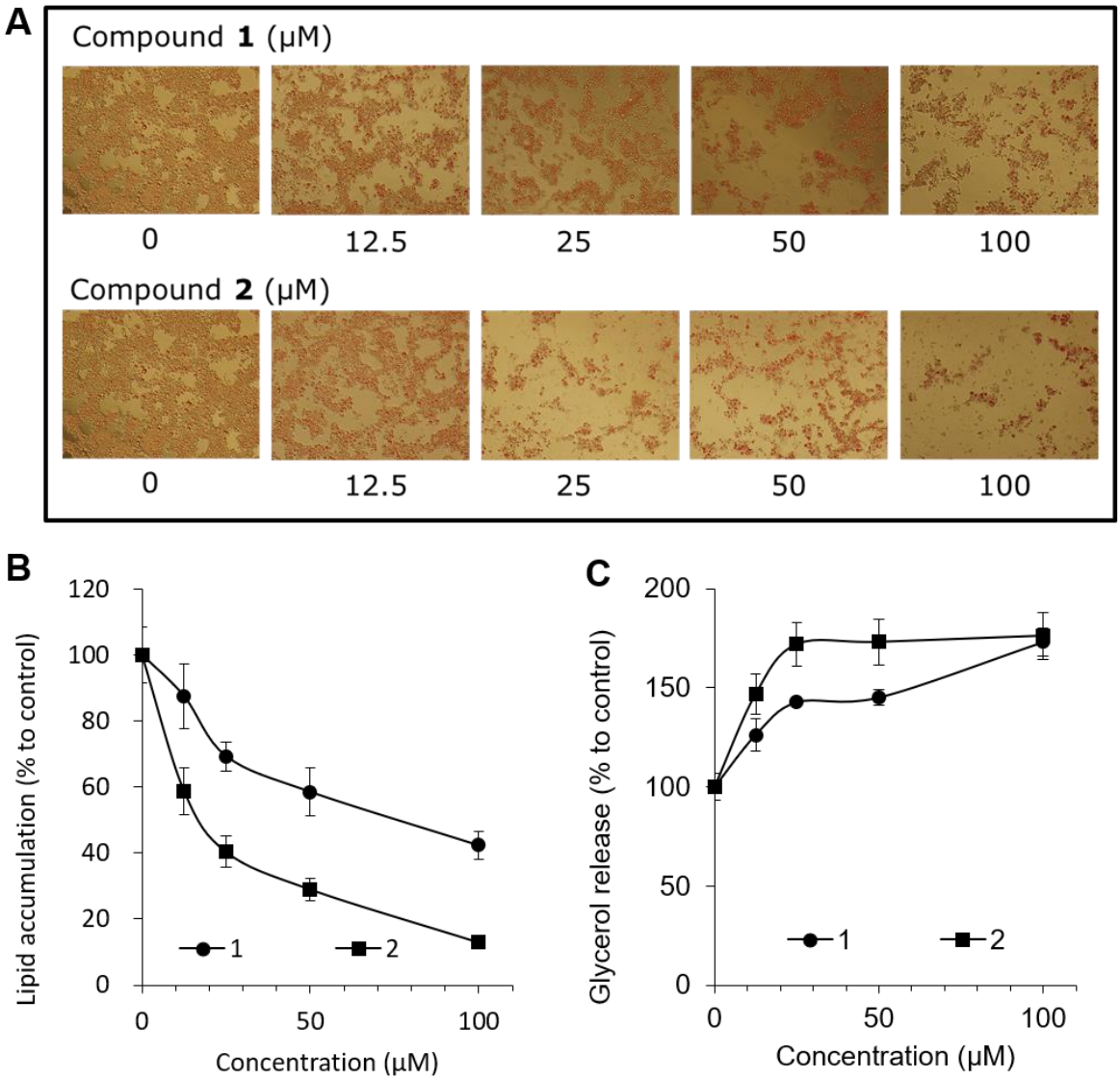

Figure 3.26 Photograph of Nile Red-stained lipid droplets under fluorescence microscope (A), lipid accumulation reduction effect (B), and glycerol release enhancement activity (C) of compounds **1** and **2** in WT-1 brown adipocytes. (A) Magnification 200x. (B) Compound **1** showed significant difference above 25 μM (p<0.01). Compound **2** showed significant difference above 12.5 μM (p<0.01). (C) Compounds **1** and **2** showed significant difference above 12.5 μM (p<0.05). Isoproterenol (1 μM) and CL 316,243 (1 μM) were used as positive control, with glycerol release 183±19% and 183±5%, respectively. Data are expressed as mean ± SEM (n=8). Dunnett's test was used.

Compounds **1** and **2** showed concentration-dependent activity in the reduction of lipid accumulation and enhancement of glycerol release as shown in Figure 3.25. For the reduction of lipid accumulation, lipid-reducing activity of compounds **1** and **2** in brown adipocytes (42 ± 4% and 13 ± 1%, at 100 μM, respectively) seemed to be stronger than that in white adipocytes (**1** and **2** (100 μM) 71 ± 2% and 63 ± 3%, respectively). However, the lipid accumulation assays were conducted in different assays; ORO for white adipocytes and Nile

Red for brown adipocytes. Using the same assay method, compounds **1** and **2** reduced lipid accumulation stronger in white adipocytes than that in brown adipocytes (**Appendix 6**). Thus, compounds **1** and **2** are more effective in reducing lipid droplets in white adipocytes, indicating selectivity in target cells. This activity difference, in fact, will serve as beneficial property of compounds **1** and **2**.

As for the glycerol release enhancing-activity, both compounds **1** and **2** demonstrated significant enhancement above 12.5 µM. At higher concentrations, however, the enhancement rate of compound **1** was slower than that of compound **2**. Similar results were also obtained in the white adipocytes, in which compound **1** exerted weaker enhancement (EC_{50}=14.6 µM) than compound **2** (EC_{50}=8.6 µM).

Even though lipolytic activity of compounds **1** and **2** in brown adipocytes (EC_{50}=11.5 µM for **2**) was slightly weaker than that in white adipocytes (EC_{50}=8.6 µM for **2**), brown adipocytes were less sensitive to the isolated compounds. These were reflected by the difference of the sample incubation time, in which brown adipocytes required longer incubation time (two days) to allow enough accumulation of glycerol in the culture medium (**Appendix 7** showed the result of the same incubation time (one-day) in brown adipocytes). These results are in agreement with previous report that measurement of glycerol release in brown adipocytes tends to underestimate lipolysis, due to a significant portion of glycerol released being re-phosphorylated (Nicholls and Locke, 1984).

Lipolysis has been known to give an acute thermogenic response in brown adipocytes. Although lipolysis can also be assayed by the release of fatty acids, the net export of fatty acids from brown adipocytes will also underestimate lipolysis by the extent to which the fatty acids are oxidized (Nicholls and Locke, 1984). Instead of being released, this fatty acid oxidation has been utilized as fuel in brown adipocytes (Ouellet et al., 2012, Townsend and Tseng, 2014).

This indication leads to the hypothesis that compounds **1** and **2** may enhance thermogenesis process in brown adipocytes, suggesting further study on the thermogenic activity of the isolated compounds in brown adipocytes. Furthermore, it is also interesting to study the target proteins in the brown adipocytes, investigating whether the compounds activate fat-browning proteins. It is expected that the results of these further studies can lead to a better understanding of the bioactivities of this compound in brown adipocytes and to explore new therapeutical target for obesity treatment.

3.2 Lipolytic activity of *Brucea javanica* (L.) Merr.

3.2.1 Bioactivities of *Brucea javanica* (L.) Merr.

In the search for lipolytic compounds from other Indonesian medicinal plants, *Brucea javanica* (L.) Merr. is a promising option, due to its rich quassinoid constituents. Initially, fruit extract of *B. javanica* (BJ) was subjected to lipid accumulation and cell viability assays (Figure 3.27).

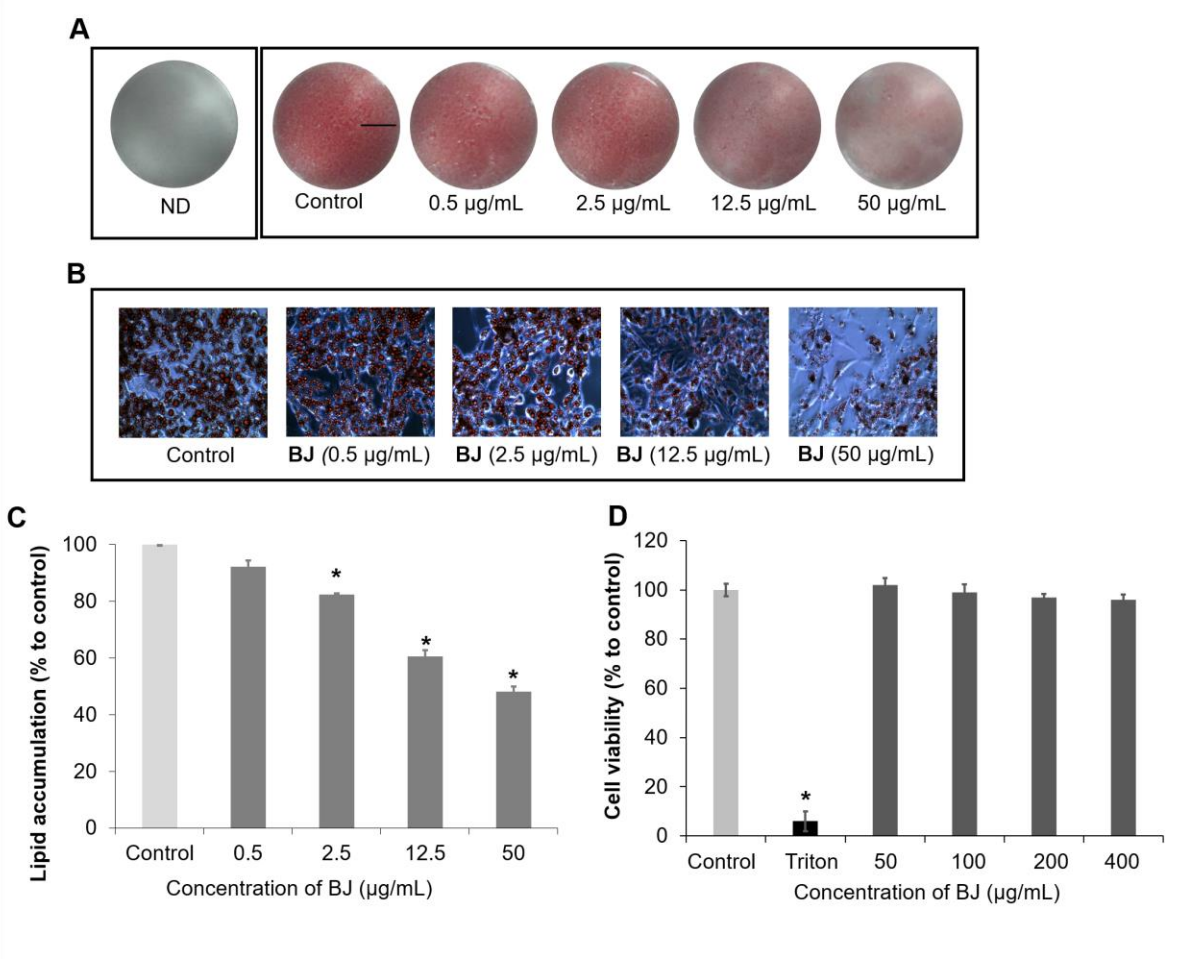

Figure 3.26 Lipid reducing-activity and cytotoxicity of BJ in 3T3-L1 adipocytes. (A) Photograph of Oil Red O-stained differentiated 3T3-L1 cells, representative from three independent experiments. Scale bar = 3 mm. ND, non-differentiation. (B) Lipid droplets as captured with microscope (200x magnification). (C) Dissolved Oil Red O was measured at the absorbance of 520 nm. (C) Cell viability of 3T3-L1 adipocytes after treatment with BJ. Data are expressed as mean ± SEM (n = 3) of three independent experiments. *p value ≤ 0.01 versus control (Student's t-test).

As demonstrated in Figure 3.26C, BJ significantly reduced lipid accumulation in 3T3-L1 white adipocytes at concentration as low as 2.5 µg/mL, when the tested concentrations ranged from 0.5 to 50 µg/mL. A cell viability assay needed to be performed to examine

whether the low lipid accumulation value is the result of lipid accumulation reduction or cytotoxicity of BJ in the white adipocytes. It is shown that the treatment with various concentrations of BJ did not cause significant cell death in the white adipocytes, even at the concentration as high as 400 µg/mL (Figure 3.26D). These results confirm the strong reduction of lipid accumulation and rule out cytotoxicity effect of BJ in the white adipocytes.

The subsequent glycerol release enhancement assay was also conducted for various concentrations of BJ (Figure 3.28).

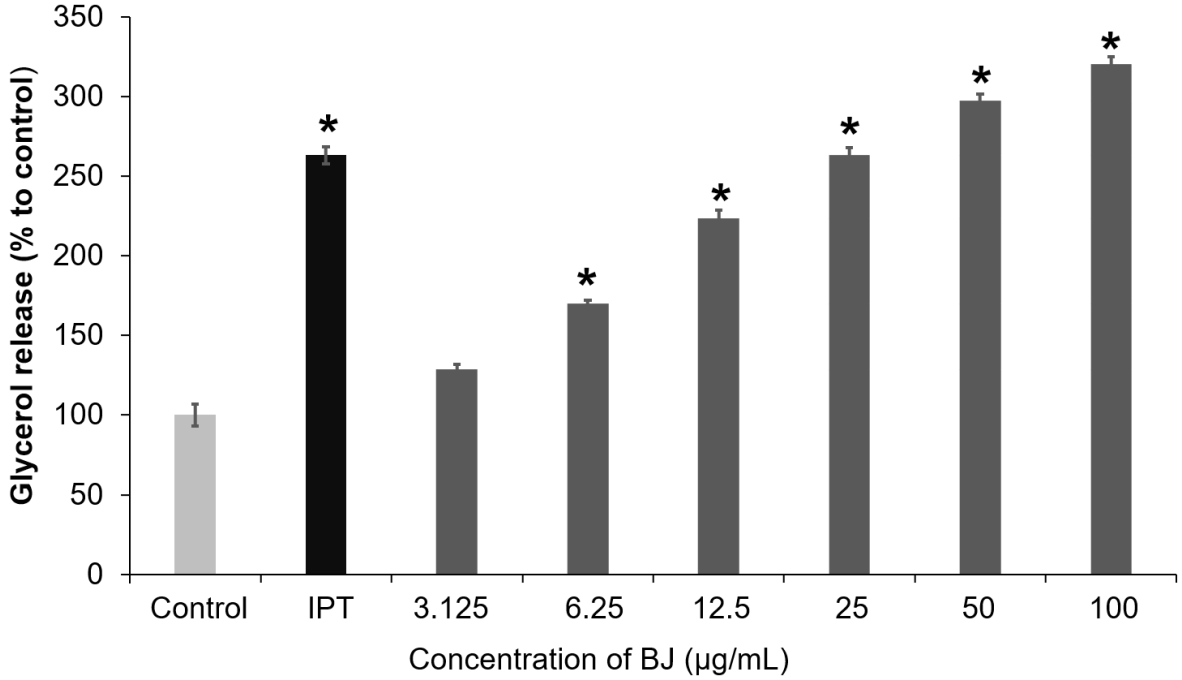

Figure 3.28 Effects of BJ on lipolysis in 3T3-L1 adipocytes. IPT, isoproterenol 1 µM was used as the positive control. Data are expressed as mean ± SEM (n = 6) and are representative of three independent experiments. ** $p < 0.01$ versus untreated cells.

BJ strongly enhanced the release of glycerol from 3T3-L1 adipocytes at a concentration as low as 3.125 µg/mL, and increased glycerol release in a concentration-dependent manner thus showing a significant lipolytic activity (Figure 3.27). In order to further study its lipolytic mechanism of action, an inhibitory challenge was performed. PKA as the major lipolytic protein was chosen as the target pathway, and the results are presented in Figure 3.29.

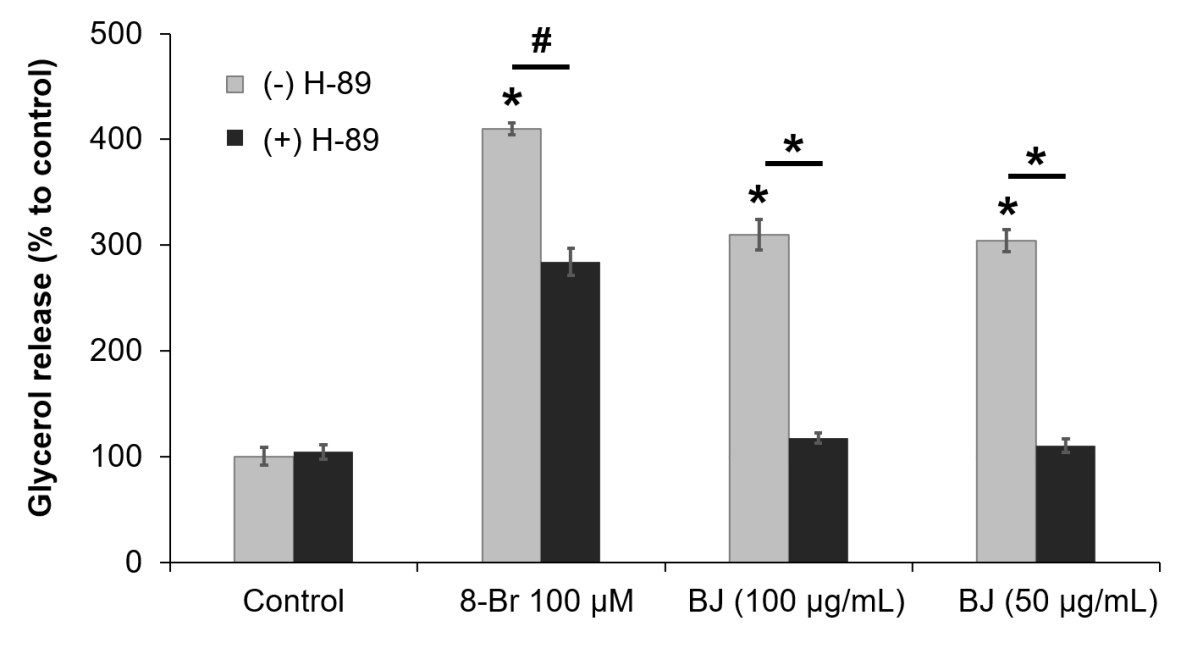

Figure 3.29 Effect of PKA inhibitor on the BJ-stimulated lipolysis. 3T3-L1 adipocytes were pre-treated with inhibitor of PKA (20 µM H-89) for 1 hour. 8-Br-cAMP (100 µM) was used as positive control. Glycerol release values are percentages to control without inhibitor. Data are expressed as mean ± SEM (n = 6). *p<0.01 versus control without inhibitor (Dunnett's test); $^{\#}p$<0.05 versus without H-89 (t-test).

As shown in Figure 3.28, inhibitor of PKA (H-89) totally diminished lipolytic activity of BJ to the basal levels. These results suggest that strong enhancement of lipolysis by BJ is mediated via PKA pathway. Due to the strong lipolytic activity of BJ, further study on the isolation of the responsible lipolytic compounds was conducted, and the following sub-section reports the results of the bioassay-guided fractionation.

3.2.2 Bioassay-guided Fractionation of Lipolytic Compounds from *Brucea javanica*

The purpose of this isolation was to elucidate the responsible compounds from *B. javanica* that enhanced lipolysis in 3T3-L1 white adipocytes. The bioassay-guided fractionation was performed using glycerol release enhancement assay in 3T3-L1 adipocytes as described in §2.6. Multiple fractionation steps of separation by column chromatography, TLC and HPLC were performed to give six purified compounds (compounds **5**-**10**). Fractionation steps of the bioassay-guided isolation and purification of the isolated compounds from the ethyl acetate layer are described in Figure 3.30.

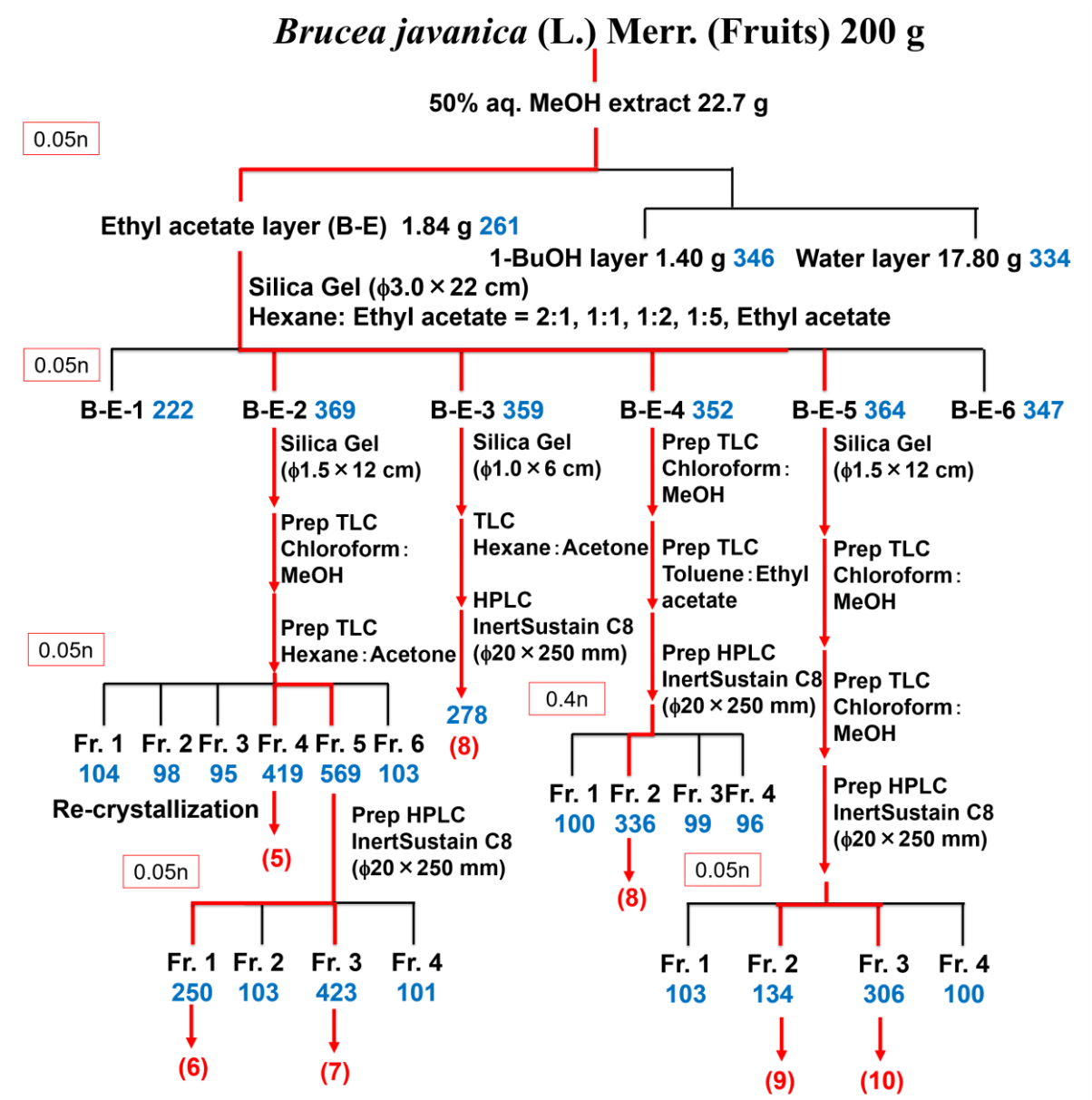

Figure 3.30 Fractionation scheme of *B. javanica* from its ethyl acetate layer.
Remarks:
200 = percentage of glycerol release (% to control)

$$1\ n = \frac{\text{extracted material (1 g)}}{\text{solution volume (10 mL)}}$$

Dried fruits of *B. javanica* was extracted with 50% (v/v) aq. methanol. The extract was dried and partitioned with water, 1-butanol, and ethyl acetate. The ethyl acetate layer, the highest active fraction, was separated by silica gel column to obtain six fractions. Through subsequent silica gel column and purification by TLC and HPLC, four fractions yielded in six lipolytic compounds **5-10**. They are known-quassinoids founds in Brucea genus, namely

bruceine A (**5**), brusatol (**6**), bruceantinol (**7**), bruceine B (**8**), 3'-hydroxybrucein A (**9**), and bruceine C (**10**). ^{1}H-NMR and ^{13}C-NMR spectra followed with ESI-MS data are presented here. Identification of the six known compounds was accomplished by comparing their spectroscopic data with those in the literature.

Bruceine A (5)

^{1}H-NMR and ^{13}C-NMR spectra of compound **5** are shown in Figure 3.31 and 3.32, respectively.

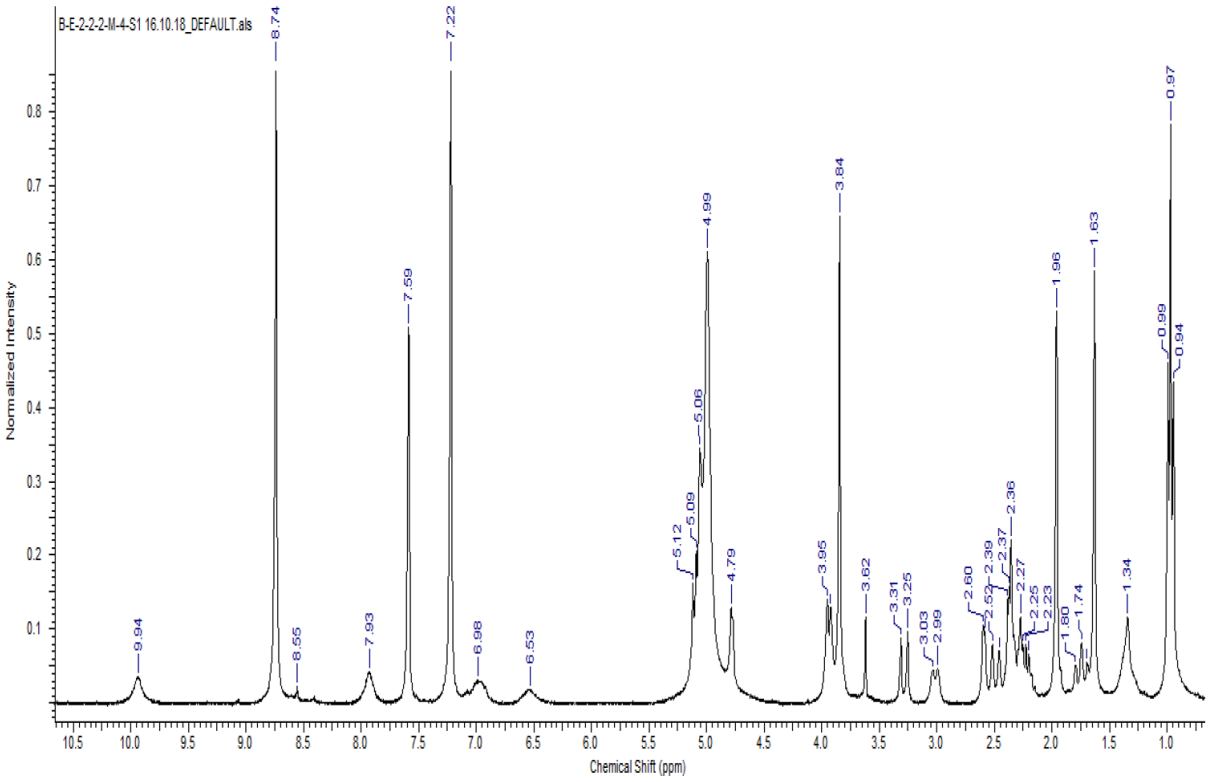

Figure 3.31 ^{1}H-NMR spectrum of compound **5**

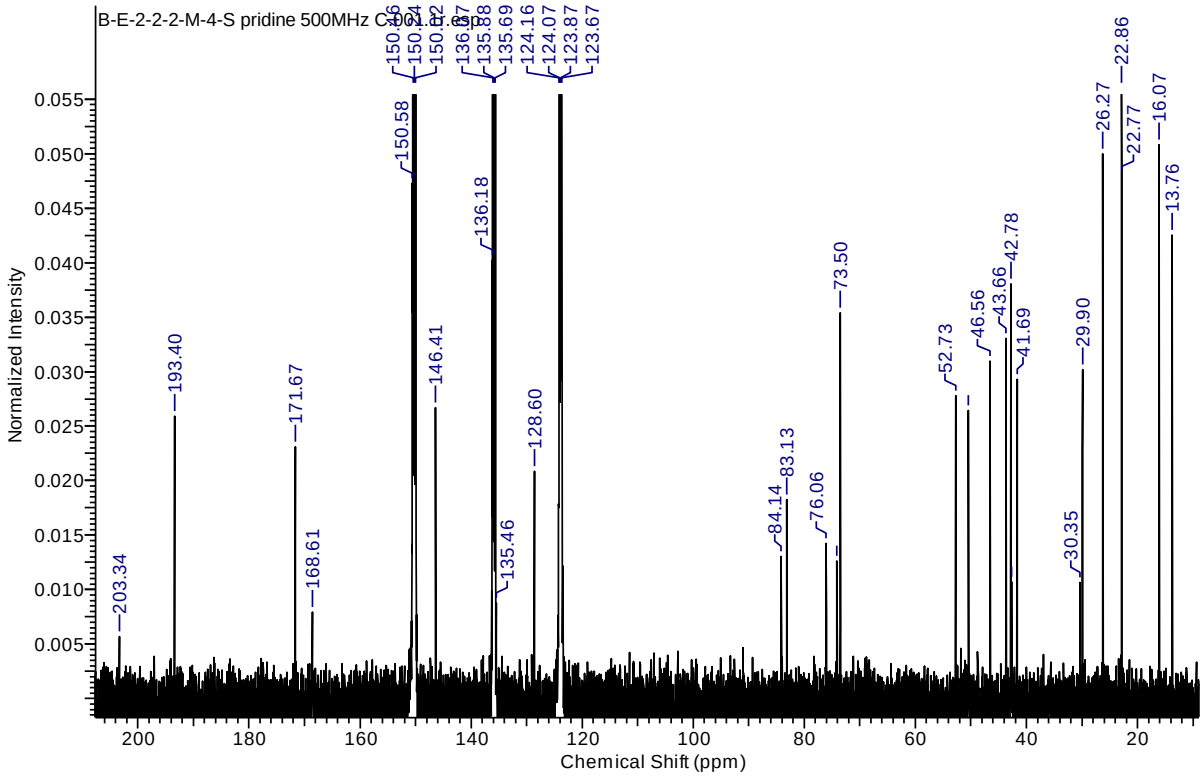

Figure 3.32 ^{13}C-NMR spectrum of compound **5**

The NMR data of compound **5** are consistent with those reported for bruceine A (Yoshimura et al., 1985), thus compound **5** was confirmed as bruceine A (Figure 3.33).

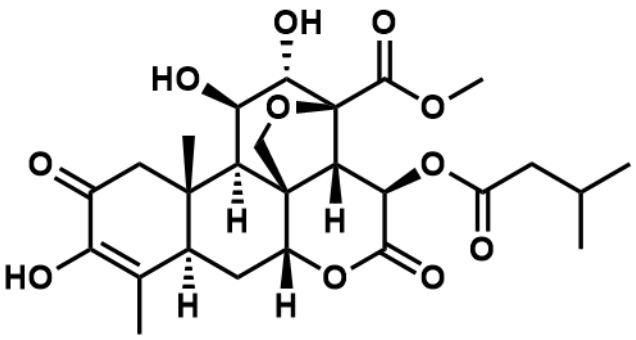

Figure 3.33 Structure of bruceine A (**5**)
^{13}C-NMR (125 MHz, pyridine-d_5, rt): 13.8, 16.1, 22.8, 22.9, 26.3, 29.9, 41.7, 42.7, 42.8, 43.7, 46.6, 50.5, 52.7 (OMe), 68.8, 73.5, 74.1, 76.1, 83.1, 84.1, 128.6, 146.4, 168.6, 171.7, 193.4 ppm. C14, C1'; not detected.
ESI-MS (positive): found m/z = 545, $[M+Na]^+$

Brusatol (6)

^{1}H-NMR and ^{13}C-NMR spectra of compound **6** are shown in Figure 3.34 and 3.35, respectively.

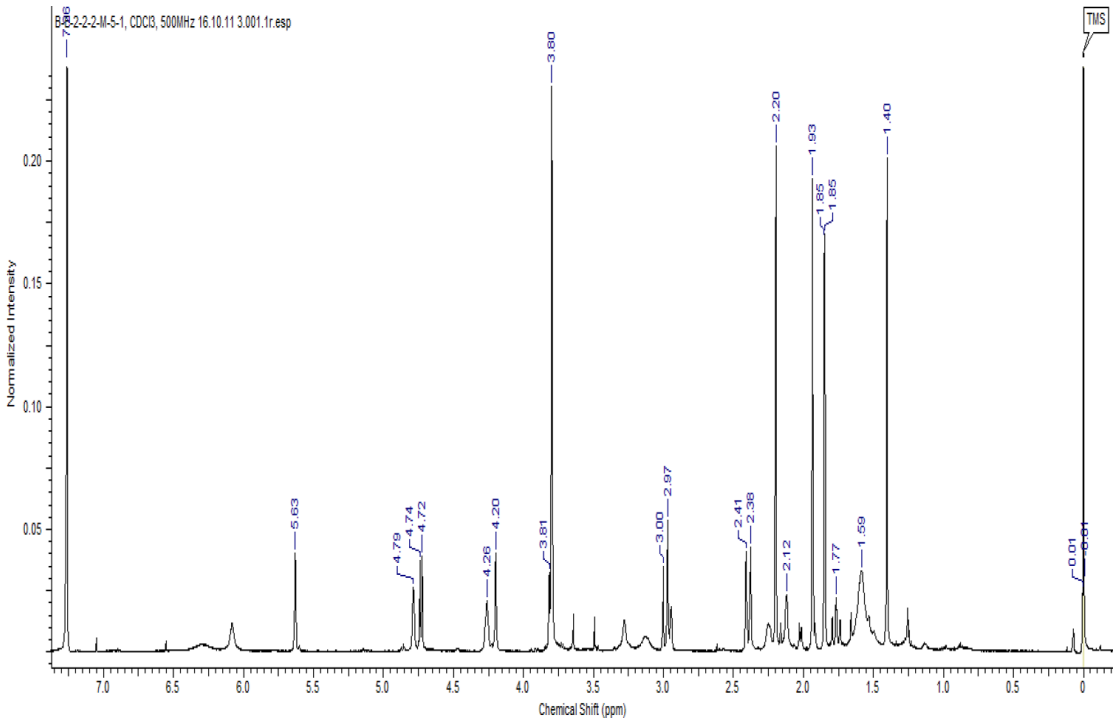

Figure 3.34 ^{1}H-NMR spectrum of compound **6**

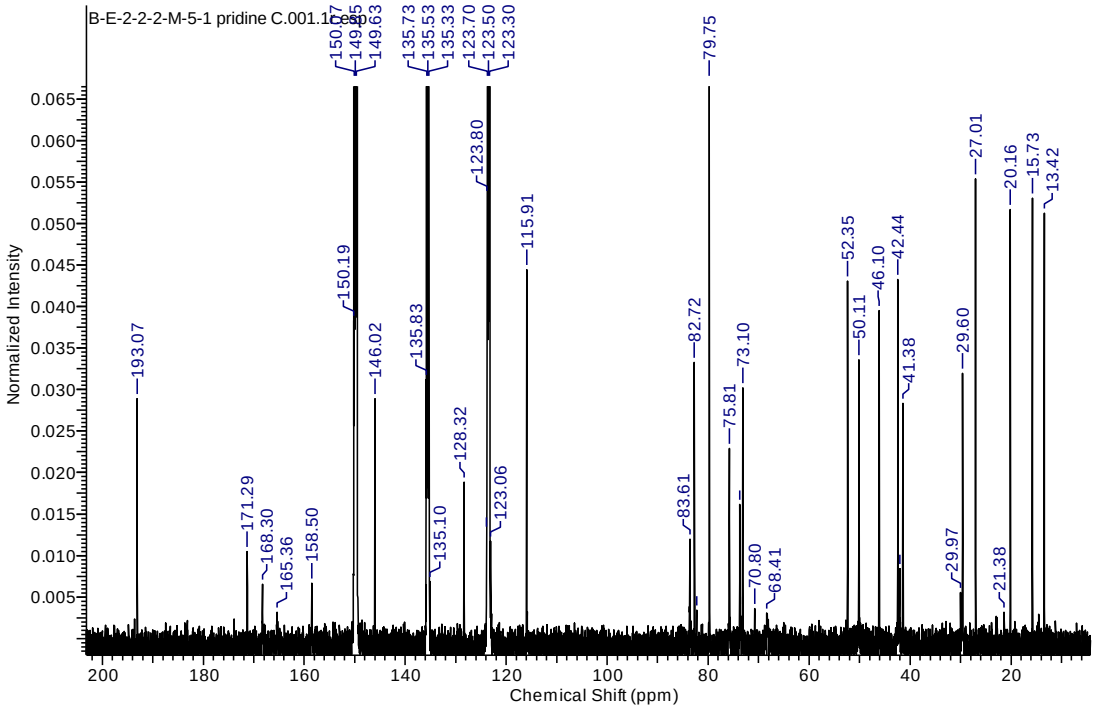

Figure 3.35 ^{13}C-NMR spectrum of compound **6**

The NMR data of compound **6** are consistent with those reported for brusatol (Yoshimura et al., 1985), thus compound **6** was confirmed as brusatol (Figure 3.36).

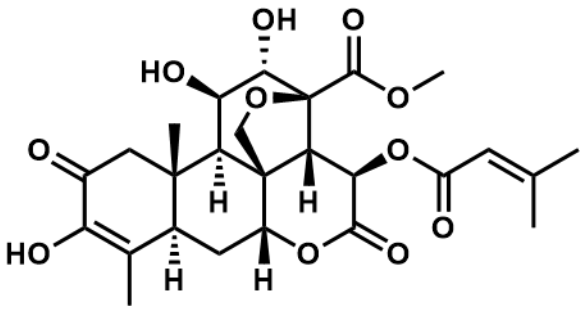

Figure 3.36 Structure of brusatol (**6**)
^{13}C-NMR (125 MHz, pyridine-d_5, rt): 13.8, 16.1, 22.8, 22.9, 26.3, 29.9, 41.7, 42.7, 42.8, 43.7, 46.6, 50.5, 52.7 (OMe), 68.8, 73.5, 74.1, 76.1, 83.1, 84.1, 128.6, 146.4, 168.6, 171.7, 193.4 ppm. C14, C1'; not detected.
ESI-MS (positive): found *m*/*z* = 543, $[M+Na]^+$

Bruceantinol (7)

^{1}H-NMR and ^{13}C-NMR spectra of compound **7** are shown in Figure 3.37 and 3.38, respectively.

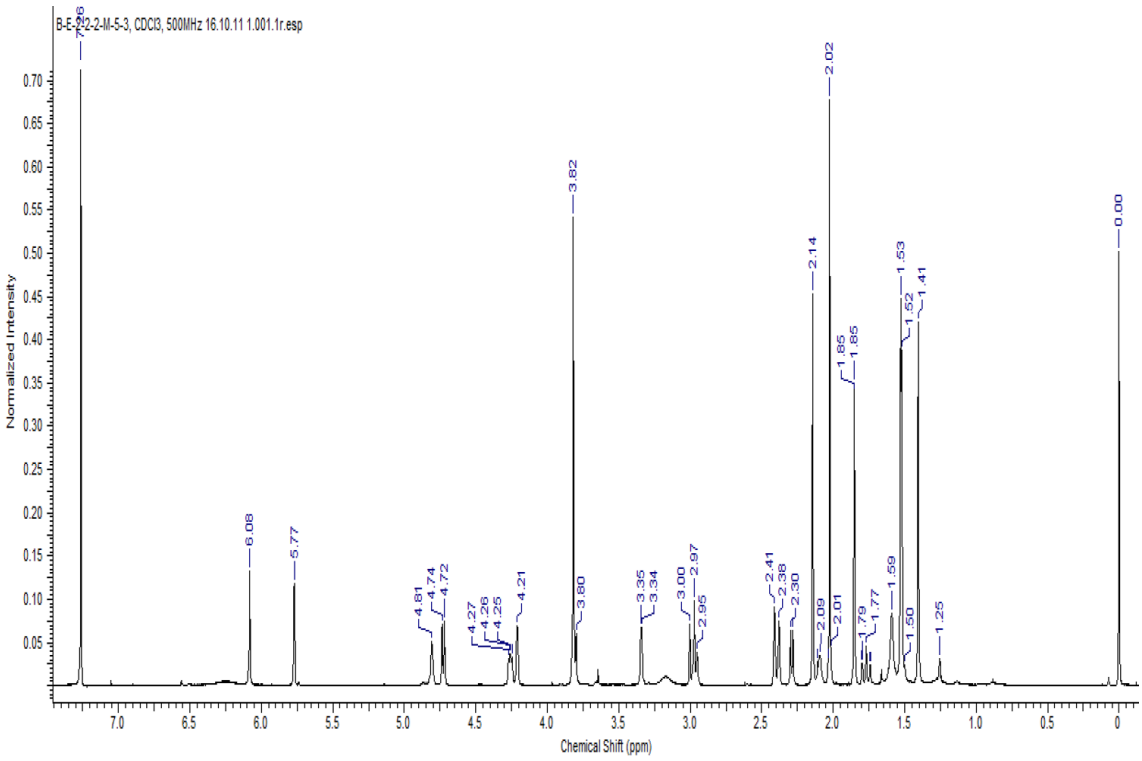

Figure 3.37 ^{1}H-NMR spectrum of compound **7**

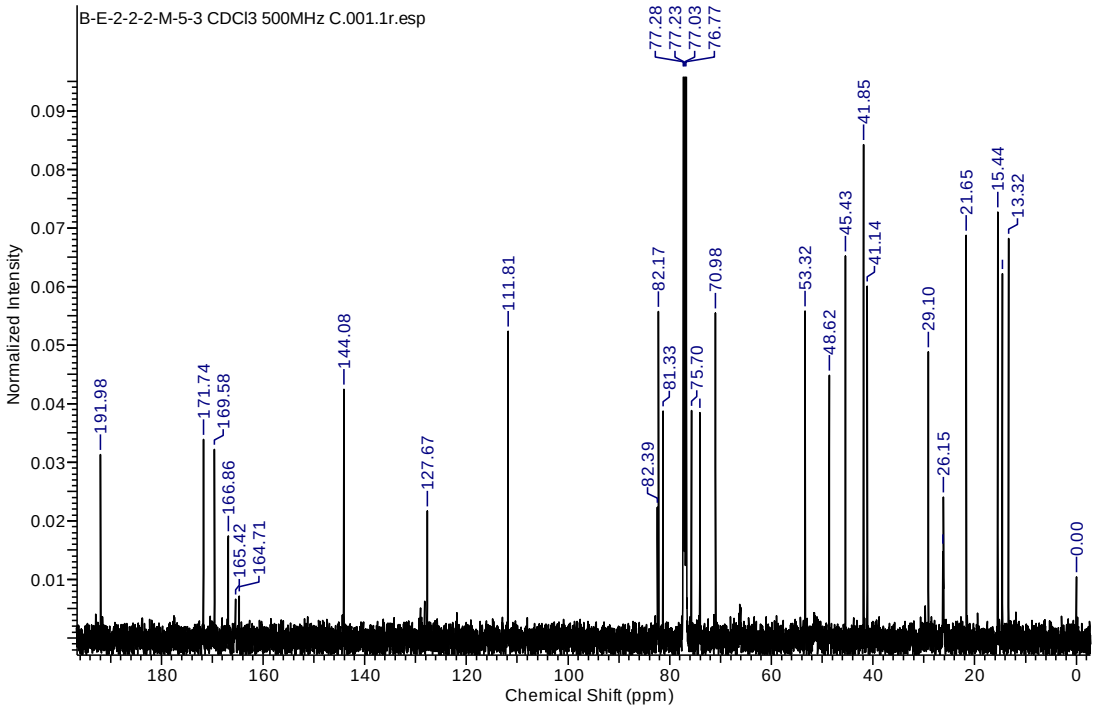

Figure 3.38 ^{13}C-NMR spectrum of compound **7**

The NMR data of compound **7** are consistent with those reported for bruceantinol (Sakaki et al. 1986), thus compound **7** was confirmed as bruceantinol (Figure 3.39).

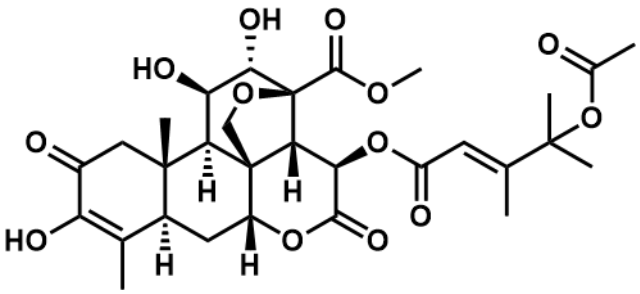

Figure 3.39 Structure of bruceantinol (**7**)
^{13}C-NMR (125 MHz, chloroform-*d*, rt): 13.32, 14.59, 15.44, 21.65, 26.15, 26.15, 26.24, 29.1, 41.14, 41.14, 41.85, 45.43, 48.62, 51.5, 53.32, 66.17, 70.98, 74.09, 77.23, 81.33, 82.17, 82.39, 111.81, 127.67, 144.08, 164.71 (OMe), 166.86, 169.58, 171.74, 184.42, 191.98 ppm.
ESI-MS (positive): found *m*/*z* = 629, $[M+Na]^+$

Bruceine B (8)

^{1}H-NMR spectrum of compound **8** are shown in Figure 3.40.

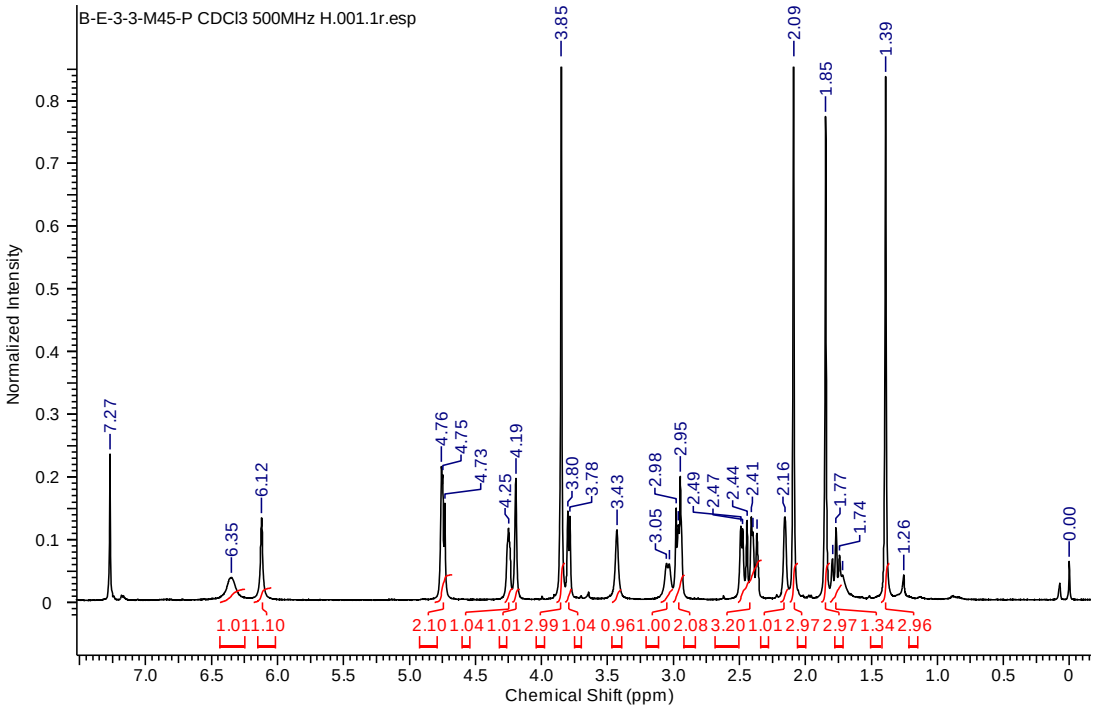

Figure 3.40 ^{1}H-NMR spectrum of compound **8**

The NMR data of compound **8** are consistent with those reported for bruceine B (Murakami et al., 2003), thus compound **8** was confirmed as bruceine B (Figure 3.41).

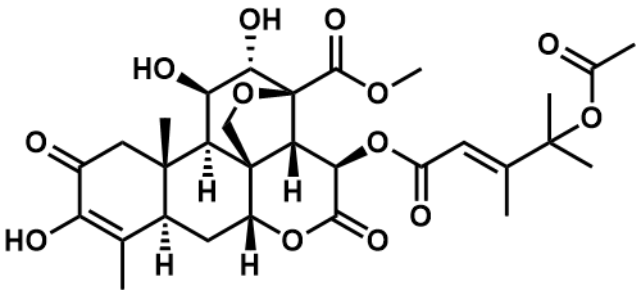

Figure 3.41 Structure of bruceine B (**8**)
^{1}H-NMR (500 MHz, chloroform-*d*, rt): 1.41 (1H, s), 1.78 (1H, td), 1.85 (1H, d), 2.1 (1H, s, OAc), 2.15 (1H, brd), 2.38 (1H, td), 2.41 (1H, brd), 2.94 (1H, brs), 2.96 (1H, brd), 2.99 (1H, brd), 3.29 (1H, brs, OH), 3.81 (1H, d), 4.74 (1H, d), 3.87 (CO2Me, s), 4.19 (1H, brs), 4.27 (1H, brs), 4.27 (1H, dd), 6.38 (1H, brs), 6.09 (1H, s, OH), ppm.
ESI-MS (positive): found *m/z* = 503, $[M+Na]^{+}$

3'-hydroxybrucein A (9)

^{1}H-NMR and ^{13}C-NMR spectra of compound **9** are shown in Figure 3.42 and 3.43, respectively.

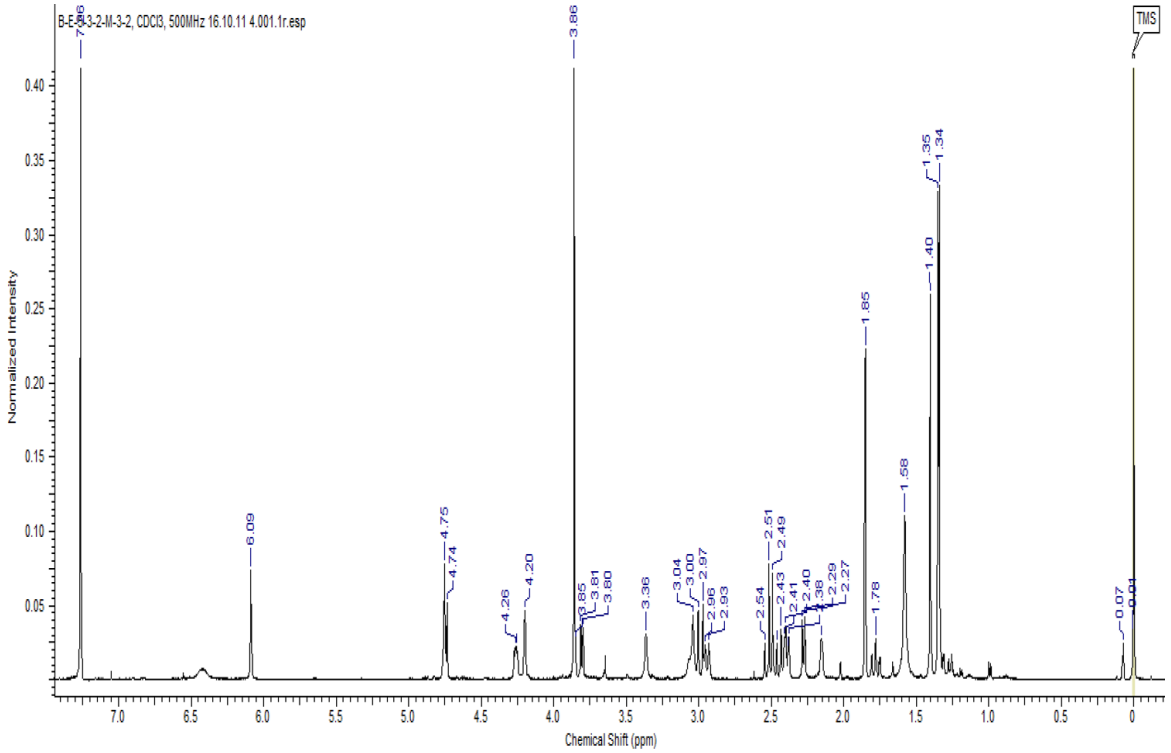

Figure 3.42 ^{1}H-NMR spectrum of compound **9**

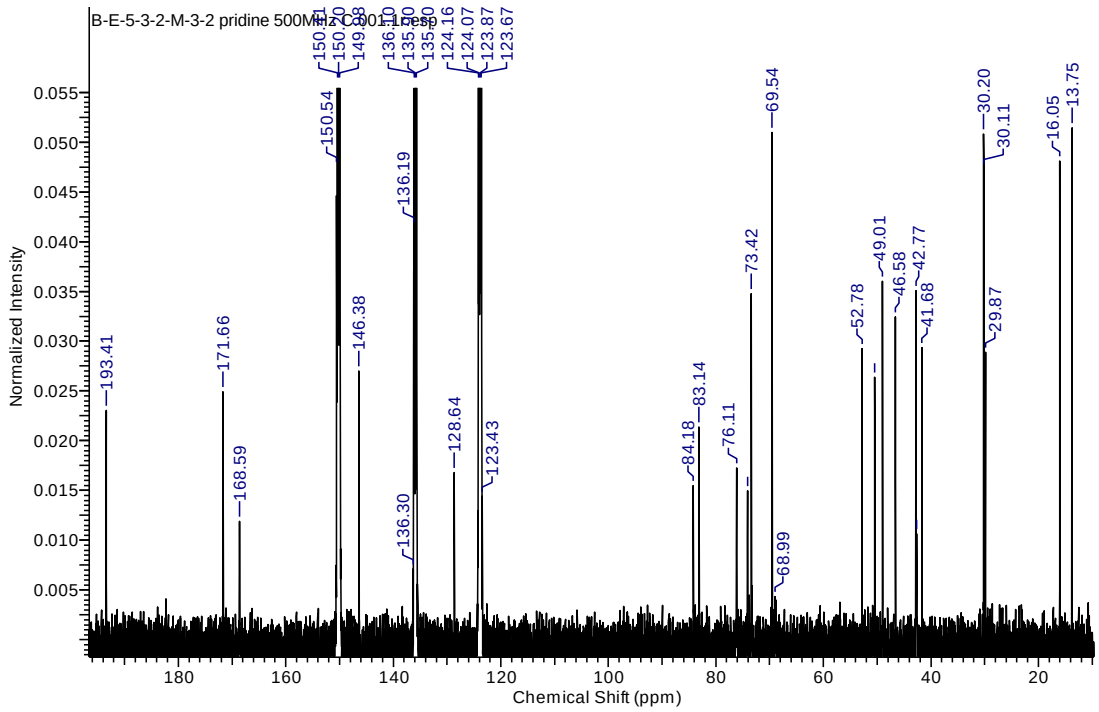

Figure 3.43 ^{13}C-NMR spectrum of compound **9**

The NMR data of compound **9** are consistent with those reported for 3'-hydroxybrucein A (Yoshimura et al., 1985), thus compound **9** was confirmed as 3'-hydroxybrucein A (Figure 3.44).

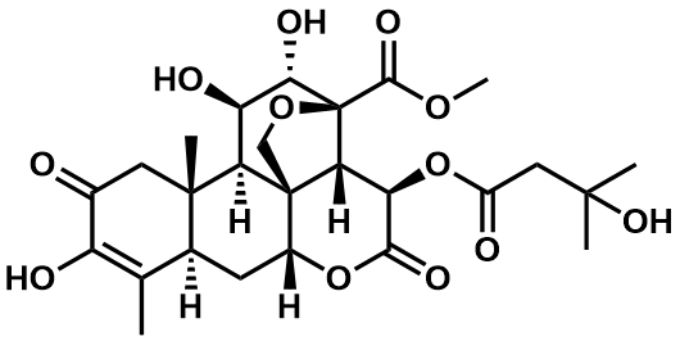

Figure 3.44 Structure of 3'-hydroxybrucein A (**9**)
^{13}C-NMR (125 MHz, pyridine-d_5, rt): 13.75, 16.05, 29.87, 30.11, 30.2, 42.63, 42.77, 46.58, 49.01, 50.43, 52.78 (OMe), 69.54, 73.42, 74.08, 74.68, 76.11, 83.14, 84.18, 128.64, 146.38, 168.59, 171.66, 193.41 ppm. C14, C15, C1'; not detected.
ESI-MS (positive): found m/z = 561, $[M+Na]^+$

Bruceine C (10)

^{1}H-NMR and ^{13}C-NMR spectra of compound **10** are shown in Figure 3.45 and 3.46, respectively.

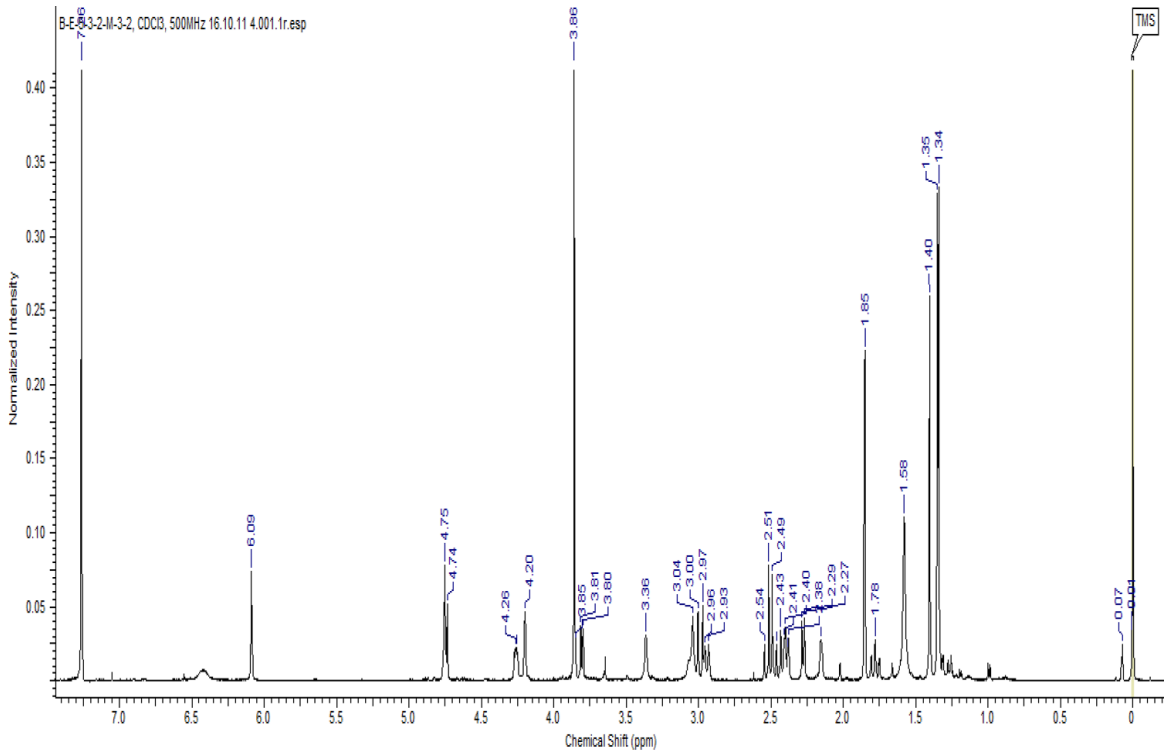

Figure 3.45 ^{1}H-NMR spectrum of compound **10**

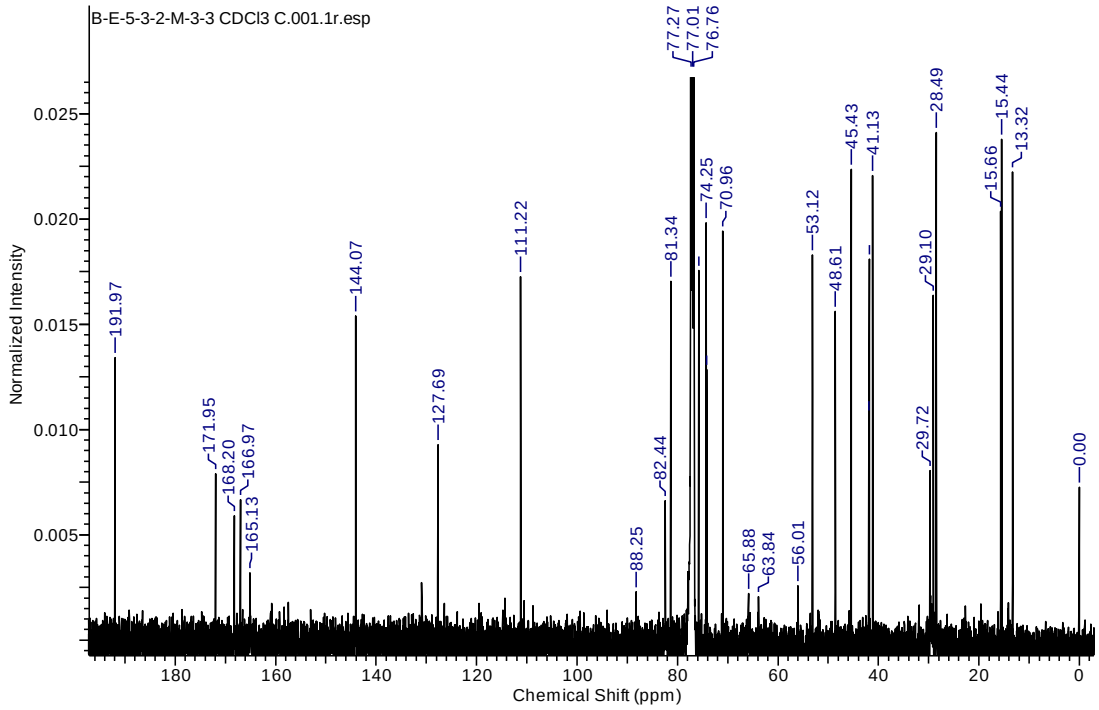

Figure 3.46 ^{13}C-NMR spectrum of compound **10**

The NMR data of compound **10** are consistent with those reported for bruceine C (Yoshimura et al., 1985), thus compound **10** was confirmed as bruceine C (Figure 3.47).

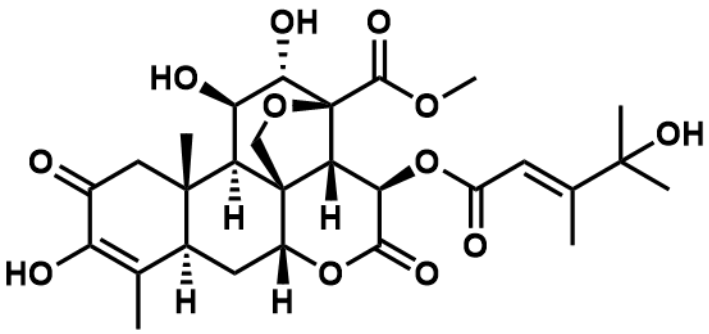

Figure 3.47 Structure of bruceine C (**10**)
^{13}C-NMR (125 MHz, chloroform-*d*, rt): 13.17, 15.3, 15.52, 28.37, 28.41, 28.98, 41.04, 41.75, 41.84, 45.35, 48.53, 51.78, 53.06 (OMe), 65.82, 70.94, 74.14, 74.23, 75.76, 81.33, 82.42, 111.27, 127.77, 144.19, 165.29, 167.13, 168.36, 172.13, 192.17 ppm.
ESI-MS (positive): found *m*/*z* = 587, $[M+Na]^+$

Following the isolation of compounds **5-10**, lipolytic activity of each compound was examined (Figure 3.48).

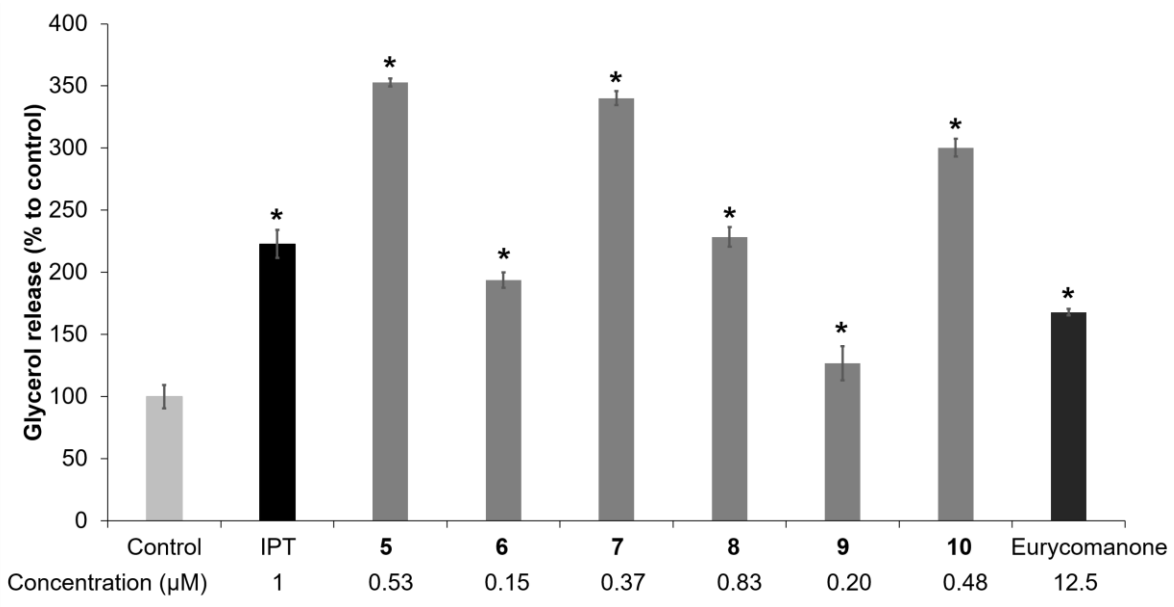

Figure 3.48 Effects of compounds **5-10** on lipolysis in 3T3-L1 adipocytes. IPT, isoproterenol 1 μM was used as the positive control. Tested compounds: bruceine A (**5**), brusatol (**6**), bruceantinol (**7**), bruceine B (**8**), 3'-hydroxybrucein A (**9**), and bruceine C (**10**). Data are expressed as mean ± SEM (n = 6) and are representative of three independent experiments. *$p < 0.01$ versus untreated cells.

As shown in Figure 3.48, compounds **5-10** significantly enhanced lipolysis in 3T3-L1 white adipocytes. Due to the low yield of the isolates, the tested concentration of **5-10** was not uniform. Nevertheless, when compared with the lipolytic activity of eurycomanone (12.5 μM), compounds **5-10** exerted stronger lipolytic activity when tested in lower concentrations than eurycomanone. These results confirm stronger lipolysis enhancement of *B. javanica* extract (Figure 3.28) than that of *E. longifolia* extract (Figure 3.2).

3.2.3 Discussion on *Brucea javanica* (L.) Merr.

In regard of bioactivity of *B. javanica* in metabolic disorders, there was not much research that studies its activity in glucose and lipid metabolism. So far, there was only one report on its hypoglycemic effects of its two quassinoids, bruceine D and E, in STZ-induced diabetic rats (Noorshahida et al., 2009). As for research in lipid metabolism, this study is the first study to explore and elucidate lipolytic compounds from *B. javanica*. Thus, it is expected that this effort can lead to the development of anti-obesity research from this species.

B. javanica exerted not only lipolytic activity, but also strong reduction of lipid accumulation. This dual mode of action suggests promising anti-obesogenic effects from this plant. As six lipolytic compounds have been isolated from *B. javanica* (compounds **5**-**10**), a future work in bioassay-guided fractionation based on anti-lipogenic activity will be of great interest. The elucidated compounds may or may not the same quassinoids possessing lipolytic activity. Thus, the results may lead to dual target of the same quassinoids or synergetic effects from different compounds with different mode of actions from *B. javanica*.

Bruceine A, B, and C (**5**, **8**, **10**) and bruceantinol (**7**) were first isolated from *Brucea amarissima*, a species from Brucea genus (Polonsky et al., 1967), in which a revised structure was made by the same research group for compound **7** (Polonsky et al., 1980). Brusatol (**6**) was first isolated from *Brucea sumatrana* Roxb., another Brucea species (Sim et al., 1967). Although a number of quassinoids from Brucea have been widely studied for anti-tumor effects, brusatol (**6**), in particular, has received extensive exposure for this activity (Lee et al., 1984, Zhang et al., 2013, Olayanju et al., 2015, Xiang et al., 2017).

Isolated compounds from Brucea genus have been widely studied for anti-tumor, anti-malaria and anti-parasite activities (Lee et al., 1984, O'Neill et al., 1987, Bawm et al., 2008), that killed or inhibited growth of other organisms. However, in this study, there was no cell death observed in 3T3-L1 white adipocytes when treated with *B. javanica* extract (Figure 3.28A). This might have been due to the strong viability of the white adipocytes, or due to the mixture of various constituents in the crude extract that cumulatively reduced its cytotoxicity. Hence, cytotoxicity assay in the white adipocytes may also be performed for each isolated compound.

3.3 Anti-obesogenic Screening of Indonesian Medicinal Plants

In the lipid metabolism regulation, anti-obesogenic effects can be generally divided into two mode of actions, anti-lipogenesis and enhancement of lipolysis (Figure 3.49). In the previous sections, *E. longifolia* and *B. javanica*, have been investigated for their activity of enhancement of lipolysis. In the effort to explore other potential plants with different mode of actions, this section reports the results of the anti-obesogenic screening of Indonesian medicinal plants. The 76 selected Indonesian plant extracts were subjected to two bioassays, namely lipid accumulation and glycerol release assays (Table 3.1).

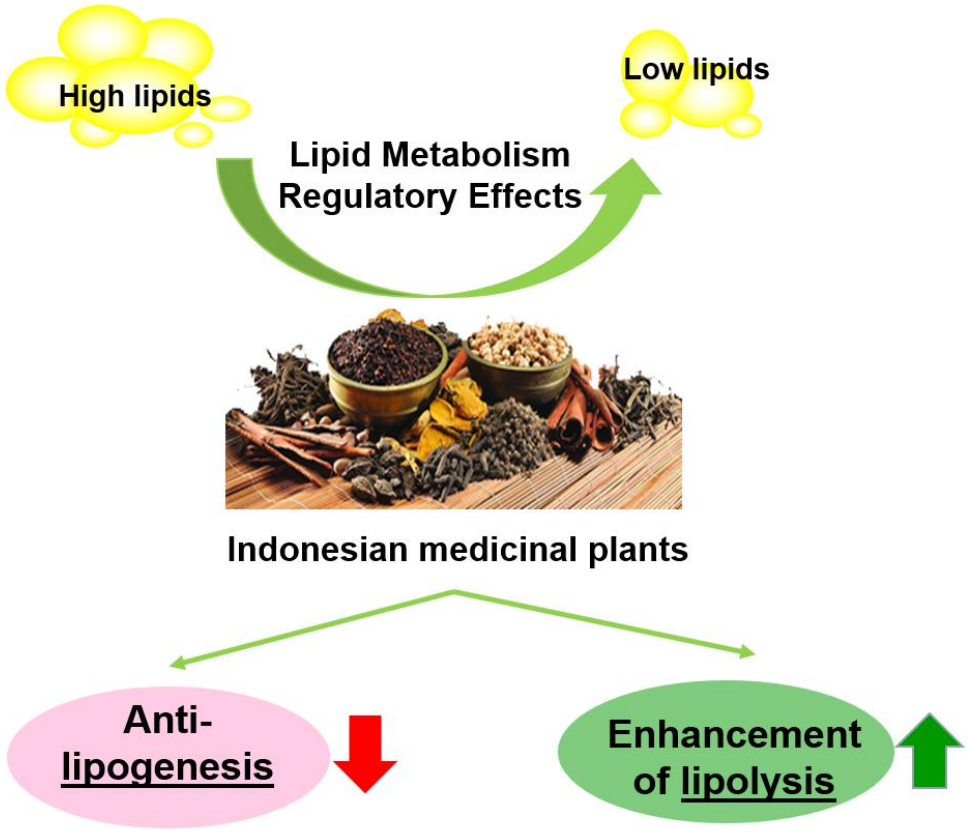

Figure 3.48 Lipid metabolism regulatory effects from Indonesian medicinal plants

Table 3.1 Lipid accumulation and glycerol release results of selected Indonesian plant extracts

Plant species	Batch number	Local name	Part used	Lipid accumulation (% to control)	Glycerol release (% to control)
Abrus precatorius L.	AP1314.052	Saga	Leaves	92.7 ± 3.2	95.5 ± 2.0
Aleurites moluccanus (L.) Willd.	AM1314.011	Kemiri	Fruits	89.7 ± 4.1	76.7 ± 2.5
Alpinia galanga (L.) Willd.	AG1314.073	Lengkuas	Rhizomes	89.6 ± 2.5	103.0 ± 3.3
Alstonia scholaris (L.) R. Br.	AS1314.004	Pule	Bark	89.0 ± 2.7	100.0 ± 1.8
Amomum cardamomum L.	AC1314.036	Kapulogo	Fruits	88.4 ± 3.1	101.4 ± 3.2
Andrographis paniculata (Burm.f.) Nees	AP1314.042	Sambiloto	Whole plant	88.6 ± 3.1	101.4 ± 6.2
Areca catechu L.	AC1314.006	Pinang	Fruits	87.6 ± 3.4	103.4 ± 2.3
Averrhoa bilimbi L.	AB1314.070	Belimbing wuluh	Leaves	92.0 ± 0.8	90.9 ± 2.8
Azadirachta indica A.Juss.	AI1314.051	Mimba	Leaves	93.8 ± 1.0	104.1 ± 3.4
Baeckea frutescens L.	BF1314.023	Jungrahab	Bark	89.3 ± 1.3	95.2 ± 2.3
Blumea balsamifera (L.) DC.	BB1314.007	Sembung	Leaves	92.0 ± 1.1	92.5 ± 2.8
Brucea javanica (L.) Merr.	BJ1314.031	Buah Makasar	Fruits	52.1 ± 1.6*	309.1 ± 5.9*
Caesalpinia sappan L.	CS1314.17	Kayu secang	Wood	90.2 ± 4.1	83.2 ± 6.0
Carica papaya L.	CP1314.049	Pepaya	Leaves	99.9 ± 3.8	95.8 ± 3.2
Centella asiatica (L.) Urb.	CA1314.041	Pegagan	Whole plant	97.2 ± 1.8	95.0 ± 5.0
Cinnamomum burmanni (Nees & T.Nees) Blume	CB1314.065	Kayu manis	Bark	83.0 ± 1.5	110.9 ± 3.6
Cinnamomum cassia (L.) J.Presl	CC1314.015	Kembang lawang	Fruits	92.9 ± 1.1	94.1 ± 4.3
Citrus hystrix DC.	CH1314.030	Daun jeruk	Leaves	90.2 ± 0.9	110.1 ± 6.0
Clerodendrum serratum (L.) Moon	CS1314.013	Akar senggugu	Roots	62.0 ± 2.0*	157.1 ± 3.2*
Coriandrum sativum L.	CS1314.068	Ketumbar	Seeds	89.7 ± 3.2	110.9 ± 4.9
Curcuma aeruginosa Roxb.	CA1314.039	Temu ireng	Rhizomes	93.4 ± 0.5	98.3 ± 1.6
Curcuma heyneana Valeton & Zijp	CH1314.038	Temu giring	Rhizomes	97.4 ± 2.7	116.8 ± 2.1

Continued on the following page

Plant species	Batch number	Local name	Part used	Lipid accumulation (% to control)	Glycerol release (% to control)
Curcuma zanthorrhiza Roxb.	CX1314.040	Temulawak	Rhizomes	96.9 ± 3.8	95.2 ± 6.2
Curcuma zedoaria (Christm.) Roscoe	CZ1213.001	Temu putih	Rhizomes	90.4 ± 3.3	107.6 ± 13.9
Cymbopogon citratus (DC.) Stapf	CC1314.053	Sere minyak	Leaves	96.3 ± 2.9	92.4 ± 1.7
Elaeocarpus grandiflorus Sm.	ES1314.064	Kayuanyang	Fruits	93.2 ± 1.2	113.4 ± 7.7
Elephantopus scaber L.	E1113.001	Tapak liman	Leaves	100.1 ± 5.8	118.7 ± 5.2
Eleutherine americana (Aubl.) Merr. ex K.Heyne	EA1314.054	Bawang sabrang	Leaves	99.5 ± 1.8	101.7 ± 8.2
Eleutherine americana (Aubl.) Merr. ex K.Heyne	EA1314.055	Bawang sabrang	Bulbs	96.1 ± 1.9	100.0 ± 4.2
Eugenia aromatica (L.) Baill.	EA1314.050	Cengkeh	Leaves	97.1 ± 2.8	96.6 ± 5.6
Eugenia polyantha Barb. Rodr.	EP1314.056	Daun salam	Leaves	101.7 ± 1.9	95.0 ± 5.0
Eurycoma longifolia Jack	EL1314.057	Pasak bumi	Roots	91.7 ± 1.2	141.7 ± 6.0*
Foeniculum vulgare Mill.	FW1314.003	Adas-Jogja	Seeds	91.4 ± 2.3	94.1 ± 10.7
Guazuma ulmifolia Lam.	GU1314.033	Jati Belanda	Leaves	91.1 ± 2.0	146.8 ± 16.4
Gynura procumbens (Lour.) Merr.	GP1314.058	Sambung nyawa	Leaves	88.8 ± 0.7	105.8 ± 7.5
Helicteres isora L.	HI1314.063	Kayu ulet	Fruits	86.7 ± 0.9	118.7 ± 9.7
Kaempferia angustifolia Roscoe	KA1314.037	Kunci pepet	Rhizomes	86.7 ± 1.6	95.9 ± 5.5
Kaempferia galanga L.	KG1314.059	Kencur	Rhizomes	82.4 ± 3.8	92.4 ± 5.8
Leucaena leucocephala (Lam.) de Wit	LL1314.075	Lamtoro	Seeds	91.4 ± 0.9	97.1 ± 5.9
Leucas lavandulifolia Sm.	LL1314.014	Leng-lengan	Whole plant	90.1 ± 1.7	123.5 ± 5.2*
Melaleuca leucadendra (L.) L.	ML1314.024	Merica bolong	Fruits	63.3 ± 0.9*	133.6 ± 13.3*
Melastoma polyanthum Burm. f.	MP1314.019	Senggani	Roots	88.4 ± 1.3	92.4 ± 6.8
Mentha arvensis L.	MA1314.060	Menta	Leaves	86.8 ± 0.5	124.8 ± 1.6*
Mimosa pigra L.	MP1314.018	Putri malu	Whole plant	84.5 ± 2.2	100.6 ± 3.0
Momordica charantia L.	MC1314.043	Pare	Fruits	74.5 ± 3.0*	110.6 ± 2.0

Continued on the following page

Plant species	Batch number	Local name	Part used	Lipid accumulation (% to control)	Glycerol release (% to control)
Morinda citrifolia L.	MC1314.029	Mengkudu	Fruits	82.6 ± 1.4	96.5 ± 6.3
Moringa oleifera Lam.	MO1314.071	Kelor	Leaves	94.9 ± 2.6	88.3 ± 5.8
Morus alba L.	MA1314.044	Bebesaran Lampung	Leaves	95.4 ± 2.1	94.7 ± 8.0
Myristica fragrans Houtt.	MY1013.001	Pala	Fruits	93.6 ± 1.8	97.7 ± 4.2
Nigella sativa L.	NS1314.028	Jintan hitam	Seeds	92.4 ± 1.5	99.4 ± 7.7
Ocimum gratissimum L.	OG1314.067	Selasih	Seeds	91.6 ± 8.5	95.9 ± 5.6
Orthosiphon aristatus (Blume) Miq.	OA1314.061	Kumis kucing	Whole plant	89.4 ± 1.2	92.4 ± 6.1
Pachystachys coccinea (Aubl.) Nees	PC1314.002	Pronojiwo	Fruits	89.6 ± 1.0	109.1 ± 2.1
Pandanus amaryllifolius Roxb.	PA1314.025	Daun pandan	Leaves	85.6 ± 0.8	102.9 ± 5.1
Phaleria macrocarpa (Scheff.) Boerl.	PM1314.034	Mahkota dewa	Fruits	84.4 ± 3.3	101.8 ± 2.1
Phyllanthus urinaria L.	PU1314.012	Meniran	Whole plant	95.5 ± 2.6	103.5 ± 7.2
Physalis angulata L.	PA1314.32	Ciplukan	Whole plant	91.0 ± 2.8	118.9 ± 1.7
Pimpinella anisum L.	PA1314.045	Adas manis	Seeds	92.8 ± 1.6	125.5 ± 12.1*
Piper betle L.	PB1314.062	Sirih	Leaves	92.1 ± 0.7	106.2 ± 2.5
Piper crocatum Ruiz & Pav.	PC1314.066	Sirih merah	Leaves	88.3 ± 0.5	142.0 ± 5.6*
Piper nigrum L.	PN1314.027	Lada hitam	Fruits	85.1 ± 1.4	74.1 ± 5.2
Piper retrofractum Vahl	PR1314.026	Cabe jawa	Fruits	88.5 ± 2.3	74.1 ± 3.0
Plantago major L.	PM1314.072	Daun sendok	Leaves	100.1 ± 1.0	100.0 ± 13.7
Ruellia tuberosa L.	RT 1314.001	Ceplikan	Fruits	90.6 ± 0.8	63.0 ± 4.8
Sapindus rarak DC.	SD1314.069	Lerak	Fruits	95.0 ± 0.7	187.0 ± 8.2*
Selaginella doederleinii Hieron.	TI1314.046	Cakar ayam	Leaves	96.9 ± 3.6	85.2 ± 3.7
Sonchus arvensis L.	SA1314.008	Tempuyung	Leaves	89.1 ± 2.1	77.8 ± 4.8
Swietenia mahagoni (L.) Jacq.	SM1314.020	Mahoni	Seeds	86.7 ± 3.5	82.6 ± 2.6

Continued on the following page

Plant species	Batch number	Local name	Part used	Lipid accumulation (% to control)	Glycerol release (% to control)
Syzygium aromaticum (L.) Merr. & L.M.Perry	SA1314.022	Cengkeh	Fruits	89.8 ± 1.5	81.5 ± 3.0
Tamarindus indica L.	TI1314.047	Asam Jawa	Fruits	84.1 ± 2.8	97.0 ± 1.7
Terminalia bellirica (Gaertn.) Roxb.	TB1314.009	Joho	Fruits	93.9 ± 1.3	92.6 ± 18.8
Tinospora crispa (L.) Hook. f. & Thomson	TC1314.021	Brotowali	Bark	92.3 ± 3.8	87.0 ± 5.6
Typhonium flagelliforme (Lodd.) Blume	TF1314.005	Keladi tikus	Rhizomes	89.4 ± 1.5	101.2 ± 4.9
Usnea barbata	UB1314.048	Kayu angin	Whole plant	88.6 ± 2.4	94.4 ± 5.6
Zingiber officinale Roscoe	ZO1314.074	Jahe merah	Rhizomes	84.6 ± 3.8	66.7 ± 7.4
Zingiber purpureum Roscoe	ZP1314.035	Bengle-Jogja	Rhizomes	80.9 ± 1.0*	181.9 ± 2.9*
Isoproterenol 1 µM					318.5 ± 6.4

Remarks:
Concentration of tested plant extracts in 3T3-L1 cells: 50 µg/mL, lipid accumulation assay using Oil Red O, data are expressed as mean ± SEM (n = 4).

For lipid accumulation using Oil Red O staining (Table 3.1), there are 5 plant extracts that showed lipid reduction more than 20% in the white adipocytes; *Brucea javanica* (L.) Merr., *Clerodendrum serratum* (L.) Moon, *Melaleuca leucadendra* (L.) L., *Momordica charantia* L., and *Zingiber purpureum* Roscoe. As of particular, *B. javanica* (BJ) and *M. leucadendra* (ML) had the highest lipid reduction, 48% and 57%, respectively, at the tested concentration of 50 µg/mL.

As for glycerol release assay, there are 11 out of 76 plant extracts that enhanced glycerol release in the white adipocytes, reflecting a lipolysis enhancing-activity (Figure 3.50).

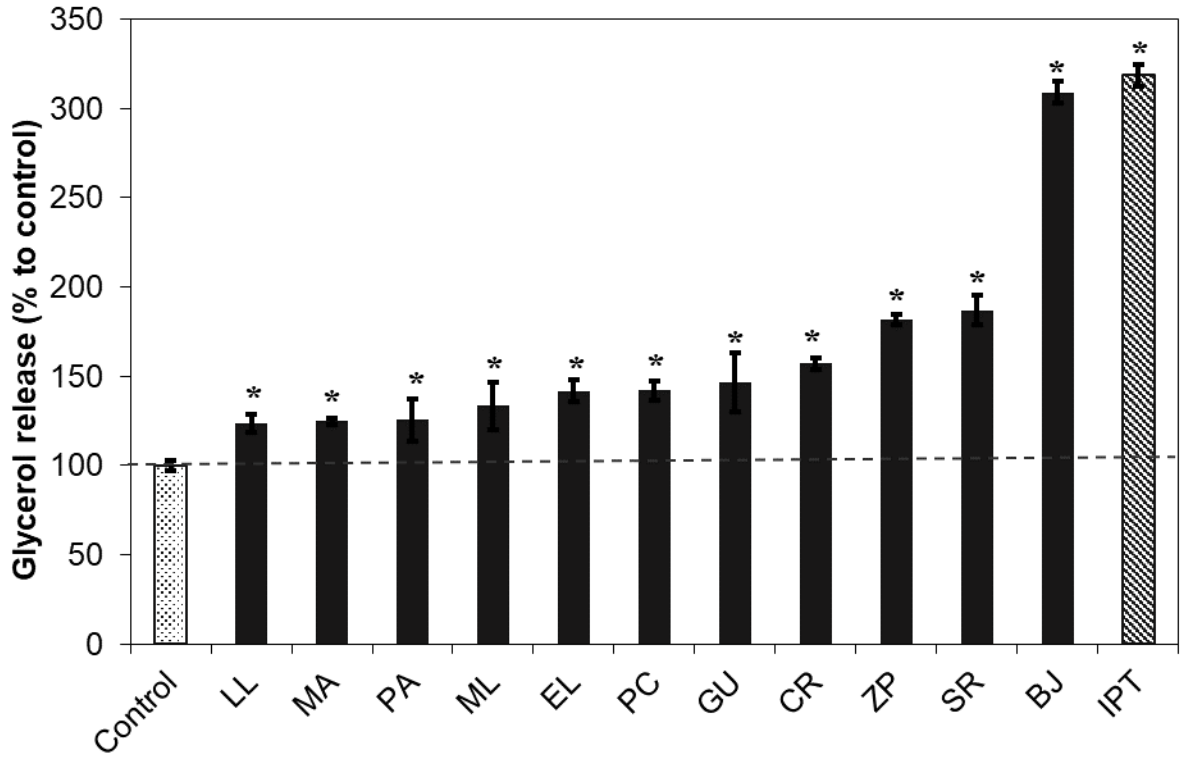

Figure 3.50 Eleven Indonesian plant extracts that enhance glycerol release. Data are expressed as mean ± SEM (n = 4), *p < 0.01 versus control). Concentration of tested plant extracts in 3T3-L1 cells: 50 µg/mL.

Figure 3.50 depicts the activity of the 11 plant extracts that enhanced glycerol release, including *Leucas lavandulifolia* Sm. (LL), *Mentha arvensis* L. (MA), *Pimpinella anisum* L (PA), *Melaleuca leucadendra* (L.) L. (ML), *Eurycoma longifolia* Jack (EL), *Piper crocatum* Ruiz & Pav. (PC), *Guazuma ulmifolia* Lam. (GU), *Clerodendrum serratum* (L.) Moon (CR), *Zingiber purpureum* Roscoe (ZP), *Sapindus rarak* DC. (SR), and *Brucea javanica* (L.) Merr. (BJ).

Based on the results of the reduction of lipid accumulation and enhancement lipolysis

(Figure 3.51), there are plants that both reduced lipid accumulation and enhanced lipolysis, such as BJ, ML, ZP and CR. There are some that enhanced lipolysis but not reduced lipid accumulation, such as LL, MA, PA, EL, PC, GU, and SR. But MC is the plant that reduced lipid accumulation but not enhance lipoysis. It indicates different mode of lipid metabolism regulation in adipocytes; suppression of lipid synthesis and enhancement of lipid catabolism. In the end, lipid accumulation is the result of lipid synthesis and lipid breakdown of the adipocytes.

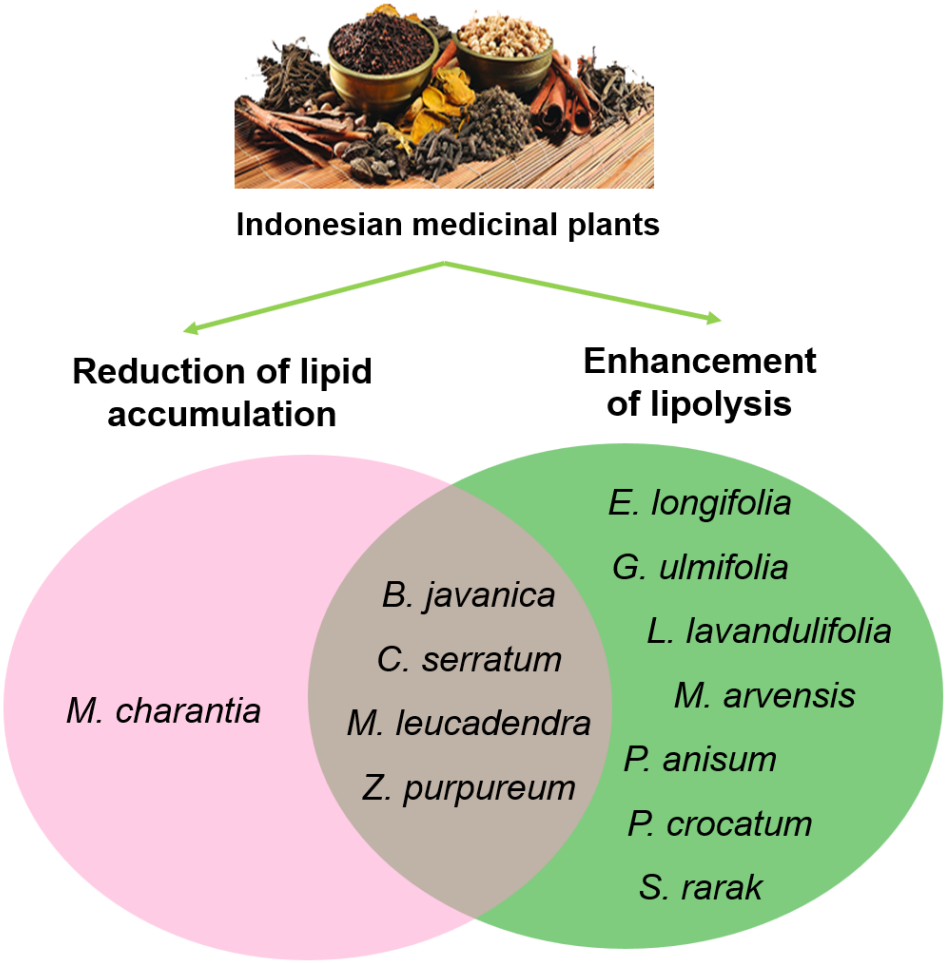

Figure 3.51 Results of anti-obesogenic screening of Indonesian medicinal plants

As for future works, the results of the screening can lead to subsequent isolation study to identify the responsible compounds for the anti-obesogenic activities, through lipid accumulation assay and/or glycerol release assay. The author recommends to perform bioassay-guided isolation using glycerol release assay for plants that showed enhancement of lipolysis (Figure 3.50). However, it is recommended to identify active compounds from *M.*

leucadendra using lipid accumulation assay because the plant showed strong reduction of lipid accumulation but moderate enhancement of lipolysis. As for *M. charantia* that showed reduction of lipid accumulation but no enhancement of lipolysis which indicated an anti-lipogenesis, a bioassay-guided isolation using lipid accumulation assay is strongly recommended (Figure 3.51).

The results of the screening have clearly demonstrated that different plant extracts possess different mode of anti-obesogenic activities, due to various chemical constituents in the extracts. Further studies on the cellular mechanisms and isolation of the active compounds will lead to a better understanding of interaction between natural products and lipid metabolism in adipocytes.

Chapter IV
Conclusions and Recommendations

This chapter summarizes the findings of the present study in relation to the research objectives presented in Section 1.3 (Chapter 1 Introduction) and makes recommendations for future works. Conclusions and recommendations are presented separately for study of lipolytic activity from *Eurycoma longifolia* Jack (Section 4.1), lipolytic activity from *Brucea javanica* (L.) Merr. (Section 4.2) and anti-obesogenic screening of Indonesian medicinal plants (Section 4.3). The conclusion sub-section presents the results of the respective study, while the second sub-section points out various recommendations that will provide readers some insights into further research and how to apply the results of this study for developing suitable drug/nutraceuticals for the treatment of obesity. The last section (Section 4.4) highlights the major contributions of the present study to the body of knowledge.

4.1 Study of Lipolytic Activity from *Eurycoma longifolia* Jack

The study of lipolytic compounds from *Eurycoma longifolia* Jack is summarized in Figure 4.1.

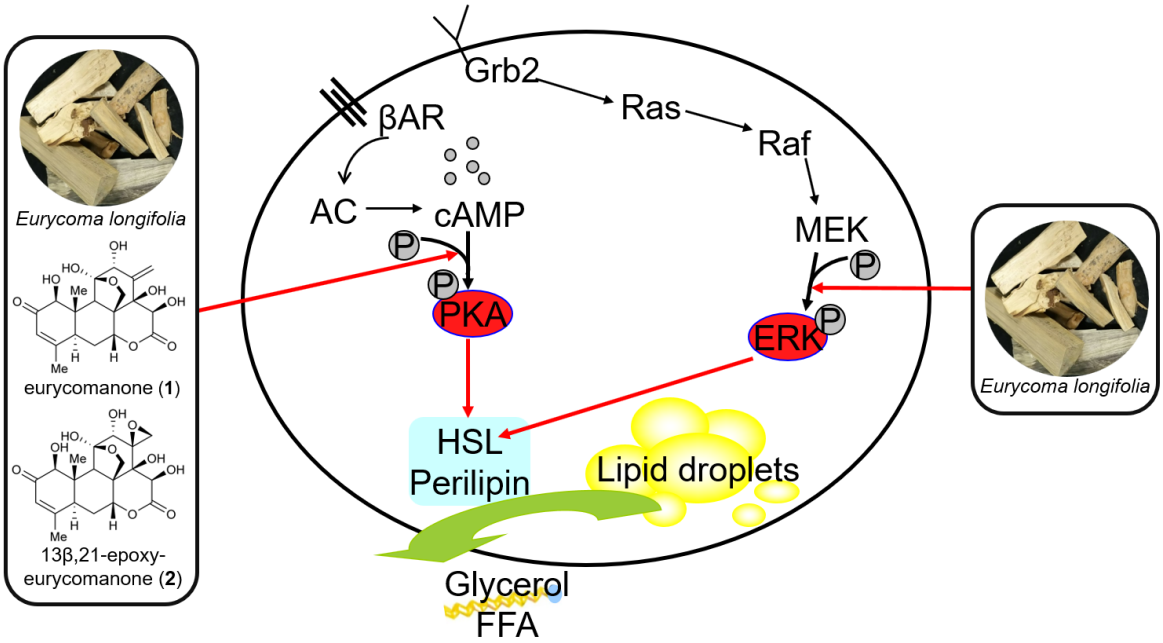

Figure 4.1 *E. longifolia* and its quassinoids stimulate lipolysis in 3T3-L1 adipocytes

4.1.1 Conclusions on Study of *Eurycoma longifolia* Jack

The study of *E. longifolia* is a series of study to address research questions raised from the results of previous study (Lahrita, 2015a). The conclusions are summarized based on the objectives presented in Section 1.3 (Chapter 1).

1. Mechanism of action of *E. longifolia* root extract
   E. longifolia root extract enhanced lipolysis through the activation of PKA and ERK kinases in 3T3-L1 white adipocytes.
2. Isolation of bioactive compounds
   Eurycomanone (**1**) and 13β,21-epoxyeurycomanone (**2**) were identified from *E. longifolia* root as the compounds responsible for the enhancement of lipolysis, with EC_{50} of 14.6 µM and 8.6 µM, respectively.
3. Mechanism of action of the bioactive compounds
   Eurycomanone (**1**) and 13β,21-epoxyeurycomanone (**2**) enhanced lipolysis through the activation of PKA.
4. Anti-obesogenic effects of the bioactive compounds in brown adipocytes
   Eurycomanone (**1**) and 13β,21-epoxyeurycomanone (**2**) reduced lipid accumulation and enhanced lipolysis in WT-1 brown adipocytes.

As a highlight, eurycomanone (**1**) is the major quassinoid in *E. longifolia*, and it is used as the marker compound in quality control of commercial products derived from this plant. Several bioactivities have been reported for this compound, but this is the first report on its anti-obesogenic activity and further study on the target protein.

4.1.2 Recommendations for Future Study on *Eurycoma longifolia* Jack

Based on the results of *E. longifolia* study, several recommendations are made to encompass the directions and strategies that can be adopted to develop *E. longifolia* and its active compounds into promising anti-obesity drugs or nutraceuticals. Recommendations for future study are presented as follows:

1. Investigation on obesity-male infertility effects of *E. longifolia*
   This plant has been traditionally used and marketed in modern days to improve male sexual performance, and this study has uncovered the activation of ERK as the target protein in lipolysis, thus there is an indication of overlapping mechanism between

lipolysis and spermatogenesis effects from this plant. A further study on the obesity-male infertility will address this increasing health problem in our male society and open up a better understanding of these complex phenomena.

2. Structure-activity relationship (SAR) study of the isolated compounds

   The stronger lipolytic activity of the epoxide derivate (**2**) than eurycomanone (**1**), and the absence of lipolytic activity of the dihydroxy derivate (**3**) indicates an essential moiety for the lipolytic activity, thus a further SAR study is warranted. It is expected that the results of the SAR study will bring these natural compounds as lead compounds for a potent anti-obesity drug.

3. Thermogenesis study of the isolated compounds in brown adipocytes

   The results of current study on the activity of compound **1** and **2** in WT-1 brown adipocytes indicate an enhancement of thermogenesis and fatty acid oxidation. Research in brown adipocytes has been increasingly explored in recent years due to the unique thermogenesis, and it may lead to a new therapeutic target for anti-obesity prevention or treatment.

4. *In vivo* study of the isolated compounds

   Based on the findings of this *in vitro* study, it is recommended to conduct a comprehensive *in vivo* study that examines not only lipid profiles, but also glucose metabolism, toxicity and spermatogenesis, after the administration of the isolated compounds. The results of *in vivo* study are necessary to provide information on the systemic effects, to support *in vitro* findings and to develop the isolated compounds for the treatment of metabolic syndromes.

4.2 Lipolytic Activity of *Brucea javanica* (L.) Merr.

The study of lipolytic activity of *Brucea javanica* (L.) Merr. is summarized in Figure 4.2.

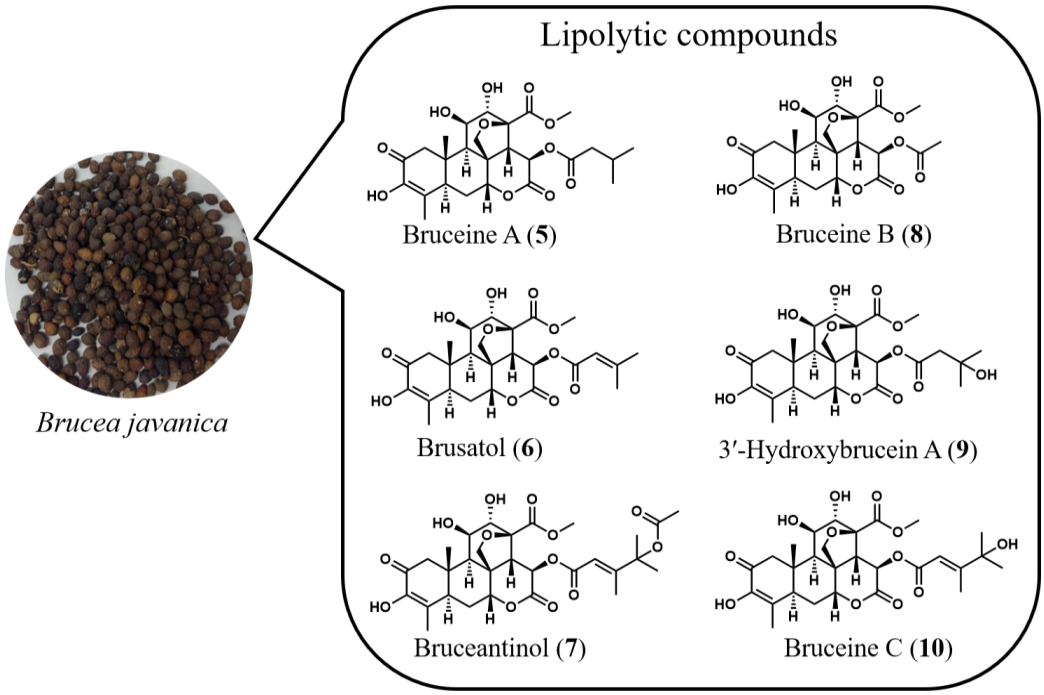

Figure 4.2 *B. javanica* and its isolated lipolytic compounds

4.2.1 Conclusions on Study of *Brucea javanica* (L.) Merr.

A couple of conclusions have been drawn from the study of lipolytic activity of *B. Javanica*.

1. Lipid metabolic-regulation of *B. javanica* fruit extract
   B. javanica also exerted strong lipolytic and lipid reducing-activity in 3T3-L1 white adipocytes.
2. Isolation of lipolytic compounds
   Bioassay-guided fractionation from *B. javanica* (L.) Merr. has isolated several lipolytic compounds, including brucein A (**5**), brusatol (**6**), brucenatinol (**7**), brucein B (**8**), 3'-hydroybrucein A (**9**), and bruceine C (**10**). Some isolated compounds from this plant have demonstrated much stronger lipolytic activity compared to two isolated compounds from *E. longifolia*.

This study is the first study to explore potential anti-obesogenic activities from *B. javanica*. Thus, it is expected that this effort can lead to the development of anti-obesity research from this plant.

4.2.2 Recommendations for Future Study on *Brucea javanica* (L.) Merr.

Because further studies on *B. javanica* and its active compounds are promising to be explored, a number of recommendations for future works are presented as follows:

1. Cellular mechanisms of actions

   As this plant strongly reduced lipid accumulation and enhanced lipolysis in the white adipocytes, it is recommended to elucidate its mechanism of actions not only for its lipolytic activity, but also for its activity in lipid synthesis of adipocytes. Mechanistic studies of the most potent isolated compounds are expected to identify their target proteins and to understand how they modulate lipid metabolism/catabolism in the adipocytes.
2. Structure-activity relationship (SAR) study of the isolated compounds

   As there were 7 isolated active compounds from this study which represented different chemical structure and strength of activity, further SAR study will lead to potent anti-obesity lead compounds in a new drug discovery.
3. *In vivo* study of the isolated compounds

   An *in vivo* study is necessary to provide systemic effects and support *in vitro* findings of anti-obesity potential from this plant and its active compounds.

4.3 Anti-obesogenic Screening of Indonesian Medicinal Plants

The anti-obesogenic bioassay screening of selected 76 Indonesian plant extracts in 3T3-L1 adipocytes is summarized in Table 4.1.

Table 4.1 Anti-obesogenic screening of Indonesian plant extracts

Indonesian Plant Extract	**Lipid Reduction**	**Lipolysis Enhancement**
Brucea javanica (L.) Merr.	○	○
Clerodendrum serratum (L.) Moon	○	○

Melaleuca leucadendra (L.) L.	○	○
Momordica charantia L.	○	
Zingiber purpureum Roscoe.	○	○
Leucas lavandulifolia Sm.		○
Mentha arvensis L.		○
Pimpinella anisum L		○
Eurycoma longifolia Jack		○
Piper crocatum Ruiz & Pav.		○
Guazuma ulmifolia Lam.		○
Sapindus rarak DC.		○

4.3.1 Conclusions on Anti-obesogenic Screening

Based on the results of the screenings, a number of conclusions have been drawn regarding Indonesian medicinal plants with different anti-obesogenic activities in the white adipocytes.

1. For enhancement of lipolysis, there are 7 plant extracts that significantly enhanced glycerol release in the white adipocytes.

   The plants are *Eurycoma longifolia* Jack, *Guazuma ulmifolia* Lam., *Leucas lavandulifolia* Sm., *Mentha arvensis* L., *Pimpinella anisum* L, *Piper crocatum* Ruiz & Pav., and *Sapindus rarak* DC.

2. For lipid reducing-activity and glycerol release enhancing-activity, there are 4 plant extracts that showed reduction of lipid accumulation more than 20% and significant enhancement of lipolysis in 3T3-L1 adipocytes.

   The plants are *Brucea javanica* (L.) Merr., *Clerodendrum serratum* (L.) Moon, *Melaleuca leucadendra* (L.) L., and *Zingiber purpureum* Roscoe.

3. For anti-lipogenesis in which there is reduction of lipid accumulation but no

enhancement of lipolysis, there is *Momordica charantia* L. that exerts this anti-obesogenic activity.

4.3.2 Recommendations for Future Study of Indonesian Medicinal Plants

Further studies are recommended to explore those potential medicinal plants for their active compounds and their mechanisms of actions. As for bioassay-guided fractionation, the author recommends to perform isolation using glycerol release assay for 11 plants shown that show lipolysis enhancement. However, it is recommended to identify lipid-reducing compounds from *M. leucadendra* using lipid accumulation assay because the plant showed strong reduction of lipid accumulation but moderate enhancement of lipolysis. Another suggestion includes a bioassay-guided isolation for *M. charantia* using lipid accumulation assay, as it showed reduction of lipid accumulation but no enhancement of lipolysis. Various results between reduction of lipid accumulation and enhancement of lipolysis from these plants also provide insights for their mechanistic studies.

4.4 Contributions to the Body of Knowledge

Particularly, the study of *E. longifolia* has uncovered cellular mechanisms of actions of its extract and active compounds, providing further information on chemical-biology field. As the author previously reported its potential anti-obesogenic effects for the first time, this study has provided further evidences on its activities in two different type of adipocytes, identification of the active compounds, and elucidation of the target proteins. The accumulated information resulted from this study will apparently contribute to a better understanding of this medicinal plant, its constituents and its effects in biology system.

In the similar way, the study of *B. javanica*, another less studied anti-obesity medicinal plant, has also opened up a new knowledge on anti-obesity research from natural products. In fact, this is the first report on potential anti-obesogenic activities of this medicinal plant *in vitro* in white adipocytes.

The findings of this study will provide significant contributions to the body of knowledge in anti-obesity research from medicinal plants. Not only has this study provided scientific basis and rationale for the use of those potential plants for medicinal purposes but it has also provided information on different mode of anti-obesogenic effects that can be used in a bioassay-guided fractionation from various natural products. Needless to say, this study

will encourage anti-obesity research from other medicinal plants. Specifically, in regard to the subject of this study, this study will corroborate the traditional use of Indonesian medicinal plants for the treatment of obesity.

Overall, research in obesity, is of a great importance, because it has attracted interest of global researchers who foresee the future negative impacts on medical costs and public health. Researchers are challenged to address this global health problem by developing new drugs to prevent/treat obesity, and by providing a better understanding of lipid metabolism in our body.

References

Ahern, K. (2012). Lipolysis. In: Berg JM, Tymoczko JL, Stryer L (eds) Biochemistry, seventh edition. W.H. Freeman and company, New York.

Ahmadian, M., Wang, Y., Sul, H.S. (2010). Medicine in focus, lipolysis in adipocytes. Int. J. Biochem. Cell Biol. *42*, 555–559.

Ahn, J., Lee, H., Kim, S. (2010). Curcumin-induced suppression of adipogenic differentiation is accompanied by activation of Wnt/β-catenin signaling. Am. J. Physiol. Cell Physiol. *298*, C1510−C1516.

Al-Salahi, O.S.A., Lam, C.K., Majid, A.M.S.A., Al-Suede, F.S.R.A., Saghir, S.A.M., Abdullah, W.Z., Ahamed, M.B.K., Yusoff, N.M. (2013). Anti-angiogenic quassinoid-rich fraction from *Eurycoma longifolia* modulates endothelial cell function. Microvascular Res. *90*, 30–39.

Almog, T., Naor, Z. (2008). Mitogen activated protein kinases (MAPKs) as regulators of spermatogenesis and spermatozoa functions. Mol. Cell. Endocrin., *282*, 39–44.

Almog, T., Naor, Z. (2010). The role of Mitogen activated protein kinase (MAPK) in sperm functions. Mol. Cell. Endocrin., *314*, 239–243.

An, S.J., Han, J.I., Kim, M.J., Park, J.S., Han, J.M., Baek, N.I., Chung, H.G., Choi, M.S., Lee, K.T., Jeong, T.S. (2010). Ethanolic extracts of *Brassica campestris* spp. *rapa* roots prevent high-fat diet-induced obesity via β_3-adrenergic regulation of white adipocyte lipolytic activity. J. Med. Food *13*, 406–414.

Ang, H.H., Hitotsuyanagi, Y., Takeya, K. (2000). Eurycolactones A–C, novel quassinoids from Eurycoma longifolia. Tetrahedron Lett. *41*, 6849–6853.

Ang, H.H., Ngai, T.H., Tan, T.H., (2003). Effects of *Eurycoma longifolia* Jack on sexual qualities in middle aged male rats. Phytomedicine *10*, 590–593.

Antel, J., Hebebrand, J. (2012). Weight-reducing side effects of the antiepileptic agents topiramate and zonisamide. In: Joost HG. (eds) Appetite Control. Handbook of Experimental Pharmacology, vol 209. Springer, Berlin, Heidelberg.

Balaji, M., Ganjayia, M.S., Gali, E.N., Kumara, H., Parima, B.N., Mopuri, R., Dasaria, S. (2016). A review on possible therapeutic targets to contain obesity: The role of phytochemicals. Obes. Res. Clin Pract. *10*, 363−380.

Ballinger, A., Peikin, S.R. (2002). Orlistat: its current status as an anti-obesity drug. Eur. J. Pharmacol. *440*, 109−17.

Bawm, S., Matsuura, H., Elkhateeb, A., Nabeta, K., Subeki, Nonaka, N., Oku, Y., Katakura, K. (2008). *In vitro* antitrypanosomal activities of quassinoid compounds from the fruits of a medicinal plant, *Brucea javanica*. Vet. Parasitol. *158*, 288–294.

Betz, M.J., Slawik, M., Lidell, M.E., Osswald, A., Heglind, M., Nilsson, D., Lichtenauer, U.D., Mauracher, B., Mussack, T., Beuschlein, F., Enerbäck, S. (2013). Presence of brown adipocytes in retroperitoneal fat from patients with benign adrenal tumors: relationship with outdoor temperature, J. Clin. Endocrinol. Metab. *19*, 635–639.

Boschmann, M., Thielecke, F. (2007). The effects of epigallocatechin-3-gallate on thermogenesis and fat oxidation in obese men: a pilot study. J. Am. Coll. Nutr. *26*, 389S–395S.

Brahma, N. P., Neman, H., Meriga, B., Mehar, S.K., Potana, S., Ramgopalrao, S. (2014). Mitigating efficacy of piperine in the physiological derangements of high fat diet induced obesity in Sprague Dawley rats. Chem. Biol. Interact. *221*, 42−51.

Burton, K.A., McKnight, G.S. (2007). PKA, Germ cells, and Fertility. Physiology *22*, 40–46.

Canning, K.L., Brown, R.E., Jamnik, V. (2014). Relationship between obesity and obesity-related morbidities weakens with aging. J. Gerontol. A Biol. Sci. Med. Sci. *69*, 87−92.

Cannon, B., Nedergaard, J. (2004). Brown adipose tissue: function and physiological significance. Physiol. Rev. *84*, 277−359.

Chan, K., Lee, S., Sam, T., Han, B. (1989). A quassinoid glycoside from the roots of *Eurycoma longifolia*. Phytochemistry *28*, 2857–2859.

Chan, K., Lee, S., Sam, T., Tan, S., Noguchi, H., Sankawa, U. (1991). 13β,18-dihydroeurycomanol, a quassinoid from *Eurycoma longifolia*. Phytochemistry *30*, 3138–3141.

Chan, K., Iitaka, Y., Noguchi, H., Sugiyama, H., Saito, I., Sankawa, U. (1992). 6β-Hydroxyeurycomalactone, a quassinoid from *Eurycoma longifolia*. Phytochemistry *31*, 4295–4298.

Chan, K.L., Choo, C.Y., Abdullah, N.R., Ismail, Z. (2004). Antiplasmodial studies of *Eurycoma longifolia* Jack using the lactate dehydrogenase assay of *Plasmodium falciparum.* J. Ethnopharmacol. *92*, 223–227.

Chang, L., Karin, M. (2001). Mammalian MAP kinase signalling cascades. Nature *410*, 37–40.

Chen, S.F., Li, Z.L., Li, W.X., Shan, Z.M., Zhu, W. (2011). Resveratrol inhibits cell differentiation in 3T3-L1 adipocytes via activation of AMPK. Can. J. Physiol. Pharm. *9*, 793–799.

Cinti, S. (2002). Adipocyte differentiation and transdifferentiation: plasticity of the adipose organ. J. Endocrinol. Invest. *25*, 823-835.

Clegg, M.E., Golsorkhi, M., Henry, C.J. (2013). Combined medium-chain triglyceride and chilli feeding increases diet-induced thermogenesis in normal weight humans. Eur. J. Nutr. *52*, 1579−1585.

Cornelius, P., MacDougald, O.A., Lane, M.D. (1994). Regulation of adipocytes development. Annu. Rev. Nutr. *14*, 99−129.

Croft, H., Houser, T.L., Jamerson, B.D. (2002). Effect on body weight of bupropion sustained-release in patients with major depression treated for 52 weeks. Clin. Ther. *24*, 662−672.

Cypess, A.M., White, A.P., Vernochet, C., Schulz, T.J., Xue, R., Sass, C.A., Huang, T.L., Roberts-Toler, C., Weiner, L.S., Sze, C., Chacko, A.T., Deschamps, L.N., Herder, L.M., Truchan, N., Glasgow, A.L., Holman, A.R., Gavrila, A., Hasselgren, P.O., Mori, M.A., Molla, M., Tseng, Y.H. (2013). Anatomical localization, gene expression profiling and functional characterization of adult human neck brown fat. Nat. Med. *19*, 635–639.

Daneschvar, H.L., Aronson, M.D., Smetana, G.W. (2016). FDA-Approved Anti-Obesity Drugs in the United States. Am. J. Med. *129*, 1−6.

Darise, M., Kohda, H., Mizutani, K., Tanaka, O. (1982). Eurycomanone and eurycomanol, quassinoids from the roots of *Eurycoma longifolia*. Phytochemistry *21*, 2091–2093.

Dojindo. (2014). Cell counting kit-8, cell proliferation assay and cytotoxicity assay, technical manual. http://www.dojindo.com/TechnicalManual/Manual_CK04.pdf Retrieved on Aug 7, 2014.

Drira, R., Matsumoto, T., Agawa, M., Sakamoto, K. (2016). Ice plant (*Mesembryanthemum crystallinum*) extract promotes lipolysis in mouse 3T3-L1 adipocytes through extracellular signal-regulated kinase activation. J. Med. Food. *19*, 274–280.

Elkhateeb, A., Yamasaki, M., Maede, Y., Katakura, K., Nabeta, K., Matsuura, H. (2008) Anti-babesial quassinoids from the fruits of *Brucea javanica*. Nat. Prod. Commun. *3*, 145–148.

Fidler, M.C., Sanchez, M., Raether, B. (2011). A one-year randomized trial of lorcaserin for weight loss in obese and overweight adults: the BLOSSOM trial. J. Clin. Endocrinol. Metab. *96*, 3067−3077.

Fukamiya, N., Okano, M., Miyamoto, M., Tagahara, K., Lee, K.H. (1992) Antitumor agents, 127. Bruceoside C, a new cytotoxic quassinoid glucoside and related compounds from *Brucea javanica*. J. Nat. Prod. *55*, 468–475.

Fink, K.B., Gothert, M. (2007). 5-HT receptor regulation of neurotransmitter release. Pharmacol. Rev. *59*, 360−417.

Gong, D.W., He, Y., Karas, M., Reitman, M. (1997). Uncoupling protein-3 is a mediator of thermogenesis regulated by thyroid hormone, β3-adrenergic agonists, and leptin. J. Biol. Chem. *272*, 24129–24132.

Green, H., Kehinde, O. (1974). Sublines of mouse 3T3 cells that accumulate lipid. Cell *1*, 113 −116.

Green, H., Kehinde, O. (1975). An established preadipose cell line and its differentiation in culture II. Factors affecting the adipose conversion. Cell *5*, 19−27.

Greenberg, A.S., Shen, W.J., Muliro, K., Patel, S., Souza, S.C., Roth, R.A., Kraemer, F.B. (2001). Stimulation of lipolysis and hormone-sensitive lipase via the extracellular signal-regulated kinase pathway. J. Biol. Chem. *276*, 45456–45461.

Halford, J.C. (2006). Obesity drugs in clinical development, Curr. Opin. Investig. Drugs *7*, 312–318.

Hall, I.H., Lee, K.H., Imakura, Y., Okano, M., Johnson, A. (1983). Anti-inflammatory agents. III. Structure–activity relationships of brusatol and related quassinoids. J. Pharm. Sci. *72*, 1282–1284.

Han, L.K., Xu, B.J., Kimura, Y., Zheng, Y.N., Okuda, H. (2000). *Platycodi radix* affects lipid metabolism in mice with high fat diet–induced obesity. J. Nutr. *130*, 2760–2764.

Han, L. K., Zheng, Y.N., Yoshikawa, M. (2005). Anti-obesity effects of chikusetsusaponins isolated from *Panax japonicus* rhizomes. BMC Compl. Altern. Med. *5*, 1–10.

Han, Y.M., Jang, M., Kim, I.S., Kim, S.H., Yoo, H.H. (2015). Simultaneous quantitation of six major quassinoids in Tongkat Ali dietary supplements by liquid chromatography with tandem mass spectrometry. J. Sep. Sci. *38*, 2260–2266.

Hasegawa, K., Satoshi H., Namekawa, H., Saga, Y. (2013). MEK/ERK signaling directly and indirectly contributes to the cyclical self-renewal of spermatogonial. Stem Cells *31*, 2517–2527.

Huang, C., Zhang, Y., Gong, Z., Sheng, X., Li, Z., Zhang, W., Qin, Y. (2006). Berberine inhibits 3T3-L1 adipocyte differentiation through the PPARgamma pathway. Biochem. Biophys. Res. Commun. *348*, 571–578.

Hwang, J.T., Park, I.J., Shin, J.I., Lee, Y.K., Lee, S.K., Baik, H.W., Ha, J., and Park, O.J. (2005). Genistein, EGCG, and capsaicin inhibit adipocyte differentiation process via activating AMP-activated protein kinase. Biochem. Biophys. Res. Commun. *338*, 694–699.

Hvizdos, K.M., Markham, A. (1999). Orlistat: a review of its use in the management of obesity. Drugs *58*, 743–760.

Ikarashi, N., Tajima, M., Suzuki, K., Toda, T., Ito, K., Ochiai, W., Sugiyama, K. (2012). Inhibition of preadipocyte differentiation and lipid accumulation by orengedokuto treatment of 3T3-L1 cultures. Phytother. Res. *26*, 91–100.

Ikram, N.K.K., Durrant, J.D., Muchtaridi, M., Zalaludin, A.S., Purwitasari, N., Mohamed, N., Rahim, A.S.A., Lam, C.K., Normi, Y.M., Rahman, N.A. (2015). A virtual screening approach for identifying plants with anti H5N1 neuraminidase activity. J. Chem. Inf. Model. *55*, 308–316.

Ishiyama, M., Miyazono, Y., Sasamoto, K., Ohkura, Y., Ueno, K. (1997). A highly water-soluble disulfonated tetrazolium salt as a chromogenic indicator for NADH as well as cell viability. Talanta *44*, 1299–1305.

Ismail, S.B., WanMohammad, Z., George, A., Hussain, N.H., Kamal, Z.M., Liske E. (2012). Randomized clinical trial on the use of PHYSTA freeze-dried water extract of *Eurycoma longifolia* for the improvement of quality of life and sexual well-being in men. Evid. Based Complement. Alternat. Med. *429268*, 1–10.

James, W.P., Caterson, I.D., Coutinho, W., Finer, N., Van Gaal, L.F., Maggioni, A.P., Torp-Pedersen, C., Sharma, A.M., Shepherd, G.M., Rode, R.A., Renz, C.L. (2010). SCOUT Investigators. Effect of sibutramine on cardiovascular outcomes in overweight and obese subjects. N. Engl. J. Med. *363*, 905–917.

Jespersen, N.Z., Larsen, T.J., Peijs, L., Daugaard, S., Homøe, P., Loft, A., De Jong, J., Mathur, N., Cannon, B., Nedergaard, J., Pedersen, B.K., Møller, K., Scheele, C. (2013). A classical brown adipose tissue mrna signature partly overlaps with brite in the supraclavicular region of adult humans. Cell Metab. *17*.

Jiwajinda, S., Santisopasri, V., Murakami, A., Sugiyama, H., Gasquet, M., Riad, E., Balansard, G., Ohigashi, H. (2002). *In vitro* anti-tumor promoting and anti-parasitic activities of the quassinoids from *Eurycoma longifolia*, a medicinal plant in Southeast Asia. J. Ethnopharmacol. *82*, 55–58.

Kang, S.I., Shin, H.S., Kim, S.J. (2015). Sinensetin enhances adipogenesis and lipolysis by increasing cyclic adenosine monophosphate levels in 3T3-L1 adipocytes. Biol. Pharm. Bull. *38*, 552–558.

Karin, C.S.L., Yang, M.F., Roberts, Phillipson, J.D. (1990). Canthin-6-one alkaloids from cell suspension cultures of *Brucea javanica*. Phytochemistry, *29*, 141–143.

Kim, I.H., Suzuki, R., Hitotsuyanagi, Y., Takeya, K. (2003). Three novel quassinoids, javanicolides A and B, and javanicoside A, from seeds of *Brucea javanica*. Tetrahedron *59*, 9985–9989.

Kim, I.H., Takashima, S., Hitotsuyanagi, Y., Hasuda, T., Takeya, K. (2004). New quassinoids javanicolides C and D and javanicosides B–F, from seeds of *Brucea javanica*. J. Nat. Prod. *67*, 863–868.

Kim, H.J., Lee, J.H., Choi, S.H., Lee, Y.S., Jahng, J.W. (2005). Fasting-induced increases of arcuate NPY mRNA and plasma corticosterone are blunted in the rat experienced neonatal maternal separation. Neuropeptides *39*, 587–594.

Kim, H.Y., Kang, M.H. (2005). Screening of Korean medicinal plants for lipase inhibitory activity. Phytother. Res. *19*, 359–361.

Kim, S., Park, H., Lee, M. (2008). Vitisin A inhibits adipocyte differentiation through cell cycle arrest in 3T3-L1 cells. Biochem. Biophys. Res. Commun. *372*, 108−113.

Kim, S.; Lee, S.; Lee, S. (2009). Rutecarpine ameliorates bodyweight gain through the inhibition of orexigenic neuropeptides NPY and AgRP in mice. Biochem. Biophys. Res. Commun. *389*, 437−442.

Kim, J., Lee, Y.S., Kim, C. (2012). Betulinic acid has an inhibitory effect on pancreatic lipase and induces adipocyte lipolysis. Phytother. Res. *26*, 1103−1106.

Kim, S.O., Sakchaisri, K., Asami, Y., Ryoo, I.J., Choo, S.J., Yoo, I.D., Soung, N.K., Kim, Y.S., Jang, J.H., Kim, B.Y., Ahn, J.S. (2014). Illudins C2 and C3 stimulate lipolysis in 3T3-L1 adipocytes and suppress adipogenesis in 3T3-L1 preadipocytes. J. Nat. Prod. *77*, 744−750.

Kim, H.J., Hong, S.H., Chang, S.H. (2016). Effects of feeding a diet containing *Gymnema sylvestre* extract: attenuating progression of obesity in C57BL/6J mice. Asian Pac. J. Trop. Med. *9*, 437−444.

Kimura, H., Ogawa, S., Jisaka, M., Kimura, Y., Katsube, T., Yokota, K. (2006). Identification of novel saponins from edible seeds of Japanese horse chestnut (*Aesculus turbinata* Blume) after treatment with wooden ashes and their nutraceutical activity. J. Pharm. Biomed. Anal. *41*, 1657–1665.

Kishino, E., Ito, T., Fujita, K., Kiuchi, Y. (2006). A mixture of the *Salacia reticulata* (Kotala himbutu) aqueous extract and cyclodextrin reduces the accumulation of visceral fat mass in mice and rats with high-fat diet–induced obesity. J. Nutr. *136*, 433–439.

Kitagawa, I., Mahmud, T., Simanjuntak, P., Hori, K., Uji, T., Shibuya, H. (1994). Indonesian medicinal plants. VIII. Chemical structures of three new triterpenoids, bruceajavanin A, dihydrobruceajavanin A, and bruceajavanin B, and a new alkaloidal glycoside, bruceacanthinoside, from the stems of *Brucea javanica* (Simaroubaceae). Chem. Pharm. Bull. *42*, 1416–1421.

Kuo, P.C., Damu, A.G., Lee, K.H., Wu, T.S. (2004). Cytotoxic and antimalarial constituents from the roots of *Eurycoma longifolia*. Biorg. Med. Chem. *12*, 537–544.

Lahrita, L., (2015a). The effects Indonesian medicinal plants on glucose uptake and lipid accumulation in 3T3-L1 adipocytes. (Master's Thesis) Hokkaido University, Sapporo.

Lahrita, L., Kato, E., Kawabata, J. (2015b). Uncovering potential of Indonesian medicinal plants for glucose uptake enhancement and lipid suppression against 3T3-L1 adipocytes. J. Ethnopharmacol. *168*, 229–236.

Lahrita, L., Hirosawa, R., Kato, E., Kawabata, J. (2017). Isolation and lipolytic activity of eurycomanone and its epoxy derivative from *Eurycoma longifolia*. Bioorg. Med. Chem. *25*, 4829–4834.

Lass, A., Zimmermann, R., Oberer, M., Zechner, R. (2011). Lipolysis - a highly regulated multi-enzyme complex mediates the catabolism of cellular fat stores. Prog. Lipid Res. *50*, 14–27.

Lee, K.H., Hayashim N., Okano, M., Ozaki, H., Motoharu, J. (1984). Brusatol and cleomiscosin-A, antileukemic principles from Brucea javanica. J. Nat. Prod. *47*, 550–551.

Lee, I.A., Lee, J.H., Baek, N.I. (2005). Antihyperlipidemic effect of crocin isolated from the fructus of *Gardenia jasminoides* and its metabolite crocetin. Biol. Pharm. Bull. *28*, 2106−2110.

Lee, Y.S., Kim, W.S., Kim, K.H., Yoon, M.J., Cho, H.J., Shen, Y., Ye, J.M., Lee, C.H., Oh, W.K., Kim, C.T., Hohnen-Behrens, C., Gosby, A., Kraegen, E.W., James, D.E., Kim, J.B. (2006). Berberine, a natural plant product, activates AMP-activated protein kinase with beneficial metabolic effects in diabetic and insulin-resistant states. Diabetes *55*, 2256–2264.

Lee, J., Jung, E., Lee, J., Kim, S., Huh, S., Kim, Y., Kim, Y., Byun, S.Y., Kim, Y.S., and Park, D. (2009a). Isorhamnetin represses adipogenesis in 3T3-L1 cells. Obesity (Silver Spring) *17*, 226–232.

Lee, Y.K., Lee, W.S., Hwang, J.T., Kwon, D.Y., Surh, Y.J., and Park, O.J. (2009b). Curcumin exerts anti differentiation effect through AMPK and PPAR-α in 3T3-L1 adipocytes and antiproliferatory effect through AMPKa-COX-2 in cancer cells. J. Agric. Food Chem. *57*, 305–310.

Lee, H., Kang, R., and Yoon, Y. (2010). Shikonin inhibits fat accumulation in 3T3-L1 adipocytes. Phytother. Res. *24*, 344–351.

Lefterova, M.I., Lazar, M.A. (2009). New developments in adipogenesis. Trends Endocrin. Met. *20*, 107–114.

Lehrke, M., Lazar, M.A. (2005). The many faces of PPARγ. Cell *123*, 993–999.

Li, F., Li, W., Fu, H.W., Zhang, Q.B., Koike, K. (2007). Pancreatic lipase-inhibiting triterpenoid saponins from fruits of *Acanthopanax senticosus*. Chem. Pharm. Bull. *55*, 1087–1089.

Lidell, M.E., Betz, M.J., Leinhard, O.D., Heglind, M., Elander, L., Slawik, M., Mussack, T., Nilsson, D., Romu, T., Nuutila, P., Virtanen, K.A., Beuschlein, F., Persson, A., Borga, M., Enerbäck, S. (2013). Evidence for two types of brown adipose tissue in humans, Nat. Med. *19*, 631–634.

Liu, J., Lee, J., Salazar Hernandez, M.A. (2015). Treatment of obesity with celastrol. Cell *161*, 999−1011.

Low, B.S., Choi, S.B., Wahab, H.A., Kumar Das, P., Chan, K.L. (2013). Eurycomanone, the major quassinoid in *Eurycoma longifolia* root extract increases spermatogenesis by inhibiting the activity of phosphodiesterase and aromatase in steroidogenesis. J. Ethnopharm. *149*, 201–207.

Luyengi, L., Suh, N., Fong, N.H.S., Pezzuto, J.M., Kinghorn, A.D. (1996). A lignan and four terpenoids from *Brucea javanica* that induce differentiation with cultured HL-60 promyelocytic leukemia cells. Phytochemistry *43*, 409–412.

Ma, X., Xu, L., Alberobello, A.T. (2015). Celastrol protects against obesity and metabolic dysfunction through activation of a HSF1-PGC1α transcriptional axis. Cell Metab. *22*, 695−708.

Mahfudh, N., Pihie, A.H.L. (2008). Eurycomanone induces apoptosis through the up-regulation of p53 in human cervical carcinoma cells. J. Cancer Mol. *4*, 109–115.

MacLean, D.B., Luo, L.G. (2004). Increased ATP content/production in the hypothalamus may be a signal for energy-sensing of satiety: studies of the anorectic mechanism of a plant steroidal glycoside. Brain Res. *1020*, 1–11.

Maeda, H., Hosokawa, M., Sashima, T., Funayama, K., Miyashita, K. (2005). Fucoxanthin from edible seaweed, *Undaria pinnatifida*, shows antiobesity effect through UCP1 expression in white adipose tissues. Biochem. Biophys. Res. Commun. *332*, 392–397.

Martinat, N., Crepieux, P., Reiter, E., Guillou, F. (2005). Extracellular signal-regulated kinases (ERK) 1, 2 are required for luteinizing hormone (LH)-induced steroidogenesis in primary Leydig cells and control steroidogenic acute regulatory (StAR) expression Reprod. Nutr. Dev. *45*, 101–108.

Mattison, Colman, R.J., Beasley, T.M., Allison, D.B., Kemnitz, J.W., Roth, G.S., Ingram, D.K., 7 Weindruch, R., Cabo, R., M. Anderson, R.M. (2017). Caloric restriction improves health and survival of rhesus monkeys. Nat. Commun. *8*, 1–12.

Meng, D., Li, X., Han, L., Zhang, L., An, W., Li, X. (2014). Four new quassinoids from the roots of *Eurycoma longifolia* Jack. Fitoterapia *92*, 105–110.

Mercader, J., Ribot, J., Murano, I., Felipe, F., Cinti, S., Bonet, L., Palou, A. (2006). Remodeling of white adipose tissue after retinoic acid administration in mice. Endocrinology *147*, 5325–5332.

Mopuri, R., Islam, S. (2017). Medicinal plants and phytochemicals with anti-obesogenic potentials: A review. Biomed. Pharmacother. *89*, 1442–1452.

Mori, S., Takizawa, M., Satou, M., Sakasai, M., Kusuoku, H., Nojiri, H., Yoshizuka, N., Hotta, M., Kitahara, T., Hase, T., Takema, Y., Saito, M., Yada, T. (2009). Enhancement of lipolytic responsiveness of adipocytes by novel plant extract in rat. Exp. Biol. Med. *234*, 1445–1449.

Morimoto, C., Satoh, Y., Hara, M., Inoue, S., Tsujita, T., Okuda, H. (2005). Anti-obese action of raspberry ketone. Life Sci. *77*, 194–204.

Morita, H., Kishi, E., Takeya, K., Itokawa, H., Tanaka, O. (1990). New quassinoids from the roots of *Eurycoma longifolia*. Chem. Lett. *5*, 749–752.

Morita, H., Kishi, E., Takeya, K., Itokawa, H., Iitaka, Y. (1993). Highly oxygenated quassinoids from *Eurycoma longifolia*. Phytochemistry *33*, 691–696.

Miyake, K., Tezuka, Y., Awale, S., Li, F., Kadota, S. (2009). Quassinoids from *Eurycoma longifolia*. J. Nat. Prod. *72*, 2135–2140.

Murakami, N., Sugimoto, M., Kawanishi, M., Tamura, S., Kim, H.S., Begum, K., Wataya, Y., Kobayashi, M. (2003). New semisynthetic quassinoids with *in vivo* antimalarial activity. J. Med. Chem. *46*, 638–641.

Nahal, S., Valery, L.L., King, J. (2012). Globesity-The Global Fight Against Obesity, Bank of America Merrill Lynch.

Nakai, M., Fukui, Y., Asami, S., Toyoda-Ono, Y., Iwashita, T., Shibata, H., Mitsunaga, T., Hashimoto, F., Kiso, Y. (2005). Inhibitory effects of oolong tea polyphenols on pancreatic lipase *in vitro*. J. Agric. Food Chem. *53*, 4593−4598.

Nicholls, D.G., Locke, R.M. (1984). Thermogenic mechanism in brown fat. Physiol. Rev *64*, 1−64.

Noorshahida, A., Wong, T.W., Choo, C.Y. (2009). Hypoglycemic effect of quassinoids from *Brucea javanica* (L.) Merr. J. Ethnopharmacol. *124*, 586–591.

O'Neill, M.J., Bray, D.H., Boardman, P., Chan, K.L., Phillipson, J.D., Warhurst, D.C., Peters, W. (1987). Plants as sources of antimalarial drugs. Part 4. Activity of *Brucea javanica* fruits against chloroquine-resistant *Plasmodium falciparum in vitro* and against *Plasmodium berghei in vivo*. J. Nat Prod. *50*, 41–48.

Ohia, S.E., Opere, C.A., LeDay, A.M. (2002). Safety and mechanism of appetite suppression by a novel hydroxycitric acid extract (HCASX). Mol. Cell. Biochem. *238*, 89−103.

Okano, M., Fukamiya, N., Tagahara, K., Cosentino, M., Lee, T.T.Y., Morris-Natshke, S., Lee, K.H. (1996). Anti-HIV activity of quassinoids. Bioorg. Med. Chem. Lett. *6*, 701–706.

Olayanjua, A., Copple, I.M., Bryana, H.K., Edge, G.T., Sison, R.L., Wong, M.W., Lai, Z.Q., Lin, Z.X., Dunn, K., Sanderson, C.M., Alghanem, A.F., Cross, M.J. Ellis, E.C., Ingelman-Sundberg M., Malik, H.Z., Kitteringhama, N.R., Christopher E. Goldring, C.E., Park, B.K. (2015). Brusatol provokes a rapid and transient inhibition of Nrf2 signaling and sensitizes mammalian cells to chemical toxicity-implications for therapeutic targeting of Nrf2. Free Radical Biol. Med. *78*, 202–212.

Ono, Y., Hattori, E., Fukaya Y., Imai, S., Ohizumi, Y. (2006). Anti-obesity effect of *Nelumbo nucifera* leaves extract in mice and rats. J. Ethnopharmacol. *106*, 238–244.

Oppi-Williams, C., Suagee, J.K., Corl, B.A. (2013). Regulation of lipid synthesis by liver X receptor α and sterol regulatory element-binding protein 1 in mammary epithelial cells. J. Dairy Sci. *96*, 112–121.

Ouellet, V., Labbé, S.M., Blondin, D.P., Phoenix, S., Guérin, B., Haman, F., Turcotte, E.E., Richard, D., Carpentier, A.C. (2012). Brown adipose tissue oxidative metabolism contributes to energy expenditure during acute cold exposure in humans. J. Clin. Invest. *122*, 545–552.

Park, S., Nhiem, N.X., Van Kiem, P., Van Minh, C., Tai, B.H., Kim, N., Yoo, H.H., Song, J.H., Ko, H.J., Kim, S.H. (2014). Five new quassinoids and cytotoxic constituents from the roots of *Eurycoma longifolia*. Bioorg. Med. Chem. Lett. *24*, 3835–3840.

Peirce, V., Carobbio, S., Vidal-Puig, A. (2014). The different shades of fat. Nature *510*, 76–83.

Polonsky, J., Baskevitvh, Z., Gaudemer A. (1967). Constituants amers de *Brucea amarissirna*, structures des bruceines A, B and C. Experientia *23*, 424–426.

Polonsky, J., Varenne, J., Prange, T., Pascard, C. (1980). Antileukaemic quassinoids: structure (X-ray analysis) of bruceine C and revised structure of bruceantinol. Tetrahedron Lett. *21*, 1853–1856.

Pramono E. (2002). The traditional use of traditional knowledge and medicinal plants in Indonesia. Multi-stakeholder dialoque on trade, intellectual property and biological resources in Asia. Rajendrapur, Bangladesh: BRAC Centre for Development Management.

Prokesch, A., Hackl, H., Hakim-Weber, R., Bornstein, S.R., Trajanoski, Z. (2009). Novel insights into adipogenesis from omics data. Curr. Med. Chem. *16*, 2952–2964.

Ramji, D.P., Foka, P. (2002). CCAT/enhancer-binding proteins: structure, function and regulation. Biochem. J. *365*, 561–575.

Richard, A.J., Burris, T.P., Sanchez-Infantes, D., Wang, Y., Ribnicky, D.M., Stephens, J.M. (2014). Artemisia extracts activate PPARγ, promote adipogenesis, and enhance insulin sensitivity in adipose tissue of obese mice. Nutrition *30*, S31–S36.

Rehman, S., Choe, K., Yoo, H. (2016). Review on a traditional herbal medicine, *Eurycoma longifolia* Jack (tongkat ali): its traditional uses, chemistry, evidence-based pharmacology and toxicology. Molecules *21*, 1–31.

Sangat-Roemantyo, H., Riswan, S. (1990). Javanese medicinal plants: their distribution and uses. Congress on Traditional Medicines and Medicinal Plants. Denpasar, Indonesia.

Sakaki, T., Yoshimura, S., Tsuyuki, T. (1986a). Two new quassinoid glycosides, yadanziosides N and O isolated from seeds of *Brucea javanica* (L.) Merr. Tetrahedron Lett. *27*, 593–596.

Sakaki, T., Yoshimura, S., Tsuyuki, T., Takahashi, T., Honda, T. (1986b). Yadanzioside P, a new antileukemic quassinoid glycoside from *Brucea javanica* (L.) Merr. with the 3-*O*-(β-D-glucopyranosyl) bruceantin structure. Chem. Pharm. Bull. *34*, 4447–4450.

Sawangjaroen, N., Sawangjaroen, K. (2005). The effects of extracts fromanti-diarrheic Thai medicinal plants on the in vitro growth of the intestinal protozoa parasite: *Blastocystis hominis*. J. Ethnopharmacol. *98*, 67–72.

Scheele, C., Nielsen, S. (2017). Metabolic regulation and the anti-obesity perspectives of human brown fat. Redox Biology *12*, 770–775.

Sethi, J.K., Vidal-Puig, A.J. (2010). Adipocyte biology. Adipose tissue function and plasticity orchestrate nutritional adaptation. http://www.mikrobik.net/page.php?id=874 Retrieved on May 17, 2018.

Sette, C., Barchi, M., Bianchini, A., Conti, M., Rossi, P., Geremia, R. (1999). Activation of the mitogen-activated protein kinase ERK1 during meiotic progression of mouse pachytene spermatocytes. J. Biol. Chem. *274*, 33571–33579.

Shamsul, K., Tajuddin, A.M., Mazina, M.Y. (2003). Tumbuhan ubatan tradisional Malaysia. (In Malay). Institut Biosains, Universiti Pertanian Malaysia Publisher, Malaysia.

Sheng, L., Qian, Z., Zheng, S. (2006). Mechanism of hypolipidemic effect of crocin in rats: crocin inhibits pancreatic lipase. Eur. J. Pharmacol. *543*, 116−122.

Shi, J.,Yan, J., Lei, Q. (2009). Intragastric administration of evodiamine suppresses NPY and AgRP gene expression in the hypothalamus and decreases food intake in rats. Brain Res. *1247*, 71−78.

Sigma-Aldrich. (2015). Free glycerol reagent, technical bulletin. https://www.sigmaaldrich.com/content/dam/sigmaaldrich/docs/Sigma/Bulletin/f6428bul.pdf Retrieved on June 2, 2015.

Sim, K.Y., Sim, J.J., Geissman, T.A. (1967). Constituents of *Brucea sumatrana* Roxb. Brusatol. J. Org. Chem. *33*, 429–431.

Smeets, A.J., Westerterp-Plantenga, M.S. (2009). The acute effects of a lunch containing capsaicin on energy and substrate utilisation, hormones, and satiety. Eur. J. Nutr. *48*, 229−234.

Smith S.R., Weissman N.J., Anderson C.M. (2010). Multicenter, placebo controlled trial of lorcaserin for weight management. N. Engl. J. Med. *363*, 245–256.

Subeki, Matsuura, H., Takahashi, K., Nabeta, K., Yamasaki, M., Maede, Y., Katakura, K. (2007). Screening of Indonesian medicinal plant extracts for antibabesial activity and isolation of new quassinoids from *Brucea javanica*. J. Nat. Prod. *70*, 1654–1657.

Tada, H., Yasuda, F., Otani, K., Doteuchi, M., Ishihara, Y., Shiro, M. (1991). New antiulcer quassinoids from *Eurycoma longifolia*. Eur. J. Med. Chem. *26*, 345–349.

Tilaar, M., Sangat-Roemantyo, H., Riswan, S. (1992). Kunyit (*Curcuma domestica*), the queen of jamu. In: Proceed. of the Conf. on Medicinal Products from Tropical Rain Forests. FRIM, Kuala Lumpur, Malaysia.

Thomsen, W.J., Grottick, A.J., Menzaghi, F. (2008). Lorcaserin, a novel selective human 5-hydroxytryptamine2C agonist: *in vitro* and *in vivo* pharmacological characterization. J Pharmacol. Exp. Ther. *325*, 577–587.

Tran, T.V.A., Malainer, C., Schwaiger, S., Atanasov, A.G., Heiss, E.H., Dirsch, V.M., Stuppner, H. (2014). NF-kB Inhibitors from *Eurycoma longifolia*. J. Nat. Prod. *77*, 483–488.

Tomoda, H., Namatame, I., Omura, S. (2002). Microbial metabolites with inhibitory activity against lipid metabolism. Proc. Japan Acad. *78*, 217–240.

Townsend, K.L., Tseng, Y.H. (2014). Brown fat fuel utilization and thermogenesis. Trends Endocrinol. Metab. *25*, 168–177.

Tsuboyama-Kasaoka, N., Takahashi, M., Kim, H., Ezaki, O., (1999). Up-regulation of liver uncoupling protein-2 mRNA by either fish oil feeding or fibrate administration in mice. Biochem. Biophys. Res. Commun. *257*, 879–885.

van Heerden, F.R., Marthinus Horak, R., Maharaj, V.J., Vleggaar, R., Senabe, J.V., Gunning, P.J. (2007). An appetite suppressant from Hoodia species. Phytochemistry *68*, 2545–2553.

Walker, W.H. (2009). Molecular mechanisms of testosterone action in spermatogenesis. Steroids *74*, 602–607.

Weigle, D.S., Cummings, D.E., Newby, P.A., Breen, P.A., Frayo, R.S., Matthys, C.C., Callahan, H.S., Purnell, J.Q. (2003). Roles of leptin and ghrelin in the loss of body weight caused by a low fat, high carbohydrate diet. Int. J. Clin. Endocrinol. Metab. *88*, 1577–1586.

Weir, M.A., Beyea, M.M., Gomes, T. (2011). Orlistat and acute kidney injury:an analysis of 953 patients. Arch. Intern. Med. *171*, 703–704.

Weiss, E.C., Galuska, D.A., Kettel-Khan, L., Serdula, M.K. (2006). Weight control practices among U.S. adults, 2001–2002. Am. J. Prev. Med. *31*, 18−24.

White, M.A., Grilo, C.M. (2013). Bupropion for overweight women with binge eating disorder: a randomized, double-blind, placebo-controlled trial. J. Clin. Psychiatry *74*, 400–406.

Withrow, D., Alter, D.A. (2011). The economic burden of obesity worldwide: a systematic review of the direct costs of obesity. Obes. Rev. *12*, 131−41.

World Health Organization. (2018). Obesity and overweight. http://www.who.int/mediacentre/factsheets/fs311/en/ Retrieved on May 18, 2018.

Won, S., Kim, S., Kim, Y. (2007). Licochalcone A, a lipase inhibitor from the roots of *Glycyrrhiza uralensis*. Food Res. Int. *40*, 1046−1050.

Wright, C.W., O'Neill, M.J., Phillipson, J.D.,Warhurst, D.C. (1988). Use of microdilution to assess in vitro antiamoebic activities of *Brucea javanica* fruits, *Simarouba amara* stem, and a number of quassinoids. Antimicrob. Agents Chemother. *32*, 1725–1729.

Xiang, Y.K., Ye, W., Huang, C.H., Lou, B., Zhang, J., Yu, D.L., Huang, X.C., Chen, B.C., Zhou, M.T. (2017). Brusatol inhibits growth and induces apoptosis in pancreatic cancer cells ia JNK/p38 MAPK/NF-kb/Stat3/Bcl-2 signaling pathway. Biochem. Biophys. Res. Commun. *387*, 820–826.

Yang, J.Y., Della-Fera, M.A., Baile, C.A. (2008). Guggulsterone inhibits adipocyte differentiation and induces apoptosis in 3T3-L1 cells. Obesity *16*, 16–22.

Yoshikawa, M., Shimoda, H., Nishida, N., Takada, M., Matsuda, H. (2002). *Salacia reticulata* and its polyphenolic constituents with lipase inhibitory and lipolytic activities have mild antiobesity effects in rats. J. Nutr. *132*, 1819–1824.

Yoshimure, S., Sakaki, T., Ishibashi, M., Tsuyuki, T., Takahashi, T., Honda, T. (1985). Onstituents of seeds of *Brucea javanica*. Structures of new bitter principles, Yadanziolides A, B, C, Yaanziosides F, I, J, and L. Bull. Chem. Soc. Jpn. *58*, 2673–2679.

Zechner, R., Zimmermann, R., Eichmann, T.O., Kohlwein, S.D., Haemmerle, G., Lass, A., Madeo, F. (2012). Fat signals-lipases and lipolysis in lipid metabolism and signaling. Cell Metabolism *15*, 279–291.

Zhang, L., Feng, X.H., Ma, D.J., Yang, J.J., Jiang, H.Y., Zhang, Y.N., He, W.Z. (2013). Brusatol isolated from *Brucea javanica* (L.) Merr. induces apoptotic death of insect cell lines. Pestic. Biochem. Phys. *107*, 18–24.

Zuhud, E.A.M., Ekarelawan, Riswan, S. (1994). Hutan tropika Indonesia sebagai sumber keanekaragaman plasma nutfah tumbuhan obat. (In Indonesian). In: Zuhud, E.A.M. and Haryanto (Eds.). Pelestarian pemanfaatan keanekaragaman tumbuhan obat hutan tropika Indonesia. 193-291, 1-15. IPB: Bogor.

Appendix 1. Curve calibration of standard glycerol solution (540 nm)

Raw data of absorbance intensity of glycerol solution

	1	2	3	4	5	6
A	0.043	0.077	0.115	0.161	0.177	0.258
B	0.043	0.076	0.115	0.125	0.169	0.188

Glycerol (µg/mL)	0	20	40	60	80	100
Absorbance (mean value)	0.043	0.0765	0.115	0.143	0.173	0.223

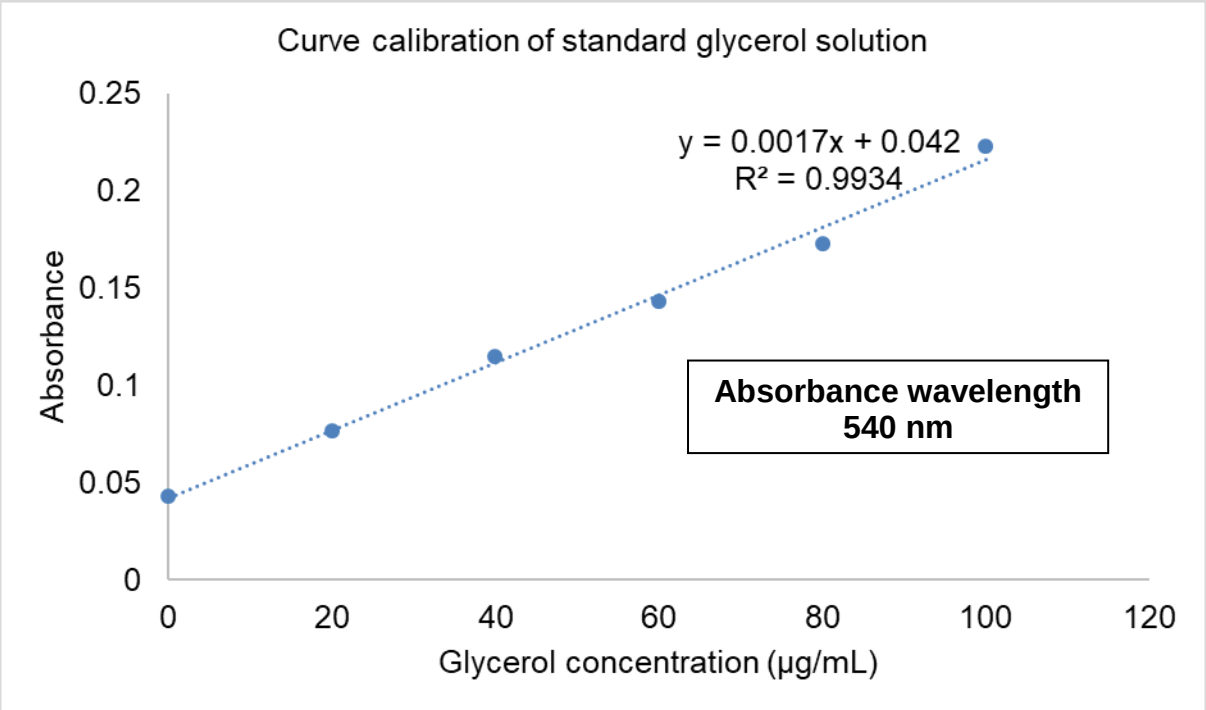

Calibration curve: y= 0.0017x + 0.042, R^2= 0.9934 where y= absorbance at wavelengths (540 nm) and x= concentration of standard glycerol solution (µg/mL). Lab. Food Biochemistry (Hokkaido University)

Appendix 2. Curve calibration of standard glycerol solution (560 nm)

Raw data of absorbance intensity of glycerol solution

	1	2	3	4	5	6	7	8
A	0.048	0.045	0.040	0.048	0.058	0.074	0.108	0.152
B	0.051	0.043	0.050	0.045	0.058	0.072	0.098	0.155

Glycerol (µg/mL)	0	3.125	6.25	12.5	25	50	100	200
Absorbance (mean value)	0.049	0.044	0.045	0.046	0.058	0.073	0.103	0.153

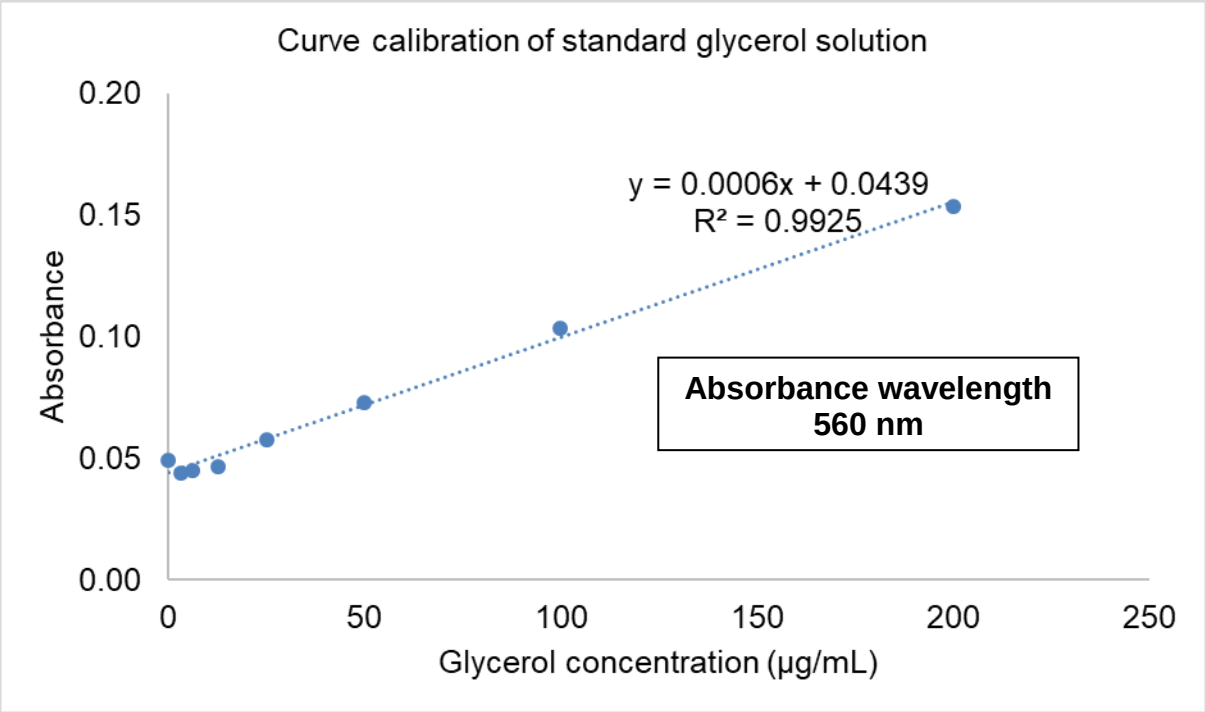

Calibration curve: y= 0.0006x + 0.0439, R^2= 0.9925 where y= absorbance at wavelengths (560 nm) and x= concentration of standard glycerol solution (µg/mL). Tseng Lab (Joslin Diabetes Center)

Appendix 3. Curve calibration of standard BSA solution (595 nm)

Raw data of absorbance intensity of BSA solution

	1	2	3	4	5	6
A	0.288	0.362	0.349	0.42	0.448	0.525
B	0.253	0.302	0.373	0.431	0.455	0.496

BSA (µg/mL)	0	200	400	600	800	1000
Absorbance (mean value)	0.271	0.332	0.361	0.426	0.452	0.511

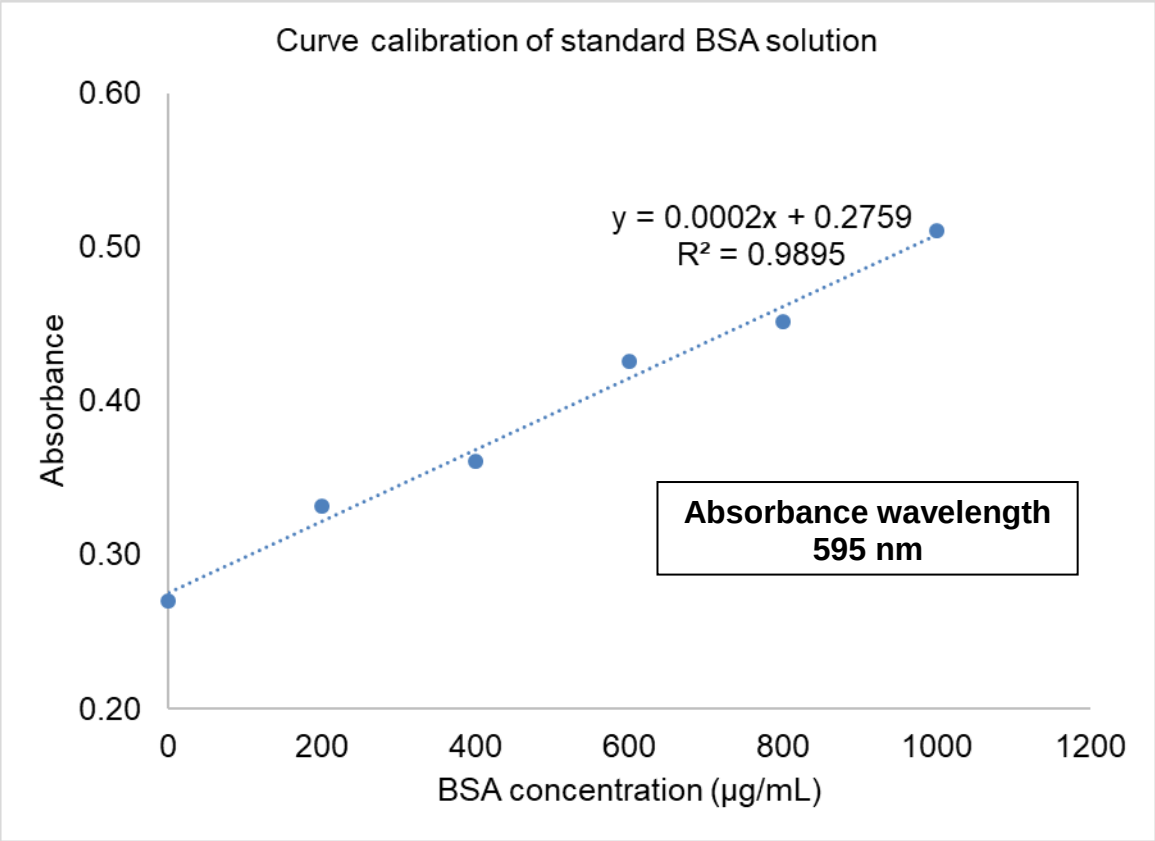

Calibration curve: y= 0.0002x + 0.2759, R^2= 0.9895 where y= absorbance at a wavelength of 595 nm and x= concentration of standard BSA solution in lysis buffer (µg/mL)

Appendix 4. 3D structure model of 13,21-epoxyeurycomanone

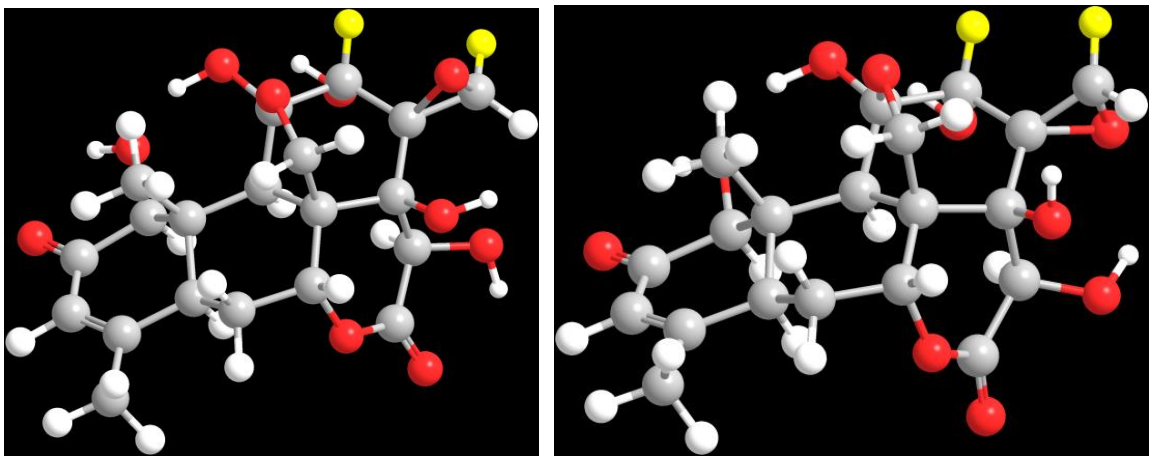

Left: β-epoxide; Right: α-epoxide. The model was created using ChemBio3D Ultra 14.0. The yellow atoms are H-12 and H_a-21. The calculated distance of H-12 and H_a-21 is 2.35 Å for β-epoxide and 2.57 Å for α-epoxide.

Appendix 5. 3D structure model of 1,15-di-*O*-acetyl-13,21-epoxyeurycomanone

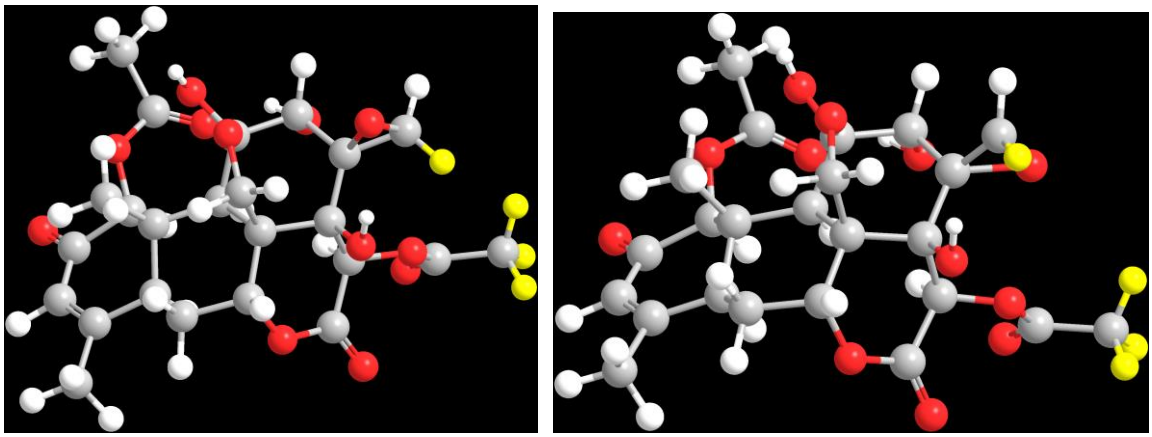

Left: β-epoxide; Right: α-epoxide. The model was created using ChemBio3D Ultra 14.0. The yellow atoms are H-12 and H_a-21. The calculated distance of H-12 and H_a-21 is 4.69 Å for β-epoxide and 3.14 Å for α-epoxide.

Appendix 6. Lipid accumulation assay of compounds 1 and 2 in 3T3-L1 white adipocytes

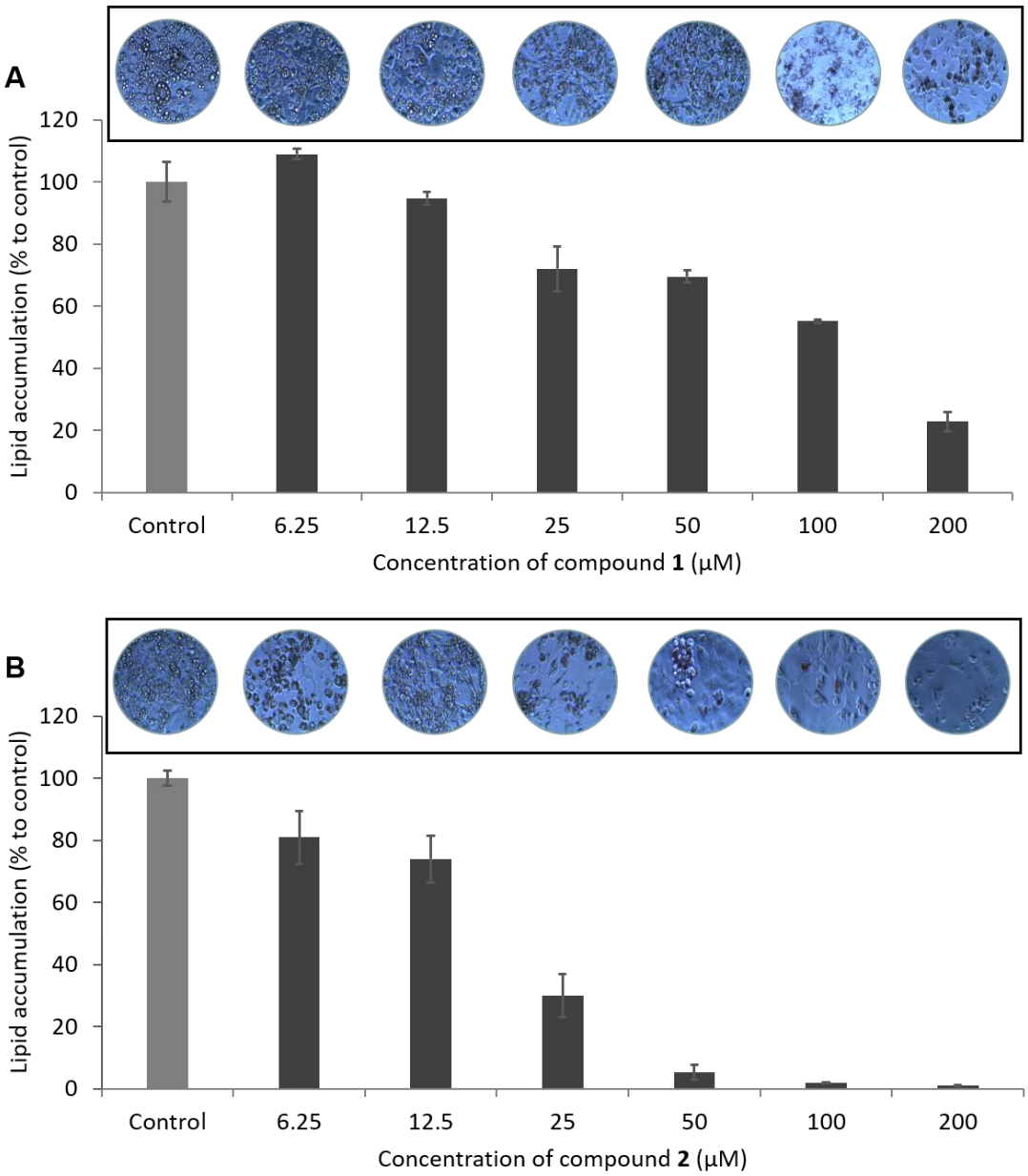

Photograph of Nile Red-stained lipid droplets under microscope and lipid accumulation reduction effect for compounds 1 (A) and 2 (B) in 3T3-L1 adipocytes. (A) Magnification 200x. (B) Compound **1** showed significant difference above 25 µM (p<0.01). Compound **2** showed significant difference above 12.5 µM (p<0.01). Data are expressed as mean ± SEM (n=6). Dunnett's test was used.

Appendix 7. Glycerol release assay of compounds 1 and 2 in WT-1 brown adipocytes

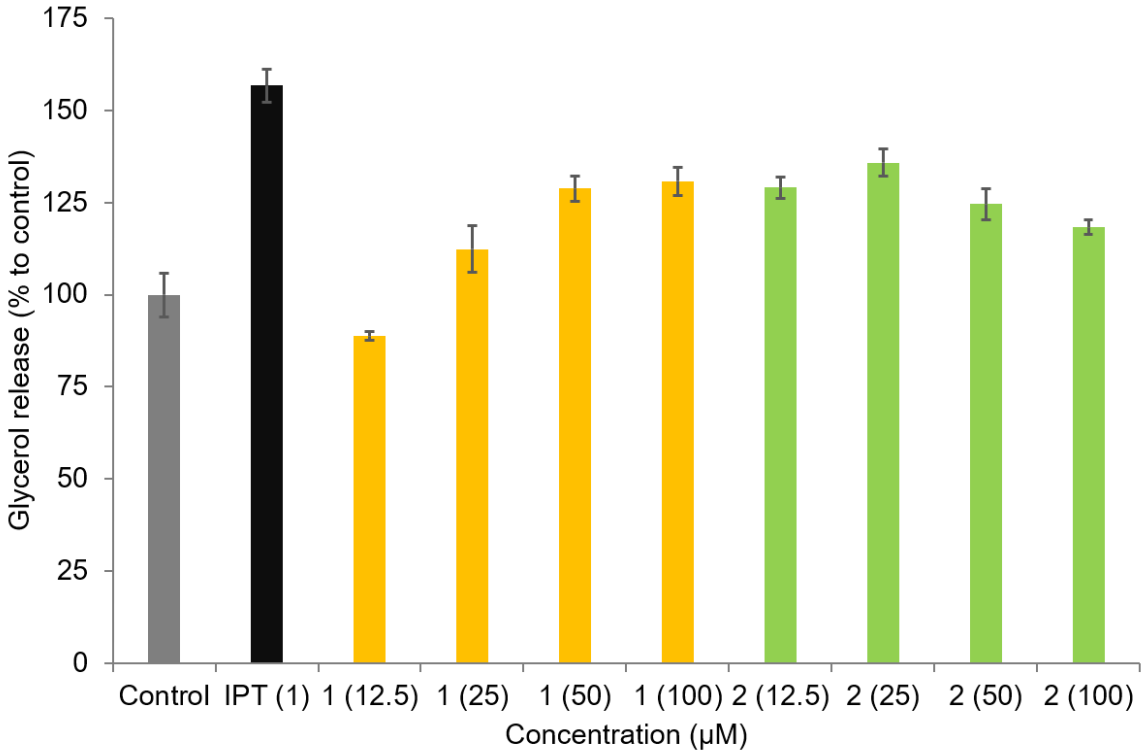

Glycerol release enhancement activity of compounds **1** and **2** in WT-1 brown adipocytes with one-day sample incubation time, same as in white adipocytes. Compounds 1 and 2 enhanced glycerol release but not statistically significant.

Appendix 8. Constituents of *E. longifolia* extract

In 1000 µg/mL *E. longifolia* extract	**Water (µg/mL)**	**50% MeOH (µg/mL)**	**MeOH (µg/mL)**	**50% EtOH (µg/mL)**	**EtOH (µg/mL)**
eurycomanone **(1)**	29.9 ± 0.9	37.3 ±1.2	**51.1 ± 0.4**	28.6 ± 0.3	14.1 ± 0.2
13β,21-epoxyeurycomanone **(2)**	2.0 ± 0.3	2.5 ± 0.1	2.1 ± 0.1	1.6 ± 0.1	0.9 ± 0.2
13β,21-dihydroxyeurycomanone **(3)**	3.6 ± 0.2	4.7 ± 0.3	4.9 ± 0.5	3.2 ± 0.6	2.3 ± 0.1

Content of eurycomanone (**1**) in *E. longifolia* extract was 5.1 % as quantified by LC-MS.

Appendix 9. Enzymatic reaction of Free Glycerol Release Reagent and eurycomanone (1)

Eurycomanone (µM)	OD (540 nm)
3.125	0.109
6.25	0.108
12.5	0.103
25	0.103
50	0.107
100	0.117

Each concentration of eurycomanone was added to 100 µg/mL glycerol standard solution (Table 2.9) before reacting with the Free Glycerol Release Reagent (Figure 2.20). OD (540 nm) values are subtracted by OD value of the blank (Milli-Q). Eurycomanone does not react with the Free Glycerol Release Reagent (Figure 2.19).